



The
University
Of
Sheffield.

Regulation of macrophage polarisation by TRIB1 and its consequences in metabolic homeostasis and atherosclerosis

By:

Jessica M. Johnston

A thesis submitted in partial fulfilment of the requirements for the
degree of
Doctor of Philosophy

The University of Sheffield
Faculty of Medicine, Dentistry & Health
Department of Infection, Immunity & Cardiovascular Disease (IICD)

January 2017

Abstract

Chronic inflammatory diseases including obesity, diabetes and cardiovascular disease cause significant morbidity and mortality worldwide. It is well established that both circulating lipid levels and macrophages have significant roles in the pathogenesis of these diseases. Single nucleotide polymorphisms (SNPs) close to the Tribbles-1 (*TRIB1*) gene have been identified in genome wide association studies (GWAS) to be associated with hyperlipidaemia and the incidence of myocardial infarction (MI).

Studies using *Trib1* full body- and liver specific knockout mice have shown hepatic expression of *Trib1* is a regulator of plasma lipid levels, one of the leading risk factors of developing heart disease. Additionally, *Trib1* has been shown to be a regulator of 'M2' (alternatively activated) macrophage polarisation. However, the interplay between *Trib1*, hepatocytes and macrophages is currently unexplored. Similarly, there has been no direct study to evaluate the role of *Trib1* in atherogenesis.

The aims of this study were to (1) investigate whether myeloid specific alterations of *Trib1* expression regulate macrophage polarisation and its consequences on plasma lipid homeostasis; (2) investigate the role of myeloid *Trib1* in experimental atherosclerosis and (3) develop immunohistochemistry staining methods to expand the analysis of macrophage phenotype in atherosclerotic plaques.

To investigate these aims, myeloid specific *Trib1* knockout (*Trib1* *fl/fl* x *LyzMCre*) and over-expressor (*ROSA26.Trib1Tg* x *LyzMCre*) mice were developed and their phenotypes were assessed. Furthermore, the molecular mechanisms by which *Trib1* affects macrophage polarisation were investigated. The role of myeloid *Trib1* in experimental atherosclerosis was determined by bone marrow transplantation into atherogenic ApoE^{-/-} mice (*Trib1*→ApoE^{-/-}) and full histological analysis was performed. Moreover, a staining and image analysis method was established to investigate the phenotype of plaque macrophages *in situ*.

Phenotypic analyses of the *Trib1* mouse models showed myeloid loss of *Trib1* promotes elevated plasma lipids and pro-inflammatory polarisation in both tissue- and bone marrow- derived macrophages (BMDMs). It was revealed that *Trib1* does this via modulating levels of C/EBP protein family members, key regulators of macrophage polarisation. Similarly, the data suggest IL-15 may in part play a role in the observations seen. Bone marrow transplantation and high-fat diet feeding exposed *Trib1* to be pro-atherogenic by increasing disease burden in the aorta and aortic sinus of the mice with substantially elevated levels of foam cell macrophages. Microarray analysis of human monocyte-derived macrophages revealed significantly elevated levels of the oxidised LDL receptor *ORLI* (LOX-1) and down-regulation of *SCARB-1*, a receptor involved in reverse cholesterol transport; a finding which was validated in *Trib1*^{Tg} BMDMs. *Trib1*^{Tg}→ApoE^{-/-} mice also presented with a metabolic phenotype including increased weight, fatty liver, enlarged adipocytes and elevated plasma glucose, which may also implicate the effect of IL-15, since previous studies have shown it to be involved in lipolysis.

In conclusion, TRIB1 is a potent regulator of lipid homeostasis, the loss of which promotes inflammation in the liver through Kupffer cell- hepatocyte cross talk. In addition, TRIB1 regulates atherosclerosis, the over-expression of which promotes atherogenesis through elevated oxLDL uptake and subsequent foam cell formation in plaque macrophages. Thus, collectively the study has uncovered previously unreported roles of TRIB1 *in vivo* that together demonstrate TRIB1 to control distinct aspects of macrophage biology that have local and systemic influence.

Declaration of Contributions

All the work presented in this thesis is my own and I confirm that approximately 85% of the experiments were carried out by myself. Data supplied by others are stated in each relevant figure legend. However for clarity and appreciation the following people are acknowledged for their contributions.

Dr. Ronald M. Krauss & colleagues performed the extensive lipid profiling data. **Dr. Adrienn Angyal** performed and analysed blood cell count data, fluorescent immunohistochemistry (F4/80 and CD206), flow cytometry and qPCR on initial characterisation of the *Trib1 x LyzMCre* mouse models. **Dr. Eva Hadadi** performed and analysed qPCR data relating to macrophage phenotype (Chapter 3). **Dr. Daniel Szili** performed and analysed western blots for C/EBP α and β . Human MDM microarrays were performed and analysed by **Professor Alison Goodall & Dr. Stephen Hamby**. Hepatic lipid measurements and qPCR data was performed by our continual supportive collaborators **Dr. Robert Bauer & Professor Daniel Rader**. qPCR relating to *TRIB1* expression (Chapter 3) were completed by **Mr. Zabran Ilyas**.

Acknowledgements

Firstly I would like to thank my supervisors Professor Endre Kiss-Toth and Professor Sheila Francis for the opportunity to join their lab and complete a PhD. I am exceptionally grateful for their continued effort and time, their invaluable encouragement, support and advice that has allowed me to become a successful scientist. Thank you to Endre for the many opportunities to travel in the name of science including to Philadelphia, San Diego, Venice and Budapest. I consider myself extremely lucky.

I would also like to thank Dr. Mabruka Alfaidi for her time and effort in the beginning for teaching me the ropes in mouse work and histology. I would also like to thank the BSU staff, particularly to Mrs. Beka Armstrong and Mrs. Rachel Sandy for their advice, thoughtful care and attention in looking after the mice. Special thanks also go to Dr. Mark Ariaans for his continual, invaluable and excellent animal technical support throughout my PhD particularly during the bone marrow transplant studies, the work could not have been done without your help.

I also thank my colleagues and friends in the lab and the O floor office, particularly to members of the Kiss-Toth group (past and present); Adri, Zabran, Yang, George and Kajus who make it *the* best place work for the laughs and stimulating conversations when experiments work and listening and helping problem solve when they don't! Special appreciations go to Zabran for his friendship and interesting Tribbles discussions and to Kajus for our monocyte/ macrophage chats!

Last but not least, I am forever appreciative for the support and encouragement my family have given me in pursuing a career in science, my (Kiwi) Dad and brothers Ross and Louie. Thanks guys, I am officially a nerd (and proud!).

Undoubtedly I wouldn't have been able to do this without support from 'the man I love the most' and my partner in crime (my 'P.I.C'), Dan, who may not fully understand my scientific ramblings but has always been there for me. Thanks for putting our lives on hold while I achieved this. You always made me feel like 'the Queen of everything'.

Finally, I am eternally indebted to my Mama who has always instilled in me the ambition to achieve anything I want to in life, and I have. Thank you for everything. This is for you.

Table of Contents

ABSTRACT.....	I
DECLARATION OF CONTRIBUTIONS.....	III
ACKNOWLEDGEMENTS	IV
TABLE OF CONTENTS	V
LIST OF FIGURES.....	XI
LIST OF TABLES.....	XIII
LIST OF ABBREVIATIONS	XIV
CHAPTER 1. GENERAL INTRODUCTION.....	1
<i>1.1 Inflammation</i>	<i>1</i>
1.1.1 Inflammation: Classical vs. metabolic	1
1.1.2 Obesity is characterised by inflammation	2
1.1.3 Macrophages are central effector cells in inflammation	2
1.1.4 Macrophages and adipocytes have overlapping signalling pathways.....	3
<i>1.2 Origins of Macrophages</i>	<i>5</i>
1.2.1 Role of tissue macrophages.....	7
1.2.2 Macrophage phenotype	9
1.2.3 Macrophage polarisation markers	10
<i>1.3 Inflammatory signalling.....</i>	<i>11</i>
1.3.2 Adipokines	12
1.3.3 Inflammatory signalling pathways	13
1.3.4 MAPK	14
1.3.5 NF- κ B.....	14
1.3.6 Toll-like receptor signalling.....	15
1.3.7 PPAR signalling at the cross roads of inflammation and metabolism ..	15
1.3.8 Tribbles proteins are modulators of inflammatory signalling.....	16
1.3.8.1 Origin of TRIBs	18
1.3.8.2 Mammalian TRIBs.....	18
1.3.8.3 TRIB interacting proteins.....	19
1.3.8.4 MAPK	19
1.3.8.5 Transcription factors relevant to Trib1 signalling.....	21
1.3.8.6 C/EBP.....	21
1.3.8.5 NF- κ B.....	22
<i>1.4 Atherosclerosis.....</i>	<i>22</i>
1.4.1 Atherosclerosis is a chronic inflammatory disease of the vessel wall ..	23
1.4.2 The pathogenesis of atherosclerosis.....	23
1.4.3 Atherosclerotic lesions	24
<i>1.5 The importance of lipid homeostasis in inflammatory disease.....</i>	<i>29</i>
1.5.1 Elevated lipids are risk factors to the development of chronic inflammatory diseases	29
1.5.2 Chronic inflammatory diseases are associated with lipid and lipoprotein abnormalities	29
1.5.3 Lipoproteins and the risk of cardiovascular disease	30
1.5.4 Lipoprotein particles	31
1.5.4.1 OxLDL	33
1.5.4.2 VLDLs.....	33
1.5.4.3 VLDL-associated lipoproteins are associated with CVD risk	34

1.5.5 Lipogenesis vs. Lipolysis	35
1.5.6 Aberration of <i>de novo</i> lipogenesis.....	35
1.6 <i>TRIB1</i> in human disease	36
1.6.1 <i>TRIB1</i> and cancer	36
1.6.2 <i>TRIB1</i> in macrophages	37
1.6.3 <i>TRIB1</i> is associated with lipid traits and is a risk factor for the development of cardiovascular disease.....	39
1.6.4 <i>Trib1</i> regulates hepatic lipogenesis.....	41
1.6.5 <i>TRIB1</i> is a potential novel therapeutic target to lower plasma cholesterol	42
1.7 <i>Molecular regulation of lipogenesis; the link between cholesterol homeostasis and inflammation</i>	43
1.7.1 Cholesterol metabolism in macrophages	47
1.7.1.1 Scavenger Receptors	47
1.7.2.2 Foam cell formation and lipoprotein uptake	48
1.7.2.3 Cholesterol efflux.....	51
1.7.2.4 Intracellular cholesterol trafficking and storage	51
1.8 <i>Summary</i>	52
1.8.1 Hypothesis.....	52
1.8.2 Aims	52
CHAPTER 2. GENERAL MATERIALS & METHODS.....	54
2.1 <i>Animals</i>	54
2.1.1 Licensing	54
2.1.2 Husbandry	54
2.1.3 Development of <i>Trib1</i> x <i>LyzMCre</i> mice	55
2.1.3.1 <i>ROSA26.Trib1Tg</i>	55
2.1.3.2 <i>Trib1 fl/fl</i>	57
2.1.5 End of procedure	58
2.2 <i>Tissue processing and Histology</i>	59
2.3 <i>Human Ethics</i>	59
2.4 <i>In vitro work</i>	60
2.4.1 Cell line maintenance.....	60
2.4.1.1 RAW 264.7 and HEPG2 cells.....	60
2.4.1.2 BMDMs.....	60
2.4.2 Polarisation of BMDMs	60
2.4.3 Transfection.....	60
2.5 <i>RNA extraction and qPCR</i>	61
2.6 <i>Western blotting</i>	62
2.7 <i>Colourimetric immunohistochemistry</i>	63
2.7.1 Standard protocol	63
2.8 <i>Statistical analysis</i>	64
CHAPTER 3. MYELOID <i>TRIB1</i> ALTERS PLASMA LIPID HOMEOSTASIS.....	65
3.1 <i>Introduction</i>	65
3.2 <i>Hypothesis</i>	66
3.3 <i>Materials & Methods</i>	66
3.3.1 Animals	66
3.3.1.1 High fat diet.....	66
3.3.1.2 Peritonitis	66
3.3.2 Morphometry.....	67
3.3.3 Lipid profiling	67

3.3.4 Immunohistochemistry.....	67
3.3.5 Flow Cytometry	68
3.3.5.1 Expression of <i>Trib1</i> - transgene (GFP) in monocytes and macrophages	69
3.3.6 Microarray	69
3.3.7 Stimulation of HepG2 cells	70
3.3.8 Hepatic Lipid measurements	70
3.3 Results	70
3.3.1 Expression of <i>Trib1</i> in <i>Trib1 x LyzMCre</i> mice.....	70
3.3.2 <i>Trib1</i> floxed <i>x LyzMCre & ROSA26.Trib1 x LyzMCre</i> mice have normal tissue anatomy.....	73
3.3.2.1 Gross anatomy.....	73
3.3.2.2 Liver and Adipose	73
3.3.3 Myeloid <i>Trib1</i> does not affect white blood cell count.....	75
3.3.4 Myeloid <i>Trib1</i> does not influence expression of macrophage markers in the spleen.....	75
3.3.5 Myeloid <i>Trib1</i> alters plasma lipid homeostasis	77
3.3.5.1 Myeloid <i>Trib1</i> alters plasma lipid homeostasis	77
3.3.5.2 Inflammatory challenge in C57BL/6 mice mirrors phenotype	77
3.3.6 <i>Trib1 x LyzMCre</i> alters Kupffer cell phenotype <i>in vivo</i>	79
3.3.6.1 Myeloid <i>Trib1</i> mice show no differences in F4/80+ macrophages in the liver or adipose	79
3.3.6.2 Loss of <i>Trib1</i> in myeloid cells increases Kupffer cell expression of IRF-5	79
3.3.6.3 Myeloid <i>Trib1</i> overexpression increases Kupffer cell expression of <i>Ym1</i>	80
3.3.7 Myeloid <i>Trib1</i> regulates macrophage polarisation in BMDMs <i>in vitro</i> ... 80	
3.3.7.1 The loss of <i>Trib1</i> promotes an ‘M1’ pro-inflammatory phenotype in BMDMs.....	81
3.3.7.2 Overexpression of <i>Trib1</i> promotes an ‘M2’ anti-inflammatory phenotype in BMDMs.....	81
3.3.8 <i>TRIB1</i> regulates macrophage polarisation by modulating <i>C/EBPα</i> and <i>C/EBPβ</i> expression	84
3.3.8.1 <i>TRIB1</i> overexpression in RAW 264.7 cells down-regulates protein expression of <i>C/EBPα</i>	84
3.3.8.2 <i>TRIB1</i> overexpression in RAW cells up-regulates protein expression of <i>C/EBPβ</i>	84
3.3.8.3 <i>TRIB1</i> regulates macrophage polarisation via miR-155 in BMDMs 84	
3.3.9 <i>TRIB1</i> expression is associated with overexpression of alternatively activated macrophage markers in human MDMs.....	86
3.3.10 Macrophage <i>Trib1</i> controls <i>IL-15</i> expression	89
3.3.11 Myeloid <i>Trib1</i> regulates hepatic lipogenesis	90
3.3.12 Hepatic <i>Trib1</i> is down regulated by inflammatory signals.....	92
3.3.13 Kupffer cell phenotype correlates with hepatic <i>Trib1</i> expression and hepatic lipid content.....	93
3.4 Summary.....	95
3.5 Discussion	96

CHAPTER 4. DISTINCT MACROPHAGE POPULATIONS CONTRIBUTE TO PLAQUE SIZE AND STABILITY IN MURINE MODELS OF ATHEROSCLEROSIS 104

.....	104
4.1 Introduction.....	104

4.2 Hypothesis	105
4.3 Materials & Methods	105
4.3.1 ApoE ^{-/-}	105
4.3.2 LDLR ^{-/-}	105
4.3.3 AAV8-PCSK9D377Y	106
4.3.4 Assessment of atherosclerosis	106
4.3.5 Histology & Morphometry	106
4.3.6 Fluorescent Immunohistochemistry	106
4.3.6.1 Development of Image Analysis using ImageJ	107
<i>Semi automated system to quantify macrophage phenotype using ImageJ</i>	108
4.3.6.2 Optimised Image J work flow	112
4.3.6.3 Macrophage populations and ratios	113
4.4 Results	114
4.4.1 Plaque macrophages can be simultaneously stained for MAC3, NOS2 and ARG1	114
4.4.2 ARG1 expressing plaque macrophages are less abundant in ApoE ^{-/-} , compared to LDLR ^{-/-} and PCSK9 animals.	114
4.4.3 Enrichment of NOS2 positive/ARG1 negative macrophages is responsible for the pro-inflammatory phenotype of ApoE ^{-/-} plaques.....	118
4.4.4 Plaque macrophage phenotype correlates with plaque size and stability.	121
4.5 Summary.....	124
4.6 Discussion	125

CHAPTER 5. OVEREXPRESSION OF <i>TRIB1</i> IN HAEMATOPOETIC CELLS INDUCES ATHEROSCLEROSIS AND METABOLIC PHENOTYPE IN APOE^{-/-} MICE.....	132
5.1 Introduction.....	132
5.2 Hypothesis.....	133
5.3 Materials & Methods	134
5.3.1 Animals	134
5.3.2 Bone marrow transplantation	134
5.3.2.1 Total body irradiation.....	134
5.3.2.2 Bone marrow cell preparation and transplantation	134
5.3.2.3 High fat diet.....	135
5.3.3 End of procedure and cardiac puncture.....	137
5.3.4 Perfusion fixation	137
5.3.5 Tissue dissection	137
5.3.5.1 Dissection of the aortic tree.....	137
5.3.6 Blood biochemistry	140
5.3.7 Histological processing and paraffin embedding of tissues.....	140
5.3.8 Histological analysis	141
5.3.8.1 <i>En Face</i> staining of the Aorta	141
5.3.8.2 Histology & Morphometry.....	141
5.3.8.3 Histological staining.....	142
5.3.9 Assessment of lesion size and macrophage infiltrate in aortic roots ..	143
5.3.9.1 Lesion size.....	143
5.3.9.2 Histological staining and plaque pathology	143
5.3.9.3 Quantification of Lesion size	143
5.3.9.4 Quantification of Mac3 and Collagen staining	145
5.4 Results	145
5.4.1 Human plaque macrophages express TRIB1	145
5.4.2 <i>Survival of Trib1 x LyzMCre → ApoE^{-/-} mice</i>	146

5.4.3 <i>Trib1 x LyzMCre</i> → <i>ApoE</i> ^{-/-} have altered atherosclerosis burden	146
5.3.2.1 Aorta	146
5.3.2.2 Lesion size and stability	149
5.4.3 <i>Trib1</i> ^{Tg} → <i>ApoE</i> ^{-/-} atheromas are rich in foamy cell macrophages	151
5.4.3.1 Mac-3 staining	151
5.4.3.2 Scavenger receptors are up regulated in <i>TRIB1</i> -high human MDMs	152
5.4.3.3 Expression of scavenger receptors are up regulated in <i>Trib1</i> transgenic BMDMs	153
5.4.4 <i>ApoE</i> ^{-/-} mice with altered levels of <i>Trib1</i> in haematopoietic cells show differences in body weight and adipose tissue size	156
5.4.4.1 Transgenic <i>Trib1</i> → <i>ApoE</i> ^{-/-} mice have altered plasma lipids	157
5.4.5 <i>Trib1</i> → <i>ApoE</i> ^{-/-} mice have a metabolic phenotype	160
5.4.5.1 <i>Trib1</i> ^{Tg} → <i>ApoE</i> ^{-/-} mice have increased hepatic steatosis	160
5.4.5.2 Adipocyte size is altered in <i>Trib1</i> → <i>ApoE</i> ^{-/-} mice	162
5.4.6 Macrophage infiltrate in metabolic tissues	164
5.4.6.1 <i>Trib1</i> → <i>ApoE</i> ^{-/-} mice have comparable numbers of macrophages in the adipose tissue	164
5.5 Summary	165
5.6 Discussion	167
CHAPTER 6. GENERAL DISCUSSION	176
6.1 Major outcomes	176
6.2 Limitations	183
6.3 Future work	187
6.3.1 The regulation of foam cell formation by <i>TRIB1</i>	187
6.3.2 Assessment of macrophage phenotype in BMT mice	187
6.3.3 High fat diet in <i>Trib1 x LyzMCre</i> mice	188
6.3.4 Measurement of lipolysis	188
6.3.5 Measurement of plasma levels of cytokines	188
6.3.6 Measurement of apoB	188
6.3.7 Measurement of fatty acid oxidation genes	189
REFERENCES	190
APPENDIX I GENOTYPING PROTOCOLS	213
8.1.1 DNA extraction from mouse earclips	213
8.1.2 DNA isolation	213
8.1.3 Primers and PCR conditions	213
8.1.3.1 <i>ROSA26.Trib1</i> transgene	213
8.1.3.2 <i>Trib1</i> floxed	214
8.1.3.3 <i>Lyz2Cre</i>	215
APPENDIX II MOUSE DIETS & DRINKING WATER	217
8.2.1 Chow diet	217
8.2.2 Western diet	217
8.2.3 Acidified drinking water	218
APPENDIX III HISTOLOGY	219
8.3.1 Fixatives	219
8.3.2 Histological stains	219
8.3.2.1 Oil Red O	219
8.3.2.2 Elastic van Gieson (EVG)	219
8.3.2.3 Haematoxylin and Eosin (H&E)	220

8.3.2.4 Maritus Scarlet Blue (MSB).....	221
APPENDIX IV IMMUNOHISTOCHEMISTRY	222
8.4.3.1 <i>Dual CD68 and TRIB1</i>	222
8.4.3.2 <i>Mac-3</i>	222
APPENDIX V RAW DATA.....	224

List of Figures

Figure 1.1: Cellular Mediators of inflammation and immunity in obesity and associated pathological consequences.	3
Figure 1.2: Macrophage and adipocytes have overlapping signalling and sensing pathways that lead to common physiological outcomes.....	5
Figure 1.3: The origins and renewal of tissue macrophages.	7
Figure 1.4: Characteristics of the different macrophage phenotypes.	10
Figure 1.5: Overview of inflammatory signalling pathways and the role of TRIB1 in modulating these pathways.....	13
Figure 1.6: Protein domain organisation of TRIBs	18
Figure 1.7: The time line of atherosclerotic lesion development.	25
Figure 1.8: The molecular pathogenesis of atherosclerosis.....	28
Figure 1.9: Cholesterol metabolism.....	30
Figure 1.10: The role of TRIB1 in human diseases.....	37
Figure 1.11: Association of <i>TRIB1</i> region with plasma triglycerides and total cholesterol levels.	40
Figure 1.12: <i>De novo</i> lipogenesis and production of triglyceride in the liver and adipose tissue.....	42
Figure 1.13: Working model of cholesterol metabolism in macrophages and the formation of foam cells.....	50
Figure 2.1: Schematic of tissue specific <i>Trib1</i> transgene and principle of Cre-Lox Recombination.....	56
Figure 2.2: Schematic of Conditional <i>Trib1</i> allele and generation of <i>Trib1^{fl/fl} x Lyz^{MCre}</i>	58
Figure 3.1: Expression of <i>Trib1</i> in myeloid <i>Trib1</i> knockout (<i>Trib1^{floxed} x Lyz^{MCre}</i>) and <i>Trib1</i> transgenic (<i>ROSA26.Trib1 x Lyz^{MCre}</i>) mice.	72
Figure 3.2: <i>Trib1</i> transgenic and KO mice have normal tissue anatomy	74
Figure 3.3: Myeloid <i>Trib1</i> does not alter white blood cell counts.	76
Figure 3.4: Myeloid <i>Trib1</i> alters plasma cholesterol levels	78
Figure 3.5: Myeloid <i>Trib1</i> alters Kupffer cell phenotype.	82
Figure 3.6: <i>Trib1</i> expression modulates macrophage polarisation in BMDMs.	83
Figure 3.7: TRIB1 regulates macrophage polarisation via modulating <i>Trib1</i> regulates macrophage polarisation via modulating C/EBP and C/EBP β expression.	85

Figure 3.8: <i>TRIB1</i> expression is associated with overexpression of alternatively activated macrophages.....	88
Figure 3.9: Macrophage <i>TRIB1</i> controls IL-15 expression.....	90
Figure 3.10: Myeloid <i>Trib1</i> induces changes in hepatic lipids.....	91
Figure 3.11: Hepatic <i>TRIB1</i> is down regulated by inflammatory signals.....	93
Figure 3.12: Kupffer cell phenotype correlates with hepatic <i>Trib1</i> expression and hepatic lipid content.....	94
Figure 3.13: Working model of myeloid <i>Trib1</i> dependent regulation of plasma lipid homeostasis.....	102
Figure 4.1: Representative images of each fluorescent channel from the Leica AF6000 fluorescent microscope.....	108
Figure 4.2: Flow chart summarising the analysis of plaque macrophage phenotype <i>in situ</i> by immunohistochemistry.....	113
Figure 4.3: Plaque macrophages can be individually characterised by multi-colour immunohistochemistry and can be quantified by ImageJ.....	114
Figure 4.4: Representative images of simultaneous staining of murine plaque macrophages.....	116
Figure 4.5: Single marker staining reveals ApoE ^{-/-} plaque macrophages are more pro-inflammatory than LDLR ^{-/-}	117
Figure 4.6: Dual marker analysis ApoE ^{-/-} have an increased population of NOS2 positive/ARG1 negative plaque macrophages.....	120
Figure 4.7: Plaque macrophage phenotype correlates with plaque size and stability.....	123
Figure 4.8: The mechanism of PCSK9 clearance of LDLR.....	127
Figure 5.1: Schematic of bone marrow transplantation into ApoE ^{-/-} mice and induction of experimental atherosclerosis.....	136
Figure 5.2: Schematic illustration of tissues excised for examination of atherosclerosis.....	139
Figure 5.3: Quantification of <i>en face</i> Oil Red O staining in whole aorta.....	142
Figure 5.4: Anatomy of the mouse aortic sinus (root).....	144
Figure 5.5: <i>TRIB1</i> expression in human plaque macrophages.....	146
Figure 5.7: <i>Trib1</i> x <i>LyzMCre</i> → ApoE ^{-/-} have altered atherosclerosis burden in the aortic sinus.....	151
Figure 5.8: <i>Trib1</i> ^{Tg} → ApoE ^{-/-} mice have increased plaque macrophage infiltrate and presence of foamy cell macrophages.....	152
Figure 5.9: Scavenger receptor expression in <i>Trib1</i> transgenic BMDMs.....	155

Figure 5.10: <i>Trib1</i> ^{Tg} →ApoE ^{-/-} mice have increased abdominal and visceral adipose tissue.	157
Figure 5.11: <i>Trib1</i> ^{Tg} → ApoE ^{-/-} mice have altered plasma lipids.	159
Figure 5.12: Transgenic <i>Trib1</i> ApoE ^{-/-} mice have significantly more steatosis.	161
Figure 5.13: Adipocyte size is altered in <i>Trib1</i> → ApoE ^{-/-} mice.	163
Figure 5.14: : Levels of F4/80+ macrophages are unchanged in <i>Trib1</i> →ApoE ^{-/-} mice.	164
Figure 5.15: Regulation of OLR1 and SCARB-1 expression.	171
Figure 5.16: Proposed working model of local (atheroma) and systemic (adipose and liver) effects of <i>Trib1</i> expression in macrophages.	175
Figure 6.1: Myeloid TRIB1 has distinct roles in macrophage biology under normal physiological conditions and inflammation.	183

List of Tables

Table 1.1: Examples of tissue resident macrophages and their function.	8
Table 1.2: Phenotypic markers of macrophage subsets in humans and mice.	11
Table 1.3: TRIB1 interacting proteins	21
Table 1.4: Stages and progression of human atherosclerotic lesions.	26
Table 1.5: Physical properties of lipoprotein particles.	32
Table 1.6: Roles of PPAR- α , PPAR- γ and LXRs in lipid homeostasis and immune responses in macrophages.	45
Table 1.7: List of known scavenger receptors and their role in atherosclerosis.	48
Table 2.1: Primer sequences for gene expression assays.	62
Table 3.1: Genes found to be differentially regulated in <i>TRIB1</i> high vs. <i>TRIB1</i> low human MDMs.	87
Table 5.1: Outline of <i>Trib1</i> x <i>LyzMCre</i> → ApoE ^{-/-} bone marrow transplantation.	137
Table 5.2: Genes found to be differentially regulated in <i>TRIB1</i> high vs. <i>TRIB1</i> low human MDMs	153
Table 6.1: Summary of the effects of PPAR ligands on atherosclerosis.	181

List of Abbreviations

A	Adventitia
AAV	Adeno-associated virus serotype
ABC	ATP-binding cassette
ACAT-1	Acetyl co-enzyme A acyl transferase
ACC	Acetyl coenzyme A Carboxylase
AcLDL	Acetylated LDL
AD	Alzheimer's disease
AggLDL	Aggregated LDL
AKT (PKB)	Protein kinase B
ALT	Alanine transaminase
AML	Acute myeloid leukaemia
AP-1	Activator protein 1
ApoE	Apolipoprotein E
Arg	Arginase
ATMs	Adipose tissue macrophages
BM	Bone marrow
BMDMs	Bone marrow derived macrophages
BMT	Bone marrow transplant
C/EBP	CCAAT-enhancer binding protein
CARE	Cholesterol and Recurrent events
cDNA	Complementary DNA
CDP	Dendritic cell progenitor
CE	Cholesterol ester
CETP	Cholesterol ester transfer protein
CHIP	Chromatin immunoprecipitation
CHOP	C/EBP homologous protein
ChREBP	Carbohydrate responsive element binding protein
COP1	Constitutive photomorphogenic 1
COPD	Chronic obstructive pulmonary disease
COX	Cyclooxygenase
Cre	Cre recombinase
CRP	C-reactive protein
CSA	Cross-sectional area
CSF	Colony stimulating factor
CVD	Cardiovascular disease
CXCL	C-X-C motif chemokine ligand
DAB	3, 3'-Diaminobenzidine
DAMPs	Damage associated molecular patterns
DAPI	4',6-diamidino-2-phenylindole
DC	Dendritic cell
DMEM	Dulbecco's modified Eagle's Medium
DNA	Deoxyribonucleic acid
DNL	<i>De novo</i> lipogenesis
DS-AMKL	Down syndrome associated acute megakaryoblastic leukaemia
ER	Endoplasmic reticulum
ERK	Extra-cellular signal regulated kinase
EVG	Elastic van Gieson
FABP	Fatty acid binding protein

FASN	Fatty acid synthase
FBS	Neutral buffered formalin
FC	Fibrous cap
FCS	Foetal calf serum
FFA	Free fatty acids
FFPE	Formalin fixed paraffin embedded
GFP	Green fluorescent protein
GWAS	Genome wide association study
H	Human
H&E	Haematoxylin & Eosin
Hb	Haemoglobin
HBSS	Hank's Balanced Salt solution
HDL	High density lipoprotein
Hem	Haemorrhage
HFD	High fat diet
HMOX	Haem oxygenase
HRP	Horse radish peroxidase
Hs	Homo sapiens
HSI	Hue, Saturation and Intensity
HUVECs	Human umbilical vein endothelial cells
I	Intima
IC	Immune complex
IDL	Intermediate density lipoprotein
IFN	Interferon
IHC	Immunohistochemistry
IHD	Ischaemic heart disease
IKK	Inhibitor of I κ B
IL	Interleukin
IL1R1	Interleukin 1 receptor
IMT	Intima-media thickness
INOS	Inducible nitric oxide synthase
IRAK	Interleukin-1 receptor associated protein kinase
IRF-5	Interferon regulatory factor-5
IVC	Individual ventilated caging
I κ B	Inhibitor of κ B
JCML	Juvenile chronic myeloid leukaemia
JIP	JNK interacting protein
JNK	c-Jun N-terminal kinase
KCs	Kupffer cells
KO	Knockout
LAL	Lipoprotein lipase
LCAT	Lecithin cholesterol acyl transferase
LDL	Low density lipoprotein
LDLR	Low density lipoprotein receptor
LOX	Lectin-like oxidised low-density lipoprotein receptor
LPS	Lipopolysaccharide
LXR	Liver X Receptor
Lyz	Lysozyme

M	Media
Mm	Mouse
MAPK	Mitogen activated protein kinase
MARS	Monitored Atherosclerosis Regression Study
Mb	Mega base pairs
MCP	Monocyte chemo-attractant protein
MCSF	Macrophage colony stimulating factor
MDMs	Monocyte derived macrophages
MDP	Monocyte/macrophage cell progenitor
MI	Myocardial infarction
miRNA	micro-RNA
MKK	MAPK-Kinase
MMP	Matrix metalloproteinase
MMR	Macrophage mannose receptor
MPO	Myeloperoxidase
MPS	Mononuclear phagocyte system
mRNA	messenger RNA
MS	Multiple Sclerosis
MSB	Martius Scarlet Blue
MTT	Microsomal triglyceride transfer protein
NAFLD	Non-alcoholic fatty liver disease
NCEH	neutral cholesteryl ester hydrolase
NEFAs	Non-esterified fatty acids
NEMO	NF- κ B essential modifier
NF- κ B	Nuclear factor kappa-light-chain enhancer of activated B cells
NFE2L2	Nuclear factor, erythroid 2 like 2
NICE	National Institute for Health and Care Excellence
NMR	Nuclear magnetic resonance
NO	Nitric oxide
NPC	Niemann Pick type C
OLR	oxLDL receptor
ORO	Oil red O
oxLDL	Oxidised low density lipoprotein
PAMPs	Pathogen associated molecular patterns
PBS	Phosphate buffered saline
PCKS9	Proprotein convertase subtilisin/kexin type 9
PD	Parkinson's disease
PE	Phycoerythrin
PFA	Paraformaldehyde
PFA	Paraformaldehyde
PIL	Procedure individual license
PKB (AKT)	Protein kinase B
PL	Phospholipid
PPAR	Peroxisome proliferator-activated receptor
PPL	Procedure project license
PPRE	PPAR response element
PRRs	Pattern recognition receptor
qPCR	Real-time polymerase chain reaction
RNA	Ribonucleic acid
ROI	Region of interest

ROS	Reactive oxygen species
RPMI	Roswell Park Memorial Institute Medium
RT	Room temperature
RXR	Retinoid X receptor
SCARB/SR-B1	Scavenger receptor B1
SCD1	Stearoyl-coenzyme A
SDS	Sodium dodecyl sulphate
SEM	Standard error of the mean
Ser	Serine
S _f	Svedberg floatation rate
siRNA	Small (short) interfering RNA
SMCs	Smooth muscle cells
SNP	Single nucleotide polymorphism
SR	Scavenger receptor
SREBP	Sterol regulatory element binding protein
SREs	Sterol regulatory elements
STAT	Signal transducer and activator of transcription
TBST	Tris-buffered saline-Tween
Tg	Transgenic
TG	Triglyceride (triacylglycerol)
TGF	Transforming growth factor
T _H	T-helper cell
Thr	Threonine
TIMP	Tissue inhibitor of matrix metalloproteinase
TIR	Toll-interleukin-1 receptor
TLR	Toll-like receptor
TNF	Tumour necrosis factor
TRAF	TNF receptor activated factor
Trib	Tribbles
Trib1_LSKO	Tribbles 1 liver specific knockout
VLDL	Very low-density lipoprotein
WAT	White adipose tissue
WHO	World Health Organisation
WT	Wild type
Ym-1	Chitinase 3-like protein

Chapter 1. General Introduction

1.1 Inflammation

1.1.1 Inflammation: Classical vs. metabolic

Inflammation is an innate and protective immune mechanism that evolved to repair tissue injury and eliminate invading pathogens. Tissue injury results in the cellular release of cytosolic components known as damage-associated molecular patterns (DAMPs); likewise, an invading pathogen will express pathogen-associated molecular patterns (PAMPs) (Akira et al., 2006). Both of these specific patterns are recognised by either intracellular or surface pattern recognition receptors (PRRs), inducing an acute inflammatory signalling response, initiating the recruitment of immune cells to eliminate pathogens and promote tissue repair (Rock et al., 2011). Classical signs of inflammation include redness, swelling and pain. The inflammatory response is a tightly regulated process and by definition is a finite process that resolves when the insult is neutralised and the process of repair is initiated (Johnston et al., 2015). However, although inflammation is a protective immune response, the inflammatory reaction and subsequent repair process can themselves cause considerable harm to normal healthy tissues. Injury associated with inflammation therefore can be entirely typical and beneficial, prolonged (e.g. when infection is severe) or even inappropriate (e.g. when it is aimed towards self-antigens in auto-immune diseases or harmless environmental antigens in allergic syndromes) (Kumar et al., 2013).

Another type of inappropriate inflammation is metabolic inflammation. It is unlike classical inflammation and instead, it is chronically sustained without adequate resolution (McNelis and Olefsky, 2014). Chronic inflammation is thought to be the underlying pathological cause of a number of diseases with high morbidity and mortality including so-called immuno-metabolic diseases such as cardiovascular disease, obesity, diabetes and cancer (Brestoff and Artis, 2015). Studies over the past decade have identified close relationships between nutrient excess and imbalances in immunity and inflammation, particularly with the involvement of macrophages and

their change in inflammatory phenotype (Lumeng and Saltiel, 2011, McNelis and Olefsky, 2014). It is thought that increase in systemic low-grade inflammation due to obesity may affect the balance of metabolic homeostasis over time, favouring pro-inflammatory immune responses in metabolic tissues such as the liver, adipose, muscle and pancreas (and blood vessels) promoting metabolic associated syndromes such as diabetes, hypertension, atherosclerosis, and fatty liver disease.

Acute inflammation triggered by either injury or infection involves the coordinated recruitment of plasma and blood leukocytes (mainly neutrophils) to the affected site. This process called the 'leukocyte adhesion cascade' is a sequence of events that induces adhesion, activation and transmigration of leukocytes into extravascular tissue (Medzhitov, 2008). This acute inflammation is usually resolved by tissue-resident and recruited macrophages. However, if the acute inflammatory response fails to eliminate the pathogen or insult, the inflammatory response persists and neutrophils are replaced with macrophages and T cells.

1.1.2 Obesity is characterised by inflammation

The pro-inflammatory cytokine TNF- α was identified as the first molecular link between obesity and inflammation (Hotamisligil et al., 1993). TNF- α has been found to be over-expressed in the adipose tissue of obese humans, furthermore macrophages co-localise with adipocytes in obesity (Hotamisligil et al., 1995, Lumeng et al., 2007). Adipokines (cytokines produced by adipose tissue) released from adipocytes can modulate inflammatory signalling. Indeed, reduced levels of the hormone leptin (inhibits hunger) may be responsible for the immunosuppression associated with starvation as leptin administration reverses immunosuppression of mice starved for 48 hours (Faggioni et al., 2000).

1.1.3 Macrophages are central effector cells in inflammation

Macrophages are a highly functionally diverse and heterogeneous population of professional phagocytic cells with roles in development, homeostasis, tissue repair and immunity. Macrophages have three main roles in the inflammatory response; phagocytosis, antigen presentation and immunomodulation. They play a critical role in the initiation, maintenance and resolution of inflammation and show remarkable plasticity to respond and adapt to the tissue microenvironment to either initiate or

resolve inflammation. However, macrophages are also central to the initiation and maintenance of chronic inflammatory diseases including atherosclerosis, obesity and non-alcoholic fatty liver disease (NAFLD). **Figure 1.1** demonstrates the consequences of chronic inflammation and highlights the significant role of macrophages in metabolic associated diseases (Lumeng and Saltiel, 2011).

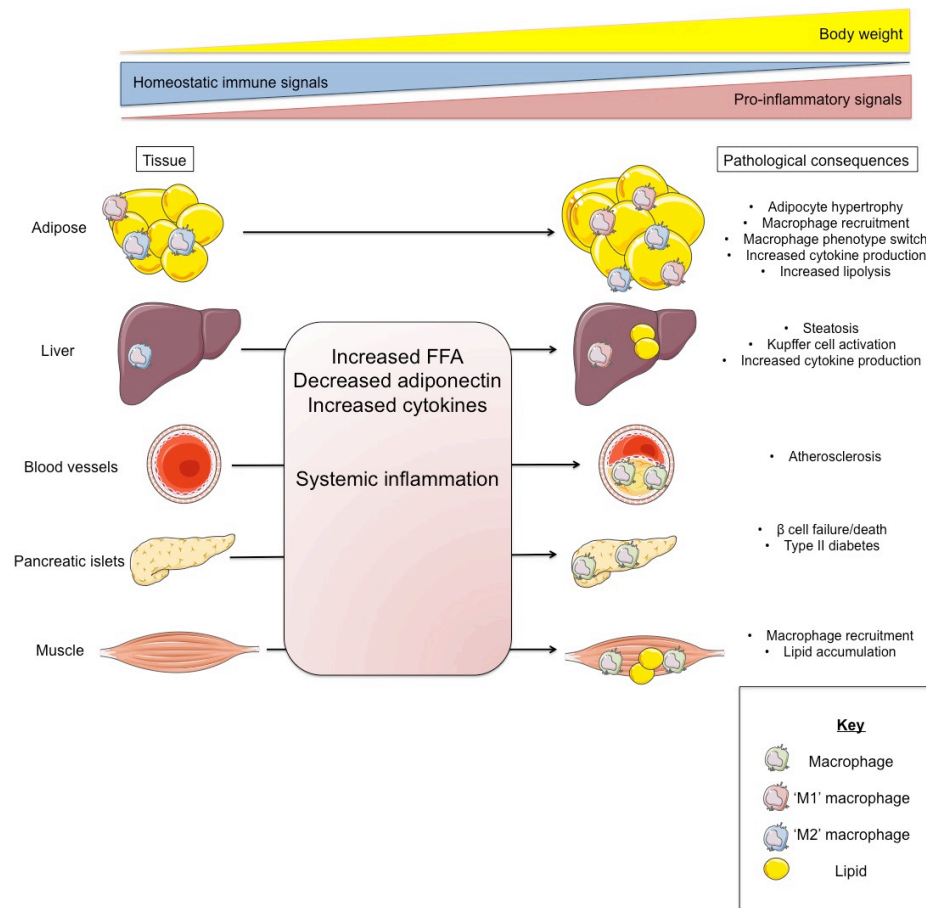


Figure 1.1: Cellular Mediators of inflammation and immunity in obesity and associated pathological consequences.

The systemic effects of obesity are linked to an imbalance in homeostatic and pro-inflammatory immune responses. Obesity initiates pro-inflammatory activation in the adipose tissue that dysregulate responses that maintain insulin and leptin sensitivity. Over time, macrophage recruitment in the adipose and phenotypic switch decrease adiponectin levels and increase the levels of free fatty acids (FFA) in the circulation. Increases in visceral adipose deposits in the liver, blood vessels, pancreas and muscle contribute to organ specific diseases and exacerbates systemic inflammation and insulin resistance accelerating the progression towards type II diabetes.

1.1.4 Macrophages and adipocytes have overlapping signalling pathways

The high level of cross talk between metabolism and inflammation is further emphasised by the overlapping biology and function of macrophages and

adipocytes. Gene expression between the two cells are highly similar, macrophages for example express many of the 'adipocyte' gene products for example FABP (fatty acid binding protein), aP2 and PPAR γ , whereas adipocytes also express many of the 'macrophage' associated proteins such as IL-6, MMPs and TNF- α (Wellen and Hotamisligil, 2005). Equally, the two cell types have overlapping functional properties; macrophages can uptake and store lipid to become macrophage foam cells in atherosclerosis. Pre-adipocytes under some conditions also have phagocytic and anti-microbial properties and are able to differentiate into macrophages (Charriere et al., 2003, Cousin et al., 1999). In the context of the immune response, macrophages secrete pro-inflammatory cytokines to initiate the immune response while adipocytes can secrete lipids that can modulate the inflammatory state or participate in the neutralisation of pathogens. Indeed, macrophages and adipocytes also share some of the same signalling pathways (e.g. PPARs, LXRs and NF- κ B that can lead to similar physiological outcomes whether this is initiated by inflammation, infection or nutrient excess (Wellen and Hotamisligil, 2005) (**Figure 1.2**). Therefore macrophages and adipocytes are likely both to contribute either alone or together in pro-inflammatory signalling induction in the context of obesity.

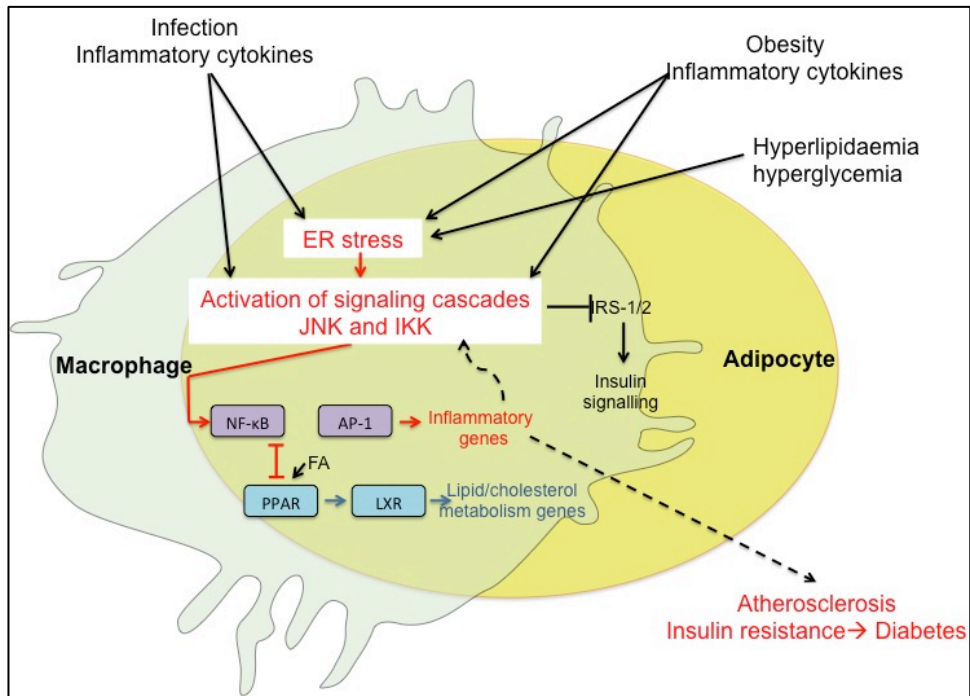


Figure 1.2: Macrophage and adipocytes have overlapping signalling and sensing pathways that lead to common physiological outcomes.

Infection, inflammatory cytokines and high levels of lipids all converge to initiate inflammatory signalling pathways including the kinases JNK and IKK. These pathways lead to the production of inflammatory mediators through NF- κ B and AP-1 transcription factors and the inhibition of insulin signalling through insulin receptor substrate (IRS). Opposing anti-inflammatory pathways are the transcription factors PPAR and LXR families which promote nutrient transport, metabolism and antagonise inflammatory activity. Cells must therefore strike a balance between metabolism and inflammation. In cases of over-nutrition however, the pathways required for nutrient utilisation (e.g. mitochondrial oxidative metabolism induces ROS and protein synthesis in the ER induces ER stress) can induce the inflammatory response leading to chronic inflammatory diseases such as atherosclerosis and diabetes.

1.2 Origins of Macrophages

Until recently, macrophages were defined as originating from the mononuclear phagocyte system (MPS); this rather rigid definition proposed all adult tissue macrophages were derived from bone marrow progenitor cells and circulating blood monocytes (Vanfurth et al., 1972). However lineage-tracing experiments have shown some populations of macrophages have embryonic origins such as microglia (macrophages of the brain and spinal cord) and are primarily derived from embryonic yolk sac progenitors (Ginhoux et al., 2010) and Langerhans cells (macrophages of the skin) originate from both the yolk sac and foetal liver (Hoeffel et al., 2012, Schulz et al., 2012). Additionally, other studies have shown that the major tissue-resident macrophage population in the skin, liver, spleen, liver and lung indeed derive from embryonic progenitors (defined as F4/80^{high}) (Schulz et al.,

2012). However, some tissue macrophages (F4/80^{low}) can also be derived from a separate self-renewing population in the bone marrow, where its progenitors give rise to circulating monocytes. Tissues such as the kidney and the lung have chimaeric populations of macrophages, which are derived from both the embryonic yolk sac and the bone marrow (Yona et al., 2013). However, it is not clear exactly what contribution embryonic derived macrophages vs. bone marrow derived macrophages have on the macrophage populations in the adult in terms of self-renewal. The rate and dependence of self-renewal of tissue macrophages from blood monocytes is highly tissue specific and its reliance varies from total independence such as in red pulp splenic macrophages and adult microglia, where blood monocytes are not relied on for renewal to total dependence in the gastro-intestinal tract, which contains a large population of resident macrophages all of which are continually replenished from blood monocytes (Wynn et al., 2013) (**Figure 1.3**). Interestingly, the origins of Kupffer cells (KCs) in the liver remain controversial and some have suggested they may originate from blood monocytes or intrahepatic precursors. A study by Klein et al. (2007) demonstrated two distinct populations of liver resident macrophages based on their sensitivity to radiation; radiosensitive population that were replaced by blood monocytes and those that were radio-resistant and long lived. More over, bone marrow transplantation experiments using CD45.1 and CD45.2 mice demonstrated that after 4 weeks, 46% of cells were of recipient origin, while the rest were bone marrow derived. Interestingly, administration of clodronate liposomes at 4 weeks post transplant, which causes tissue macrophage apoptosis, showed only 1% of cells were of recipient origin and the vast majority were repopulated by the bone marrow (Klein et al., 2007)

. These experiments highlight the complexity of macrophage populations whose renewal may be context specific.

Additionally, recent fate-mapping experiments have further explored the origins of tissue macrophages and have suggested these cells may originate from a different population entirely. Experiments by Perdiguero et al. (2015) showed that the majority of tissue macrophages in the liver (KCs), brain (microglia), epidermis (Langerhans cells) and lung (alveolar macrophages) originate independently of *Myb*; a transcription factor required for haematopoietic stem cells (HSCs). The group of cells are thought to generate erythro-myeloid progenitors (EMP) that are distinct from HSCs (Perdiguero et al., 2015).

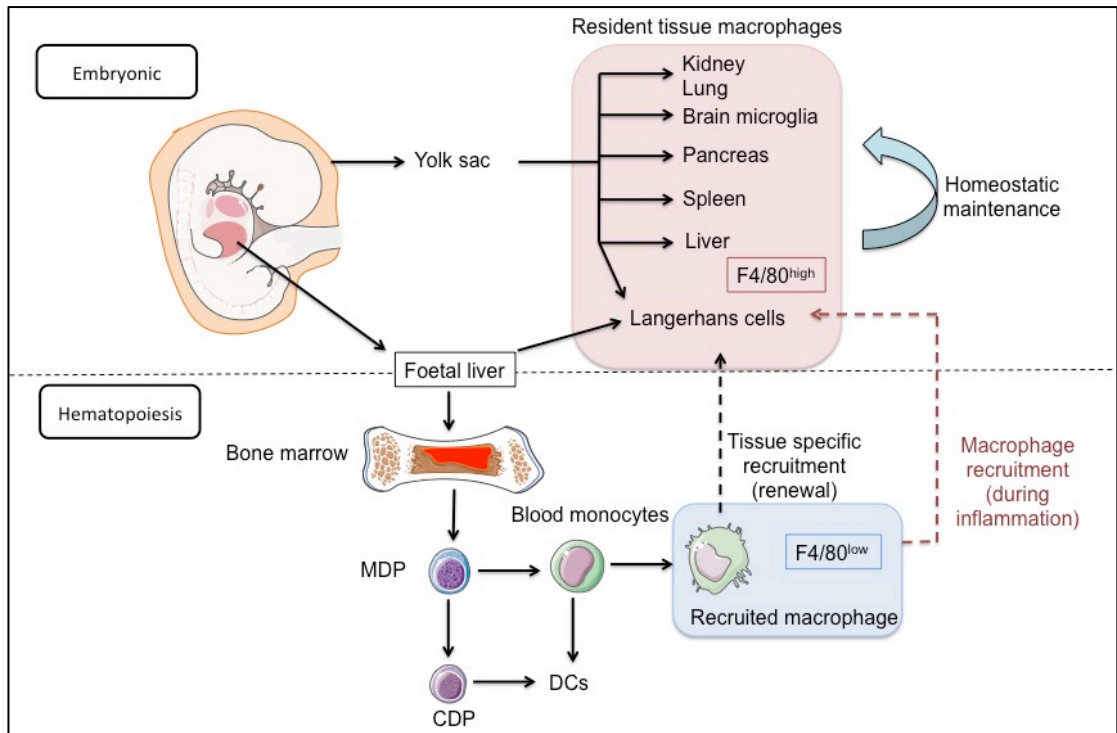


Figure 1.3: The origins and renewal of tissue macrophages.

Recent studies suggest macrophages in adults are derived from three distinct pools; the yolk sac, foetal liver and adult bone marrow. Macrophages derived in early embryogenesis from the yolk sac give rise tissue macrophages such as the Langerhans cells and brain microglia (known as $F4/80^{\text{high}}$ resident macrophages). The foetal liver contributes to the production of adult Langerhans cells, possibly through progenitor cells derived from the yolk sac. Haematopoiesis in the bone marrow gives rise to monocyte (and dendritic cell) progenitors and their progeny of macrophages ($F4/80^{\text{low}}$). Low level of homeostatic self-renewal is sufficient to maintain many tissue resident populations. Some tissue-resident populations require renewal from recruited monocyte-derived macrophages. The extent of recruitment is tissue specific. Note macrophage recruitment to tissues occurs during the innate and adaptive immune response during inflammation. The exact contribution of bone marrow-/ monocyte-derived macrophages to the resident tissue macrophage pool is unclear.

1.2.1 Role of tissue macrophages

Tissue resident macrophages are highly diverse both in terms of functional capabilities and transcriptional profiles owing to their discrete micro-anatomical niches and hence differing microenvironments (Wynn et al., 2013). **Table 1.1** describes the various examples and function of tissue resident macrophages. One such important (but not the only) role of tissue macrophages is that they act as immune sentinels to detect invading pathogens and are an important component of the innate and adaptive immune response. Tissue macrophages express both PAMPs and DAMPs to recognise invading pathogens or damaged cells, once recognition has occurred (through e.g. Toll-like receptors) they initiate a local inflammatory

response by promoting the influx of pro-inflammatory monocyte-derived macrophages (amongst other cells) to eliminate pathogens and promote tissue repair. However, some tissue resident macrophages also have additional metabolic roles. Liver tissue macrophages known as Kupffer cells (KCs) have roles in lipid metabolism, furthermore adipose tissue macrophages (ATMs) directly contribute to maintaining insulin sensitivity and have roles in adipogenesis. However, their activation and consequent promotion of chronic low-grade inflammation has major consequences in the context of metabolic disorders such as diseases of the liver and obesity.

Table 1.1: Examples of tissue resident macrophages and their function.

Adapted from Italiani and Boraschi (2014) and Davies et al. (2013).

Tissue resident macrophage	Tissue	Function	Role in disease
Adipose tissue macrophages (ATMs)	Adipose tissue	Metabolism, adipogenesis, adaptive thermogenesis	Obesity, insulin resistance
Kupffer cells	Liver	Toxin removal, lipid metabolism, erythrocyte clearance, clearance of debris	NAFLD
Alveolar macrophages	Lung	Surfactant clearance, immune surveillance for inhaled pathogens	Chronic obstructive pulmonary disease (COPD)
Monocytes	Blood	Surveillance	Initiation of atherosclerosis and plaque phenotype
Osteoclasts/ osteoblasts	Bone	Bone remodelling	Bone disease, bone cancer metastasis
Microglia	Brain	Brain development, immune surveillance	Neurotoxic (PD, MS, AD) and neuro-protective (ischemia, tissue injury, MS, AS)
Intestinal macrophages	Gut	Tolerance to microbiota, pathogen defence, intestinal homeostasis	Crohn's disease
Langerhans	Skin	Immune surveillance	
Marginal zone, red pulp	Spleen	Erythrocyte clearance, capture of microbes from blood	
Bone marrow	Bone marrow	Reservoir of monocytes, waste disposal	
Tumour-associated macrophages (TAMs)	Tumours		Cancer; inhibit and promote tumour development

1.2.2 Macrophage phenotype

The nature and definition of macrophage polarisation is the subject of on-going debate and has continually changed over time. Traditionally, macrophage activation has been classified into two groups with opposing phenotypes mimicking T-helper (T_H) cell nomenclature; Pro-inflammatory ‘M1’ or ‘classically’ activated macrophages vs. anti-inflammatory ‘M2’ or ‘alternatively’ activated macrophages. Classically activated macrophages are typically induced by T_H1 cytokines such as $IFN-\gamma$, $TNF-\alpha$ or bacterial lipopolysaccharide (LPS) and produce high levels of IL-12 and IL-23 and low levels of IL-10. They produce high levels of pro-inflammatory cytokines such as IL-6 and IL-1 β and serve to remove pathogens through for example, the generation of reactive oxygen species (ROS) (Verreck et al., 2004, Chinetti-Gbaguidi et al., 2015). Chronic activation of pro-inflammatory macrophages result in tissue damage as well as impairment of wound healing. Alternatively activated macrophages however have anti-inflammatory properties and produce high levels of anti-inflammatory cytokines such as IL-10 and IL-4 that promote the resolution of inflammation and wound healing (Chinetti-Gbaguidi et al., 2015). However the paradigm of ‘M1/M2’ macrophage classification fails to encompass the true heterogeneity of macrophages as cells of high functional plasticity that respond to specific micro-environments and instead should be considered as cells on a phenotypic spectrum rather than belonging to rigid classification sub-groups (Martinez and Gordon, 2014). To that end, additional macrophage subclasses of ‘M2’ macrophages have been characterised including ‘M2a’ (wound healing), ‘M2b’ and ‘M2c’ (regulatory) (Gordon, 2003). Moreover, emerging evidence has suggested other and distinct macrophage phenotypes (Mox, Mhem and M4) can be driven by complex microenvironments in the atherosclerotic plaque (Chinetti-Gbaguidi et al., 2015) and can influence not only structure but also the evolution and regression of atherosclerotic lesions which is of high clinical interest and will be discussed later in detail in **section 1.4**. As classification of macrophage phenotype is potentially complex, for the sake of clarity in particular to the role of TRIB1, I will largely generalise macrophages as either ‘M1’/ pro-inflammatory or ‘M2’/ anti-inflammatory. However it must be appreciated

macrophages are highly plastic with heterogeneous phenotypes. **Figure 1.4** shows the various macrophage subtypes that have been identified to date.

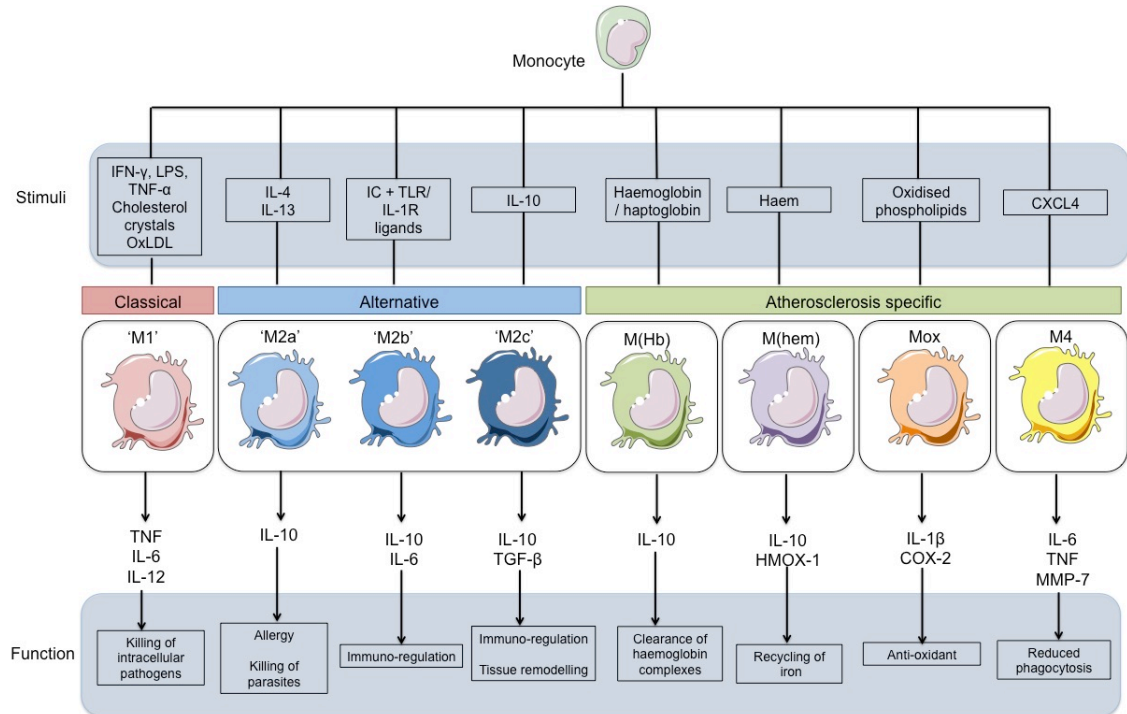


Figure 1.4: Characteristics of the different macrophage phenotypes.

Specific stimuli in the tissue drive monocyte differentiation towards different macrophage phenotypes. Stimuli along with secreted factors and function are described. Adapted from Chinetti-Gbaguidi et al. (2015) and Martinez and Gordon (2014). Abbreviations: IC, immune complexes; TLR, toll-like receptor; CXCL, C-X-C motif chemokine ligand.

1.2.3 Macrophage polarisation markers

Despite the identification of a number of macrophage subtypes, the simple classifications and assignment of phenotypic markers have mostly derived from *in vitro* studies and therefore may oversimplify complex macrophage phenotypes seen *in vivo*. Adding to the complexity, although the properties of each macrophage subtype are conserved between species, their markers are not. For example, the markers Arginase-1 and Ym-1 (chitinase 3-like protein) are specific for ‘M2’ macrophages in mice but not in humans. Some markers also appear to be specific for a given phenotype but others can also be shared across different subsets. Therefore careful consideration must be given to define macrophage phenotype particularly when translating findings from mice to human tissues and quantitative

rather than qualitative differences should be considered (Chinetti-Gbaguidi et al., 2015). **Table 1.2** outlines the different macrophage phenotypes and their markers in human and mice, most of which have been identified through *in vitro* studies and may not have been observed *in vivo*. Moreover, no single marker can distinctly identify a particular macrophage subtype.

Table 1.2: Phenotypic markers of macrophage subsets in humans and mice.

Phenotype	Traditional classification	Polarised by	Markers		Presence in atherosclerotic plaques?	References
			In human	In mice		
M1	Classically activated/ Pro-inflammatory	T _H 1 cytokines (IFN- γ , TNF- α , IL-1 β) or LPS	IL-1 β , TNF, IL-6, IL12, IL-23, CXCL9, CXCL10, CXCL11	IL-1 β , TNF, IL-6, IL12, IL-23, CXCL9, CXCL10, CXCL11, Arg-II, iNOS*	H, Mm	
M2a	Alternatively activated/ Anti-inflammatory	T _H 2 cytokines (IL-4, IL-13)	MMR, IL-1RA, factor XIIIa, CD200R, CCL18, stabilin-1, CD163	Arg-I, resistin-like α , Ym1, Ym2, MMGL, stabilin-1, CD163	H, Mm	
M2b	Alternatively activated/ Anti-inflammatory	Immune complexes or LPS	IL-10 ^{high} , IL-12 ^{low}	IL-10 ^{high} , IL-12 ^{low}	H, Mm	
M2c	Alternatively activated/ Anti-inflammatory	IL-10, TGF- β	MMR	Arg-I*	H, Mm	
M(Hb)	N/A	Haemoglobin-haptoglobin complexes	CD163, MMR	CD163, MMR	H	
M(Hem)	N/A	Haem	CD163, ATF-1	CD163, ATF-1	H, Mm	
Mox	N/A	Oxidised phospholipids	HO-1, sulfiredoxin-1, TR, NFE2L2	HO-1, sulfiredoxin-1, TR, NFE2L2	Mm	
M4	N/A	CXCL4	MMP-7, S100-A8, MMR	MMP-7, S100-A8, MMR	H	

*Only in mice. H, human; Mm, mouse.

1.3 Inflammatory signalling

The role of the inflammatory response as discussed is to combat infection and tissue injury whilst also promoting healing. Macrophages along with other innate immune cells function to initiate intracellular inflammatory signalling pathways that result in the release of factors (e.g. cytokines) that can promote several activities including recruitment of leukocytes. Indeed, cell signalling is a complex system of communication that coordinates the basic activities of cells and allows them to respond to their microenvironment appropriately and is fundamental to development, immunity, tissue repair and homeostasis.

1.3.2 Adipokines

Adipose tissue is also the source of many bioactive molecules known as adipokines that are implicated in both lipid metabolism and inflammation. Adipokines like cytokines can be either pro- or anti-inflammatory and include TNF- α , IL-6, leptin, adiponectin and free fatty acids (FFAs). Altered expression of adipokines through obesity or adipocyte dysregulation contributes to development and sustainment of chronic inflammatory diseases including insulin resistance and atherosclerosis (Molica et al., 2015).

1.3.3 Inflammatory signalling pathways

The TRIB family of pseudokinase proteins have been shown to modulate components of key inflammatory signalling pathways including MAPK, NF- κ B and toll/interleukin 1 (TLR) signalling (Hegedus et al., 2007, Hegedus et al., 2006). To understand the role of TRIBs therefore, key inflammatory signalling pathways are discussed below. **Figure 1.5** illustrates inflammatory signalling and known roles of TRIB1 in modulating these pathways, which will be discussed in the following sections.

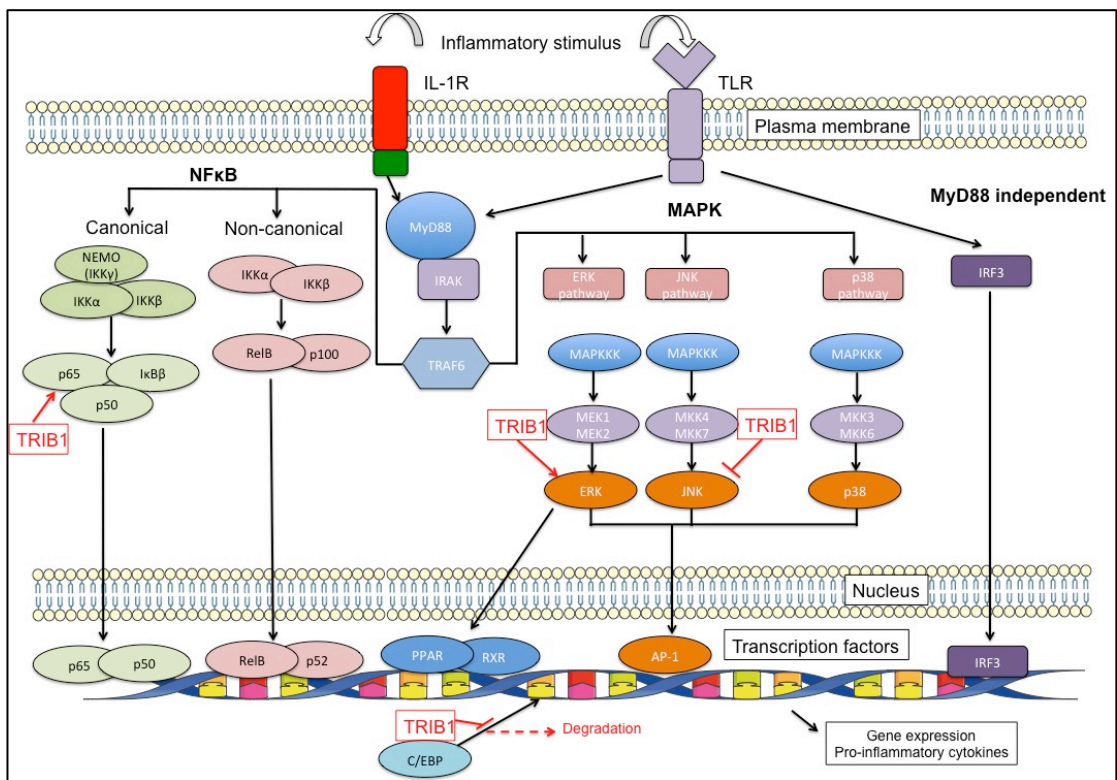


Figure 1.5: Overview of inflammatory signalling pathways and the role of TRIB1 in modulating these pathways.

Inflammatory stimuli initiate the signal transduction pathways where membrane associated events can activate down-stream components resulting in the activation of transcription factors and inducing a biological response. There are three elements of the MAPK pathway; the extracellular-signal-regulated kinase (ERK), JUN N-terminal kinase (JNK) and p38 pathways. The Toll-interleukin-1 receptor (TIR) is also activated by inflammatory stimulus and once activated recruits adaptor proteins such as MyD88 which associate with various IL-1R associated kinases (IRAK 1, 2, 4) and adaptor proteins such as TRAF6. TRAF6 can initiate cross talk to the MAPK pathway and activates the Nf κ B and IRF pathways. TRIB1 has shown to be an important regulator of these pathways. Among them, it has been shown that TRIB1 may regulate the Nf κ B pathway by enhancing I κ B α phosphorylation and therefore its degradation. It also regulates the MAPK pathway by interacting with MEK1 and enhancing the phosphorylation of ERK and also interacts with MKK4, a JNK activator inhibiting this pathway. Interestingly, TRIB1 can also regulate transcription factors such as C/EBP α by recruiting COP1, an E3 ligase which catalyses the ubiquitination of C/EBP α resulting in its degradation via the proteasome.

1.3.4 MAPK

Mitogen activated protein (MAP) kinase signalling involves multi-tiered pathways that are highly regulated and can be subdivided into three distinct pathways involving ERKs (extra-cellular signal-regulated kinases), JNKs (c-Jun N-terminal kinases) and p38 MAPKs. The ERK MAPKs are primarily activated by growth factors (mitogens), while JNK and p38 MAPKs are activated by environmental stimuli including stress and pro-inflammatory cytokines. Once MAPK are activated, a phospho-relay is initiated where each component is phosphorylated to activate one another. The pathways however are not mutually exclusive and a stimulus may activate more than one, which is cell type dependent, and may cooperate or antagonise one another. The pathways like NF- κ B converge to promote the binding of transcription factors on responsive genes and induce gene expression (Tedgui and Mallat, 2006).

1.3.5 NF- κ B

NF- κ B is one of the main signalling pathways that is initiated by pro-inflammatory cytokines. NF- κ B is a dimeric transcription factor formed by the hetero- or homodimerisation of proteins of the Rel family including p50, p52, p65 (Rel-A), c-Rel and RelB. In its inactive form NF- κ B is bound to inhibitor of κ B (I- κ B α/β). Localisation of the NF- κ B complex to the nucleus induces transcription of genes involved in a wide range of cellular processes including cell proliferation, survival, migration and immune responses such as the expression of pro-inflammatory cytokines and adhesion molecules. NF- κ B signalling can be divided into two pathways; the canonical pathway and the non-canonical pathway (Akira et al., 2001). Canonical NF- κ B is a rapid acting pathway that can induce gene expression in as little as 30 minutes after activation. This pathway mainly employs binding of the p65-p50 heterodimers to DNA. However, the much slower (~4 hours for gene expression changes) non-canonical pathway employs binding of RelB-p52 heterodimer for gene transcription. Signalling through the canonical pathway involves the activation of IKK (inhibitor of NF- κ B (I κ B) kinase). The IKK complex contains two kinases IKK1/IKK α and IKK2/IKK β and the regulatory protein NEMO (NF- κ B essential modifier/ IKK γ). The activation of IKK initiates phosphorylation of I κ B α/β , which is subsequently ubiquitinated leading to its degradation via the proteasome. The degradation of its inhibitor therefore allows the release of NF- κ B dimers from the cytoplasmic complex to translocate to the nucleus and inducing

transcription of genes with κ B binding sites including pro-inflammatory cytokines (Akira et al., 2001).

1.3.6 Toll-like receptor signalling

Traditionally, toll-like receptor (TLR) signalling is a mechanism by which the innate immunity can detect the invasion of microorganisms. TLRs can recognise PAMPs expressed by invading microbes, which induces specific gene expression activating the innate immune pathway including an inflammatory response. TLRs are a type of PRRs that can also recognise endogenous ligands as well as microbial ones to induce the inflammatory response. TLRs, together with interleukin 1 (IL-1) receptors, form a group of receptors termed the interleukin-1 receptor/ toll-like receptor super-family. Members of the super-family all contain an intracellular toll-IL receptor (TIR) domain that initiates the signalling cascade. TLRs are expressed differentially among immune cells and appear to respond to different stimuli (Akira et al., 2001).

As the cytoplasmic sequences of TLRs are similar to the IL-1R family, they also share components of the down-stream signalling pathway. Once activated, they recruit adaptor proteins such as MyD88 that links the IL-1R to various IL-1R associated protein kinases (IRAK) and adaptor proteins such as tumour necrosis factor (TNF) receptor activated factor 6 (TRAF6). Upon ligand binding and activation, IRAK becomes phosphorylated and subsequently disassociates from TRAF6. This results in the activation of JNK and p38 kinases of the MAPK pathway and NF- κ B. This pathway is known as the MyD88 dependent pathway. However the MyD88 independent pathway also exists and involves the activation of interferon (IFN) regulatory genes by the phosphorylation and nuclear translocation of interferon regulatory factors (IRF) (Akira et al., 2001).

1.3.7 PPAR signalling at the cross roads of inflammation and metabolism

The peroxisome proliferator-activated receptors (PPARs) are members of the nuclear receptor superfamily of ligand-inducible transcription factors that are key regulators of lipid metabolism, adipogenesis and metabolic homeostasis. Recent evidence also suggests these factors along with other nuclear regulators of cholesterol homeostasis (e.g. SREBP and LXR, discussed later in **section 1.7**) have

important roles in regulating inflammatory processes too. PPARs play major roles in signalling that is initiated from both the dietary intake of lipids and inflammation (Daynes and Jones, 2002). They also have anti-inflammatory properties in macrophages, where by they inhibit the expression of pro-inflammatory cytokines and promote alternative activation in macrophages (Tyagi et al., 2011). The PPARs are stimulated upon a wide range of ligand binding including lipid-derivatives such as fatty acids and metabolites as well as inflammatory events. Three isoforms of PPAR have been identified with distinct functions and tissue expression; PPAR α (NR1C1), PPAR β/δ (NR1C2) and PPAR γ (NR1C3). Each PPAR forms heterodimers with retinoid X receptor (RXR) and bind to genes with PPAR-responsive elements (PPREs). PPAR α is predominately expressed in the liver, heart and brown adipose tissue where it is a major activator of fatty acid oxidation. PPAR β/δ also functions as a major activator of fatty acid oxidation but it is expressed ubiquitously. PPAR γ is the most highly expressed in both white and brown adipose tissue where it is a master regulator of adipogenesis and lipid metabolism, however it is also expressed in macrophages and is involved in macrophage lipid metabolism and their inflammatory activation (Lee and Evans, 2002, Ahmadian et al., 2013). PPARs are able to modulate gene expression by transcriptional repression by modulating the activity of transcription factors such as NF- κ B, AP-1 and STATs. PPARs are phospho-proteins and activation depends on their phosphorylation state, which can be altered by regulation through the MAPK pathway, for example, ERK1 can directly phosphorylate PPAR γ rendering it inactive to bind to PPREs (Burns and Vanden Heuvel, 2007). It is important to note that inflammatory signalling occurs through a tightly regulated network and the individual pathways illustrated may be simultaneously active.

1.3.8 Tribbles proteins are modulators of inflammatory signalling

To maintain control of cellular signalling and homeostasis, mechanisms have evolved to regulate the spatio-temporal components of signalling pathways. These include mechanisms that involve catalytic proteins such as kinases, phosphatases and lipases but also regulatory proteins. Regulatory proteins do not have catalytic function but can activate components through physical association and have important roles in the localisation and assembly for signalling complexes such as receptor binding proteins like MyD88 or adaptor/scaffold proteins such as JIP (Akira

et al., 2001, Whitmarsh, 2006, Hegedus et al., 2006). These so-called scaffold proteins are able to directly bind or associate with proteins and activate or inhibit signalling cascades including MAPK function.

The Tribbles (TRIB) family of proteins however, are an unusual class of adaptor proteins. TRIBs possess a kinase-like domain but with no reported catalytic activity (pseudo-kinase) and also lack some protein-protein interaction domains characteristic of other kinases and scaffold/adaptor proteins (e.g SH2, SH3, PDZ) (**Figure 1.6**). The literature suggests that TRIBs belong to a functional niche where they balance the activation of a number of signalling pathways (Hegedus et al., 2007, Hegedus et al., 2006). Indeed TRIBs have been implicated in the regulation of MAPK, NF κ B and C/EBP in inflammation and in the development of human diseases including leukaemia, metabolic syndromes, lipid metabolism, insulin resistance and cardiovascular disease. Since the kinase-like domain is similar to MAPK, it has been suggested that TRIBs may compete with MAPK for binding sites, thereby regulating their action (Sung et al., 2007). It is interesting to note however that according to current knowledge, the effects of TRIBs may be cell type specific and 'normal' cell signalling occurs when TRIBs are expressed at 'normal' physiological levels. Altered TRIB levels are likely to lead to dysfunctional signalling and ultimately the development of disease (Johnston et al., 2015).

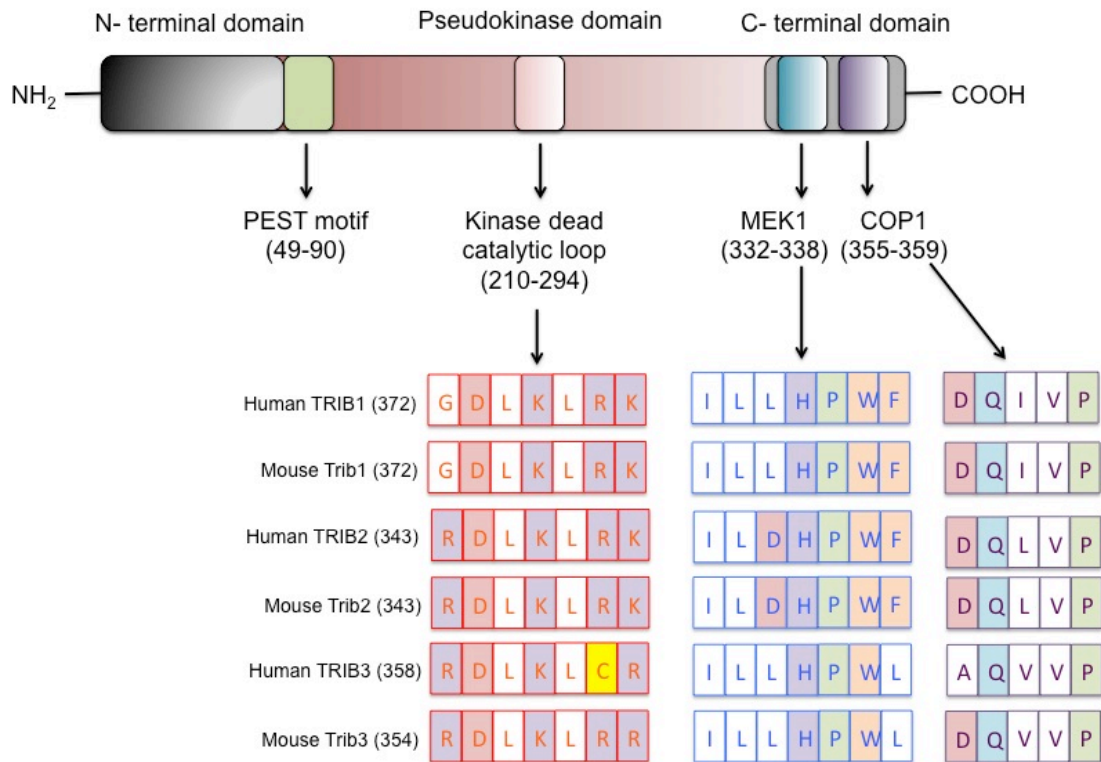


Figure 1.6: Protein domain organisation of TRIBs

TRIBs contain an N-terminal, pseudokinase and C-terminal domains. It contains four protein motifs; a putative PEST sequence (signal peptide for protein degradation), a kinase dead catalytic loop, a MEK1 binding and COP1 binding motif. The characteristic amino acid sequence for each TRIB and motif is shown along with its location. Conserved amino acids that are characteristic to the kinase superfamily are indicated with red background. The size of each protein (in amino acids) is indicated in brackets.

1.3.8.1 Origin of TRIBs

TRIB proteins were first discovered in *Drosophila* as a negative regulator of *string/Cdc25* where when over-expressed directly inhibited mitosis (Grosshans and Wieschaus, 2000). Simultaneously, TRIBs were found to promote the degradation of *string* via the proteasome pathway (Mata et al., 2000). Since then several orthologs in both invertebrates and vertebrates have been identified of which several interactions between signalling pathway components have been recognised.

1.3.8.2 Mammalian TRIBs

Currently, three highly conserved mammalian homologues of *Trib* genes exist; *Trib1/C8FW/SKIP1*, *Trib2/C5FW/SKIP2* and *Trib3/NIPK/SKIP3*. The TRIB family of proteins are characterised by a single central Ser/Thr kinase-like (pseudokinase)

domain, an N-terminal domain of 60-80 residues and a C-terminal domain of 35-40 residues. TRIBs also possess amino acid sequences that are characteristic motifs (**Figure 1.6**) of MEK-1 (MAPKK) and COP1 (ubiquitin ligase) binding, both of which are important in the interaction with MEK-1 in the MAPK pathway and in the proteasomal mediated degradation of C/EBP family of transcription factors, discussed in more detail in **section 1.3.8.6**. Despite the similar amino acid sequences between the TRIBs (TRIB1/TRIB2, 71.3%; TRIB1/TRIB3, 53.3%; TRIB2/TRIB3, 53.7%), each TRIB seems to have distinct roles in a particular tissue or cell type.

Studies have shown that in particular Trib3 is an important controller of fatty acid synthesis and is implicated in the development of type II diabetes and cardiovascular disease (Qi et al., 2006, Du et al., 2003, Prudente et al., 2005). More recently however, TRIB1 has become the subject of much focus as has been identified in GWAS for genes involved in hyperlipidaemia and as a risk for developing coronary heart disease (Edmondson et al., 2011, Varbo et al., 2011).

1.3.8.3 TRIB interacting proteins

As the subject of this research entirely focuses on the role of TRIB1, the main emphasis will be to highlight key studies that have demonstrated the function of TRIB1. However, important studies involving TRIB2 and TRIB3 are included for clarity and relevance, as recent studies have revealed TRIB3 in particular to have significant roles in immuno-metabolic diseases, that may or may not overlap with the role of Trib1.

A comprehensive list of TRIB1 interacting proteins is detailed in **Table 1.3**. However, some of the most relevant are discussed in detail below.

1.3.8.4 MAPK

Studies have shown specific interactions with MEK-1 (ERK activator) of the MAPK pathway and have implicated TRIB1 as an oncogene in the pathogenesis of acute myeloid leukaemia (AML) (Kiss-Toth et al., 2004, Yokoyama et al., 2010). Normally, MEK-1 phosphorylates ERK, which in turn promotes cell proliferation and suppresses apoptosis. The interaction between Trib and MEK-1 via the

ILLHPWF motif however enhances ERK phosphorylation and thus cell proliferation. In addition, TRIB1 also recruits the ubiquitin ligase COP1 to the transcription factor C/EBP α . Addition of ubiquitin to C/EBP α promotes its degradation via the proteasome. The post-translational suppression of C/EBP α promotes myeloid differentiation resulting in AML. Similarly, specific interactions with MEK1 and TRIB2 and TRIB3 have been demonstrated (Eder et al., 2008, Kiss-Toth et al., 2004).

Protein complementation assays have also shown TRIBS to interact with MKK4/SEK1 and MKK7 a JNK activator and implicated in the migration and proliferation of smooth muscle, a key characteristic of atherosclerosis progression (Sung, *et al* 2007).

Table 1.3: TRIB1 interacting proteins

Tissue/ cells	Protein	Mode of interaction	Biological consequences	Ref.
Macrophages	C/EBP α (COP1)	COP1 via the C-terminal motif, proteasomal degradation of C/EBP α	Critical for M2- macrophage polarisation Over-expression: AML (Acute myeloid leukaemia)	Satoh et al. (2013); Yokoyama et al. (2010)
Hepatocytes	C/EBP α	Regulation of lipogenesis genes via C/EBP α by post transcriptional regulation	Deficiency: increases plasma triglyceride and cholesterol by reducing VLDL production Over-expression: decreases plasma triglyceride and cholesterol by reducing VLDL production	Burkhardt et al. (2010), Bauer et al. (2015)
	ERK (MEK1)	MEK1 via C-terminal motif, enhances ERK phosphorylation	Enhances phosphorylation, promotes cell proliferation; AML	Yokoyama et al. (2010), Kiss-Toth et al. (2004)
	JNK (MKK4)	Via C-terminal domain	Suppression of vascular smooth muscle migration	Sung et al. (2007)
RAW 267.4 cells (murine monocyte/macrophage cell line)	Pro-inflammatory cytokines	Inhibits IL-6 and IL-12 induction	Suppression of inflammation	Sung et al. (2012)
	C/EBP β	Via MEK1 binding domain	Regulation of lipogenesis genes	Ishizuka et al. (2014)
	NF κ B	RelA subunit	Adipocyte inflammation	Ostertag et al. (2010)

1.3.8.5 Transcription factors relevant to TRIB1 signalling

1.3.8.6 C/EBP

As discussed, TRIBs negatively regulate the C/EBP family of transcription factors. Studies by Keeshan et al. (2006) demonstrated over-expression of TRIB2 reduced C/EBP α protein expression in a proteasome-dependent manner resulting in myeloid differentiation. Similarly, TRIB2 also increases the degradation of C/EBP β ,

suppressing adipocyte differentiation. Furthermore, *Trib1* knockout mice show an up-regulation of C/EBP β (Naiki et al., 2007, Yamamoto et al., 2007). In a recent study, Bauer et al. (2015) demonstrated that TRIB1 regulates hepatic lipogenesis through post-transcriptional regulation of C/EBP α , a major regulator of hepatic lipogenesis genes. They propose that not only is TRIB1 a regulator of C/EBP α , C/EBP α also strongly promotes the transcription of TRIB1 suggesting they are both part of a regulatory feedback loop. Interestingly, TRIB3 interacts with C/EBP homologous protein (CHOP). CHOP regulates the expression of genes in both an inhibitory and activating manner. It inhibits the binding of C/EBP members to target genes and also activates genes with CHOP-C/EBP binding motifs, over-expression of TRIB3 suppresses the transcriptional activity of CHOP, suggesting TRIB3 may also be involved in a regulatory loop with C/EBPs (Ohoka, *et al* 2005).

1.3.8.5 NF- κ B

TRIB1 also binds to the RelA/p65 subunit of NF- κ B acting as a nuclear transcriptional co-activator of NF- κ B signalling, thereby promoting the induction of pro-inflammatory cytokines. Indeed, haplo-insufficiency of TRIB1 protects mice against diet induced obesity (Ostertag et al., 2010). Additionally, TRIB2 also binds RelA/p65 but is a negative regulator by inhibiting its phosphorylation and induction of NF- κ B signalling (Wu et al., 2003).

1.4 Atherosclerosis

The survival of multi-cellular organisms depends on the ability to fight infection, heal the damage and the ability to store energy to use when nutrients are deprived or when high energy is needed. Therefore metabolic and immune pathways have evolved to be closely linked and interdependent. Under normal conditions, the close relationship of metabolism and immunity is beneficial, however the balance can be disrupted either through starvation and nutrient deprivation at one end or through obesity and nutrient excess at the other. Whatever the direction of balance shift, both can have detrimental consequences. This is best exemplified by high rates of infection in areas of widespread famine and by the high incidence of obesity in modern times that has increased complications that are associated with immunity

and metabolism such as obesity-linked diseases including diabetes, fatty liver disease and atherosclerosis (Wellen and Hotamisligil, 2005).

1.4.1 Atherosclerosis is a chronic inflammatory disease of the vessel wall

Cardiovascular diseases (CVDs) are the number one cause of death globally. With an estimated 17.5 million people dying from CVDs in 2012, CVDs represent 31% of all deaths (W.H.O, 2016). Atherosclerosis is the main cause of CVDs where it occurs mainly in large and medium sized elastic arteries. Macrophage accumulation within the vessel wall is a classical hallmark of atherosclerosis. The recruitment and retention of these cells at early stages of atheroma development leads to sustained inflammatory response and subsequent lesion formation. Macrophages are not only important in the initial lesion development but are central to lesion progression and have postulated roles in plaque stability and rupture, the main cause of cardiovascular associated events such as myocardial infarction (MI) and stroke. **Figure 1.7** and **Table 1.4** Shows the stages of atherosclerotic lesion development from early foam cell infiltrate to lesion rupture (Libby et al., 2011).

1.4.2 The pathogenesis of atherosclerosis

Atherosclerosis is a chronic inflammatory disease characterised by thickening of the artery wall caused by an accumulation of lipids, cholesterol and calcium. The principal risk factor for atherosclerosis is high plasma concentrations of cholesterol, particularly concentrations of low-density lipoprotein (LDL) cholesterol. However despite increasing public knowledge, lifestyle changes and pharmacological interventions, CVDs still remain the leading cause of death (Hansson, 2005, Ross, 1999).

Atherosclerosis is a highly complex inflammatory disease involving the interplay of many cell types. In principle, high levels of cholesterol (hypercholesterolaemia) and altered patterns of blood flow cause local activation of the artery endothelium. Activation of the endothelium promotes LDL retention (**Figure 1.8A**) and simultaneously promotes the recruitment of circulating monocytes by up-regulating adhesion molecules on the surface of the endothelium in a leukocyte adhesion cascade (Moore et al., 2013). Chemokines such as CC-chemokine ligand 5 (CCL5)

and CXC-chemokine ligand 1 (CXCL1) on endothelial cells regulate the capture and rolling of leukocytes by expression of chemokine receptors on the surface of leukocytes. Monocytes transmigrate through the endothelium and can enter the developing plaque (Moore et al., 2013) (**Figure 1.8B**). Oxidative and enzymatic oxidation of LDLs by differentiated monocytes causes the release of inflammatory mediators consequently activating the endothelium again increasing cell surface adhesion molecule expression thereby recruiting more inflammatory cells, causing a continual cycle of inflammation. (**Figure 1.8C**). Endothelial activation also causes platelet aggregation; this process eventually leads to the development of an atherosclerotic lesion.

1.4.3 Atherosclerotic lesions

Atherosclerotic lesions or atheromas are characterised by an asymmetric focal thickening of the intima (the most inner layer of the artery). Atheromas are mostly composed of macrophages, foam cells (lipid laden macrophages), cellular debris, lipids, vascular endothelial cells, smooth muscle cells and fibrous and connective tissue. Foam cells and extracellular lipid droplets form a core region capped by a smooth muscle layer and a collagen rich matrix. An infarction occurs when the atheroma progresses to restrict blood flow through the artery. It has been thought previously that luminal narrowing due to increased smooth muscle growth was the cause of infarction but it is now thought that plaque activation and rupture is the main cause resulting in the development of an obstructing thrombus on the surface of the plaque (Hansson, 2005). Lesions however are not randomly distributed throughout the vasculature but instead tend to form at curvatures and branch points of arteries of which are the subject of much research. At branch points, laminar flow within the artery is disturbed causing the normally quiescent endothelium cells to become activated. The activation leads to increased cell permeability to circulating lipoproteins to accumulate and recruit circulating monocytes to the endothelium thereby initiating the inflammatory process (Traub and Berk, 1998).

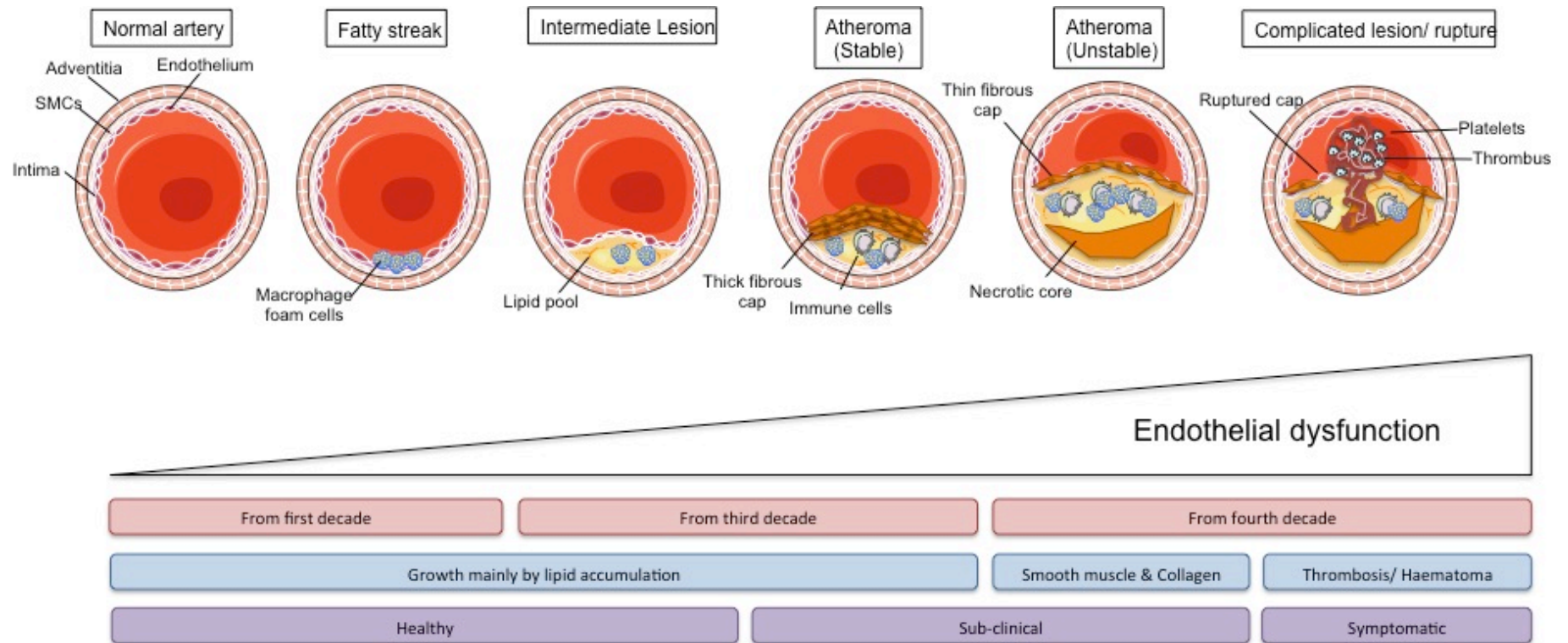


Figure 1.7: The time line of atherosclerotic lesion development.

Injury to the vessel wall caused by a number of factors including elevated levels of circulating LDL causes endothelial cell activation. Local retention of LDL and subsequent infiltrate of inflammatory cells drives macrophage foam cell formation known as a fatty streak. A chronic cycle of inflammation in the vessel wall drives atheroma formation. Stable atheromas, characterised by a thick fibrous cap of smooth muscle cells are clinically silent. However progression to unstable atheromas characterised by a weakened thin fibrous cap and necrotic core full of dead inflammatory cells are prone to rupture. Finally, a complicated/ ruptured lesion occurs when there is a break in the fibrous cap, contact between cells of the lesion and the circulating blood stream triggers the coagulation cascade resulting in thrombus formation, the cause of CVD associated events such as MI and stroke which can be fatal. Figure adapted from Libby et al. (2011) and Pepine (1998).

Table 1.4: Stages and progression of human atherosclerotic lesions.

Human atherosclerotic lesions progress from type I (initial lesion) to type VI (complicated lesion) that are associated with clinical events. The table illustrates the main histological characteristics between each type and the associated cellular changes and clinical events. Lesion progression is further illustrated by the flow diagram. The loop between types V and VI indicates how lesions increase in thickness when thrombotic deposits form on the surface (Stary et al., 1995)

Nomenclature	Main histology	Sequence of progression	Main growth mechanisms	Earliest onset	Clinical correlation	
Type I (Initial lesion)	Isolated macrophage foam cells	<pre> graph TD I((I)) --> II((II)) II --> III((III)) III --> IV((IV)) IV --> V((V)) V --> VI((VI)) VI --> V </pre>	Growth mainly by lipid accumulation	From first decade	Clinically silent	
Type II (fatty streak) lesion	Mainly intracellular lipid accumulation		From third decade			
Type III (intermediate) lesion	Type II changes & small extracellular			Accelerated smooth muscle and collagen increase	From fourth decade	Clinically silent or overt
Type IV (atheroma) lesions	Type II changes & core of extracellular lipid					
Type V (fibro-atheroma) lesion	Lipid core & fibrotic layer or multiple lipid cores & fibrotic layers or mainly calcific or mainly fibrotic			Thrombosis, haematoma		
Type VI (complicated) lesions	Surface defect; haematoma-haemorrhage, thrombus					

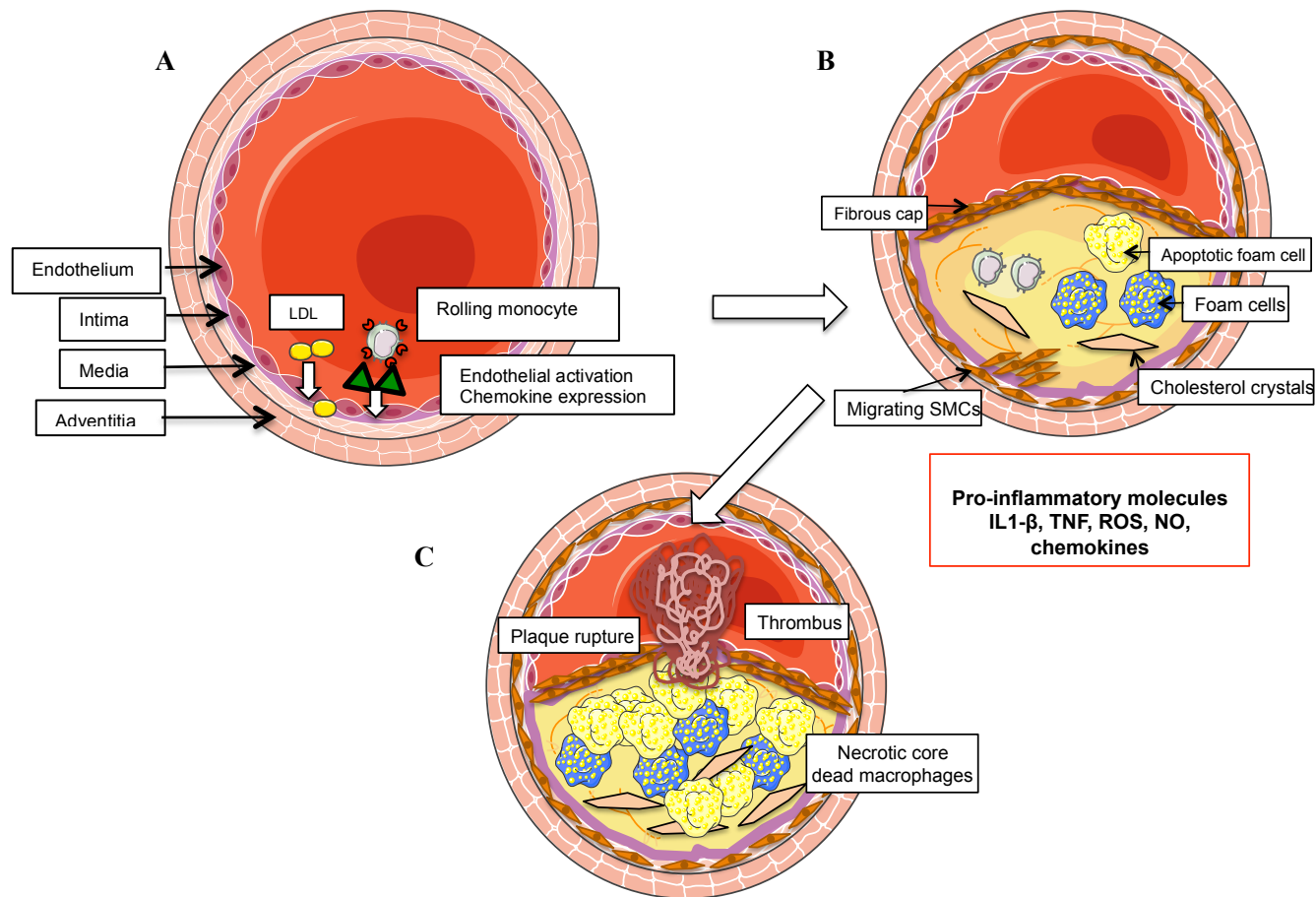


Figure 1.8: The molecular pathogenesis of atherosclerosis.

The normal artery contains three layers. The inner layer; tunica intima is lined by a monolayer of endothelial cells that is in contact with blood (lumen) and in the human contains some SMCs. The middle layer; tunica media contains a vast SMC layer containing layers of elastic lamina. The outer layer; tunica adventitia contains mast cells, nerve endings and microvessels. **(A)** In the early stages of atherogenesis, the endothelium is activated by excess LDL (hypercholesterolaemia) in the blood infiltrates the artery wall and is retained in the intima. Endothelial activation causes upregulation of adhesion molecules (CCL5, CXCL1) on the surface thereby recruiting circulating monocytes and directed migration into the intima. **(B)** Monocytes differentiate into mature macrophages and phagocytose lipids. Enzymatic modification of LDL results in oxLDL (oxidative LDL). If oxLDL cannot be mobilised, it accumulates as cytosolic droplets and macrophages eventually evolve and progress into lipid laden foam cells. During this process macrophages release inflammatory mediators thereby attracting more inflammatory cells to the plaque. Apoptotic and dead macrophages release their contents and initiate the formation of a necrotic core. Plaque progression involves the migration of SMCs from the media into the intima and resident intimal SMCs begin to proliferate and synthesise matrix molecules such as collagen, elastic and proteoglycans. **(C)** Both SMCs and macrophages continue to die and apoptose and extracellular lipid accumulates in the centre of the plaque (necrotic core). Thrombosis the ultimate complication of atherosclerosis occurs when the plaque ruptures due to increased necrotic core formation and weakening fibrous cap. Weakening of the cap results in plaque cells being exposed to circulating platelets and consequently triggering the coagulation cascade and thrombus formation affecting blood flow resulting in cardiovascular events and complications. . Figure and legend adapted from Hansson et al (2005) and Libby et al (2011).

1.5 The importance of lipid homeostasis in inflammatory disease

1.5.1 Elevated lipids are risk factors to the development of chronic inflammatory diseases

Excessive supply of energy-rich nutrients (particularly lipids and carbohydrates) is sufficient to induce insulin resistance and elevated plasma fatty acids are enough to activate a pro-inflammatory response in the liver (Boden et al., 2005). Lipids (and products of their metabolism) can also induce cellular damage through oxidative stress. Indeed, elevated plasma free fatty acids can directly bind TLR4 (LPS recognition) and initiate a pro-inflammatory response. Lipids therefore can coordinate and regulate metabolic, innate immunity and inflammation and are a significant risk factor in not only developing but the maintenance of chronic inflammatory diseases (Wymann and Schneider, 2008). **Figure 1.9** illustrates the process of cholesterol metabolism.

1.5.2 Chronic inflammatory diseases are associated with lipid and lipoprotein abnormalities

Not only do lipids increase chronic inflammation, infectious disease or chronic inflammation also induce alterations in lipid metabolism that is thought to initially help dampen inflammation or fight infection, however if chronically sustained could lead to increased risk of CVD. Several studies have demonstrated an increased risk of CVD in patients with chronic inflammatory diseases including rheumatoid arthritis (50% increased risk) (Avina-Zubieta et al., 2008), systemic lupus erythematosus (50x increased risk) (Manzi et al., 1997) and psoriasis (3x increased risk) (Samarasekera et al., 2013).

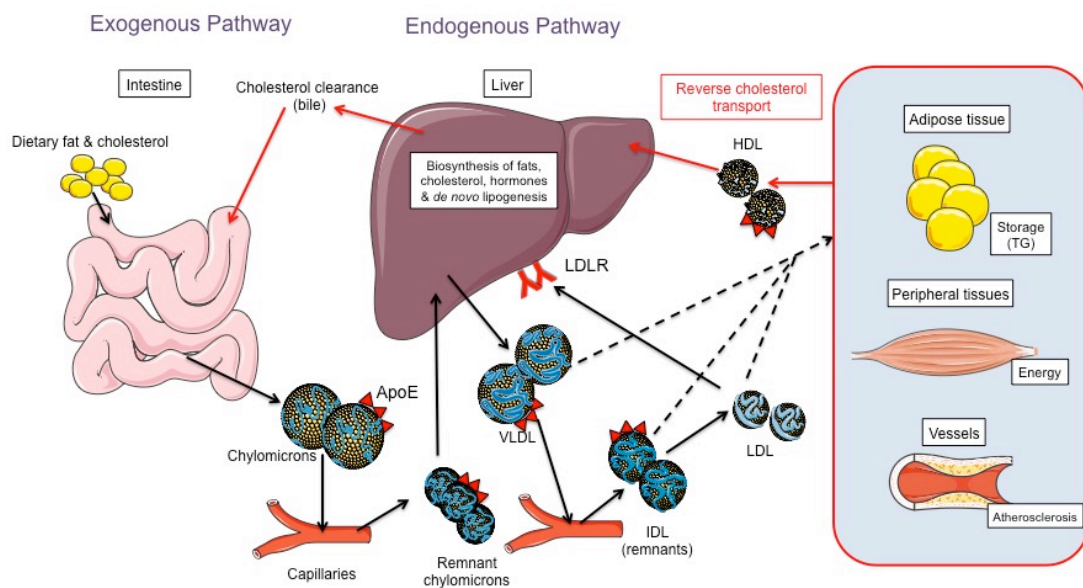


Figure 1.9: Cholesterol metabolism.

Lipid metabolism and transport occurs via lipoproteins. Lipoproteins are complex aggregates of lipids and proteins that enable the transport of lipids in the bloodstream. There are five types of lipoproteins involved with the transport of cholesterol in the body including chylomicrons, VLDL (very-low density lipoprotein), IDL (intermediate density lipoprotein), LDL (low density lipoprotein) and HDL (high density lipoprotein). Cholesterol transport occurs via two pathways; the exogenous and the endogenous pathways. The exogenous ('outside cholesterol') pathway begins as dietary fats and cholesterol are mobilised from the intestines into nascent chylomicrons where they adhere to the inner surface of capillaries of skeletal and adipose tissue. The fats inside (not cholesterol) are hydrolysed by lipoprotein lipase freeing fatty acids and monoacylglycerol. The resulting particles are termed chylomicron remnants that contain cholesterol. The remnants re-enter the circulation and are taken up by the liver thereby commencing the endogenous pathway ('inside cholesterol'). The liver synthesises VLDLs and like chylomicrons are hydrolysed by lipoprotein lipase, repeating the cycle. The remnants of VLDL found in the circulation are termed IDL and LDL particles. This process involves the sequential removal of all proteins (except ApoB-100) from their surfaces and esterification of most of the cholesterol present by lecithin cholesterol acyl transferase (LCAT). Exogenous cholesterol (in the form of LDL) can be taken up by the liver where it is used in the biosynthesis of fats and cholesterol and hormone synthesis. VLDL, IDL and LDL particles can also deposit in various tissues for to be used as an energy source (peripheral tissues) or storage as triglyceride (adipose tissue), excess lipid is also deposited in the vessel wall initiating atherosclerosis. HDL remove cholesterol from cells and tissues of the body and transports it to the liver, this is termed 'reverse cholesterol transport' (red arrows). Nascent HDL particles are assembled in the liver from other degraded lipoproteins where they take up cholesterol from peripheral tissues to form mature HDL particles that take cholesterol back to the liver. The liver either uses cholesterol for further biosynthesis of fats and cholesterol or clears cholesterol in the bile. Atherosclerosis occurs in ApoE null and LDLR null mice due to them being unable to uptake dietary cholesterol in the liver and remove it from tissues, consequently high cholesterol levels remain in the plasma inducing atherosclerosis. ApoE is a class of lipoprotein present on chylomicrons, VLDLs and HDLs. ApoE acts as a ligand for apolipoprotein receptors present in the liver that mediates clearance of these particles. Amongst the receptors that recognises apolipoproteins including ApoE is the LDL receptor.

1.5.3 Lipoproteins and the risk of cardiovascular disease

Lipids have a central role in the pathogenesis of cardiovascular disease, especially in the initiation and progression of the developing plaque. Epidemiological studies have implicated the levels of total cholesterol as a risk factor of coronary heart

disease. However total cholesterol does not accurately predict risk of disease due to all lipoprotein particles being included in the measurement including the potentially atherogenic VLDL, IDL and LDL particles and anti-atherogenic particles (HDL). To this end, LDL measurements have become the gold standard measurement in both the prediction of future coronary events as well as the target of therapeutics to reduce cardiovascular disease risk.

1.5.4 Lipoprotein particles

As lipids are inherently insoluble in water and have to be transported in the blood, almost all lipids found in the blood (except for a small percentage of free fatty acids associated with albumin) are found in lipoproteins- arrangements of lipid and proteins. Lipoproteins are a heterogeneous spectrum of particles that differ in size, density, lipid and apo-lipoprotein composition. Since the first attempt of separating lipoprotein sub-fractions based on size using ultracentrifugation, attempts have been made to investigate which sub-fractions provide the most accurate risk of predicting cardiovascular disease. Lipoprotein particles are defined based on their ultracentrifugation flotation rates in high salt solutions known as the Svedberg flotation rate (S_f). Most recent techniques have focused used nuclear magnetic resonance (NMR) and ion mobility with quantitative measurements of size fractions. Using NMR typically involves de-convolution of magnetic resonance signal from plasma into components corresponding to lipoproteins of various sizes. However, ion mobility procedure is based on physical separation and counting of individual ionised lipoprotein particles whose mobility in an electric field are based on size (Otvos et al., 1992, Caulfield et al., 2008). Since then several subclasses of the major lipoprotein particles; LDL, IDL, VLDL and HDL have been identified (**Table 1.5**).

Table 1.5: Physical properties of lipoprotein particles.

Adapted from Berneis and Krauss (2002).

Lipo-protein	Subclass	Floatation coefficient (S _f)	Floatation coefficient (F _{1,2}) (HDL only)	Diameter (Å)	% Protein	Major Lipids	Apoproteins
VLDL	VLDL-1	60-400		330-700	5-10	TG	B-100, C, E
	VLDL-2	20-60		300-330		PL CE	
IDL	IDL 1	12-20		285-300	15-20	CE	B-100, C, E
	IDL 2	10-16		272-285		TG PL	
LDL	LDL-I	7-12		272-285	20-25	CE PL	B-100
	LDL-II	5-7		256-272			
	LDL-III	3-5		242-256			
	LDL-IV	0-3		220-242			
HDL	HDL1		9-20	~120	40-55	PL CE	A, C, D, E
	HDL2		3.5-9	103-104			
	HDL3		0-3.5	73-99			

Abbreviations: CE, cholesterol ester; TG, triacylglycerol (triglycerides); PL, phospholipid

Elevated levels of LDL are associated with more than three-fold increase risk in coronary artery disease. This has been demonstrated in several case-control studies of MI and coronary heart disease (reviewed Berneis and Krauss (2002)) and therapeutic interventions (e.g. statins) that lower plasma LDL also reduce the risk of cardiovascular diseases. Despite LDL cholesterol remaining the primary target of therapeutics that reduce the risk of cardiovascular disease, in some patients, despite long term statin use, there is still a considerable residual risk of cardiovascular disease, suggesting that treatments to lower LDL levels even further could provide

clinical benefit to these patients (Libby, 2005). Interestingly, it has also been recognised that heterogeneity of LDL particles and particles other than LDL itself (including oxLDL, VLDL and lipoproteins) may contribute to the pathogenesis of atherosclerosis.

1.5.4.1 OxLDL

Oxidative stress, particularly oxidised LDL may also induce atherosclerosis. It is well known the oxidation of LDL particles by plaque macrophages and subsequent formation into foam cells is a key step in the initiation and progression of atheroma development (**Figure 1.8**). However, it has also been suggested circulating oxLDL may also induce atherosclerosis. oxLDL along with age, sex, HDL cholesterol levels, hypertension, smoking and diabetes is included in the global measurements to identify individuals with an increased risk of CVDs. A study published by Hulthe and Fagerberg (2002) showed circulating oxLDL is associated with sub-clinical atherosclerosis (clinically silent disease but with atherosclerotic changes in the arteries) and levels of inflammatory markers such as C-reactive protein, IL-6 and TNF- α .

1.5.4.2 VLDLs

Population based meta-analysis have indicated elevated levels of triglyceride (hypertriglyceridaemia) to be an independent risk factor for the development of cardiovascular disease (Cullen, 2000). However, rather than being atherogenic themselves, elevated triglycerides may in fact serve as a marker for increases in triglyceride-rich remnant lipoproteins. It is thought that these particles may be involved in atherosclerosis development (Carmena et al., 2004).

Studies have suggested there is an inverse relationship between the size of lipoprotein particle and their capacity to cross the endothelium into the arterial intima. Chylomicrons and large VLDL particles (S_f 60-400) are thought not to be able to cross into the arterial wall. However, smaller particles such as small VLDLs (S_f 20-60) and IDLs (S_f 12-20) can cross the endothelial barrier into the arterial wall, and are thought to be highly atherogenic (Carmena et al., 2004).

There are several published studies that have suggested small VLDLs (and IDLs) may be involved in both the pathogenesis of atherosclerosis and may have predictive value.

1.5.4.3 VLDL-associated lipoproteins are associated with CVD risk

ApoC-III (a small VLDL-associated lipoprotein) is significantly correlated with the development of coronary stenosis (Phillips et al., 1993). Similarly, results from the Monitored Atherosclerosis Regression Study (MARS) show lipoproteins in the S_F 12-60 range (IDLs and small VLDLs) were independently correlated with the development of coronary atherosclerosis (Hodis et al., 1994). Intriguingly, triglyceride rich particles such as small VLDLs and those rich in apoC-III were related to the progression of mild or moderate coronary artery disease (<50% stenosis) rather than severe disease (>50% stenosis), indicating that these small VLDL particles may be involved in the initiation of atherosclerosis. Interestingly, lesions of <50% stenosis seemed to be highly predictive of future clinical coronary events. Similarly, a sub-study of the Cholesterol and Recurrent events (CARE) trial indicated that plasma concentrations of VLDL particles and apo C-III in VLDL and LDL were more specific measures of coronary heart disease than plasma triglycerides (Sacks et al., 2000).

1.5.5 Lipogenesis vs. Lipolysis

Lipids in the body that are derived from dietary fat and are metabolised as described in **Figure 1.9**. However, an alternative source of lipids is *de novo* lipogenesis (DNL) that converts excess carbohydrates into fatty acids and into eventual triglycerides, which can be used as energy later via β -oxidation. Most serum triglycerides are derived from the diet but some suggest DNL has a significant contribution to serum triglycerides, especially those who are on a high carbohydrate diet (Ameer et al., 2014). DNL occurs in both the liver and adipose tissue and involve a coordinated series of enzymatic reactions that convert citrate (derived from glycolysis and the citric acid cycle) to acetyl CoA and eventually into fatty acids. These fatty acids can then be incorporated into triglycerides for energy storage. Increase in excess carbohydrate in the diet, like lipid can increase the synthesis and release of VLDL particles into the circulation and deposition in tissues. White adipose tissue is the main storage site for excess triglycerides. The FFA acids derived from lipoprotein particles are re-esterified and stored as triglycerides or oxidised for energy. During fasting however, hydrolysis of triglycerides in the adipose tissue liberates FFA in a process known as lipolysis. The FFA can re-enter the liver and incorporated into triglycerides and VLDL particles (Ameer et al., 2014).

1.5.6 Aberration of *de novo* lipogenesis

The deregulation of DNL is often observed in many metabolic disorders including NAFLD, obesity, hyper-insulinaemia and insulin resistance. The deregulation occurs when the delivery of fat and the subsequent secretion or metabolism is imbalanced. Elevated rates of DNL and triglyceride production, particularly in the liver through a number of factors including excess dietary intake of carbohydrates increases lipid deposits in the liver known as hepatic steatosis. Inefficient oxidation of fatty acids can also lead to the production of ROS that may induce inflammation in the liver (Jaeschke and Ramachandran, 2011). Inflammatory environments in the liver have been shown to be important in the pathogenesis of NAFLD. Inflammation can also be derived from activated Kupffer cells (KCs) and can directly influence lipogenesis in the liver (Huang et al., 2010). Similarly, activated macrophages in the adipose tissue known as adipose tissue macrophages (ATMs) can influence the secretion of adipokines, cytokines involved in the remodelling of adipose tissue including lipolysis (Weisberg et al., 2003).

1.6 TRIB1 in human disease

TRIB1 is intimately involved in inflammatory signalling but also appears to be involved in a number of diseases such as cancer (Yokoyama et al., 2010, Yokoyama and Nakamura, 2011), metabolic disease (Ostertag et al., 2010, Bauer et al., 2015) and atherosclerosis, (Sung et al., 2012, Sung et al., 2007) that have an inflammatory component including inflammatory signalling itself or cells of inflammation such as monocytes and macrophages (Sato et al., 2013) (**Figure 1.11**).

1.6.1 TRIB1 and cancer

As discussed, TRIB1 has been identified as an oncogene in the development of AML, a neoplastic disease of myeloid cells. Not only does TRIB1 enhance the phosphorylation of ERK and the degradation of C/EBP α it also collaborates together with *Hoxa9* and *Meis1* (Jin et al., 2007). Genes that collaborate with *Hoxa9/Meis1* have been identified as common targets of retroviral integration when retrovirus was used as an insertional mutagen. *Trib1* was identified as the most frequent common integration site of *Hoxa9/Meis1* retrovirus in AML. Although *Trib1* by itself is a transforming gene in myeloid cells, it greatly accelerates the progression of *Hoxa9/Meis1* AML (Nakamura, 2005).

Amplification or increased expression of the oncogene *c-MYC* is implicated in a range of human cancers. *Trib1* is located 1.5 Mb away from *c-MYC* on chromosome 8q24 and a study showed that in at least some cases of AML, *Trib1* is over-expressed with 8q24 amplification while *c-MYC* is not detected, although *c-MYC* is significant in the development of AML, it suggests that *Trib1* may also have a cooperative role with this oncogene (Storlazzi et al., 2006, Roethlisberger et al., 2007). Similar cooperative roles with *Trib1* have been described for *Gata2* in Down syndrome associated acute megakaryoblastic leukaemia (DS-AMKL) and loss of *Nf1* in juvenile chronic myeloid leukaemia (JCML) through *Bcl1a* and *Nf1* mutations (Yokoyama and Nakamura, 2011).

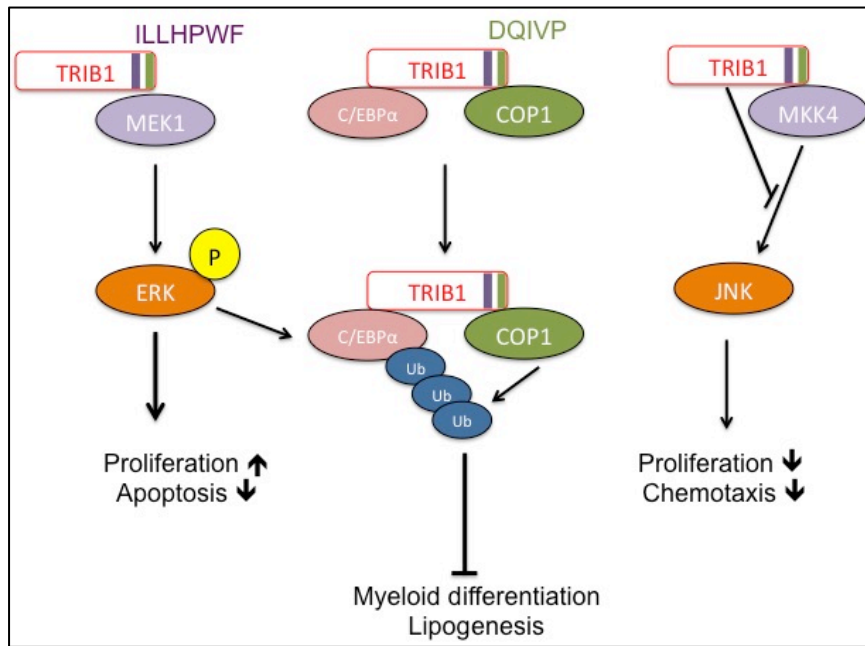


Figure 1.10: The role of TRIB1 in human diseases.

TRIB1 functions as an adaptor and interacts with MEK1 through its MEK1 binding domain (ILLHPWF) to enhance the phosphorylation of ERK which promotes cell proliferation and inhibition of apoptosis, the pathway has been implicated in the pathogenesis of AML. Similarly, TRIB1 interacts with the ubiquitin ligase COP1 through DQIVP to enhance the ubiquitination of the transcription factor C/EBP α and its degradation via the proteasome which is implicated in myeloid differentiation in AML and hepatic lipogenesis, note that phosphorylation of ERK also promotes the ubiquitination of C/EBP α . TRIB1 also interacts with MKK4 of the MAPK pathway to control the proliferation and chemotaxis of smooth muscle cells via inhibition of JNK.

1.6.2 TRIB1 in macrophages

As well as the described role of TRIB1 in myeloid cells in cancer, TRIB1 has been shown to be a critical regulator of macrophage function and polarisation by altering C/EBP α levels in a COP1 dependent manner. A prominent paper published by Akira's group demonstrated that TRIB1 may be a regulator of macrophage polarisation (Sato et al., 2013). Full body *Trib1* knockout mice were shown to be deficient in 'M2' alternatively activated macrophages in various organs including the spleen and adipose tissue. Haematopoietic derived *Trib1* may also impact adipose tissue lipolysis and markers of metabolic disorders, as bone marrow transplantation of *Trib1*^{-/-} bone marrow into WT mice resulted in reduced adipose tissue mass while transplantation of WT bone marrow into *Trib1*^{-/-} mice did not. The lipodystrophic phenotype observed was attributed to lack of 'M2' macrophages as *Trib1*^{-/-} mice supplemented with 'M2' macrophages had increased

adipose tissue mass and adipocyte size vs. PBS-treated mice. The lack of *Trib1* in bone marrow derived cells was shown to increase serum levels of non-esterified fatty acids (NEFAs) and glycerol, attributed to increase in lipolysis. Additionally, increased levels of pro-inflammatory cytokine expression (TNF- α and iNOS), known factors that contribute to adipose inflammation and lipolysis were observed. Interestingly, measurements associated with metabolic disorders (e.g. cholesterol, insulin, glucose and triglycerides) were not detected when both *Trib1*^{-/-} and *Trib1*^{-/-} \rightarrow WT transplanted mice were sustained on a normal chow diet but only emerged when mice were fed a high-fat diet. Both models developed glucose intolerance and insulin resistance on high-fat diet suggesting that myeloid- *Trib1* may have complex roles in homeostasis that may become apparent in only in the context of metabolic inflammation due to increased intake of diets rich in fats and carbohydrates which is relevant to the broadening epidemic of human obesity.

Akira's study interestingly used full body *Trib1*^{-/-} mice, the viability of which has been questioned by several laboratories including our own (discussed in more detail in **section 3.5**) to conclude macrophage derived *Trib1* is responsible for the observed phenotype. However, bone marrow consists of cells of multiple lineage and not just macrophages, which complicates their conclusion and does not reveal specifically if monocytes/macrophages are responsible. This project however will aim to determine the exact contribution of myeloid-TRIB1 in relation to lipid homeostasis and metabolic disorders by using tissue specific knockout and over-expressor mice.

TRIB1 has also been shown to be involved in macrophage migration, through interactions with C/EBP β and TNF- α . Silencing of *Trib1* in RAW 264.7 cells resulted in attenuation in migration behaviour. Interestingly, this also caused an increase of TNF- α , the authors propose that TRIB1 plays a role in the pro-inflammatory response by attenuating TNF- α and inhibiting monocyte migration (Liu et al., 2013).

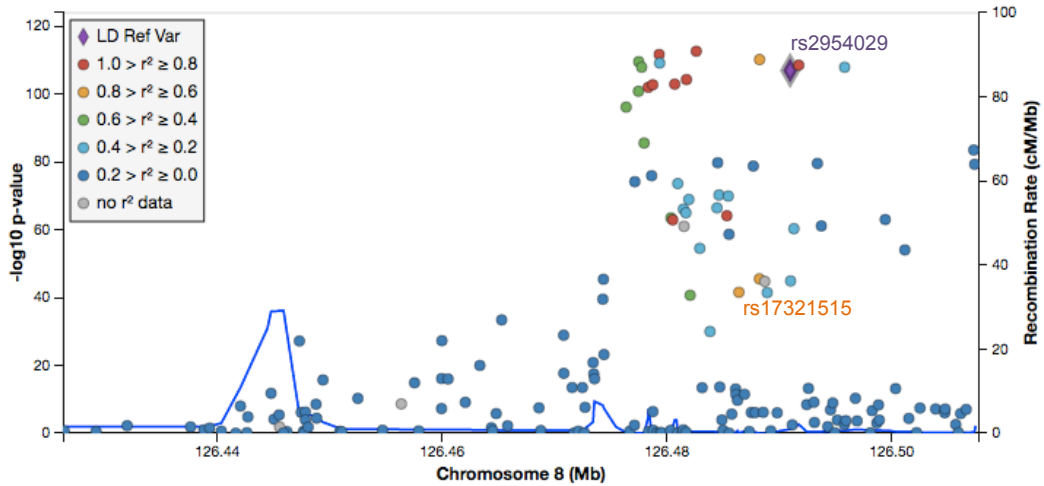
In the context of atherosclerosis, in plaque macrophages specifically, the percentage of TRIB1-expressing macrophages is reduced in the lesions of mice that lack the IL-1 receptor and therefore cannot signal via IL-1 (ApoE^{-/-}/IL1R1^{-/-} double knockout) compared to controls (ApoE^{-/-}), suggesting *Trib1* may be involved in a regulatory feedback loop with IL1 receptor-signalling (Sung et al., 2012).

1.6.3 *TRIB1* is associated with lipid traits and is a risk factor for the development of cardiovascular disease

Several GWAS have shown allelic variations e.g. rs2954029 and rs17321515 (single nucleotide polymorphisms; SNPs) in areas close to the *TRIB1* gene are associated with all the major lipid traits including triglycerides, total cholesterol, low-density lipoprotein cholesterol (LDL-C) and high-density lipoprotein cholesterol (HDL-C) (**Figure 1.12**). The same variants are also significantly associated with levels of alanine transaminase (ALT; a marker of hepatocellular injury) and increased risk in ischaemic heart disease and MI (Chambers et al., 2011). Interestingly, for rs2954029, TT to TA to AA genotypes were associated with a step-wise increase in the levels of triglyceride, remnant cholesterol, and levels of apoB. HDL cholesterol levels also decreased stepwise through the genotypes. Additionally the genotype variations were significantly associated with increased risk of ischemic heart disease (IHD) and increase risk of MI (Edmondson, *et al* 2011, Varbo, *et al* 2011). A bivariate analysis showed *TRIB1* expression to be specifically associated with triglyceride/elevated blood pressure and triglyceride/ HDL-cholesterol suggesting that *TRIB1* may be involved in a specific feature of lipid homeostasis rather than having a general and non specific role (Kraja, *et al* 2011). *TRIB1* expression interestingly is ubiquitous but is found at high levels in the liver, the major site for the formation, secretion and clearance of circulating lipoproteins (Burkhardt, *et al* 2010).

These initial studies were further validated using full-body knockout and hepatic-specific overexpression mouse models by Burkhardt et al. (2010). Full body *Trib1*^{-/-} mice had elevated levels of triglyceride and cholesterol due to increased VLDL production. Similarly, hepatic *Trib1* overexpression using adeno-associated virus serotype 8 (AAV8) vector resulted in reduced levels of triglyceride, cholesterol due to reduced production of VLDL.

Willer CJ 2013 - Triglycerides meta-analysis



Willer CJ 2013 - Total cholesterol meta-analysis

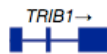
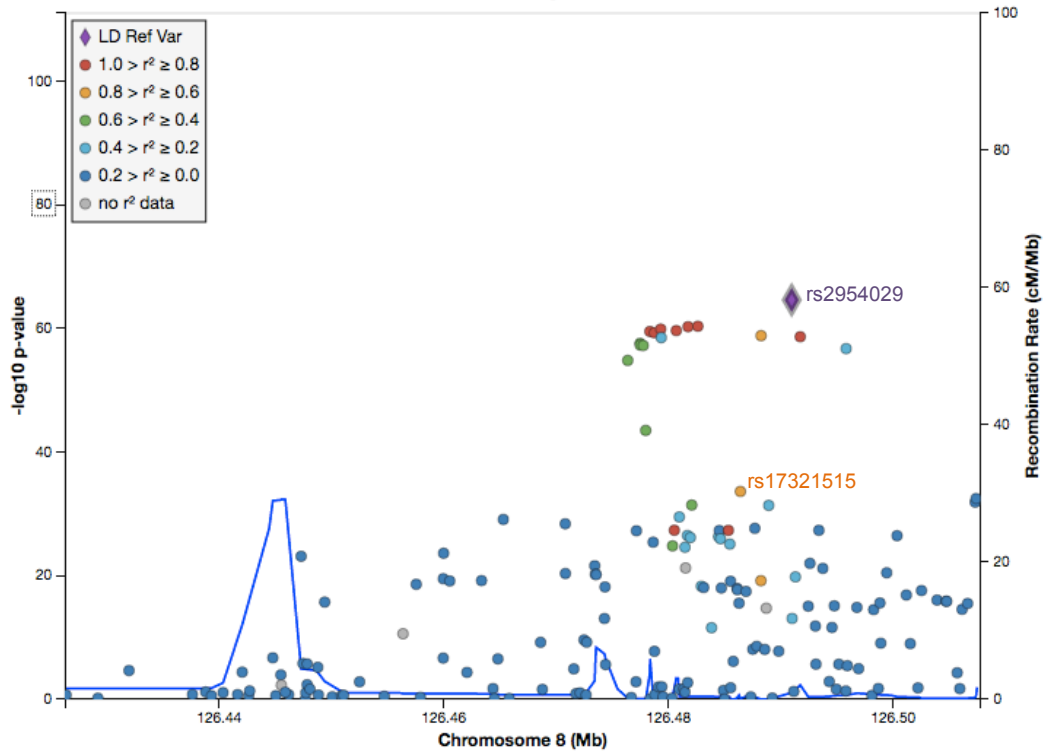


Figure 1.11: Association of *TRIB1* region with plasma triglycerides and total cholesterol levels.

Chromosome 8q24 is shown along with the location of *TRIB1* gene. Location of downstream SNPs identified as having significant association with (A) plasma triglyceride and (B) total cholesterol levels in humans. The left y-axis shows the associated p value of the SNPs and each colour represents its r^2 value relative to the lead SNP (rs2954029). The locations of discussed SNPs (rs2954029 and rs17321515) are illustrated. Association data was taken from the GLGC (2013) study of triglycerides and total cholesterol meta-analysis (Willer et al., 2013). Figure was generated using LocusZoom (Pruim et al., 2010).

1.6.4 *Trib1* regulates hepatic lipogenesis

Despite various studies implicating *Trib1* in plasma lipid homeostasis, the exact molecular mechanisms of how this is regulated are still unclear. However, the mRNA expression of various genes involved in lipogenesis were investigated in the livers of *Trib1*-deficient and –overexpressing mice. **Figure 1.13** illustrates the process of lipogenesis. It was found that genes involved in fatty acid oxidation (*Cpt1a*, *Cpt2m* and *Acox1*) were significantly decreased in *Trib1*^{-/-} mice. Similarly, key genes involved in lipogenesis; acetyl-coA carboxylase (*Acc1*), fatty acid synthase (*Fasn*) and stearoyl-coenzyme A desaturase 1 (*Scd1*) were significantly down-regulated in mice over-expressing *Trib1* and were significantly up-regulated in *Trib1*-overexpressing mice (Burkhardt et al., 2010). Interestingly, further work using liver specific *Trib1*-KO mice (*Trib1*_LSKO) demonstrated an increase in lipogenesis gene expression (*Acaca*, *Fasn*, *Scd1* and *Dgat2*), interestingly an increase in de novo lipogenesis and hepatic steatosis was also observed. These effects were largely due to increase protein levels of the transcription factor C/EBP α . ChIP-Seq data verified C/EBP α occupancy near lipogenic genes and pathway analysis revealed significant increase in the transcription of C/EBP α target genes. The authors suggest that TRIB1 regulates lipogenesis through C/EBP α via up-regulating fatty acid-synthesis genes, however the regulation appears to be independent of the master regulators of fatty acid synthesis such as ChREBP, LXR and SREBP1. Indeed, TRIB1 regulation of C/EBP α also appears to occur in a regulatory feedback loop that is both transcriptional and translational that occurs by C/EBP α transcriptionally up-regulating *Trib1*, while simultaneously TRIB1 protein post-transcriptionally down regulates C/EBP α protein (Bauer et al., 2015). C/EBP α is known to be involved in the regulation of lipogenesis in adipocytes and some studies have also implicated it in the regulation of lipogenesis genes and hepatic steatosis in mice (Matusue et al., 2004, Qiao et al., 2006).

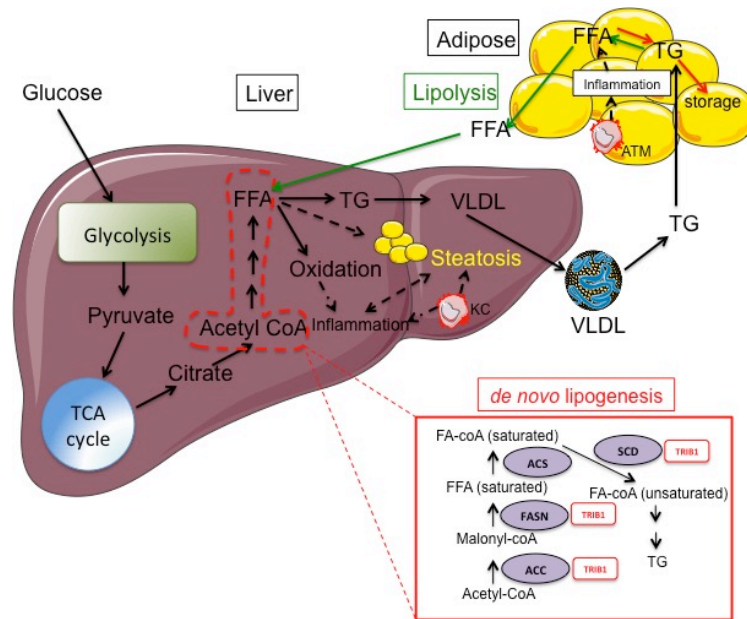


Figure 1.12: De novo lipogenesis and production of triglyceride in the liver and adipose tissue.

DNL is a coordinated series of enzymatic reactions. Glucose taken up by the glucose transporter enters the liver and enters the glycolysis pathway to produce pyruvate. Pyruvate is converted into citrate via the tricarboxylic acid (TCA) cycle in the mitochondria. The citrate leaves the mitochondria and is converted to acetyl-CoA and enters the lipogenesis (fatty acid synthesis) pathway (outlined in red) to produce complex free fatty acids (FFA). FFA are either oxidised for energy or esterified into triacylglycerol (TG) and either exported as VLDL particles or stored as lipid droplets. VLDL particles are rapidly hydrolysed by lipoprotein lipase where TG is rapidly hydrolysed to FFA. FFA can be re-esterified to TG for storage or when needed re-enters the circulation and are available for uptake in cells. FFA enters the liver and can re-enter the lipogenesis pathway. Lipid intermediates, reactive oxygen species (generated by FA oxidation), excessive TG accumulation (steatosis) and KC activation can all contribute to inflammation. Similarly, inflammation in the adipose (through ATM activation or excess nutrients) induces lipolysis freeing fatty acids into the circulation, exacerbating pro-inflammatory pathways in the liver. Enzymes that catalyse DNL are shown (inset), lipogenesis genes which are known to be regulated by TRIB1 are also indicated.

1.6.5 *TRIB1* is a potential novel therapeutic target to lower plasma cholesterol

Epidemiological studies have long demonstrated that levels of LDL-cholesterol and triglycerides are strong risk factors for the development of coronary artery disease. Most LDL-C is removed from the circulation through LDL-receptor mediated uptake in the liver. Indeed, therapeutics that increase the levels of the LDL receptor (LDLR) have proven to be effective in lowering plasma LDL-C and lowering the risk of cardiovascular disease (Nagiec et al., 2015). The widely used class of drugs called statins act through inhibition of HMG CoA reductase and block cholesterol synthesis in the liver leading to the activation of sterol regulatory element binding protein-2 (SREBP-2) promoting the transcription and expression of LDLR. However, the clinical efficacy of statins are limited as stimulation of SREBP-2 regulated gene expression also increases levels of proprotein convertase subtilisin/kexin type 9 (PCSK9) which acts to promote the uptake

and degradation of LDLR (Horton et al., 2003). Therefore, the limitations of statins and reported side effects (including hepatic fat accumulation and liver toxicity) to reduce levels of LDL-C have promoted the development of new therapeutic strategies. New approaches include inhibition of PCSK9, apolipoprotein-B100 (apoB, component of LDL and VLDL particles), cholesterol ester transport protein (CETP) and microsomal triglyceride transfer protein (MTT), reviewed in Noto et al. (2014). Certainly, results from recent clinical trials using monoclonal antibodies to PCSK9 have proved promising (Desai et al., 2014, Raal et al., 2012), however the first outcomes of two large-scale clinical trials (Regeneron CVOT and Odessey Outcomes) are not expected until late 2017. Recently, it has been shown TRIB1 could be a suitable bona fide therapeutic target to tackle hypercholesterolaemia. A group performed a high throughput phenotypic screen based on quantitative RT-PCR assay to identify compounds that induce *TRIB1* expression in human HepG2 cells in the hopes to treat hypercholesterolaemia (Nagiec et al., 2015). They identified a series of benzofuran-based compounds that upregulate *TRIB1* expression and inhibit triglyceride synthesis and apoB secretion in cells. Characterisation of one of the compounds, BRD0418 showed that treatment resulted in decreased rate of VLDL production and increased rate of LDL uptake in cells by modifying and reprogramming lipogenesis and could prove a promising basis for future therapy.

1.7 Molecular regulation of lipogenesis; the link between cholesterol homeostasis and inflammation

Since dysregulated inflammation is responsible for immuno-metabolic disorders, it is important to consider the pathways that overlap both factors; inflammation and metabolism. Hyperglycaemia (high glucose), hyperinsulinaemia (high insulin) and hypercholesterolaemia trigger both lipogenesis and glycolysis through activation of transcription factors that can also induce inflammatory gene expression. Such transcription factors include sterol regulatory element binding protein (SREBP), PPARs, carbohydrate responsive element-binding protein (ChREBP) and liver X receptors (LXR). These transcription factors promote the transcription of lipogenesis genes including ones regulated by TRIB1 (*Acc*, *Fas*, *Scd1*) (Bauer et al., 2015). However, inappropriate activation is implicated in the pathogenesis of NAFLD and in the case of SREBP can activate pro-inflammatory cytokine gene expression through NF- κ B and the inflammasome (Ferre and Fougelle, 2010). Likewise, LXR activation is known to be important for cholesterol efflux in and promoting anti-inflammatory effects in

macrophages. The PPAR transcription factors in particular have been shown to have a central role in macrophage lipid metabolism by promoting cholesterol efflux and have anti-inflammatory properties by reducing expression of pro-inflammatory mediators (e.g iNOS) and are also involved in macrophage activation itself (reviewed in Rigamonti et al. (2008)). PPAR- γ expression has been shown to enhance the differentiation of monocytes into alternatively activated/ anti-inflammatory macrophages (Odegaard et al., 2007). The roles of PPAR- α , PPAR- γ and LXRs in macrophage lipid metabolism and immune responses are illustrated in **Table 1.6**.

Table 1.6: Roles of PPAR- α , PPAR- γ and LXRs in lipid homeostasis and immune responses in macrophages

Function in cholesterol metabolism		PPAR- α		Mechanism	PPAR- γ		Mechanism	LXR		Mechanism
		H	M		H	M		H	M	
Cholesterol accumulation										
	TG- rich lipoprotein uptake	↓		↓ apoB-48R	↓		↓ apoB-48R			
	In vivo model of foam cell formation		↓	n.d.		↓	↑ ↓ CD36 SR-A			
Cholesterol trafficking		↑	X	↑ NPC1 ↑ NPC2	n.d.	n.d.	n.d.	↑	X	↑ NPC1 ↑ NPC2
Cholesterol esterification		↓	X	↑ CPT-I ↓ ACAT1 activity ↑ NCEH	↓	↓	↓ ACAT1 (H) ↑ NCEH (H) n.d. (M)	↓	n.d.	↓ ACAT1
Cholesterol efflux		↑	X	↑ SR-B1 ↑ ABCA1 ↑ LXR α	↑	↑	↑ SR-B1 ↑ ABCA1 ↑ LXR α ↑ ApoE ↑ ABCG1 ↑ Caveolin (H)	↑	↑	↑ ABCA1 ↑ ABCG1 ↑ ABCG4 ↑ ApoE ↑ Caveolin
Function in immune response										
	Production of inflammatory mediators	↓	↓	1) NF- κ B pathway inhibition 2) AP-1 pathway inhibition	↓	↓	1) NF- κ B pathway inhibition 2) AP-1 pathway inhibition	↓	↓	1) NF- κ B pathway inhibition 2) AP-1 pathway inhibition 3) SUMOylation (M)

							3) SUMOylation (M) 4) ↑ IL-1Ra (H) 5) ↑ Alternative Macrophage activation			4) ↑ arginase II (M)
	Anti-bacterial activity	↑	↑	↑ ROS production ↑ NAPDH oxidase subunits ↑ MPO (H)	↑	↑	↑apoptotic neutrophil uptake (H) ↑ MPO (H) ↑ CD36	↑	↑	↑ TLR-4 (H) ↑ NAPDH oxidase subunits ↑ Macrophage survival (M)

Abbreviations: X, not regulated; n.d., not determined; H, human; M, mouse; ABC, ATP binding cassette transporter; ACAT-1, Acyl-coA:cholesterol acyltransferase-1; MPO, myeloperoxidase; NECH, neutral cholesteryl ester hydrolase; NPC, Niemann Pick type C; ROS, reactive oxygen species; SR, scavenger receptor. Adapted from Rigamonti et al. (2008)

1.7.1 Cholesterol metabolism in macrophages

Since TRIB1 has been shown to have significant roles in hepatic lipid metabolism and the polarisation state of macrophages. It is important to consider the process of lipid metabolism in macrophages themselves.

1.7.1.1 Scavenger Receptors





Since the first description of binding and internalisation of modified LDL into macrophages through scavenger receptors by Brown and Goldstein (Brown et al., 1979), the scavenger receptor family has expanded to include 8 different subclasses (A-H) of structurally heterogeneous receptors. It is now appreciated that scavenger receptor expression has a critical role in atherosclerosis development, by promoting foam cell formation, the initial stage of disease that triggers the inflammatory response and progression of disease.

Scavenger receptors bind and ‘scavenge’ a wide range of ligands including apoptotic cells, anionic phospholipids, amyloid and pathogen components and are thought to belong to pattern recognition receptors that are important in the innate immune response (Kzhyshkowska et al., 2012).

However, scavenger receptors also recognise endogenous neo-antigens present in modified forms of LDL, in some cases through molecular mimicry of pathogenic ligands, for example oxidised phosphorylcholine is identical to antigens from *Streptococcus pneumoniae* (Shaw et al., 2000, Moore and Freeman, 2006). Although most scavenger receptor identification has derived from its ability to bind and internalise acetylated- LDL (AcLDL), AcLDL itself is not a naturally occurring ligand (Moore and Freeman, 2006). Even though the internalisation of modified lipoproteins by these receptors is thought to be central to the formation of foam cells, it is thought that they also are pivotal in stimulating pro-inflammatory phenotypes in plaque macrophages including initiating signalling cascades (e.g JNK and NF- κ B) that are involved in lipid metabolism, macrophage activation and inflammation that may effect plaque development and stability. It is also recognised that scavenger receptors have roles in cell apoptosis, apoptotic cell clearance and pathogen recognition that could affect early and late more complex lesions (Moore

and Freeman, 2006). They can also participate in reverse cholesterol transport (e.g. SCARB-1) by mediating cholesterol transport from cells to HDL particles. **Table 1.7** summarises the known scavenger receptors along with their respective ligands and expression profiles.

Table 1.7: List of known scavenger receptors and their role in atherosclerosis.

Class	Name	Ligands (Relevant to atherosclerosis)	Expression on monocytes and plaque macrophages in atherosclerosis	Atherogenic?
A	SR-AI/SR-AII	oxLDL, acLDL, cholesterol, apo A-I, apo E	Myeloid cells (macrophages and subpopulations of DCs) Vascular endothelial cells Plaque smooth muscle cells	
A	MARCO	oxLDL>acLDL	Macrophage subpopulations (spleen marginal zone, medullary lymph nodes, resident peritoneal)	
B	CD36	acLDL, oxLDL, VLDL, LDL, HDL, oxidised phospholipids	Macrophages, DCs, microglia, vascular endothelial cells, hepatocytes, adipocytes	
B	SRB-I (SCARB-1)	acLDL, oxLDL, VLDL, LDL, HDL, oxidised phospholipids, cholesterol	Macrophages, hepatocytes	
E	LOX-1 (OLR1)	oxLDL phosphatidylserine	Endothelial cells, macrophages, smooth muscle cells	
F	SREC-I/SREC-II	oxLDL, acLDL	Endothelial cells, macrophages	
G	SR-PSOX/CXCL16	oxLDL, phosphatidylserine	DCs, macrophages,	
H	Stabilin/FEEL-1	acLDL, apoptotic cells	sinusoidal endothelial cells, monocytes/macrophages	

1.7.2.2 Foam cell formation and lipoprotein uptake

The detrimental lipid uptake and consequent foam cell formation of plaque macrophages is a fundamental event in the development of atherosclerosis. Normal cholesterol homeostasis in macrophages is balanced between cholesterol influx, intracellular metabolism and efflux pathways. Macrophage foam cell formation

however is known to occur when the homeostatic controls of these pathways are disrupted (**Figure 1.14**).

Lipid uptake in the form of lipoproteins in macrophages can occur through both non-receptor and receptor mediated uptake of both normal and modified lipoproteins. Although LDL uptake by macrophages through the LDL receptor (LDLR) is limited due to negative feedback inhibition of LDLR expression by cholesterol levels in the cell, the rapid and un-inhibited uptake of modified LDL (AcLDL, oxLDL) through scavenger receptors is largely unregulated and consequently has a significant contribution to foam cell formation. Several receptors have been implicated in the uptake of oxLDL in macrophages including CD36 and SR-A, which are thought to be the main contributors to cholesterol uptake in macrophages (de Villiers and Smart, 1999, Chistiakov et al., 2016). Lectin-like oxidised low-density lipoprotein receptor-1 (LOX-1), product of the *ORL-1* gene can also bind modified LDL and is a major oxLDL-binding receptor in endothelial cells and its expression is thought to be inducible in macrophages and smooth muscle cells (Mehta et al., 2006).

Interestingly, modification of LDL through oxidation or acetylation can render LDL more recognisable to specific scavenger receptors than in its native form (Berliner et al., 1990). Lipid uptake through other means such as phagocytosis of aggregated LDLs and macropinocytosis of native or modified LDLs can also contribute to the formation of foam cells (Ghosh, 2011). The question remains by which mechanism is more significant to atherogenesis, however it is likely all contribute towards foam cell formation and removal of one mechanism may be compensated by another (McLaren et al., 2011).

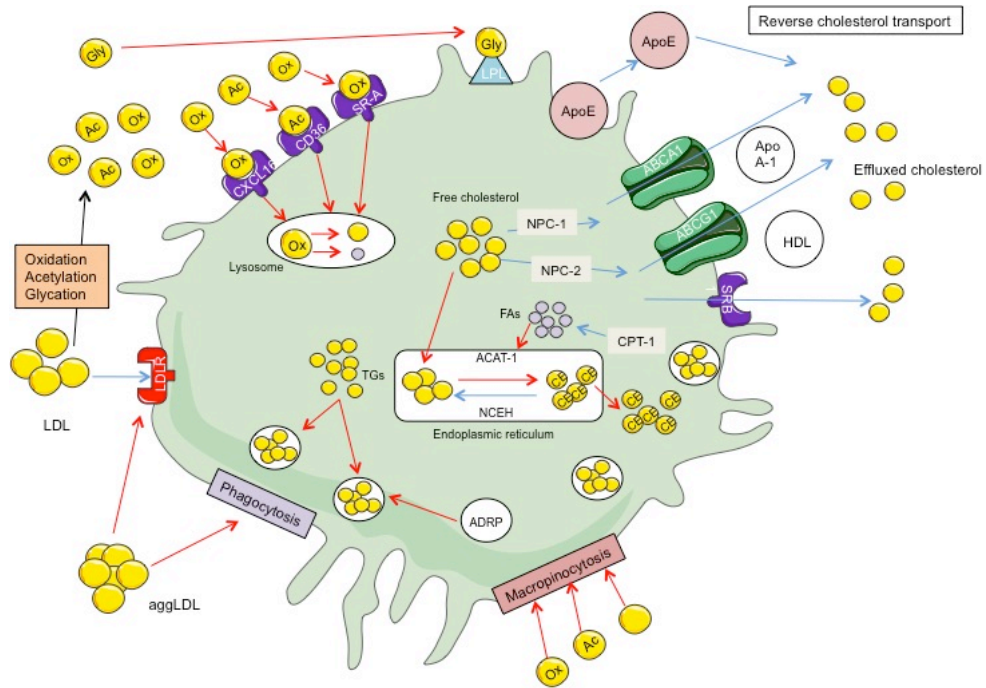


Figure 1.13: Working model of cholesterol metabolism in macrophages and the formation of foam cells.

Macrophage foam cell formation involves the disruption of cholesterol homeostasis. This mechanism involves unmodified and modified LDL uptake, efflux of cholesterol by reverse cholesterol transport and intracellular mechanisms that store, traffic and esterify cholesterol. In foam cells however the homeostatic mechanism becomes imbalanced, favouring excessive intracellular accumulation of cholesterol. This occurs by the enhancement of modified LDL uptake, dampening of cholesterol efflux machinery such as the transporters ABCA-1 and ABCG-1 and extensive intracellular storage and esterification. The red arrows indicate pathways that promote foam cell formation whereas the blue arrows indicate pathways that suppress foam cell formation. Abbreviations: ABC, ATP binding cassette transporter; Ac, acetylated; ACAT1, Acyl-coA:cholesterol acyltransferase-1; ADRP, adipocyte differentiation-related proteins; AggLDL, aggregated LDL; CE, cholesteryl ester; CPT1, carnitine palmitoyl transferase-1; FAs, fatty acids; Gly, glycated; LAL, lipoprotein lipase; NCEH, neutral cholesteryl ester hydrolase; NPC, Niemann Pick type C; SR-A, scavenger receptor A; SR-B1, scavenger receptor B1 (SCARB1).

1.7.2.3 Cholesterol efflux

Normal cholesterol efflux serves to remove cholesterol from the cell to the liver. However the formation of foam cells reduces cholesterol efflux to favour cholesterol deposition in the form of lipid droplets inside the cell. Efflux can occur via reverse cholesterol transport and HDL-mediated passive diffusion. Indeed, efflux from macrophages is stimulated by HDL particles and also the apolipoprotein A-I principally through ATP-binding cassette transporters (ABC); ABCG-1 and ABCA-1 respectively. However, efflux can also occur independently of these transporters. The lipoprotein apoE also contributes to macrophage cholesterol efflux. The role of apoE in cholesterol metabolism is mostly attributed to its systemic effect on lipoprotein metabolism, however apoE also contributes towards cholesterol efflux from cells through its expression in macrophages. Interestingly, a study by Zanotti et al. (2011) demonstrated that macrophage and not systemic expression of apoE is needed for functional macrophage reverse cholesterol transport *in vivo*. Scavenger receptors can also play a role in this process, the scavenger receptor SCARB1 has dual roles and can participate in both the internalisation of oxLDL and also stimulates the apolipoprotein-independent cholesterol efflux.

1.7.2.4 Intracellular cholesterol trafficking and storage

The intracellular metabolism of cholesterol is also disrupted in foam cells. Characteristically, foam cells have a high cytoplasmic accumulation of cholesteryl-ester and triacylglycerol-rich droplets. Following uptake, oxLDL is hydrolysed in late endosomes/lysosomes into free cholesterol and fatty acids by lysosomal acid lipase, which can be trafficked to the plasma membrane for transport. Excess cholesterol however, is transported to the endoplasmic reticulum where it is re-esterified by acyl-coenzyme A: cholesterol acyltransferase (ACAT1) and stored in cytoplasmic lipid droplets. The initial re-esterification is beneficial to prevent cellular toxicity, however under conditions of unregulated or increased uptake of LDL (through mechanisms described above) it leads to increased accumulation of cholesteryl esters in lipid droplets which gives the macrophages their classic 'foamy' appearance. Cellular cholesteryl esters continually undergo hydrolysis by neutral cholesteryl ester hydrolase (NCEH) and re-esterification in what is known as the 'cholesteryl ester cycle'. NCEH can also liberate free cholesterol from lipid droplets that either re-enter the esterification cycle or are trafficked to the membrane for cholesterol

efflux via transporters (ABCA1 and ABCG1). Interestingly, macrophages with high NCEH activity accumulate fewer cholesterol esters in the presence of VLDL compared to macrophages with low NCEH activity (Ishii et al., 1992).

1.8 Summary

The review of the literature has shown TRIB1 to be an adaptor protein that has been shown to have direct interactions with and can modulate key inflammatory signalling pathways and cellular processes. Our current understanding has illustrated TRIB1 to be intimately involved in lipid homeostasis and is a risk factor for hyperlipidaemia, MI and CVD. It has also been shown to be a key regulator in macrophage polarisation, which is a key factor in inflammation in the pathogenesis of chronic inflammatory diseases.

However the potential interplay of macrophages and TRIB1 in the context of lipid metabolism has not been fully explored. Despite its significant link to the development of cardiovascular disease, there has been no study to define the role of TRIB1 in atherosclerosis, particularly in myeloid cells, which are central to the initiation and progression of the disease.

1.8.1 Hypothesis

Based on current knowledge, I hypothesise that *Trib1* expression in myeloid cells controls macrophage function and polarisation and in doing so influences lipid metabolism both in metabolic tissues and macrophages that may affect the development of cardiovascular disease.

1.8.2 Aims

The project aims to:

- Investigate the functional consequences of *Trib1* –overexpression and knockout in macrophages using myeloid-specific *Trib1* conditional knockout (*Trib1* *fl/fl* x *LyzMCre*) and over-expressor (*ROSA26.Trib1* x *LyzMCre*) mouse models by assessing macrophage phenotype in the liver and their contribution to plasma lipid homeostasis.

- Contribute to the understanding of the role of hematopoietic- derived *Trib1* in experimental atherosclerosis by generating *Trib1*-ApoE^{-/-} chimera mice using bone marrow transplants (BMTs).
- Develop immunohistochemistry (IHC) staining methods to expand the analysis of macrophage phenotype in atherosclerotic plaques.

Chapter 2. General Materials & Methods

This materials and methods chapter will include general techniques that have been used throughout the work; relevant methods related to specific chapters will be described at the beginning of each results chapter.

2.1 Animals

2.1.1 Licensing

All experiments were performed in accordance with UK legislation under the 1986 Animals (Scientific Procedures) Act). All animal experiments were approved by the University of Sheffield Project Review Committee and carried out under a UK Home Office Project Licence (PPL), 70/7992 (Professor S.E Francis and by personal licence holder (procedure individual licence; PIL) J. Johnston 40/10901. Tissue samples that derived from mice in the USA conformed to the Guide for the Care and Use of Laboratory Animals published by the US National Institutes of Health (NIH Publication No. 85-23, revised 1996).

2.1.2 Husbandry

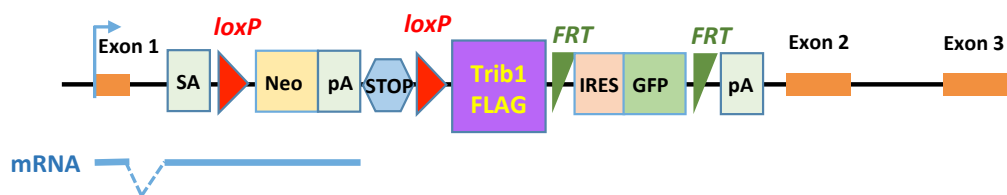
Mice were housed in a controlled environment with a 12h light/dark cycle at 22°C. Where possible, litter mates were housed together at no more than 6 mice per cage. All mice were fed *ad libitum* on standard chow diet (Harlan 18% protein rodent diet) unless otherwise stated.

2.1.3 Development of *Trib1* x *LyzMCre* mice

2.1.3.1 *ROSA26.Trib1Tg*

The myeloid-specific transgenic (Tg) mouse strain (*Trib1^{Tg}*) were created by inserting a ROSA26-STOP-*Trib1*-EGFP cassette into the *Rosa26* locus (**Figure 2.1**) of C57BL/6N mice, similar to previous studies (Sasaki et al., 2006). These mice were then crossed with mice that express Cre recombinase transgene under the control of the *Lyz2* promoter (*Lyz2-Cre*; (B6.129P2-*Lyz2^{tm1(cre)lfo}*/J; jax.org), thereby specifically deleting the STOP cassette in myeloid cells and generating a myeloid specific transgene. **Figure 2.1B** illustrates the principle of Cre-Lox recombination used to generate the mouse lines used in this study.

A: Tissue specific *Trib1* transgene



B: Cre-Lox Recombination

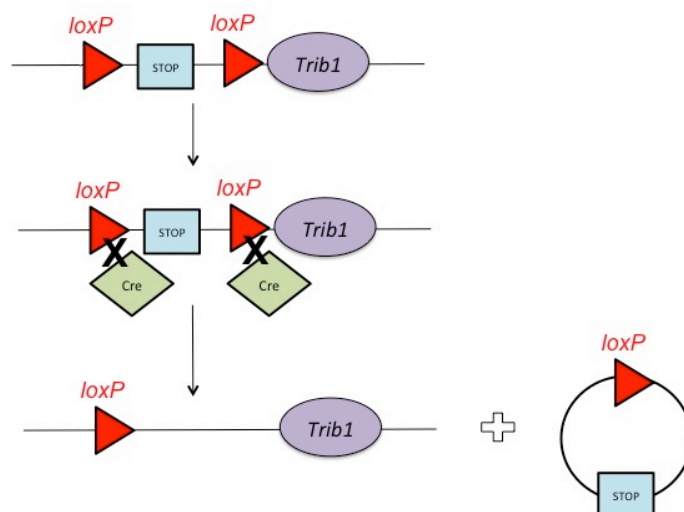


Figure 2.1: Schematic of tissue specific *Trib1* transgene and principle of Cre-Lox Recombination.

(A) The targeting construct incorporated the following key features: homology regions to the first intron of the *Rosa26* locus (5' and 3' arm), a splicing acceptor (SA) site to facilitate correct RNA maturation, a neomycin resistance gene (Neo) for positive selection in embryonic stem (ES) cells, SV40 transcriptional terminator to prevent transcription of the transgene in the targeted allele, prior to crossing with the Cre strain (STOP), a Cre recognition site to remove the neo-STOP region, enabling transcription of the *Trib1* transgene (*loxP*), a bi-cistronic expression cassette encoding for the FLAG tagged mouse Trib1 and EGFP proteins (Trib1-FLAG-IRES-EGFP). Abbreviations: pA, polyadenylation site; IRES, internal ribosomal entry site (allowing for translation in an end-independent manner). (B) Cre recombinase recognises specific sequences called LoxP sites. These are 34bp sequences of DNA that comprises of an 8bp spacer region and two palindromic sequences (13bp long each). When Cre is expressed, it recognises and binds to the LoxP sites and mediates DNA cutting. In this example and used in developing the *Rosa26.Trib1^{Tg}* mice, LoxP sites flank a STOP codon. When Cre is expressed, the STOP codon is excised allowing expression of *Trib1*.

2.1.3.2 *Trib1* fl/fl

An ES clone was purchased from KOMP (EPD0099_5_D04) and was used to generate a mouse with a *Trib1* conditional knockout allele on a C57BL/6N background. The targeting cassette (flanked by FRT sites) was inserted into the first intron of *Trib1*. It comprised of a splice acceptor site (SA), followed by an internal ribosomal entry site (IRES), followed by lacZ expression cassette (lacZ-pA). The construct also contained an expression cassette for Neomycin (Neo-pA). In addition, the second exon of *Trib1* (which encodes for the majority of the TRIB1 protein coding region) was flanked by loxP sites. In this strain (tm1a) therefore, a hybrid mRNA encoding the first exon of *Trib1* and lacZ is made, consequently generating a null allele (**Figure 2.3A**).

Tm1a mice containing the targeted *Trib1* locus were then crossed with a “deletor” strain expressing the FRT recombinase in germline cells, therefore excising the targeting cassette by flippase-mediated recombination (analogous to Cre-mediated recombination). In this strain (tm1c) therefore, *Trib1* is transcribed under the control of its endogenous promoter and wild-type *Trib1* mRNA is expressed (**Figure 2.2B**).

To produce mice lacking *Trib1* in myeloid cells (tm1d), female mice homozygous for a floxed *Trib1* allele that contained loxP sites flanking exon 2 of *Trib1* (Figure 2.2A) were crossed with male mice carrying a Cre recombinase transgene under the control of *Lyz2* promoter (B6.129P2-*Lyz2*^{tm1(cre)lfo}/J; jax.org). The Cre mediated deletion of the second exon of *Trib1* is predicted to lead to transcription of an mRNA encoding for a truncated TRIB1 protein (120aa), that lacks the central kinase-like domain and the C-terminal region, thus effectively generating a null allele (**Figure 2.2C**).

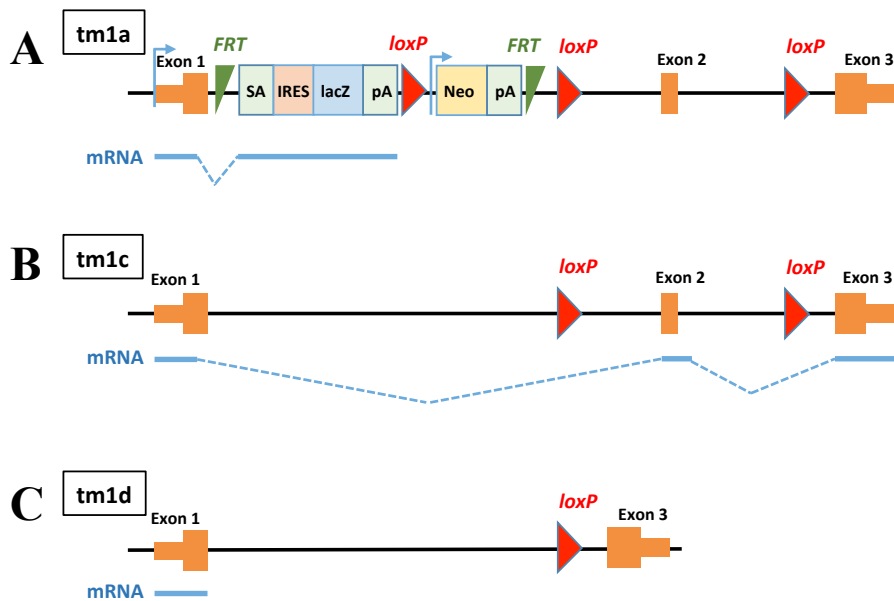


Figure 2.2: Schematic of Conditional *Trib1* allele and generation of *Trib1* fl/fl x *Lyz*MCre.

(A) Targeting construct inserted by homologous recombination into the *Trib1* locus of the mouse embryonic stem cell (ES) clone EPD0099_5_D04. (B) After flippase-mediated recombination, *Trib1* is transcribed under the control of its endogenous promoter (tm1c). (C) To produce mice with reduced expression of *Trib1* in myeloid cells, *Trib1*-floxed and *Lyz2*-Cre mice were crossed. The Cre-mediated deletion of the second exon of *Trib1* is predicted to produce an incorrectly spliced transcript encoding the first 120aa of TRIB1, followed by 3 aberrant amino acid residues, effectively producing a null allele. Abbreviations: SA; splice acceptor site; IRES, internal ribosomal entry site; pA, polyadenylation site.

2.1.4 Genotyping

Genotyping was performed in house at the University of Leeds, specific details of protocols can be found in **Appendix II**.

2.1.5 End of procedure

Mice were weighed and culled via pharmacological overdose of 0.2ml sodium pentobarbital (200mg/ml) given into the peritoneal cavity. If blood was required, cardiac puncture was performed following pentobarbital injection and prior to cessation of breathing.

Blood for plasma was taken directly from the heart through the chest wall into a heparinised syringe following loss of pedal reflex. Blood was centrifuged at 2000x g for 5 minutes at room temperature. Plasma was immediately frozen and stored at -80°C.

2.2 Tissue processing and Histology

Tissues were taken by blunt dissection and either placed in 10% (v/v) buffered formalin or snap frozen in liquid nitrogen. Tissues of interest were processed, dehydrated and embedded in paraffin wax for histological analysis as follows; the tissue was sandwiched between two sheets of Whatman Grade 1 filter paper and placed inside a processing cassette. The tissue was dehydrated sequentially in the following order: 50% (v/v) ethanol 1 hour, 70% (v/v) ethanol 1 hour/ overnight, 90% (v/v) ethanol 1 hour, 100% (v/v) ethanol 1 hour, 100% (v/v) ethanol 1 hour, 50:50 (v/v) ethanol/ xylene 1 hour, xylene 1 hour and xylene for 1 hour. Tissue cassettes were placed in molten paraffin at 60°C to infiltrate overnight. Tissues were then placed into paraffin moulds and filled with molten paraffin. Embedding cassettes were then placed on top and left to set overnight. To section, wax blocks were placed on melting ice 1 hour prior to sectioning. Blocks were trimmed until the desired area was reached and then subsequently cut at 5-10µm thickness using a microtome. The sections were placed in a pre-heated (~40°C) mounting bath and mounted on glass microscope slides. The slides were then dried at room temperature and transferred to a 37°C drying oven overnight.

To assess tissue morphology, tissues were stained with haematoxylin and eosin (H&E). Images were captured using a standard bright field microscope (Nikon Eclipse E600). Specific details of histological stains are detailed in the relevant chapters. Histological staining protocols are detailed in **Appendix IV**.

2.3 Human Ethics

Human atheromas derived from coronary endarterectomies were used for immunohistochemistry. Patients underwent surgery to remove the affected portion of the vessel and the excised tissue was fixed in 10% (v/v) formalin and embedded in paraffin wax. Sections were cut to 5µm thickness onto Poly-L-lysine coated slides (Thermo Scientific) and stored at RT until use. All samples were collected under protocols approved by the University of Sheffield and Sheffield Teaching Hospitals Trust review board and conformed to the declaration of Helsinki (Ref. STH 16346).

2.4 *In vitro* work

2.4.1 Cell line maintenance

2.4.1.1 RAW 264.7 and HEPG2 cells

RAW 264.7 (mouse leukaemic monocyte macrophage) cells were cultured in DMEM media with 10% (v/v) low endotoxin, heat inactivated FCS (Gibco) in a T75 flask. Cells were sub-cultured every 48 hours at 1:3 and maintained at 37°C at 5% CO₂.

HepG2 (human hepatocellular carcinoma) cells were cultured in low glucose (1g/L) DMEM media with L-glutamine, 25mM HEPES, pyruvate (Gibco), 10% (v/v) FCS, 1% (v/v) streptomycin/penicillin. Cells were sub-cultured every 48 hours at 1:5-1:10 and maintained at 37°C at 5% CO₂.

2.4.1.2 BMDMs

Mouse Bone marrow derived macrophages (BMDMs) were isolated from the femurs and tibias under aseptic conditions using RPMI-1640 medium + 10% (v/v) heat inactivated FCS using a syringe and 26-gauge needle. The cell suspension was passed through a 40µm cell strainer and centrifuged at 500x g for 5 minutes.

2.4.2 Polarisation of BMDMs

Bone marrow derived macrophages (BMDMs) were isolated by flushing the femurs and tibiae of *Trib1* x *LyzMCre* mice and culturing in conditioned medium for five days (DMEM, 10% (v/v) low-endotoxin FCS, penicillin-streptomycin and 10% (v/v) L929 medium). On day six, BMDMs were polarised to 'M1' (20ng/ml IFN-γ and 100ng/ml LPS), 'M2a' (20ng/ml IL-4) or 'M2c' (20ng/ml IL-10) for 24 hours.

2.4.3 Transfection

Cells were seeded at an appropriate density 24 hours prior to transfection in standard growth medium and were observed prior to experimentation to confirm healthy density and uniform distribution. Cells were transfected with the appropriate volume

of transfection reagent (Dharmafect Duo, Thermo Scientific) to the manufacturer's instructions.

2.5 RNA extraction and qPCR

Total RNA was isolated using ReliaPrep™ kit (Promega). cDNA was produced from 400ng of total RNA using iScript cDNA synthesis kit (Bio-Rad) according to the manufacturer's instructions. Real-time PCR was performed using specific primers (**Table 2.1**) and PrecisionPLUS SYBR-Green master mix (Primer design) or using standard Taqman Gene expression probes (Invitrogen) on a Bio-Rad i-Cycler PCR machine, all assays were performed in triplicate and are normalised to levels of β -Actin house keeping gene or GAPDH. Fold changes were calculated using the $\Delta\Delta C_t$ method. Total miRNA was isolated using PureLink miRNA isolation kit (Invitrogen). cDNA was prepared and qPCR was performed using Taqman miRNA Assays (Life Technologies) according to the manufacturer's protocol, all assays were performed in triplicate and are normalised to levels of U6.

Table 2.1: Primer sequences for gene expression assays.

Gene	Sense/ Forward primer 5'→3'	Anti-sense/ Reverse primer 5'→3'
<i>mTrib1</i>	GTCCCGTGCCTTTTGCCTGAG	CCCGCGTCGTCCGTGTCCAG
<i>hsTRIB1</i> (Taqman)	CCCCAAAGCCAGGTGCCT	TACCCGGGTTCCAAGACG
	Probe: CAGCCTCTTGAGACGGGGA	
<i>hsTRIB1</i>	CCGAATTCATGCGGGTCGGTCCG GTGCGC	CGCGGCCGCTTAGCAGAAGAAGGA ACTAATG
<i>mNOS2</i>	AAGAGGC AAAAATAGAGGAACA TC	TGGTAGGTTCTGTTGTTTCTAT
	Probe: TCCTTTGTTACAGCTTCCAGCCTGGCAAAGGA	
<i>mCD206</i> (MRC1, Taqman)	AGATGGGTGGGTTATTTACAAAG A	ATATTTCCATAGAACTTCTTTTCA CTT
	Probe: CACTCGCGCATTGTCCATGGTTTCCTTCTCGAGTG	
<i>mARG1</i>	CGGAGACCACAGTTTGGC	TGGTTGTCAGTGGAGTGTG
	Probe: CTGTCAGTGTGAGCATCCACCCAAATGACTCTGACAG	
<i>mIL-15</i>	GACACCACTTTATACACTGACAG TG	TCACATTCCTTGCAGCCAGA
<i>mAcaca</i>	Gene Expression Assay #4331182 (Invitrogen)	
<i>mFasn</i>		
<i>mScd1</i>		
<i>mGapdh</i>		
<i>mβ-Actin</i>	GGGACCTGACAGACTACCTCATG	GTCACGCACGATTTCCCTCTCAGC
<i>mOLR1</i>	AGATAGACACCCTCACCTTGAA	TGTGGACAAGGACCTGAAAAGT
<i>mCXCL16</i>	GAGCGCAAAGAGTGTGGA ACT	GACTATGTGCAGGGGTGCTC
<i>mSCARB1</i>	GATGGAGAGCAAGCCTGTGA	CGAAGGGATCGTCATAGCCC
<i>mCD68</i>	AAGGGGGCTCTTGGGA ACTA	CCAAGCCCTCTTTAAGCCCC
<i>mMARCO</i>	GACAAGCCCTTCTTCTCGCT	AGTTGCTCCTGGCTGGTATG
<i>mCD163</i>	CAGCGTAGTCTGCTCACGAT	TAGATTGGGCAACCCACAC

Abbreviations: Hs, Homo sapiens; m, mouse.

2.6 Western blotting

Cells were lysed in ice-cold lysis buffer (1% Triton v/v X-100, 50mM Hepes, 100mM NaF, 10mM EDTA, 10mM sodium-pyrophosphate, 10% (v/v) glycerol) in the presence of phosphatase inhibitors (PhosphoSTOP, Roche) and protease inhibitors (cOmplete mini protease inhibitor cocktail, Roche) as per manufacturer's instruction. If necessary, cells were sonicated three times for 15 seconds to complete cell lysis and shear DNA. Cell lysates were centrifuged at 15,000x g for 15 minutes

at 4°C and the supernatant was transferred to a fresh eppendorf tube and pellet was discarded. 20µg of sample protein was added to equal volume of 2x laemmli buffer (4% SDS (w/v), 10% (v/v) 2-mercaptoethanol, 20% (v/v) glycerol, 0.0004% (w/v) bromophenol blue, 0.125M Tris-HCl, pH 6.8). Each cell lysate was then boiled for 5 minutes at 95°C. Equal amounts of protein was loaded into the wells of a NuPAGE® 4-12% Bis-Tris SDS-PAGE gel (Novex®) together with a standard protein size marker and electrophoresed at 200V for 35 minutes in MES SDS Running buffer (50mM MES, 50mM Tris Base, 0.1% (w/v) SDS, 1mM EDTA, pH 7.3, Novex®). Proteins were transferred onto a nitrocellulose membrane at 35V for 1 hour in 1x transfer buffer (5% (v/v) 20x transfer buffer, 0.1% (v/v) antioxidant (NuPAGE®), 20% (v/v) methanol, Novex®). To confirm efficient transfer, the membrane was stained with Ponceau S (0.2% (w/v) Ponceau S, 5% glacial acetic acid) and washed in 5% (w/v) Marvel TBST (20mM Tris pH 7.5m 150mM NaCl, 0.1% (v/v) Tween 20). The membrane was blocked in 5% (w/v) Marvel TBST for 1 hour RT or overnight at 4°C. TRIB1 primary antibody (Rabbit polyclonal, Millipore) was diluted 1:1000 in 5% (w/v) Marvel TBST for 1 hour RT or overnight at 4°C. The membrane was washed 3 x for 5 minutes in TBST and incubated with anti-rabbit HRP-conjugated secondary antibody (1:2000, Marvel TBST, Vector Laboratories) for 1 hour RT. The membrane was washed again 3 x 5 minutes in TBST. Specific protein bands were detected by the addition of chemiluminescent substrate (ECL prime western blotting detection reagent, GE Healthcare) and exposure to x-ray film (Fuji). The membrane was stripped in 1x ReBlot solution (Millipore) for 20 minutes at RT and probed for tubulin loading control protein (1:1000, Marvel TBST, Santa Cruz) using anti-mouse HRP-conjugated secondary antibody (1:2000, Vector Laboratories).

2.7 Colourimetric immunohistochemistry

2.7.1 Standard protocol

Slides were de-waxed and re-hydrated through graded alcohols to water as follows; xylene (10 minutes minimum), 100% (v/v) EtOH; 100% (v/v) EtOH; 90% (v/v) EtOH; 70% (v/v) EtOH; 50% (v/v) EtOH, water). Endogenous peroxidases were blocked by incubation in 3% (v/v) hydrogen peroxide for 10 minutes and rinsed in tap water. To block non-specific binding of the secondary antibody, slides were incubated using appropriate blocking buffer (1% (w/v) Marvel buffer or 5% serum)

for 30 minutes at room temperature. Slides were then incubated with 1° antibody in PBS for 1 hour at RT or overnight at 4°C in a humidified chamber and subsequently washed 3x in PBS for 5 minutes each. Slides were incubated with biotinylated 2° antibody in PBS for 30 minutes at RT and washed 3 x in PBS for 5 minutes each. Slides were then incubated with VECTASTAIN® Avidin/Biotinylated enzyme complex (ABC) or VECTASTAIN® ABC Horse radish peroxidase (HRP) enzyme complex (Vector laboratories) for 30 minutes at room temperature and again washed 3 times in PBS for 5 minutes. Enzyme substrate (SIGMAFAST 3, 3'-Diaminobenzidine; DAB or Vector Red Alkaline phosphatase substrate, Vector laboratories) was added to the slides for ~10 minutes and rinsed in tap water. Nuclei were counterstained with Carazzi's Haematoxylin for 1 minute followed by rinsing in tap water. Slides were de-hydrated through graded alcohols (opposite to first step) to xylene and mounted with coverslips using DPX mountant. Specific staining methods and antibody information is detailed in **Appendix IV**.

2.8 Statistical analysis

All data presented are shown as mean \pm SEM. Results were then analysed by appropriate statistical test by either Student's t test or analysis of variance (ANOVA) with specific post test as described in the figure legends. Linear regression and Pearson correlation coefficient were calculated to determine correlation. R^2 is reported along with level of significance, set at $p < 0.05$ for all data. Graphs were generated and analysis performed using GraphPad Prism software.

Chapter 3. Myeloid TRIB1 alters plasma lipid homeostasis

3.1 Introduction

Genome wide association studies have provided novel insight into genetic loci associated with plasma lipid traits, among them is the genomic region 8q24 at which a group of non-coding variants are associated with major plasma lipid traits including low-density lipoprotein cholesterol (LDL), high-density lipoprotein cholesterol (HDL) and triglycerides (TG) (Willer et al., 2013, Teslovich et al., 2010). Interestingly however, the same region is also significantly associated with developing coronary artery disease including MI (Deloukas et al., 2013). *TRIB1* has been identified as the only gene that is associated with *all* the traits. Previous studies using full body *Trib1* knockout and hepatic specific over-expression models validated the GWAS findings and demonstrated *TRIB1* to be a regulator of plasma lipid levels, where loss of *Trib1* elevated levels of plasma triglyceride and cholesterol. Equally, hepatic over-expression of *Trib1* reduced plasma triglyceride and cholesterol (Burkhardt et al., 2010).

Similarly, studies by Satoh et al. (2013) demonstrated *Trib1* to be a critical regulator of macrophage polarisation, the loss of which results in a severe reduction in ‘M2’ anti-inflammatory macrophages in various organs.

The liver is the main site of plasma lipid homeostasis and contains tissue-resident macrophages. However, the potential interplay between *Trib1*, macrophages and hepatocytes remains unexplored.

To explore this further, *Trib1*-knockout ($Trib1^{KO}$) and *Trib1*-transgenic mice ($Trib1^{Tg}$) were generated and crossed with a strain of mice expressing Cre recombinase under the control of the well characterised *Lyz2* promoter to generate myeloid specific transgenic and knockout strains (**Figure 2.1, 2.2**) Cre-mediated deletion is a useful and efficient tool to enable activation of gene expression in a tissue specific manner when under the control of specific promoters (Abram et al., 2014). In these mice, the activity of Cre recombinase was mediated under the control of the *Lyz2* promoter, a promoter that is expressed in granulocytes (monocytes, macrophages and neutrophils). Using this system therefore it was possible to delete

or overexpress *Trib1* in monocytes and tissue macrophages. The activity of Cre recombinase has been shown to be highly efficient and causes 60% deletion in blood monocytes and 40-100% deletion in tissue macrophages such as peritoneal and splenic macrophages (Abram et al., 2014).. Similarly, the *Rosa26* locus ubiquitously expresses high levels of inserted transgene uniformly in all tissues with no side effects to offspring. Since its first discovery, *Rosa26* has been widely used to permit stable transgene expression (Friedrich and Soriano, 1991). In this study, the use of loxP sites flanking the STOP codon in *Rosa26.Trib1^{Tg}* mice enabled activation of gene expression in myeloid cells by Cre mediated recombination (*Lyz2Cre*).

3.2 Hypothesis

In this chapter, myeloid specific (*LyzMCre*) *Trib1* conditional knockout (KO) and over-expressor mice were developed and the consequences were fully characterised. Based on the literature, I hypothesise myeloid expression of *Trib1* regulates plasma lipid homeostasis and the polarisation state of macrophages that may contribute towards metabolic syndromes.

3.3 Materials & Methods

3.3.1 Animals

Trib1 x *LyzMCre* mice were fed *ad libitum* on standard chow diet. The majority of experiments used wild-type *Trib1* littermates as controls. Where required, male C57BL/6 mice were used as controls and were obtained from Charles River Laboratories and fed *ad libitum* on a standard chow diet. Where appropriate the use of C57BL/6 mice are clearly described in the figure legends.

3.3.1.1 High fat diet

Male C57BL/6 mice were fed on 60% high fat diet for 12 weeks (Special Diet Services, Witham, UK).

3.3.1.2 Peritonitis

C56BL/6 mice received an intraperitoneal injection of 1 ml of 4% thioglycollate broth and were sacrificed 24 hrs post-injection. Plasma lipid fractions were analysed as described below.

3.3.2 Morphometry

To assess tissue morphology, adipose and liver tissues were stained with haematoxylin and eosin (H&E). Images were captured using a standard bright field microscope (Nikon Eclipse E600), mean area of adipocytes were measured by NIS-Elements Software (Nikon Instruments, UK) by obtaining measurements from at least 15 cells per field of view (3 fields of view per mouse). A detailed description of tissue processing and analysis can be found in **section 2.2**.

3.3.3 Lipid profiling

Plasma was obtained from blood as described in **section 2.1.5** and stored at -80°C until analysis. Frozen plasma was sent to Royal Hallamshire Hospital (Sheffield Teaching Hospitals) Department of Clinical Chemistry. A full lipid profile including total cholesterol, low- (LDL) and high- density lipoproteins (HDL), triglycerides and glucose was obtained using Roche Cobas 8000 modular analyser series (study code CVTRIB- 70/7992). For detailed analyses into lipid subclasses, plasma was sent to Professor Ronald Krauss, Children's Hospital Oakland Research Institute, California, USA for analyses. Plasma lipids were directly measured as a function of their size and ion mobility, a technique based on gas-differential electric mobility as described previously (Caulfield et al., 2008, Otvos et al., 1992).

3.3.4 Immunohistochemistry

Immunohistochemistry was carried out on frozen mouse spleens to assess presence of 'M2' macrophages. Tissues were sectioned using a cryostat (7µm) and left overnight at room temperature to air dry. Tissues were fixed in ice-cold acetone for 5 minutes and air-dried. Sections were re-hydrated by dipping in PBS. Sections were blocked with 5% (v/v) BSA, room temperature for 30 minutes and incubated with either F4/80 (PE- rat anti-mouse F4/80, BioLegend) or CD206 (Alexa Fluor- rat anti-mouse CD206, BioLegend) directly- conjugated primary antibodies at 1:200 (PBS), 1 hour at room temperature. Sections were washed 3x PBS, 5 minutes and mounted using coverslips and Aquamount (Thermo Scientific). Images were visualised on a Leica inverted wide-field fluorescence microscope (Leica AF-6000).

To assess Kupffer cell phenotype, FFPE liver tissue was stained with macrophage phenotype markers. Sections were de-waxed and rehydrated and endogenous peroxidases were blocked by incubation in 3% hydrogen peroxide for 10 minutes, room temperature followed by enzyme induced antigen retrieval by treating with trypsin (A. Menarini Diagnostics, UK) for 15 minutes according to the manufacturer's protocol and permeabilised with 0.1% (v/v) Triton x-100 for 15 minutes. Tissues were incubated with rat anti-F4/80 (1:50) for 1h at room temperature and then with a secondary biotinylated rabbit anti-rat antibody (1:200, Vector Laboratories, UK). Finally, tissues were incubated with Streptavidin-PE (1:20, Biolegend) for 30 minutes, room temperature. Sections were re-blocked in 5% (v/v) donkey serum and incubated with either mouse anti-mouse IRF-5 (Interferon regulatory factor-5, Abcam) or rabbit anti-mouse Ym1 (Anti-Chitinase like-protein 3, Abcam). Tissues were then incubated with either donkey anti-mouse or donkey anti-rabbit NL493 (1:100, Northern Lights) for 1h at room temperature. Tissues were mounted using ProLong Gold anti-fade mountant with DAPI (Molecular Probes) and visualised on a Leica inverted wide-field fluorescence microscope (Leica AF-6000). Fluorescent images were analysed by ImageJ and although both F4/80-positive and F4/80-negative cells were positive for IRF-5 or Ym1, only cells that were F4/80-positive were included in the analysis to ensure Kupffer cell specificity. Relative IRF-5 or Ym-1 staining is normalised to levels of F4/80-positive cells.

3.3.5 Flow Cytometry

Macrophage phenotype was assessed using BMDMs by fluorescence activated cell sorting (FACs). Bone marrow was flushed from the tibiae of *Trib1 x LyzMCre* mice as described in **section 2.4.1.2** and polarised to 'M1', 'M2a' or 'M2c'. An Fc block was performed (1µg/pellet/100,000 cells). Staining was performed in FACs buffer (1x PBS, 5% (v/v) FCS) using 0.1µg antibody (Alexa Fluor 647 rat anti-mouse CD206, BioLegend or Alexa Fluor 488 rat anti-mouse CD204, AD Serotec) per sample for 15 minutes at 4°C. Cells were washed twice with FACs buffer by centrifugation (450xg, 5 minutes) and re-suspended in 200µl FACs buffer before analysis via flow cytometry (BD LSRII). Data was analysed using FlowJo software. Isotype and 'fluorescence minus one' (FMO) controls were used to determine positively stained cells in each sample. Samples were gated according to the strategy described in Bou Ghosn et al. (2010).

3.3.5.1 Expression of *Trib1*- transgene (GFP) in monocytes and macrophages

Peripheral blood from mice was collected by cardiac puncture in the presence of heparin as an anti-coagulant. Blood from 3-4 mice was pooled according with experimental requirements and were subject to density gradient centrifugation by incubation with 1.25% (w/v) dextran, RT for 30 minutes. Monocytes were isolated using positive selection by magnetic beads conjugated with F4/80 and CD115 (Miltenyi Biotec). After centrifugation PBMCs were resuspended in 80µl MACS buffer (Miltenyi Biotec) and 20µl of F4/80 and CD115 microbeads were added (per 10^7 total cell) to each sample. Cells were incubated at 4°C for 15 minutes. Samples were washed with MACS buffer and magnetically sorted using MS Columns (Miltenyi Biotec). Purified monocytes were washed, resuspended in MACS buffer and subject to flow cytometry (BD LSRII) for the presence of GFP. Data was analysed using FlowJo software.

3.3.6 Microarray

Human MDM data was derived from published microarray datasets from the Cardiogenics study which includes patients with coronary disease and healthy individuals of European descent recruited in five centres; Cambridge (UK), Leicester (UK), Lübeck, Regensburg and Paris (Heinig et al., 2010, Rotival et al., 2011, Schunkert et al., 2011). Re-analyses of the data set was performed in collaboration with Professor Alison Goodall and Dr. Stephen Hamby (University of Leicester, UK). For full method details referring to the Cardiogenics dataset, please refer to the cited publications. Briefly however, total RNA from human MDMs was isolated from whole blood. Gene expression profiling was performed using the Illumina's Human Ref-8 Sentrix Bead Chip arrays (Illumina Inc., San Diego, CA) containing 24,516 probes corresponding to 8,311 distinct genes and 21,793 Ref Seq annotated transcripts. mRNA was amplified and labelled using the Immunia Total Prep RNA Amplification Kit (Ambion). After hybridisation, array images were scanned using the Illumina BeadArray Reader and probe intensities were extracted using the Gene expression module of the Illumina's Bead Studio software. Raw intensities were processed in R statistical environment using the Lumi and beadarray packages. All array outliers were excluded and only arrays with high concordance in

terms of gene expression measures (pairwise Spearman correlation coefficients within each cell type >0.85) were included in the analyses. Identification of pathways was performed using QuSAGE (Yaari et al., 2013). The study was approved by the Institutional Ethical Committee of each participating centre.

3.3.7 Stimulation of HepG2 cells

HepG2 cells were maintained in appropriate growth medium (detailed in **section 2.4.1**) at 37°C in a humidified 5% CO₂ incubator. Cells at ~80% confluence were trypsinised and washed with PBS before being seeded in a 6 well plate. 24 hours after seeding, cells were stimulated with 100ng/ml IL-1β (Peprotech) and 50mM glucose for 24 hours. Treatment was stopped by washing the cells with PBS, cell pellets were then frozen at -80°C for RNA extraction.

3.3.8 Hepatic Lipid measurements

Hepatic triglyceride was measured by colorimetric assay (Thermo Scientific™ Triglycerides reagent) using 20mg of liver tissue homogenized in PBS from *Trib1* WT, *Trib1* knockout (*Trib1 fl/fl* x *LyzMCre*) and *Trib1* transgenic (*ROSA26.Trib1* x *LyzMCre*) mice. Cholesterol content was also measured by colorimetric assay (Thermo Scientific™ Total Cholesterol reagents) from the same liver homogenates.

3.3 Results

3.3.1 Expression of *Trib1* in *Trib1* x *LyzMCre* mice

To validate expression of *Trib1* in myeloid cells, *Trib1* mRNA levels were measured in BMDMs derived from *Trib1 fl/fl* x *LyzMCre* mice via qPCR. **Figure 3.1A(i)** shows *Trib1* expression to be reduced by approximately 70% compared to litter mate control mice (p<0.01).

To validate expression of *Trib1* in the *ROSA26.Trib1* x *LyzMCre* mice, expression of *Trib1* mRNA in BMDMs derived from these mice were measured via qPCR.

Figure 3.1A(ii) shows *Trib1* expression is overexpressed by approximately 2-fold compared to WT BMDMs ($p < 0.01$).

To validate *Trib1*-transgene expression further, the transgene tag GFP was used as a surrogate marker. **Figure 3.1B** shows the percentage positive GFP cells in both blood monocytes and peritoneal macrophages as measured by FACs. 60-80% of monocytes and macrophages are GFP positive indicating a good level of transgene expression. Tissue expression of GFP was also assessed of GFP by examining frozen liver tissue sections from these mice by fluorescence microscopy, GFP expression was seen in the livers of ROSA26.*Trib1* mice and no detectable GFP expression in litter-mate control mice (**Figure 3.1C**).

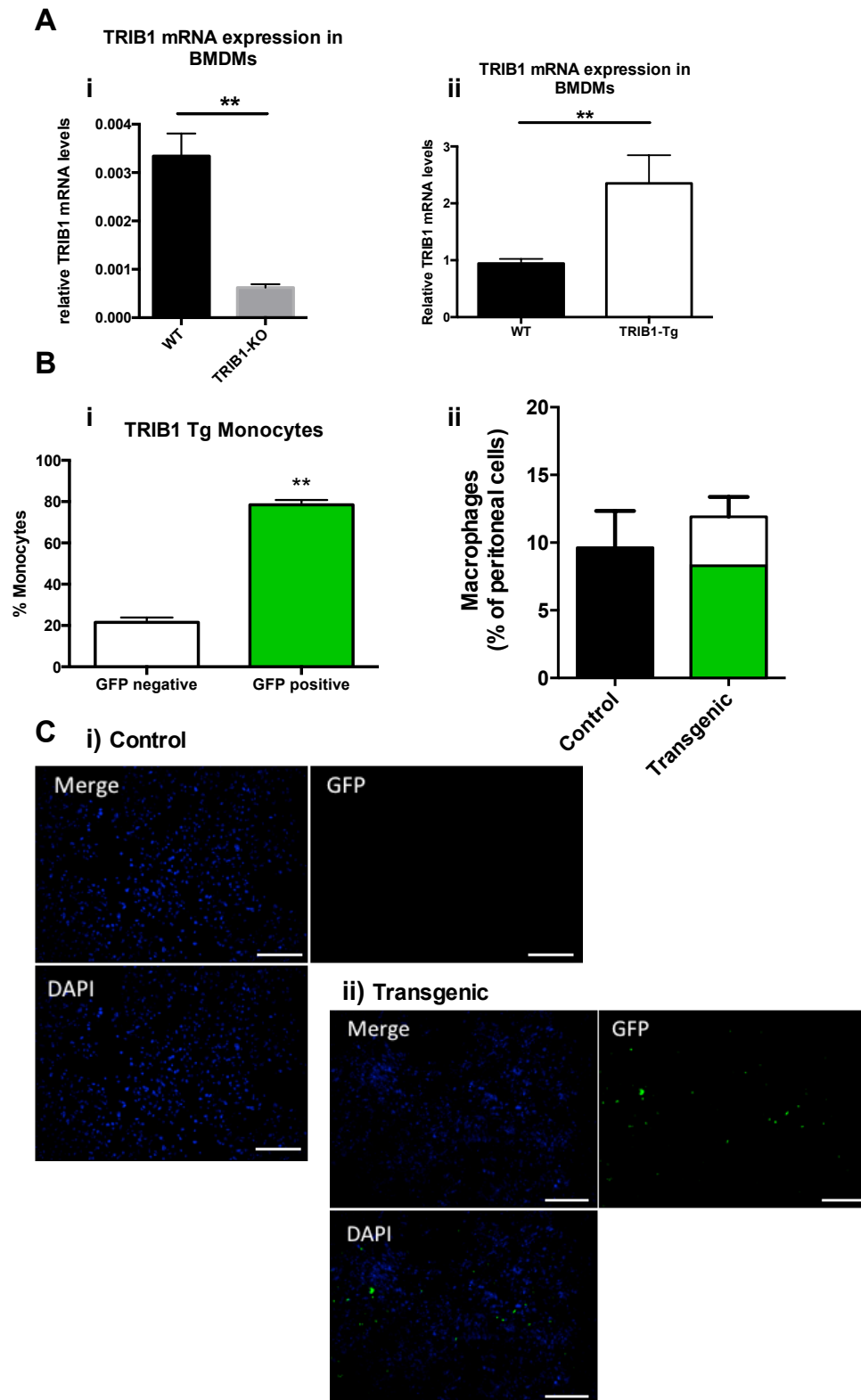


Figure 3.1: Expression of *Trib1* in myeloid *Trib1* knockout (*Trib1* floxed \times *LyzMCre*) and *Trib1* transgenic (*ROSA26.Trib1* \times *LyzMCre*) mice.

(A) Total RNA was purified from *Trib1* knockout (i), *Trib1* transgenic (ii) and WT littermate BMDMs. The level of *Trib1* mRNA expression was assessed by qPCR and normalised to β -Actin (house keeping control) (n=3-9/ group). (B) *Trib1* transgene expression was measured by assessing % GFP positive cells in blood monocytes (n=3) and peritoneal macrophages (n=3) from *ROSA26.Trib1* (transgenic) mice by flow cytometry. (C) *Trib1* transgene expression in liver tissue sections of *ROSA26.Trib1* mice (ii) and littermate controls visualised via fluorescence microscopy (Leica AF6000) (i). Graphs represent mean \pm SEM, **p<0.01, two-tailed Student's t test (A & B). Data in A(i) and B(i) were generated and provided by A.Angyal.

3.3.2 *Trib1* floxed x *LyzMCre* & *ROSA26.Trib1* x *LyzMCre* mice have normal tissue anatomy

As my group were the first documented study to generate myeloid specific *Trib1* knockout and transgenic mice, it was important to characterise tissue anatomy and compare our model to other models in the literature. A study published by Yamamoto et al. (2007) using a *Trib1*^{-/-} mouse model reported that they had a slight growth retardation with reduced body weight. Similarly, a study published by Satoh et al. (2013) reported lipodystrophy in WT mice transplanted with *Trib1*^{-/-} bone marrow.

3.3.2.1 Gross anatomy

Upon dissection of these mice it appeared they had normal and comparable tissue anatomy to their WT littermates with no obvious enlargements or tissue atrophy. Representative gross anatomy photos of each mouse model together with mean body weight at 13 weeks of age can be found in **Figure 3.2** and suggests normal body weight and no evidence of growth retardation.

3.3.2.2 Liver and Adipose

Tissue was characterised further by staining FFPE liver and adipose tissue sections with haematoxylin and eosin (H&E). **Figure 3.2C** shows liver tissue cross sections with no notable pathology. Similarly, adipose tissue cross-sections were unremarkable, quantification of adipocyte size showed no differences and lack of lipodystrophy (**Figure 3.2D**).

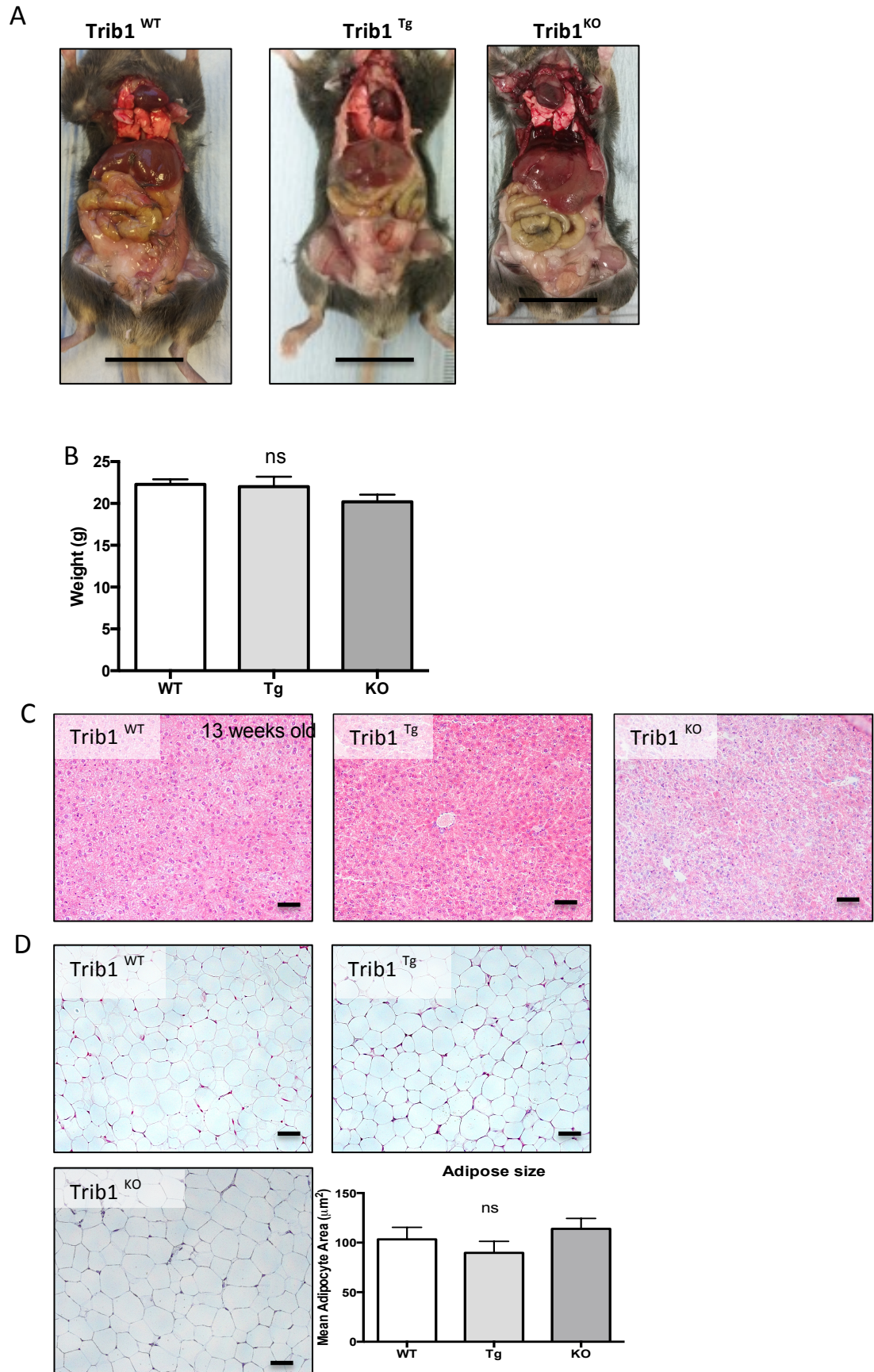


Figure 3.2: *Trib1* transgenic and KO mice have normal tissue anatomy

(A) Gross anatomy photos of *Trib1*^{WT} littermate controls, *Trib1*^{Tg} and *Trib1*^{KO} mice (scale=2cm) showing comparable anatomy and no difference in weight at 13 weeks of age (n=5-9) (B). FFPE Liver (C) and adipose tissue (D) cross sections from these mice were stained with haematoxylin and eosin (H&E) and show normal tissue anatomy and comparable adipocyte size, n= 3-7, scale = 20 μ m. Images were taken using a light microscope x200 magnification (Nikon Eclipse E600) and analysed using NIS Elements Software (Nikon Instruments, Kingston Upon Thames, UK). Representative images are shown. Graphs represent the mean \pm SEM, ns= non significant

3.3.3 Myeloid *Trib1* does not affect white blood cell count

Satoh et al. (2013) reported reduced levels of monocytes, neutrophils and eosinophils in their *Trib1*^{-/-} mouse. To ascertain if these mouse models also had reduced levels of white blood cells, whole blood counts were measured from myeloid *Trib1* knockout mice. As shown in **Figure 3.3A**, no differences in the level of white blood cells including lymphocytes, monocytes and neutrophils were found.

3.3.4 Myeloid *Trib1* does not influence expression of macrophage markers in the spleen

Satoh et al. (2013) also showed that *Trib1* deficiency results in a severe reduction in M2 (anti-inflammatory) macrophages in various organs including the spleen. They also reported the absence of tissue macrophages in splenic red pulp. Macrophages located in splenic red pulp are critical for maintenance of blood homeostasis and actively phagocytose injured and senescent red blood cells. Frozen spleen sections were examined and stained with the pan macrophage marker F4/80 and the M2 marker CD206 (mannose receptor) from the *Trib1* x *LyzMCre* mice. Contrary to Satoh et al. (2013), F4/80+ macrophages were abundantly present in the red pulp in the spleen with no obvious differences between each of the mouse models (**Figure 3.3B**). Similarly, there was no reduction in M2 macrophage marker expression in the spleen.

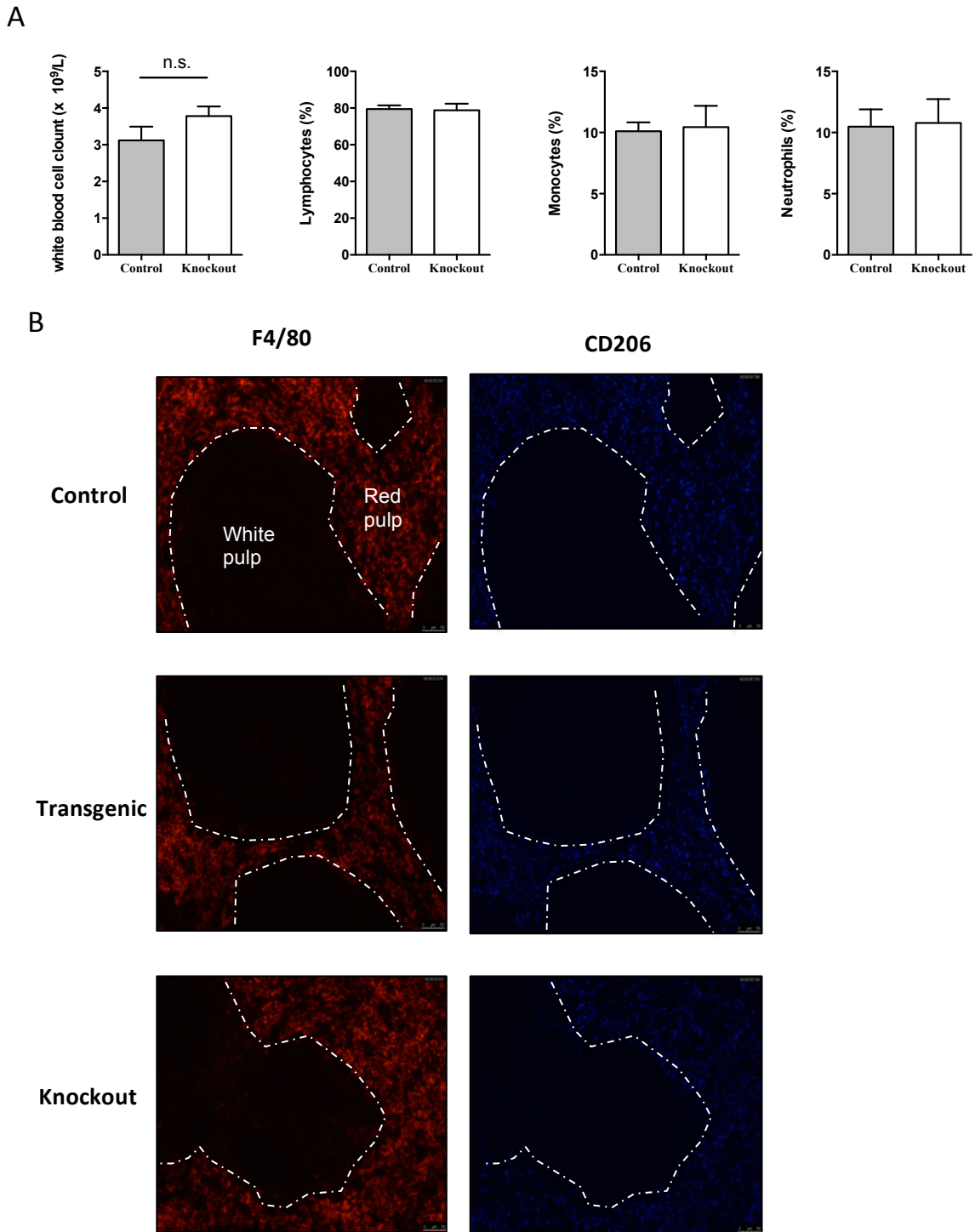


Figure 3.3: Myeloid *Trib1* does not alter white blood cell counts.

(A) Whole heparinised blood was taken via cardiac puncture from myeloid *Trib1* KO mice and WT littermate controls (n=5-6). White blood cell count together with percentage lymphocytes, monocytes and neutrophils were measured using a Sysmex whole blood counter. (B) Frozen spleens from *Trib1* transgenic and KO mice were stained for macrophage markers F4/80 (red) and CD206 (mannose receptor, blue). The spleens contained comparable levels of macrophages in the red pulp. Scale bars = 50 μ m. Representative images are shown. Graphs represent mean \pm SEM, n.s= non significant. Data was generated and provided by A.Angyal.

3.3.5 Myeloid *Trib1* alters plasma lipid homeostasis

3.3.5.1 Myeloid *Trib1* alters plasma lipid homeostasis

Numerous studies have shown hepatic TRIB1 to regulate lipogenesis (Burkhardt et al., 2010, Bauer et al., 2015) however, the potential effects of *myeloid Trib1* on hepatic lipogenesis have not been investigated. Plasma was subjected to lipid analyses and found that myeloid deficiency or over-expression of *Trib1* mirrors the phenotype of hepatic-specific *Trib1* models reported in the literature. **Figure 3.4A** shows that *Trib1* KO mice have significantly ($p < 0.05$) elevated levels of both triglyceride and VLDL cholesterol compared to control mice. *Trib1* transgenic mice however had reduced levels of VLDL cholesterol and statistically significant ($p < 0.05$) increased levels of the beneficial lipoprotein subclass; HDL-cholesterol.

3.3.5.2 Inflammatory challenge in C57BL/6 mice mirrors phenotype

Since, TRIB1 has been reported to specifically modulate VLDL production in mice (Burkhardt et al., 2010), the different subclasses of VLDL cholesterol were measured by ion mobility. Chronic inflammation and infection are known to cause increases in serum triglycerides and VLDL cholesterol. Therefore the VLDL cholesterol subclasses were measured in C57BL/6 mice that were subjected to high fat diet feeding and induction of peritonitis. **Figure 3.4B-C** shows that in both cases, the proportion of small VLDL particles were significantly ($p < 0.0001$) reduced in mice subjected to inflammation through diet or infection. Similarly, the proportion of large VLDL particles was also significantly ($p < 0.001$) increased in both models. Interestingly, the pattern seen in C57BL/6 mice was mirrored in *Trib1* KO mice, while *Trib1* transgenic mice showed the opposite. **Figure 3.4D** shows *Trib1* KO mice had an increased proportion of large VLDL cholesterol and reduced proportion of small VLDL cholesterol, suggesting that the loss of *Trib1* in myeloid cells may also induce systemic inflammation.

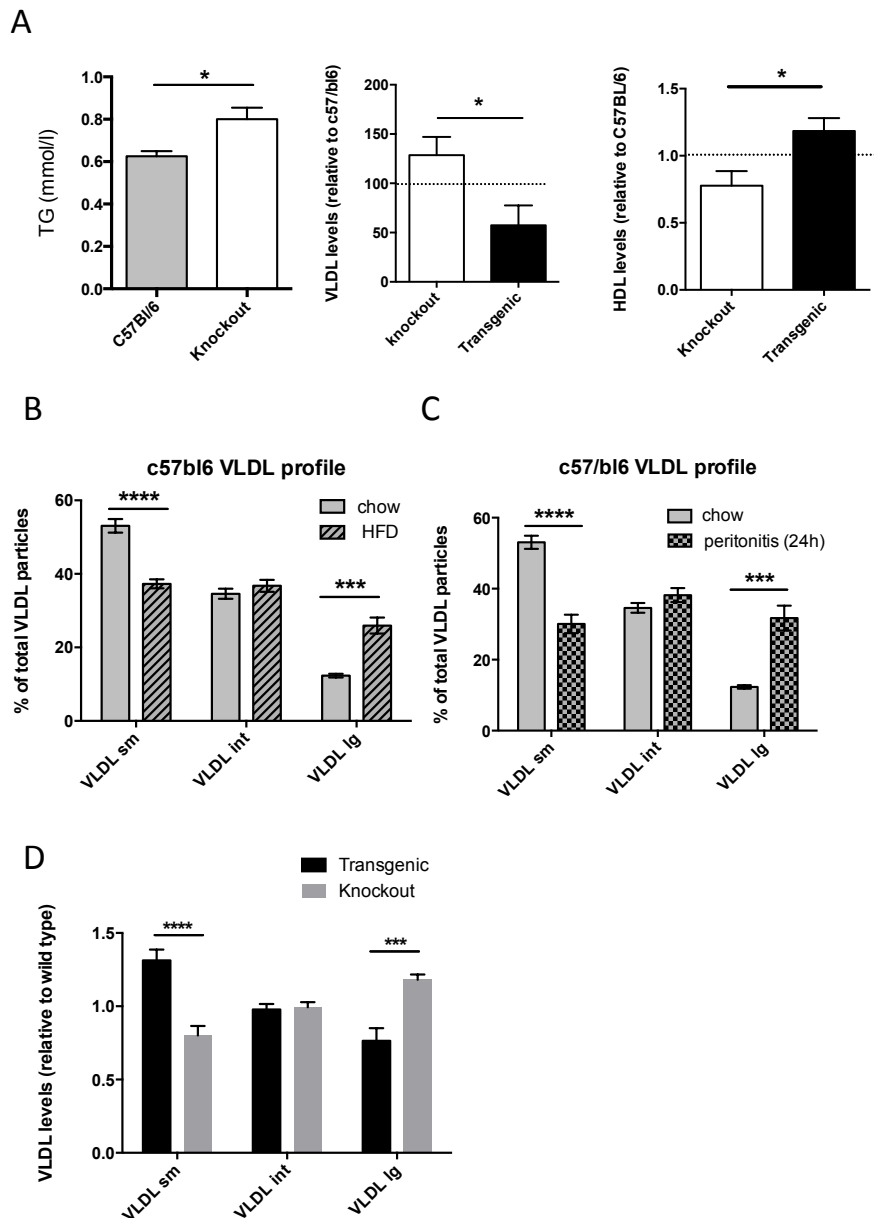


Figure 3.4: Myeloid *Trib1* alters plasma cholesterol levels

(A) Plasma lipid levels of *Trib1* mice. Ion mobility analysis was used for high resolution profiling of the abundance of lipoprotein fractions and the relative abundance of lipid fractions calculated for each mouse (A-D). (B) Male C57BL/6 mice were fed on chow vs. metabolic diet for 12 weeks and relative abundance of their lipid fractions were compared n=4-7, (C and E) C57BL/6 mice were injected with thioglycollate broth for 24 hrs n=3-7, (D) abundance of VLDL fractions was compared to and expressed relative that of wild type mice n=3-4. Analysis was performed in collaboration with Dr. Ron Krauss (Children's Hospital Oakland Research Institute). Graphs represent mean \pm SEM, *p<0.05, ***p<0.001, ****p<0.0001, unpaired student's t-test (A), ordinary two-way ANOVA (B & C).

3.3.6 *Trib1* x *LyzMCre* alters Kupffer cell phenotype *in vivo*

The results presented thus far have indicated myeloid specific *Trib1* alters plasma lipid levels. The liver is the site of most lipid metabolism in the body and since *Trib1* has been shown to be critical for the differentiation of tissue-resident M2-like macrophages (Sato et al., 2013) I hypothesised that the phenotype of tissue-resident cells in the liver known as Kupffer cells (KCs) may be altered. KCs are a major component of the endothelium lining of the blood vessels in the liver and act to phagocytose damaged red blood cells. The activation of KCs has been shown to be responsible for early ethanol-induced liver injury commonly seen in chronic alcoholics KC activation can lead to an increase of pro-inflammatory cytokine secretion which if sustained leads to liver fibrosis, cirrhosis and eventual failure (Wheeler, 2003, Beier and McClain, 2010). Evidence also exists that suggests KC activation is involved in the pathogenesis of non-alcoholic fatty liver disease (NAFLD) leading to discordant lipid metabolism and regulation (Dey et al., 2015). Therefore, *Trib1* may alter macrophage polarisation and thus the activation of KCs, which may alter the liver microenvironment and drive lipogenesis in this context.

3.3.6.1 Myeloid *Trib1* mice show no differences in F4/80+ macrophages in the liver or adipose

Increase in the level of macrophages through tissue infiltration is associated with chronic inflammation and this alone can modulate tissue environment (Lumeng et al., 2007, Lumeng and Saltiel, 2011). To ascertain if the level of tissue macrophages were responsible for the described phenotype, liver and subcutaneous adipose tissue sections were stained with F4/80 (n=3). **Figure 3.5A** indicates that there were no significant differences in the levels of tissue macrophages both in the liver and adipose tissue. As no differences were found in the level of macrophages, the phenotype of liver resident tissue macrophages were investigated.

3.3.6.2 Loss of *Trib1* in myeloid cells increases Kupffer cell expression of IRF-5

FFPE liver sections were dual stained with the pan-macrophage marker F4/80 and the pro-inflammatory marker IRF-5; which has been successfully used previously (Robbe et al., 2015). Although some cells were single and double positive for each

marker, only cells that were F4/80+ were included in the analysis to ensure macrophage specificity (**Figure 3.5B**). Despite the total number of macrophages not changing in the liver however, the proportion of IRF-positive macrophages were significantly increased (two-fold) in myeloid *Trib1* KO mice ($p < 0.01$), while *Trib1* transgenic mice show a significant (~50%) reduction in levels of IRF-5-positive macrophages ($p < 0.05$). Together this data suggest that the loss of *Trib1* in myeloid cells promotes a pro-inflammatory phenotype in liver tissue macrophages (**Figure 3.5C**).

3.3.6.3 Myeloid *Trib1* overexpression increases Kupffer cell expression of Ym1

Kupffer cells were also dual stained F4/80 and Ym1, an anti-inflammatory marker. **Figure 3.5D** shows that the proportion of anti-inflammatory macrophages were increased by ~70% ($p < 0.01$) in *Trib1* transgenic mice and reduced in *Trib1* KO mice by approximately 40% however, the data was not statistically significant ($p = 0.3$) (**Figure 3.5E**).

By combining the data, it was possible to calculate the M1/M2 phenotypic (IRF-5/Ym1) ratio of the Kupffer cells in the mice, where a ratio > 1 indicates a pro-inflammatory phenotype and a ratio of < 1 indicates an anti-inflammatory phenotype. **Figure 3.5F** illustrates that the loss of *Trib1* in myeloid cells activates Kupffer cells by shifting them to a pro-inflammatory phenotype ($p < 0.01$). Conversely, *Trib1* overexpression shifts the Kupffer cell phenotype to anti-inflammatory ($p < 0.05$).

Taken together, the data suggests *Trib1* is a modulator of macrophage phenotype both *in vitro* and *in vivo* and in agreement with published data (Satoh et al., 2013) indicates TRIB1 has anti-inflammatory actions.

3.3.7 Myeloid *Trib1* regulates macrophage polarisation in BMDMs *in vitro*

Next I wanted to investigate the molecular mechanisms by which *Trib1* may regulate macrophage polarisation.

3.3.7.1 The loss of *Trib1* promotes an ‘M1’ pro-inflammatory phenotype in BMDMs

To investigate mechanisms that underpins the observations seen *in vivo*, bone marrow from *Trib1* KO and *Trib1* transgenic mice were harvested from the femurs and tibiae and differentiated into bone marrow derived macrophages (BMDMs). BMDMs were then polarised to ‘M1’ and ‘M2a/c’ macrophage phenotypes. Markers of ‘M1’ and ‘M2’ macrophage polarisation were then assessed using qPCR (**Figure 3.6 A, D & E**) or flow cytometry (**Figure 3.6 B & C**). **Figure 3.6A** shows that the ‘M1’ pro-inflammatory marker NOS2 increased by three-fold in *Trib1* KO BMDMs compared to WT mice ($p < 0.05$).

3.3.7.2 Overexpression of *Trib1* promotes an ‘M2’ anti-inflammatory phenotype in BMDMs

Similarly, the ‘M2’ markers CD206 (mannose receptor) and CD204 (**Figure 3.5B-C**) were significantly decreased in *Trib1* KO BMDMs ($p < 0.01$) suggesting that macrophages that are deficient in *Trib1* exhibit a pro-inflammatory phenotype. Equally, *Trib1* transgenic BMDMs polarised to ‘M1’ show a significant decrease in the pro-inflammatory marker NOS2 ($p < 0.05$) and significant increase in the classic ‘M2’ marker ARG1 ($p < 0.05$). Together, this data suggests that macrophages overexpressing *Trib1* exhibit an anti-inflammatory phenotype *in vitro*.

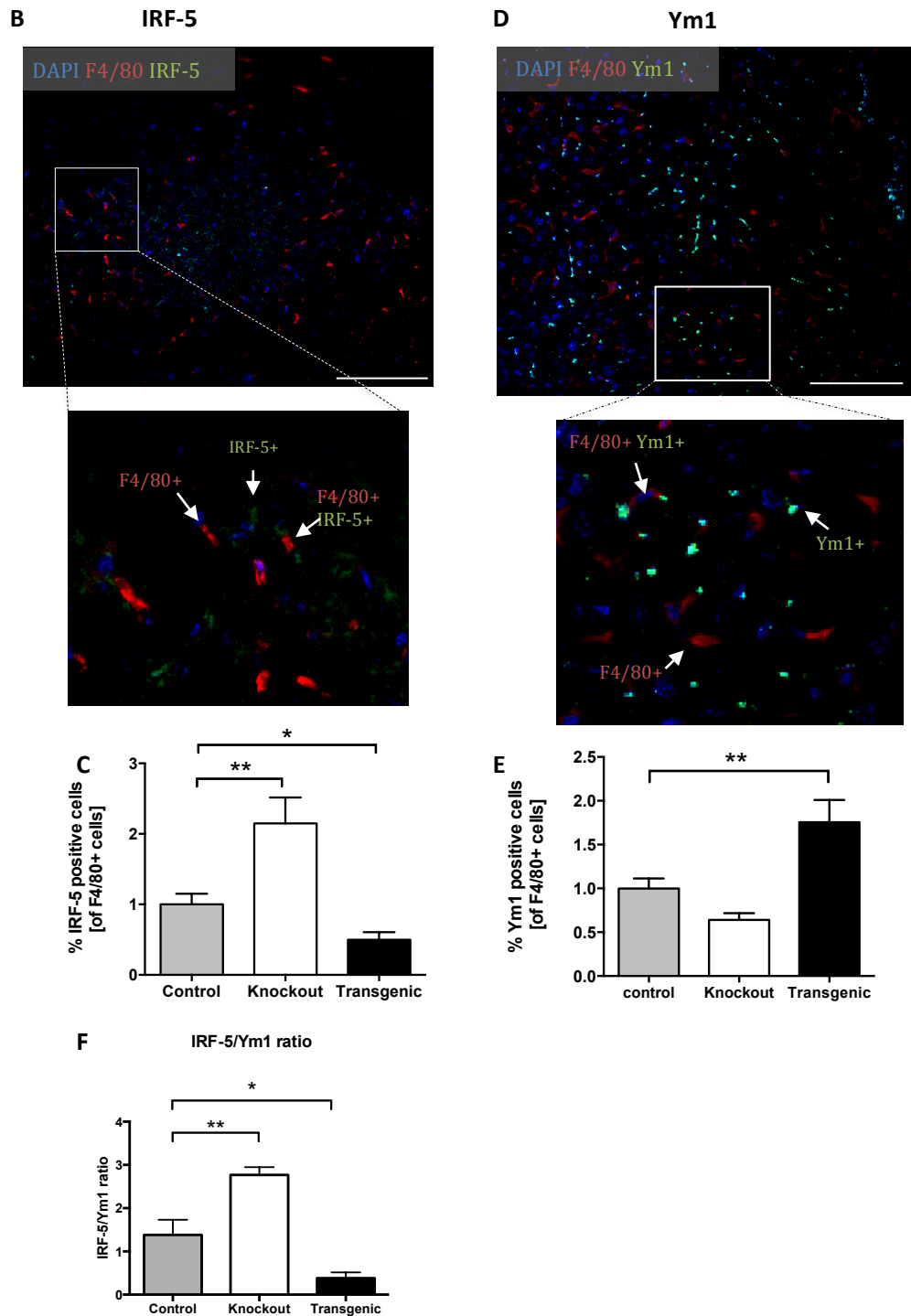


Figure 3.5: Myeloid *Trib1* alters Kupffer cell phenotype.

Formalin fixed paraffin embedded (FFPE) liver were dual stained with F4/80 and either the pro-inflammatory marker IRF-5 or the anti-inflammatory marker Ym1 to assess their phenotype. (A) The levels of F4/80+ cells in the liver and adipose were comparable between the groups (n=3). (B) Representative image of dual staining for F4/80 (red) and IRF-5 (green), although some cells were single and double positive for each marker (inset), cells that were only F4/80+ were included in the analysis ensuring macrophage specificity. (C) The resulting images were analysed by ImageJ and the graph shows % IRF-5 positive F4/80 cells (n=7-16). (D) Representative image of dual staining of F4/80 (red) and M2/anti-inflammatory marker Ym1 (chitinase like-3, green). (E) Graph shows the % positive Ym1 F4/80 cells (n=8-12). (F) M1:M2 (IRF-5:Ym1) ratio. Images were taken using Leica AF6000 fluorescent microscope (x20 lens), scale = 100 μ m. Graphs are presented as Mean \pm SEM, *p<0.05, **p<0.005, ordinary one-way ANOVA with Dunnett's multiple comparisons post test.

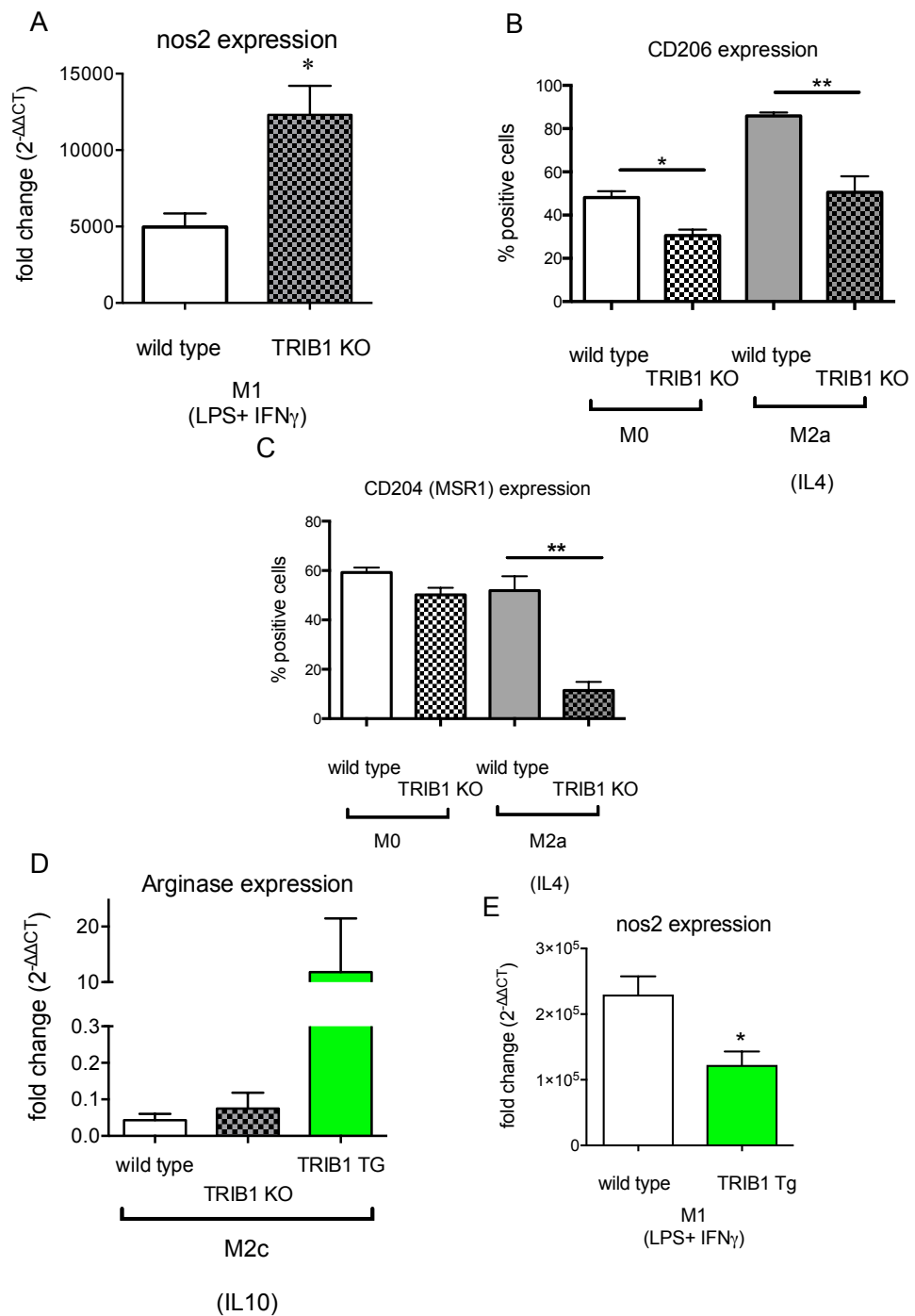


Figure 3.6: *Trib1* expression modulates macrophage polarisation in BMDMs.

Bone marrow derived macrophages (BMDMs) from *Trib1* KO (*Trib1 fl/fl x LyzMCre*) were generated using standard protocols and polarised into ‘M1’ macrophages with 100ng/ml LPS and 20ng/ml IFN- γ or ‘M2a’ with 20ng/ml IL-10 or ‘M2c’ with 20ng/ml IL-4 for 24 hours. (A) Expression of the pro-inflammatory marker *nos2* was assessed by qPCR along with anti-inflammatory markers CD206 (B) and CD204 (C) were assessed in *TRIB1* KO mice by flow cytometry (D) Similarly, expression of *Nos2* and the anti-inflammatory marker *Arg1* (E) was assessed in *Trib1* transgenic (*ROSA26.Trib1 x LyzMCre*) BMDMs polarised as above by qRT-PCR. Graphs represent the mean \pm SEM. * p <0.05, ** p <0.01; Student’s t-test (A,E), Ordinary one way ANOVA with Sidak’s multiple comparisons test (B-D). Data was generated and provided by A.Angyal & E.Hadadi.

3.3.8 TRIB1 regulates macrophage polarisation by modulating C/EBP α and C/EBP β expression

3.3.8.1 TRIB1 overexpression in RAW 264.7 cells down-regulates protein expression of C/EBP α

To investigate the molecular mechanisms of TRIB1 dependent modulation of macrophage polarisation, the protein expression levels of C/EBP α and C/EBP β were measured. C/EBP α and C/EBP β are both known transcription factors that regulate macrophage polarisation and have been shown to be themselves regulated by TRIB1. **Figure 3.7A** shows a representative western blot of C/EBP α from RAW264.7 (mouse monocyte-macrophage cell line) cell lysates transfected with a TRIB1-overexpression plasmid. Densitometry quantification revealed TRIB1 overexpression significantly down-regulates both C/EBP α isoforms p28 and p42 by $35 \pm 7\%$ ($p < 0.01$) and $17 \pm 6\%$ ($p < 0.05$), respectively (**Figure 3.7B**).

3.3.8.2 TRIB1 overexpression in RAW cells up-regulates protein expression of C/EBP β

Similarly, **Figure 3.7C** shows a representative western blot of C/EBP β , quantification revealed TRIB1 overexpression significantly up-regulates levels of C/EBP β in RAW cells by $58 \pm 20\%$ ($p < 0.05$) (**Figure 3.7D**).

3.3.8.3 TRIB1 regulates macrophage polarisation via miR-155 in BMDMs

The regulation of C/EBP α by TRIB1 via the ubiquitin ligase COP1 has been well documented in the literature (Satoh et al., 2013). However, it is unknown how TRIB1 may regulate C/EBP β expression. A recent publication by Arranz et al. (2012) showed that the PI3K induced kinase, Akt2 inhibits M2 polarisation by up-regulating miR-155. Interestingly, deletion of Akt2 reduced miR-155 expression, which in turn lead to increased levels of C/EBP β . As TRIBs are Akt inhibitors (Du et al., 2003), therefore I hypothesised that TRIB1 may be upstream of miR-155, modulating levels of C/EBP β expression. **Figure 3.7E** illustrates that when WT BMDMs were polarised to M2 macrophages (20ng/ml IL-10, 24 hours), the levels of miR-155 expression increased by 80%. However, in M2 polarised *Trib1* transgenic BMDMs, there is a failure to induce miR-155 expression, suggesting *Trib1* inhibits its expression. **Figure 3.7F** illustrates the proposed molecular mechanism of macrophage polarisation regulated by *Trib1*.

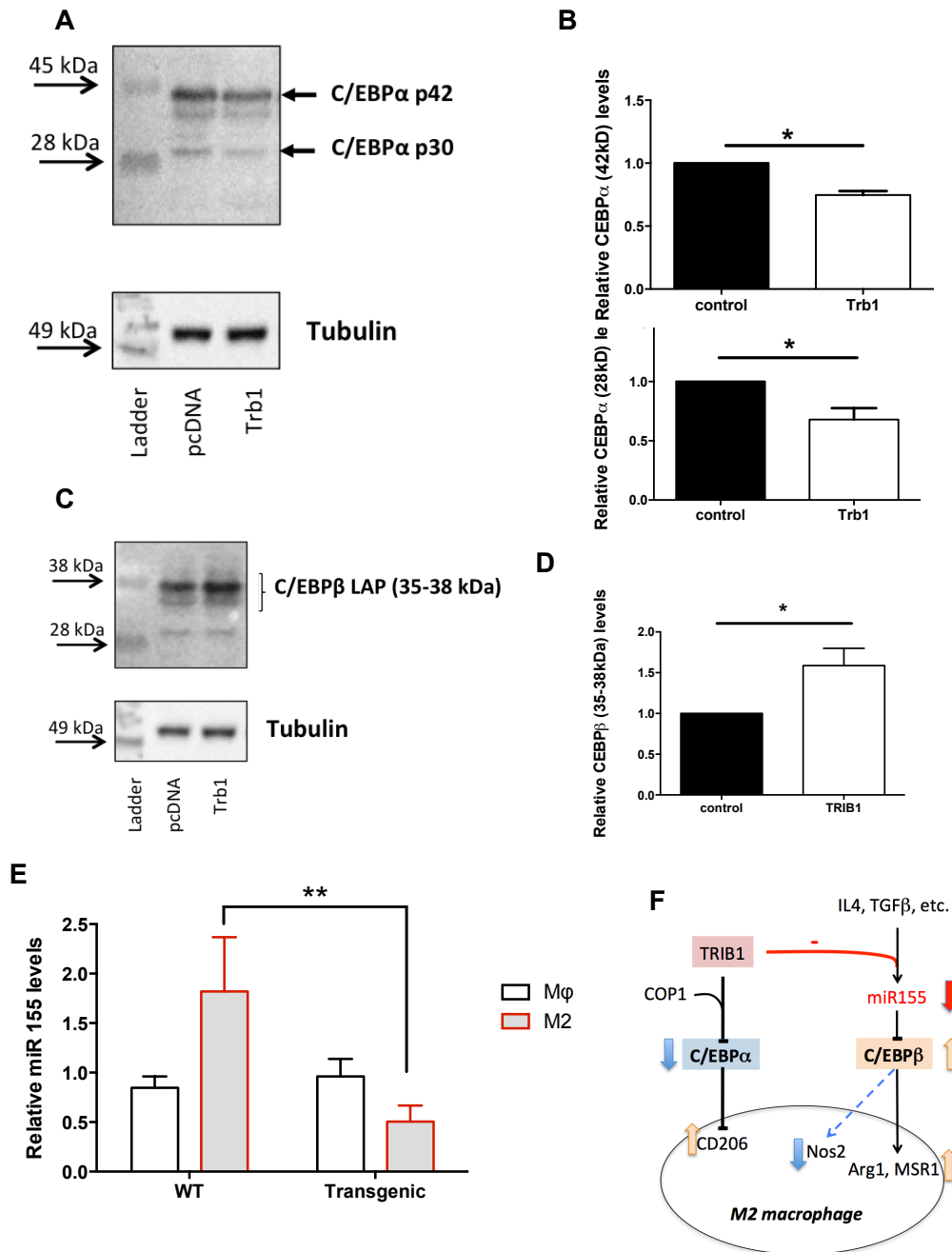


Figure 3.7: TRIB1 regulates macrophage polarisation via modulating *Trib1* regulates macrophage polarisation via modulating *C/EBPα* and *C/EBPβ* expression.

(A) RAW 264.7 cells were transfected with a TRIB1 over-expression plasmid and protein expression levels of C/EBP family members were assessed by western blotting. Representative blots of C/EBPα p42 and p39 are shown. (B) Quantification revealed over-expression of TRIB1 significantly reduces expression of both C/EBPα p42 and p39 isoforms. Results were obtained from three independent experiments. Levels of C/EBPα are normalised to tubulin. (C) Representative blot of C/EBPβ in TRIB1 transfected RAW264.7 cells, quantification shows levels of C/EBPβ is significantly increased (D), results were obtained from three independent experiments. Levels of C/EBPβ are normalised to tubulin. Graphs show Mean ± SEM, unpaired t-test, *p<0.05. (E) Expression levels of miR-155 in unpolarised (Mφ) and M2 polarised (20ng/ml IL-10, 24 hours) WT and *Trib1* transgenic BMDMs assessed by qRT-PCR (n=3-6). Levels of miR-155 expression is normalised to U6. Graphs show Mean ± SEM, two way ANOVA with Sidak's multiple comparisons test, **p<0.01. (F) Molecular mechanism by which TRIB1 controls macrophage polarisation by down-regulating C/EBPα through binding the ubiquitin ligase COP1 and up-regulating C/EBPβ via inhibiting miR-155, of which C/EBPβ is a known target. Data used in A-D was generated and provided by D.Szili.

3.3.9 *TRIB1* expression is associated with overexpression of alternatively activated macrophage markers in human MDMs

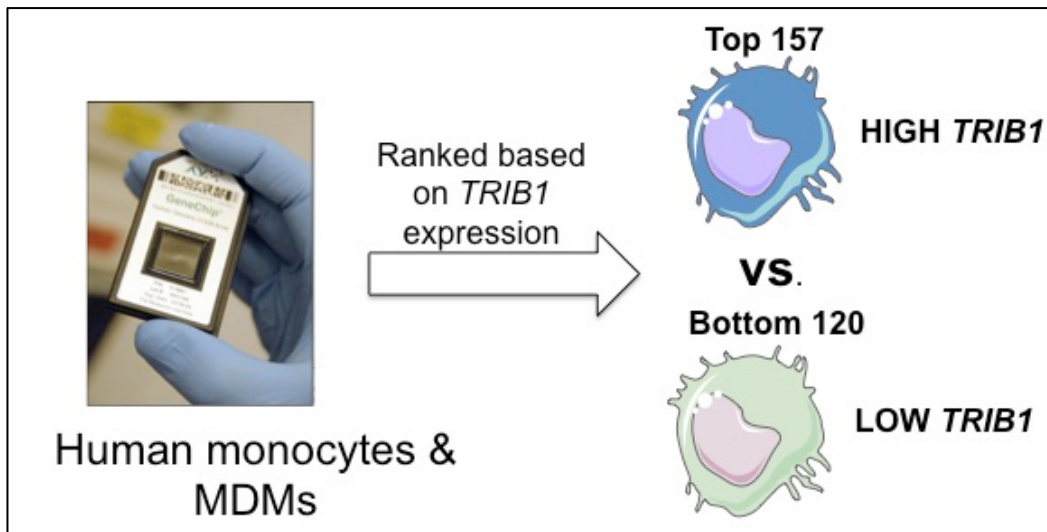
The data presented thus far has largely characterised the role of *TRIB1* in *mouse* macrophages. Therefore to establish if the observations seen in the mouse also occur in humans and to provide potential insight into the pathways affected, the Cardiogenics Consortium transcriptomic data set (Heinig et al., 2010, Rotival et al., 2011, Schunkert et al., 2011) were analysed (in collaboration with Professor Alison Goodall and Dr. Stephen Hamby, University of Leicester). Since monocytes are important in the pathogenesis of atherosclerosis, data from human monocytes as well as human monocyte derived macrophages (MDMs) were used. The data set contained RNA profiles of monocytes (n=758) and MDMS from 596 of these individuals that were subjected to microarray analyses (Illumina's Human Ref-8 Sentrix Bead Chip arrays (Illumina Inc., San Diego, CA)) and ranked based on *TRIB1* expression (**Figure 3.8A**), the top and bottom 25% were taken forward for analyses for expression of macrophage-subclass polarisation markers. The analyses found that there was no selective expression of M1 vs. non-M1 (alternative activation) markers in *TRIB1*-high *monocytes* (**Figure 3.8B**). However, in *TRIB1*-high *macrophages*, there was a selective up-regulation of alternative activation markers (**Figure 3.8B**). **Table 3.1 and Figure 3.8C** shows some of the most significant and highly regulated genes in *TRIB1* high macrophages vs. *TRIB1*-high monocytes. Among the *TRIB1*-high macrophages the non-M1 markers MMP7 (2.19-fold, $p=2.9 \times 10^{-17}$), CCL22 (2.18-fold, $p=1.14 \times 10^{-19}$), MMP12 (1.39-fold, $p=1.1 \times 10^{-9}$) and TGM2 (1.31-fold, $p=3.83 \times 10^{-7}$) are up regulated as well as the M1 marker CCL5 (1.71-fold, $p=3.44 \times 10^{-18}$). Interestingly, the non-M1 marker PPAR γ was down-regulated (0.89-fold, $p=2.89 \times 10^{-6}$) in *TRIB1*-high macrophages.

Table 3.1: Genes found to be differentially regulated in *TRIB1* high vs. *TRIB1* low human MDMs.

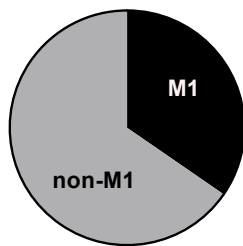
Table shows NCBI gene accession number and name along with fold changes with p- (significance set at <0.05) and q-values (set at <0.05) are reported. The associated macrophage subclass is listed along with reported roles in atherosclerosis.

NCBI gene	Name	Associated Macrophage subclass	log.fold	fold. change	p.values	q.values	Atherogenic ?	Notes	Reference
4316	<i>MMP7</i>	Non-M1	1.1347	2.1958	2.90E-17	7.24E-15	No change, may influence stability	↑ smooth muscle apoptosis	Johnson et al. (2005)
25	<i>CCL22</i>	Non-M1	1.1258	2.1822	1.14E-19	4.58E-17			
10	<i>CCL5</i>	M1	0.7788	1.7158	3.44E-18	1.13E-15	↑	↑ monocyte recruitment into lesion	Zernecke et al. (2008)
4321	<i>MMP12</i>	Non-M1	0.4798	1.3946	1.10E-09	3.95E-08	↑	↑ lesion size ↑ instability	Johnson et al. (2005)
12	<i>CCL8</i>	M1	0.4433	1.3597	4.38E-06	5.80E-05			
7052	<i>TGM2</i>	Non-M1	0.3968	1.3166	3.83E-07	6.88E-06	↑	TGM2 ^{-/-} mice have reduced monocyte adherence on endothelium	Matlung et al. (2012)
3	<i>CCL3</i>	M1	0.3843	1.3052	8.83E-12	5.78E-10	↑?	↑ expression in advanced atherosclerosis / foam cells	Lutgens et al. (2005)
3553	<i>IL1B</i>	Mixed	0.2248	1.1686	0.0102	0.0386			
6347	<i>CCL2</i>	M1	0.1913	1.1418	0.0286	0.0858			
5743	<i>PTGS2</i>	M1	0.1418	1.1033	0.0005	0.0033	↑	COX-2 ^{-/-} mice ↓ atherosclerosis	Burleigh et al. (2005)
41	<i>TNF</i>	M1	0.0447	1.0315	0.4433	0.6172			
5468	<i>PPARG</i>	Non-M1	-0.1599	0.8951	2.89E-06	4.05E-05	↓	↓ foam cell formation	Li et al. (2004)

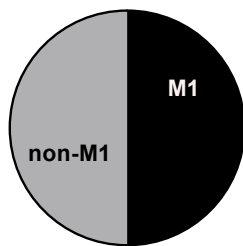
A



B Upregulated polarisation markers in *TRIB1*-high macrophages



Upregulated polarisation markers in *TRIB1*-high monocytes



C **TRIB1 associated macrophage polarisation markers**

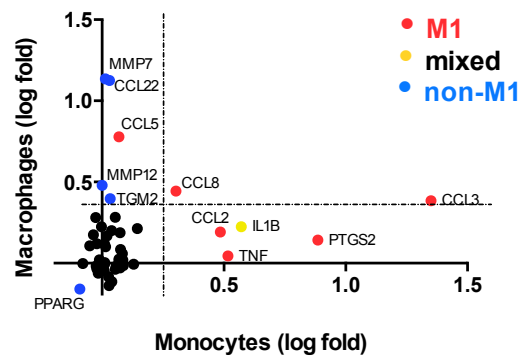


Figure 3.8: *TRIB1* expression is associated with overexpression of alternatively activated macrophages.

(A) Microarrays from human monocytes (n=758) and monocyte derived macrophages (MDMs) (n=596) were analysed and ranked based on *TRIB1* expression. The top 25% 'high expressors' and bottom 25% 'low expressors' were taken forward for analysis. (B) Analysis revealed polarisation markers of M1 and 'non-M1' phenotypes were equal in monocytes but there was an elevated expression of 'non-M1' markers in *TRIB1*-high macrophages. (C) Log-fold changes of individual *TRIB1*-associated gene expression in macrophages vs. monocytes. Identification of pathways was performed with QuSAGE.

3.3.10 Macrophage *Trib1* controls IL-15 expression

The activation of Kupffer cells leads to pro-inflammatory cytokine secretion in the liver and when sustained contributes to liver injury and the pathogenesis of non-alcoholic fatty liver disease (Baffy, 2009). To identify potential cytokines Kupffer cells may secrete and the mechanism by which myeloid *Trib1* regulates hepatic lipogenesis, the same microarray data as presented in **Figure 3.9A** was probed for *TRIB1* associated cytokines (**Table 3.2**). **Figure 3.8A** shows the fold expression levels of cytokines in *TRIB1*-high monocytes and macrophages. The ones most relevant or significant are labelled. The analysis revealed that IL-6 is significantly up-regulated in *TRIB1*-high macrophages while both TXLNA and IL-15 are significantly down-regulated in *TRIB1*-high macrophages. Interestingly, IL-15 has been shown to be produced by Kupffer cells in the liver and promotes diet induced NAFLD by modulating lipid metabolism in hepatocytes and also exacerbates inflammatory responses in the liver (Cepero-Donates et al., 2016). To validate IL-15 expression is altered and relevant in the *Trib1* x *LyzMcre* mice. Expression of IL-15 was measured in *Trib1* BMDMs, **Figure 3.9B** shows that IL-15 expression is significantly ($p < 0.001$) reduced in transgenic BMDMs.

Table 3.2: Cytokines differentially regulated in *TRIB1* high vs. *TRIB1* low human MDMs.

Table shows NCBI gene accession number and name along with fold changes with p- (significance set at < 0.05) and q-values (set at < 0.05).

NCBI Gene	Name	log.fold	fold.change	p.values	q.values
2	IL1B	0.224756563	1.168580048	0.010152387	0.038567347
37	TGFA	0.207188734	1.154436432	1.56E-06	2.36E-05
7	IL6	0.167480069	1.12309508	0.005873463	0.025052036
24	IL18	0.103550285	1.074414206	3.56E-05	0.000356452
41	TNF	0.044674406	1.031450371	0.443267647	0.617170552
16	TXLNA	-0.094605134	0.93652854	7.84E-06	9.57E-05
17	IL15	-0.132764427	0.912082084	0.000637749	0.004049335
9	IL8	-0.240822871	0.846262491	0.020399632	0.066415676

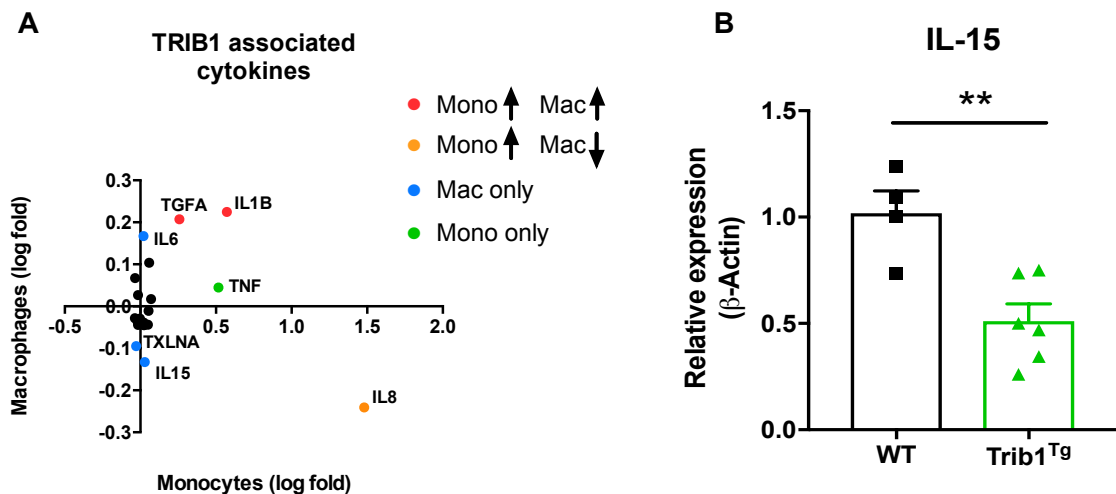


Figure 3.9: Macrophage *TRIB1* controls IL-15 expression.

(A) *TRIB1* associated cytokines in human macrophages vs. monocytes were analysed from microarrays described in Figure 3.8. IL-15, a pro-inflammatory cytokine and known to be important in liver disease pathogenesis was identified as significantly down regulated in *TRIB1* high macrophages. (B) IL-15 expression was validated in *Trib1*-transgenic BMDMs by qPCR. IL-15 levels are normalised to β -actin. Graphs represent mean \pm SEM, **p<0.01, student's t-test Expression levels of IL-15 in *Trib1* transgenic vs. WT M Φ BMDMs measured by qRT-PCR. IL-15 expression levels were normalised to β -Actin, n=4-6. p<0.05, unpaired student's t-test.

3.3.11 Myeloid *Trib1* regulates hepatic lipogenesis

As IL-15 has been shown to be involved in modulating lipid metabolism, the lipid content of *Trib1* x *LyzMcre* mice livers were investigated via a colorimetric assay. Frozen livers were sent to collaborators Dr. Robert Bauer and Professor Daniel Rader at the University of Pennsylvania, Philadelphia, USA for analysis. It was found myeloid *Trib1* KO mice had significantly (p<0.01) increased hepatic triglycerides (22.84 ± 1.6 mg/g) compared to control mice (7.7 ± 1.5 mg/g) (Figure 3.10A). However, no significant differences were found in the *Trib1* transgenic mice (7.4 ± 1.2 mg/g). *Trib1* KO mice also had increased hepatic cholesterol (7.8 ± 1.6 mg/g, *Trib1* KO vs. 5.1 ± 0.4 mg/g, control), however the difference was not significant (p=0.08). Similarly, hepatic cholesterol levels in *Trib1* transgenic mice was comparable to control mice (4.8 ± 0.9 mg/g, *Trib1* transgenic vs. 5.1 ± 0.4 mg/g, control) (Figure 3.10B).

To investigate further, qPCR analyses of lipogenesis genes that are known to be regulated by TRIB1 (Bauer et al., 2015) revealed that there were no differences in the expression of these genes; *Acaca*, *Fasn* and *Scd1* in the livers of the mice, suggesting that myeloid *Trib1* regulation of lipogenesis in the hepatocytes may occur via another mechanism e.g. post-transcriptionally (**Figure 3.10C**)

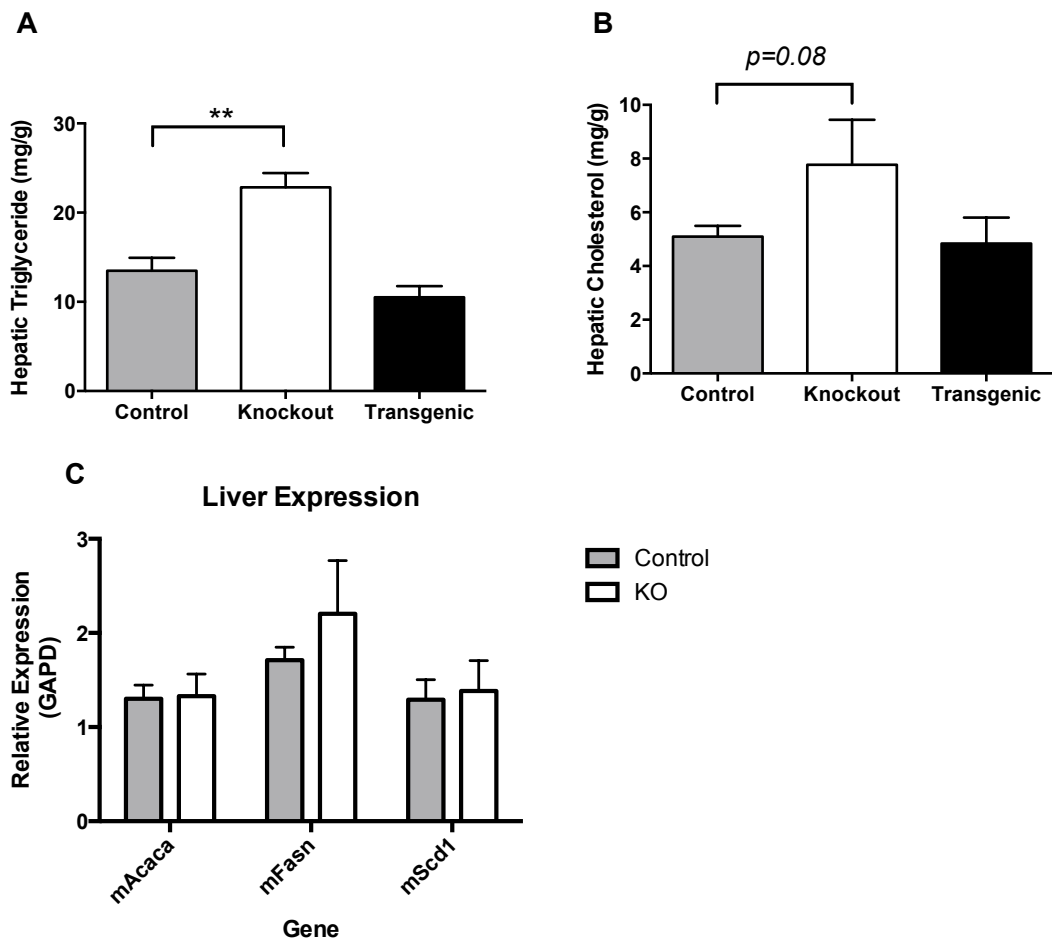


Figure 3.10: Myeloid *Trib1* induces changes in hepatic lipids.

(A) Hepatic triglyceride was measured by colorimetric assay using homogenized liver from *Trib1* WT, *Trib1* knockout (*Trib1* *fl/fl* *x* *LyzMCre*) and *Trib1* transgenic (*ROSA26.Trib1* *x* *LyzMCre*) mice. (B) Cholesterol content was measured by colorimetric assay from the same liver homogenates used in (A). (C) qRT-PCR of hepatic *Trib1* and lipogenesis genes *Acaca*, *Fasn*, *Scd1*. Gene expression was normalised to GAPDH house keeping gene. Graphs represent the Mean \pm SEM (n=4-10), **p<0.005, ordinary one-way ANOVA. Data was generated and provided by R.Bauer.

3.3.12 Hepatic *Trib1* is down regulated by inflammatory signals

Next the effects of increased inflammation on hepatic expression of *Trib1* were investigated. qPCR analyses found that *Trib1* expression was down-regulated in the livers of myeloid *Trib1* KO mice by 58% (0.43 ± 0.06 , control vs. 0.25 ± 0.06 , *Trib1* KO) although the difference was not significant ($p=0.07$) (**Figure 3.11A**), despite this the data suggests hepatic TRIB1 may be a sensor to inflammatory environments. To explore further, human liver (HepG2) cells were stimulated with 100ng IL-1 β , a potent pro-inflammatory cytokine and 50mM of glucose. *TRIB1* expression in HepG2 cells was significantly down regulated by 90% ($\pm 6.2\%$, $p<0.001$). Glucose stimulation also caused a modest but significant decrease in expression of *TRIB1* ($22 \pm 3.2\%$, $p<0.05$). Stimulation with both IL-1 β and glucose simultaneously showed some synergistic effect but this was not significant ($22 \pm 3.2\%$, IL-1 β vs. $18 \pm 7.7\%$, IL-1 β + glucose) (**Figure 3.11B**). Similarly, C57BL/6 mice were fed a HFD for 12 weeks as a model of systemic inflammation. **Figure 3.11C** shows that *Trib1* expression was significantly down regulated in the livers of HFD fed mice compared to those on chow diet ($p<0.001$).

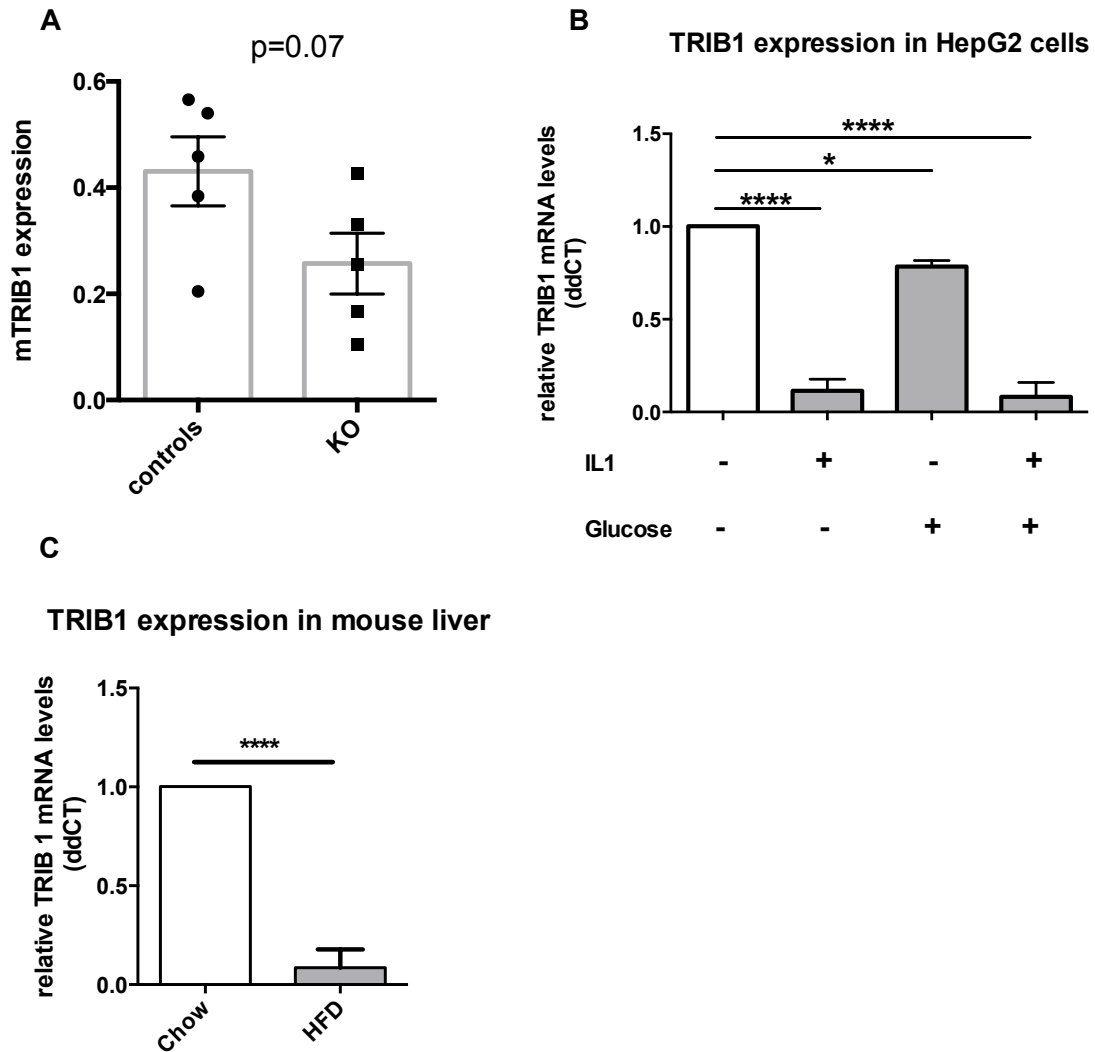


Figure 3.11: Hepatic TRIB1 is down regulated by inflammatory signals.

(A) *Trib1* is down regulated in KO liver tissue measured by qRT-PCR. Data is normalised to levels of β -Actin (n=5). (B) To mimic a pro-inflammatory environment in the liver HepG2 cells were stimulated with 100 ng/ml IL-1 β and glucose for 24 hours. Levels of *TRIB1* expression were measured by qRT-PCR, normalised to β -Actin, n=5 independent experiments. (C) C57BL/6 mice were fed on either chow or high-fat diet (HFD) for 12 weeks as a model of systemic inflammation. Levels of *TRIB1* were measured by qRT-PCR and normalised to β -Actin, n=5. Graphs represent Mean \pm SEM, * $p < 0.05$, **** $p < 0.001$, student's t-test (A), ordinary one-way ANOVA (B-C). Data from (A) was generated by R.Bauer. Data from (B-C) was generated by Z.Ilyas

3.3.13 Kupffer cell phenotype correlates with hepatic *Trib1* expression and hepatic lipid content

Given the data presented thus far showing *Trib1* is down-regulated by inflammatory signals in the liver (Figure 3.11) and a suggestion that *Trib1* is indeed down regulated in the livers of *Trib1* KO mice (Figure 3.12A), I wanted to investigate if KC phenotype based on Ym1 and IRF-5 staining directly correlates with expression of hepatic *Trib1* in the *Trib1* x *Ly2MCre* mice, irrespective of genotype. Interestingly, it was found Ym1 (anti-inflammatory marker) shows a significant

positive correlation with expression of *Trib1* ($R^2=0.4935$, $p<0.05$). The correlation between KC expression of Ym1 and hepatic triglycerides were also assessed. **Figure 3.12B** shows a significant and positive correlation between KC Ym1 expression and the presence of hepatic triglycerides ($R^2=0.4056$, $p<0.05$). Correlation between KC IRF-5 vs. *Trib1* expression and hepatic lipid content was also investigated and although showed the expected trend, the results were not significant (not shown).

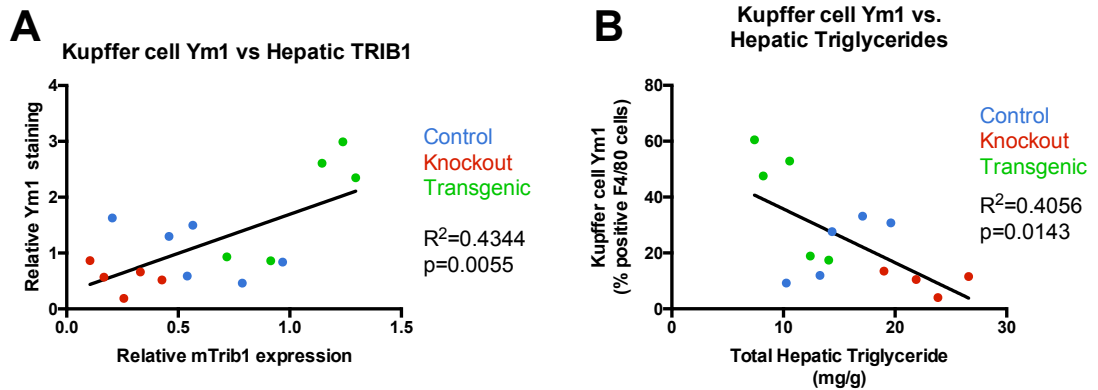


Figure 3.12: Kupffer cell phenotype correlates with hepatic *Trib1* expression and hepatic lipid content.

(A) Correlation between Kupffer cell expression of Ym1 and hepatic *Trib1* expression. (B) Correlation between Kupffer cell expression of Ym1 and hepatic triglyceride content. Data points represent the mean of one individual mouse ($n=15-16$). Linear regression and Pearson correlation coefficient were performed to determine correlation. R^2 is reported along with level of statistical significance, set at $p<0.05$.

3.4 Summary

The work presented in this chapter fully characterises myeloid specific *Trib1* knockout and over-expressor mouse models and defines the role of myeloid *Trib1*. We conclude that myeloid TRIB1 is a potent regulator of lipid homeostasis, the loss of which promotes inflammation in the liver. The observations provide circumstantial evidence of a novel TRIB1/IL-15 dependent molecular mechanism of Kupffer cell- hepatocyte cross talk. In summary:

- *Trib1* fl/fl x *LyzMCre* mice have approximately 70% reduction in *Trib1* expression.
- *ROSA26. Trib1* x *LyzMCre* mice have good levels of transgene expression both in blood monocytes and tissue macrophages.
- *Trib1* x *LyzMCre* mice have normal tissue anatomy and comparable body weight.
- White blood cell count is not altered in *Trib1* x *LyzMCre* mice.
- *Trib1* x *LyzMCre* mice show normal levels of splenic F4/80+ macrophages and the levels of M2 macrophages are not altered.
- *Trib1* x *LyzMCre* mice have altered plasma lipids. Loss of myeloid *Trib1* increases levels of circulating triglycerides and VLDL. Over-expression of *Trib1* reduces VLDL and increases HDL levels.
- Myeloid *Trib1* alters Kupffer cell phenotype; the loss of which promotes Kupffer cell activation by increasing expression of the M1/ pro-inflammatory marker IRF-5. Over-expression of *Trib1* promotes expression of the M2/anti-inflammatory marker Ym1.
- The phenotype is mirrored in *Trib1* BMDMs.
- *Trib1* regulates distinct pathways involved in macrophage polarisation by down-regulating C/EBP α and up-regulating C/EBP β via miR-155.
- The observations presented in the mouse also occur in humans, where *TRIB1* expression is associated with expression of M2/ anti-inflammatory macrophage markers.
- TRIB1 controls IL-15 (pro-inflammatory cytokine) expression in human MDMs and mouse BMDMs.

- Mice that lack *Trib1* in myeloid cells have increased hepatic triglyceride and cholesterol, however lipogenesis genes were not altered suggesting myeloid *Trib1* may regulate lipogenesis post-translationally.
- Pro-inflammatory cytokines down regulate *Trib1* in hepatic cells both *in vitro* and to some extent *in vivo*
- I propose TRIB1 is involved in Kupffer cell- hepatocyte cross talk through the pro-inflammatory cytokine IL-15, thereby regulating lipogenesis in the liver.

3.5 Discussion

Investigating the role of TRIB1 particularly its role in lipid homeostasis has been performed in a variety of animal models including full body knockout and hepatic-specific over-expression using adeno-associated virus (Yamamoto et al., 2007, Burkhardt et al., 2010, Satoh et al., 2013). However, since TRIB1 is important in the polarisation of macrophages also, myeloid specific knockout and over-expression of *Trib1* models were developed to investigate these two characteristics and their consequences further.

A high profile paper documented the significance of *Trib1* knockout in haematopoietic cells on the differentiation of tissue resident macrophages, the loss of which severely reduced tissue resident anti-inflammatory ‘M2’ macrophage in various organs, decreased abdominal adipose deposits, decreased body weight and showed slight growth retardation (Satoh et al., 2013). However, our myeloid specific *Trib1* KO and over-expression mice did not display any of the described features and showed no growth retardation, with normal comparable body weight and unremarkable histology in both the liver and adipose tissue despite a good level of *Trib1* gene expression changes in tissues. Similarly, there was no evidence of reduced numbers of macrophages in the spleen, particularly no reduction of ‘M2’ anti-inflammatory macrophages as described by Satoh et al. (2013). To reconcile these differences, it is interesting to note that the study used full body *Trib1* knockout rather than tissue specific. Full body *Trib1* knockout is reported to display high perinatal mortality (Satoh, unpublished data, cited in Ostertag et al. (2010)). In this lab and Dr. Kiss-Toth’s collaborator Professor Rader’s (University of Pennsylvania, USA) have both independently attempted to generate full body *Trib1*

knockout mice but in both cases *Trib1* homozygous mice have perinatal mortality and were non-viable on a *c57bl/6* background and had some viability (~25%) on a *m129 x c57bl/6* mixed background (unpublished data). Therefore the data should be treated with some caution to assess precisely the contributions of the loss of *Trib1* in *haemopoietic cells vs. full body* expression especially if a high proportion of mouse pups are still non-viable. It is clear from this data however that TRIB1 may have a role in mammalian development as demonstrated in *Drosophila* and *Xenopus* models (Dobens and Bouyain, 2012).

The polarisation and spectral phenotype of macrophages play a pivotal role in health and disease (discussed in more detail in Chapter 4). Here I show; *Trib1* is involved in the polarisation of both tissue- and bone marrow derived macrophages (both in mice and humans), the loss of which skews macrophages towards a pro-inflammatory ‘M1’ phenotype. In agreement with this data, TRIB1 expression attenuates the production of inflammatory cytokines suggesting an anti-inflammatory role (Sung et al., 2012).

The C/EBP family of transcription factors has important roles in both myeloid development and macrophage activation. Previous studies have shown that TRIB1 regulates the turnover of these transcription factors, specifically C/EBP α through cooperation with the ubiquitin E3 ligase COP1 targeting it for degradation (Yoshida et al., 2013). In the context of macrophage function and polarisation however, less is known. Satoh et al. (2013) suggested the loss of *Trib1* leads to elevated levels of C/EBP α expression and therefore may inhibit expression of genes involved in M2 polarisation of macrophages. However, they did not provide evidence that this was due to a defect in *Trib1* in myeloid cells directly. However, in the myeloid specific *Trib1 x LyzMCre* mice, I have shown that over-expression of *Trib1* indeed reduces protein expression of C/EBP α , suggesting that *Trib1* modulates C/EBP α levels and in agreement with Satoh et al. (2013), may control signaling pathways involved in macrophage activation by inhibiting M2 polarisation. The role of C/EBP β though is much more characterised. C/EBP β induces M2-specific gene expression by regulating the promoters of M2-specific genes such as *il10* and *Arg-1* (Ruffell et al., 2009). However there is evidence to suggest C/EBP β itself may be regulated by competition between other transcription factors too (Nerlov, 2008). The data presented in this chapter shows C/EBP β protein levels decrease when TRIB1 is

over-expressed (the opposite to C/EBP α), furthermore *Trib1* knockout mice have elevated levels of C/EBP β (Yamamoto et al., 2007). C/EBP β has been shown to have opposing effects to C/EBP α in regulating CD36 expression in adipocytes and therefore the opposing effects TRIB1 has on C/EBP α and C/EBP β expression may account for the influence on skewing macrophage polarisation (Qiao et al., 2008).

As discussed (**in section 3.3.8.3**) miR-155 directly regulates C/EBP β expression, although there has been no reported evidence of how TRIB1 may regulate C/EBP β expression. Therefore I proposed TRIB1 may be upstream of miR-155, indeed transgenic *Trib1* BMDMs fail to show an induction of miR-155 expression when polarised to M2 macrophages. Therefore it appears *Trib1* controls C/EBP β expression through a pathway that involves miR-155.

Indeed, outside the context of macrophages, the C/EBP family of transcription factors are known to have an extensive role in both the liver and adipose. C/EBP α for example, promotes steatosis in ageing mice through the regulation of triglyceride-synthetic enzymes and in the adipose tissue regulates expression of lipogenic genes (Matsusue et al., 2004, Jin et al., 2013, Qiao et al., 2006). A recent paper published demonstrated TRIB1 regulates hepatic lipogenesis through C/EBP α in hepatic cells (Bauer et al., 2015). Liver specific knockout of *Trib1* (*Trib1_LSKO*) display increased lipogenesis accompanied with increased levels of both C/EBP α and C/EBP β , interestingly, the authors propose the role of $-\beta$ is redundant to $-\alpha$. However, this may be another example of differences between different tissues and specific *Trib1* models. Interestingly, C/EBP α overexpression increased both lipogenesis and fatty acid synthesis while C/EBP α deletion in *Trib1_LKSO* animals ablated the lipogenic effects of *Trib1* deletion suggesting C/EBP α is required for the effects (Bauer et al., 2015). Both TRIB1 and C/EBP α maybe involved in a regulatory feedback loop to control lipogenesis in the liver.

Interestingly, plasma lipid levels were not changed in the C/EBP α deletion mice in the study performed by Bauer et al. (2015), suggesting a C/EBP α independent mechanism as well. Intriguingly, hepatic lipid content was elevated in our *Trib1 x LyzMCre* mice and given the overlap of TRIB1 regulation in both hepatocytes and myeloid cells through C/EBP transcription factors, I proposed a communication between Kupffer cells and hepatocytes.

The liver resident macrophages known as Kupffer cells (KCs) have been long thought as merely scavenger cells removing particulate material and red blood cells from the circulation. However, emerging evidence from animal studies have shown KCs are involved in the pathogenesis of a variety of liver diseases such as viral hepatitis, liver fibrosis, activation or rejection of liver transplants, both alcoholic and non-alcoholic liver disease and steatosis and can participate in KC-hepatocyte communication via inflammatory mediators (Kolios et al., 2006).

KCs are found in the sinusoidal lining of the liver and form part of the non-parenchymal cell populations along with sinusoidal endothelial and stellate cells. KCs comprise 80-90% of tissue macrophages in the mononuclear phagocyte system and approximately 15% of total cell population in the liver (Kolios et al., 2006). KCs, like circulating monocytes can become activated and are a major source of pro-inflammatory cytokines such as TNF- α , IL-1 and NO, which cause damage to neighbouring hepatocytes; promoting injury and fibrosis (Su, 2002). KCs form part of the hosts immune response to infection and become activated by the presence of bacterial LPS, the vast majority of which enters via the gastrointestinal (GI) tract of the host. The liver is situated at the entry to the portal blood flow that drains the GI tract, therefore preventing GI bacteria from entering the systemic blood stream.

KCs however, have also shown to become activated in chronic alcoholic liver disease through a variety of ways (reviewed in (Gao and Bataller, 2011)). Interestingly, GI leakage of bacterial endotoxins through increased gut permeability due to chronic alcohol use is known to directly activate KCs. Indeed, patients with alcohol-induced liver injury have increased levels of KCs in the portal tracts in the liver and increased systemic concentrations of pro-inflammatory cytokines including TNF- α and IL-6 (Thurman, 1998, Karakucuk et al., 1989) and inactivation of these cytokines prevents fatty liver disease (Zhan and An, 2010). However, more relevant to this study KC activation also occurs in non-alcoholic fatty liver disease (NAFLD); fatty liver deposits occurring due to other factors than alcohol. The main predisposing factors include obesity, diabetes, hypertension and more interestingly, hyperlipidaemia (Cepero-Donates et al., 2016b).

In this study varying levels of *Trib1* alter KC phenotype, the loss of which promotes activation/ pro-inflammatory phenotype and accumulation of hepatic triglycerides. However, can KCs directly participate in regulating hepatic lipid storage? In agreement with my data, Stienstra *et al.* (2010) directly showed that KCs can participate in the regulation of lipid storage in the liver. C57BL/6 mice were high-fat diet chronically to induce obesity and steatotic livers. The KCs were then depleted using clondronate liposomes and they found loss of KCs significantly decreases liver triglycerides and also increases expression of genes involved in fatty acid oxidation such as PPAR- α . However, no differences were found in the levels of lipogenesis genes suggesting the regulation may be post-translational.

Following this data, IL-15 was identified as a *TRIB1* associated cytokine in human monocyte derived macrophages and its expression was validated in *Trib1* transgenic BMDMs. Indeed, IL-15 has been identified in numerous studies to be involved in KC-hepatocyte communication and critical for the development, homeostasis and functioning of cells of the innate and adaptive immune system (Stienstra *et al.*, 2010, Cepero-Donates *et al.*, 2016b, Li *et al.*, 2002). IL-15 can be produced from both hepatocytes and KCs (Li *et al.*, 2002). In validation of the data, full body IL-15 KO and IL-15R α KO mice have reduced hepatic lipids and are protected against the development of NAFLD (Cepero-Donates *et al.*, 2016b, Cepero-Donates *et al.*, 2016a). IL-15 suppresses mitochondrial respiration in mouse primary hepatocytes and drives lipid accumulation in the liver by attenuating fatty acid oxidation by down-regulating PPAR- α and up-regulating PPAR- γ , key players of lipid metabolism (Cepero-Donates *et al.*, 2016a).

Given that TNF- α has shown to up-regulated in fatty liver disease, it is interesting to note that IL-15 also induces TNF- α expression in rheumatoid arthritis and TNF- α deletion in macrophages reduces hepatic steatosis and NAFLD in mice (McInnes *et al.*, 1997, Tosello-Tramont *et al.*, 2012). Therefore it appears evident that IL-15 promotes fatty liver disease by regulating both lipid metabolism and exacerbating inflammatory responses in the liver of which TRIB1 is a central modulator between KC and hepatocytes.

Interestingly, all of the studies discussed have demonstrated the effects of KC activation and IL-15 in chronically high-fat diet fed mice. In this study however,

Trib1 x *LyzMCre* mice were fed on chow diet suggesting the basal level of *Trib1* expression in these models is enough to drive KC activation and altered lipogenesis through IL-15.

Fascinatingly, miR-155 has been implicated in the pathogenesis of hepatic steatosis through regulation of PPAR α . A study by Bala et al. (2016) demonstrated miR-155 KO mice were protected against alcohol induced steatosis and inflammation. Likewise, they also showed previously that miR-155 is a regulator of increased KC activation and TNF- α production in macrophages (Bala et al., 2011).

It seems evident therefore that TRIB1 most likely modulates pro-inflammatory programs in both macrophages and hepatocytes that contribute towards general inflammation in the liver thereby influencing lipogenesis. Since increased hepatic and circulating plasma lipids also contribute towards inflammation and KC activation it appears there is a continual cycle of activation between the KCs and hepatocytes, exacerbating the initial challenge. However, no change in the expression of lipogenesis genes was seen in the livers of *Trib1* x *LyzM* mice. It is possible to speculate that the increase in hepatic lipid is regulated post-translationally. However, it is also possible that this may not account fully for the observations seen and the influence of adipose tissue may account for the lack of change in gene expression. The adipose is a complex tissue not just involved in the storage of excess calories; adipocytes themselves secrete factors with paracrine and systemic endocrine functions. Adipose tissue macrophages (ATMs) can become activated analogous to activation in liver Kupffer cells. Activation through systemic factors (e.g. obesity and increase in plasma lipid levels, or indeed TRIB1 deficiency) causes release of pro-inflammatory cytokines such as TNF- α , IL-6 and IL1- β , which contribute to systemic inflammation. However, activation can also alter adipokine secretion from adipocytes, consequently leading to increased adipocyte lipolysis and excess circulating levels of free fatty acids, which is taken up by the liver. Indeed, increased lipid accumulation in the liver can trigger KC activation and exacerbate liver steatosis further (reviewed in Olefsky and Glass (2010)). Certainly, excess fatty acids in the liver have been shown to stimulate VLDL secretion with subsequent hyperlipidemia (Fabbrini et al., 2010). As much of the mechanism responsible for the phenotypes observed in these mice is speculative, it is no doubt the subject of future work to fully characterise these changes, particularly investigating the

involvement of adipose tissue. However, **Figure 3.13** depicts the proposed molecular mechanism by which myeloid *Trib1* may regulate lipid homeostasis through KC and ATM activation.

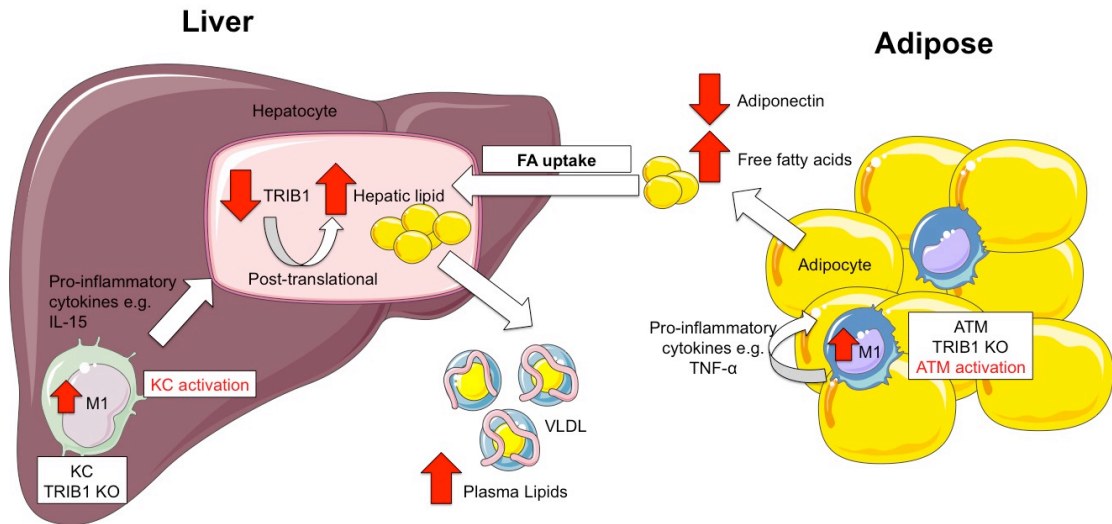


Figure 3.13: Working model of myeloid *Trib1* dependent regulation of plasma lipid homeostasis.

Myeloid *Trib1* deficiency induces pro-inflammatory macrophage polarisation and activation in tissue resident macrophages in the liver (Kupffer cells; KC) and adipose (adipose tissue macrophages; ATM). Tissue macrophage activation promotes secretion of pro-inflammatory cytokines such as IL-15 in the liver and TNF- α in adipose tissue exacerbating local and systemic inflammation. Inflammation in the liver down-regulates the expression of *TRIB1* in hepatocytes and through post-translational modifications of lipogenesis gene products upregulates production of hepatic lipid and thus secretion of lipid into the circulation in the form of VLDL particles. Inflammation in the adipose tissue alters adipokine secretion leading to increased adipocyte lipolysis and the release of free fatty acids (FFA). FFA from subcutaneous stores enter the peripheral circulation, visceral stores travel directly to the liver by the hepatic blood supply increasing hepatic lipid content and secretion of lipid into the circulation.

Lastly, the role of *TRIB1* in atherosclerosis has not yet been investigated until now **(presented in Chapter 5)**. However, the lipid profile data in **section 3.3.5** showed that despite *Trib1* KO mice having increased overall levels of VLDL cholesterol, they had significantly reduced levels of small VLDL particles compared to *Trib1*-transgenic mice which are thought to be pro-atherogenic due to their small size and proposed propensity to cross the vascular wall (Carmena et al., 2004). Atherosclerosis by nature is a localised inflammatory disease of the vascular wall, and therefore changes that occur locally may be specific to atherosclerosis and have

large consequences in relation to the initiation and progression of atheromatous lesions including lipoprotein infiltration.

Trib1^{KO} mice therefore may be protected against development atherosclerosis due to in part their reduced levels of pro-atherogenic lipoprotein particles. Similarly, data presented in **Figure 3.9** shows differentially expressed cytokine genes in TRIB1-high human MDMs along with their roles in atherosclerosis. The data suggests that Trib1^{Tg} mice may be predisposed to developing atherosclerosis do to in part increased small VLDL levels but also increased levels of pro-atherogenic cytokines (**Table 3.1**).

Chapter 4. Distinct macrophage populations contribute to plaque size and stability in murine models of atherosclerosis

4.1 Introduction

Macrophage accumulation within the vessel wall is a classic hallmark of atherosclerosis resulting in ischaemic heart disease, the leading cause of both morbidity and mortality worldwide. Whilst macrophages are important effector cells in innate immunity, the recruitment and retention of these cells in the vessel wall at early stages of atheroma development leads to a sustained inflammatory response and promotes lesion formation.

Macrophages are not only important in the initial lesion development but are central to lesion progression and also have postulated roles in plaque stability and rupture, the main cause of cardiovascular associated events such as myocardial infarction (MI) and stroke (Chinetti-Gbaguidi et al., 2015).

Classically activated macrophages are activated by cytokines such as IFN- γ or lipopolysaccharide (LPS) present on bacteria and secrete pro-inflammatory cytokines such as TNF- α , IL-6 and IL-1 β . Pro-inflammatory macrophages can be typically found in rupture prone shoulder regions (Stoger et al., 2012). Alternatively activated or ‘anti-inflammatory’ macrophages typically secrete anti-inflammatory cytokines such as IL-10 and TGF- β and act to scavenge cell debris, promote wound healing and are often found in more stable areas of the plaque away from the lipid core (Chinetti-Gbaguidi et al., 2011). However, this simple classification of macrophages has mostly been derived from *in vitro* studies and thus may oversimplify complex macrophage phenotypes present *in vivo* and may also underestimate their remarkable plasticity depending on environmental cues.

Therefore, despite considerable work demonstrating the presence of various macrophage subsets *in vivo*, there have been no studies that have characterised plaque macrophage phenotype at a single cell level *in situ*. Immunohistochemical analysis of plaque macrophages typically focuses on the use of single markers

therefore potentially missing or underestimating the complexity of macrophage populations in atheromas. In this study, a staining strategy was used to examine two well-established phenotypic markers *simultaneously* in plaque macrophages and compare the cell populations from high-fat/high cholesterol diet fed mice.

Additionally, an image analysis approach to quantify macrophages individually rather than in the lesion as a whole was designed (as described in **section 4.3.6.1**). The plaque macrophages from two of the most commonly used high-fat diet fed murine models for atherosclerosis research; ApoE^{-/-} and LDLR^{-/-} and a relatively new and less characterised model; mice with hyperlipidaemia induced by AAV-mediated overexpression of a gain of function human PCSK9 mutant (AAV-Pcsk9D377Y), which results in an LDLR^{-/-} like phenotype were fully characterised (Bjorklund et al., 2014, Somanathan et al., 2014, Maxwell and Breslow, 2004).

4.2 Hypothesis

Due to the biological similarity and way of inducing hypercholesterolaemia between LDLR^{-/-} mice and PCSK9 injected mice, I hypothesise that these mice will have similar macrophage populations based on ARG1 and NOS2 staining. Since ApoE^{-/-} mice are reported to have more severe lesions than LDLR^{-/-} mice (Whitman, 2004), I also hypothesise that plaque macrophages from ApoE^{-/-} mice are more pro-inflammatory.

4.3 Materials & Methods

4.3.1 ApoE^{-/-}

Apolipoprotein E null (ApoE^{-/-}) mice on C57BL/6J background were bred in house at the University of Sheffield. Male ApoE^{-/-} (n=4) samples were analysed. All animals were fed on chow diet until commencement of Western diet. Mice were then fed on cholate free-Western diet (Special Diet Services, Essex, UK) for 12 weeks and euthanized by pharmacological overdose of pentobarbital (Watt et al., 2011).

4.3.2 LDLR^{-/-}

Low-density lipoprotein receptor null (LDLR^{-/-}) mice on C57BL/6J background were obtained from Jackson Laboratories. Male LDLR^{-/-} (n=6) samples were

investigated. All animals were fed a standard chow diet until commencement of Western diet. Mice were fed a high fat diet (Arieblok Diet W, cat 4021.06 consisting of 15% w/v cocoa butter, 1% v/v corn oil, 0.25% (w/v) cholesterol, 40.5% (w/v) sucrose, 10% (w/v) cornstarch, 20% (w/v) casein, cholate free, total fat content 16% by weight). After 12 weeks of high-fat diet mice were euthanized by pharmacological overdose of pentobarbital (Steiner et al., 2014).

4.3.3 AAV8-PCSK9D377Y

Male Black 6 (B6NTac) (Taconic, USA) mice (n=4) were injected with 3×10^{11} genome copies of AAV8-PCSK9D377Y (Adeno-associated virus serotype 8-Proprotein convertase subtilisin kexin type 9) intra-peritoneally at 8 weeks of age and immediately placed on a western diet (#D12079Bi, Research Diets Inc., USA) for 16 weeks. Experiments were carried out at the University of Pennsylvania and Dr. Robert Bauer and Professor Daniel Rader, University of Pennsylvania, USA provided aortic root tissue sections from PCSK9 mice.

4.3.4 Assessment of atherosclerosis

The aortic sinus was dissected and embedded in paraffin and serially sectioned (5-7 μ m). Detailed methods can be found in **Chapter 5**.

4.3.5 Histology & Morphometry

Plaque stability was assessed by staining for collagen using Martius Scarlet Blue (MSB). Quantification of collagen was performed in the same way as quantification of Oil red O in the aorta described in **section 5.3.8.2**.

4.3.6 Fluorescent Immunohistochemistry

Formalin fixed paraffin embedded (FFPE) aortic roots were simultaneously stained for the pan macrophage marker, MAC3 and pro- vs. anti- inflammatory macrophage markers inducible nitric oxide synthase (NOS2) and Arginase 1 (ARG1). Aortic root sections were de-waxed in xylene and rehydrated through graded ethanol to water. Sections were pre-treated with 3% hydrogen peroxide for 10 minutes to block endogenous peroxidases and heat mediated antigen retrieval was performed by incubating the sections in 10 mM citrate buffer, pH 6 for 20 minutes at 95 °C and for a further 20 minutes at room temperature. Non-specific binding was blocked by

incubating the tissue in 5% donkey serum, 1% BSA for 30 minutes at room temperature. Tissues were then incubated with MAC3 (Rat Biotin anti-mouse Mac 3 (CD107b) antibody (1:100, #108508, Biolegend, San Diego, CA, USA) and pro- vs. anti- inflammatory macrophage markers NOS2 (mouse, anti-mouse (1:500, #ab129372, Abcam, Cambridge, UK) and ARG1 (rabbit, anti-mouse Arginase I (1:500, #PA5-22009, Thermo Scientific, Rockland, IL, USA). Positive staining was detected by incubating with Streptavidin-NL637, Anti-mouse NL493 and Anti-rabbit NL557 (Northern Lights™, R&D Systems) and nuclei were counterstained with ProLong Anti-fade Mountant with DAPI (Molecular Probes, Life Technologies). Images were captured using Leica inverted wide field fluorescence microscope AF6000 with 20x lens NA 0.7.

4.3.6.1 Development of Image Analysis using ImageJ

Once the staining protocol was optimised to stain simultaneously for macrophage phenotype markers, I aimed to develop a semi-automated image analysis protocol to quantify the level of expression of each marker using ImageJ. Previous studies exploring macrophage phenotype in tissue sections have typically identified cells expressing macrophage polarisation markers as either ‘positive’ or ‘negative’ and have not considered that expression of polarisation markers may exist in a spectrum. This approach will provide a unique insight into macrophage phenotype within plaques *in vivo* and will enhance our understanding of the contribution of macrophages to plaque phenotype and stability. The method of analysing plaque macrophages is shown in detail below. Briefly, however individual MAC-3 positive cells were selected as the region of interest (ROI) and corresponding NOS2 and ARG1 positive staining was evaluated. The analysis allowed consideration for the spectrum of M1/M2 associated marker expression and enabled characterisation of individual cells based on staining intensity. Using this approach it is possible to reveal and quantify complex populations of plaque macrophages *in situ*.

Semi automated system to quantify macrophage phenotype using ImageJ

Prior to quantification, images from separate channels were exported from Leica AF

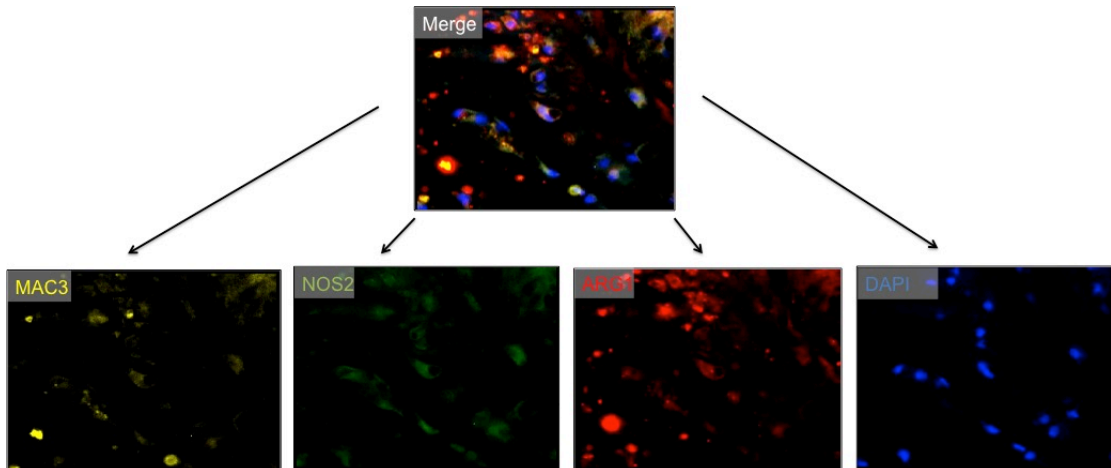
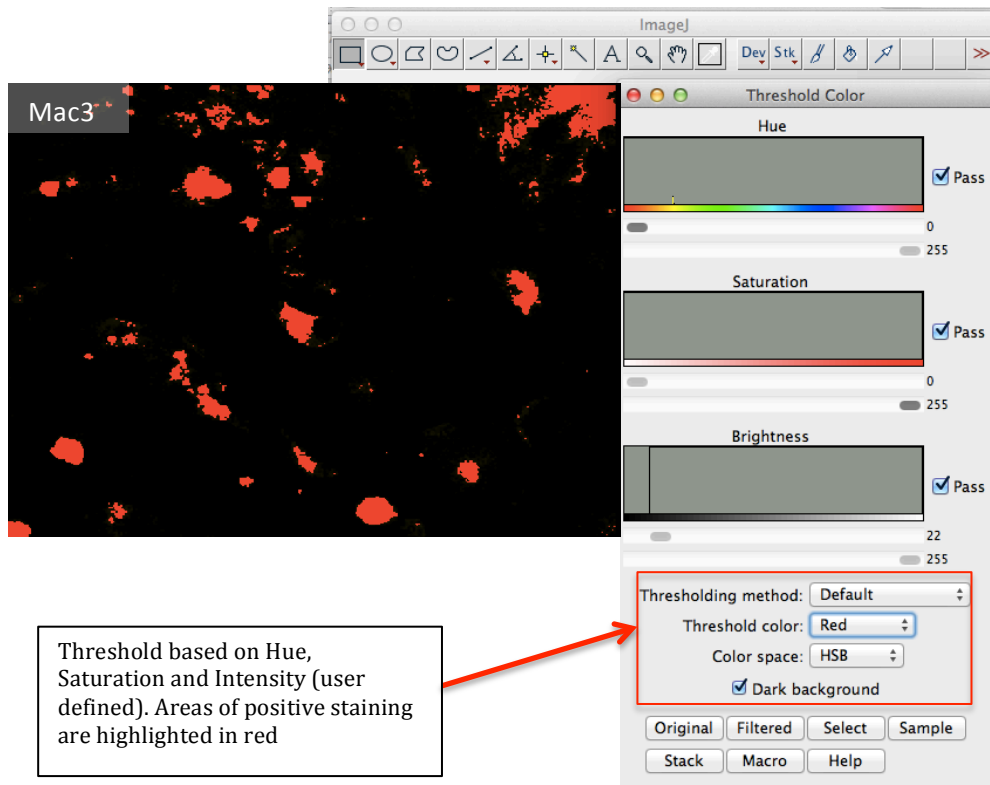


Figure 4.1: Representative images of each fluorescent channel from the Leica AF6000 fluorescent microscope

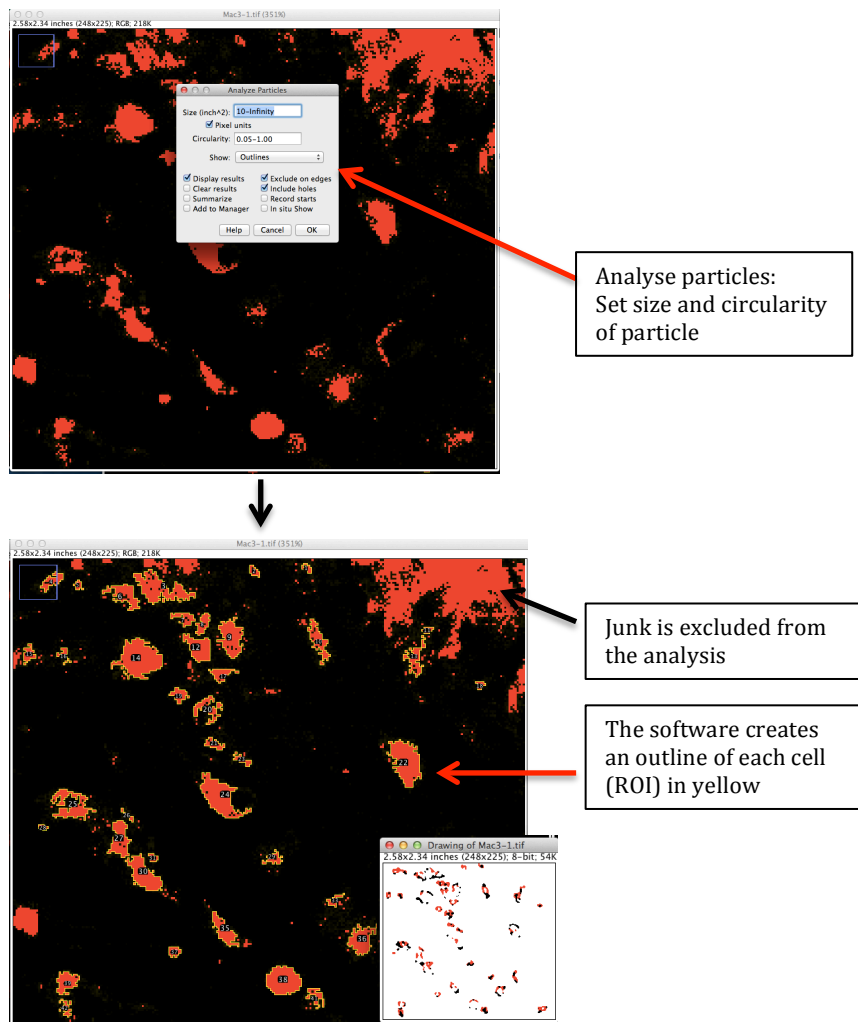
Y5, far red (MAC3), L5, green (NOS2), N3, red (ARG1) and A4, blue (DAPI). Mac3 positive cells (macrophages) were selected based on selecting a threshold based on hue, saturation and brightness (user defined).

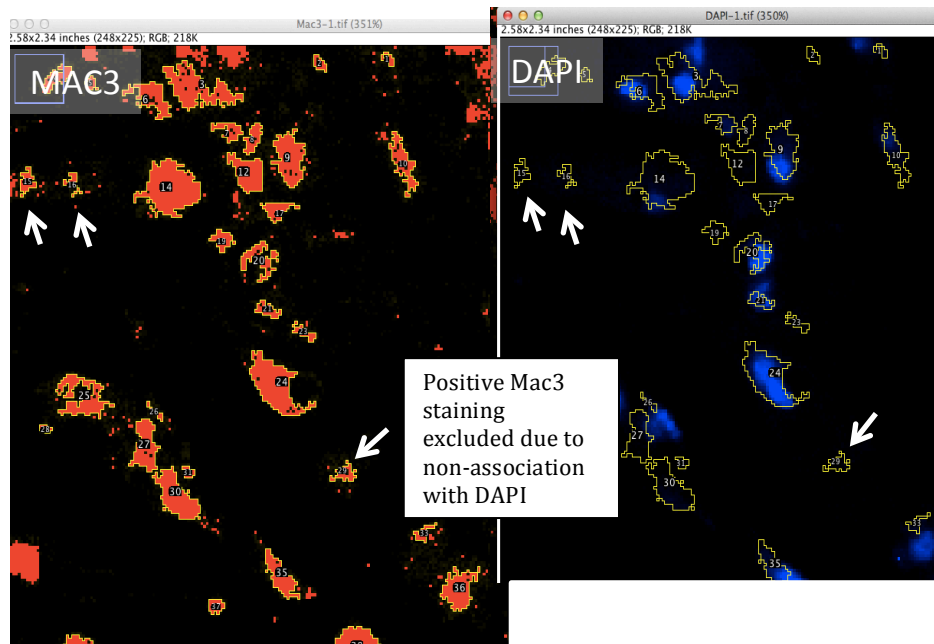


Image>Adjust>Colour threshold

Once areas of positive Mac3 staining were highlighted. It was possible to outline these areas as a region of interests (ROIs). By using the 'analyse particles' tool, features of threshold images can be extracted based on size and circularity. This enables junk or staining debris that may be counted as positive staining to be excluded. Particles with a size (area) out of the range were ignored; similarly, particles with size circularity outside the range were ignored. Circularity sizes range from 0 (infinitely elongated) to 1 (perfect circle).

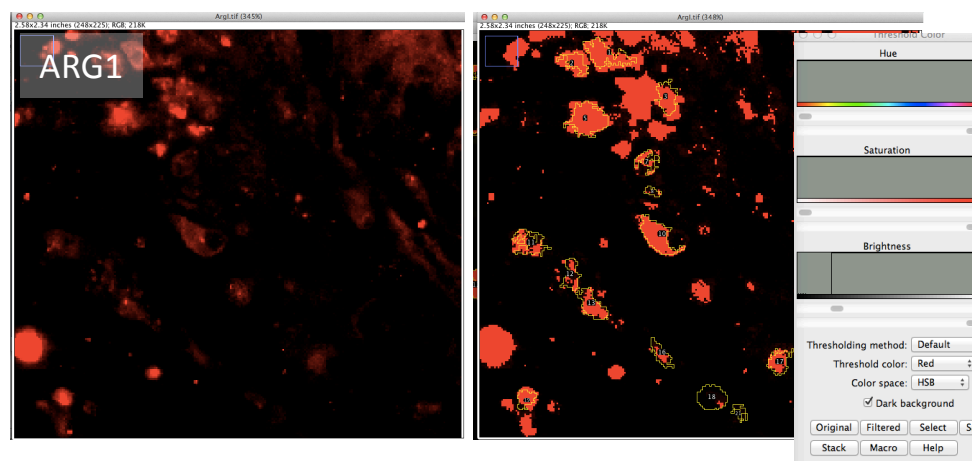
Analyse>Analyse particles
Size (inch²=10-infinity)
Circularity (0.05-10)



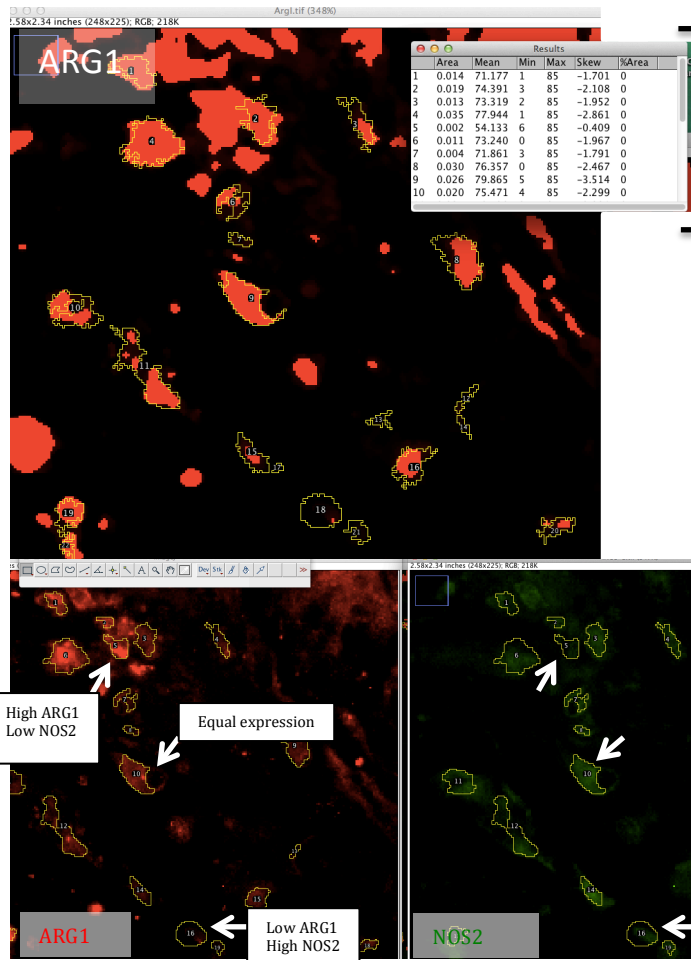


The ROIs were then overlaid to the DAPI image to ensure cell specificity. Areas that were not DAPI (cells) associated were manually excluded. To assess ArgI staining per ROI (Mac3+ cell), ROIs were overlaid to ArgI image and positive staining was thresholded by hue, saturation and brightness as before.

Image>Overlay>From ROI manager



Using 'measure' function, intensity statistics were generated for each ROI that is representative of staining intensity.



Intensity statistics

The method was repeated for NOS2 staining. Intensity statistics per ROI were compared to give relative ARG1 and NOS2 staining, enabling a population of macrophages to be characterised.

4.3.6.2 Optimised Image J work flow

Prior to quantification, raw images from separate fluorescence channels were exported from Leica AF Lite software as a TIFF file to ImageJ. ImageJ was used to quantify levels of expression of each marker (NOS2 and ARG1) in MAC3 positive cells only (**Figure 4.2**). Firstly, MAC3 positive cells were selected based on images from the Y5 channel. Regions of interest (ROI)/ MAC3 positive cells were selected by setting a threshold based on hue, saturation and brightness. The 'analyse particle' tool was used to examine particles based on size and circularity (size pixel²=10-infinity, circularity- 0.05-10) to exclude debris. This allowed MAC3 positive cells (macrophages) to be selected as ROIs. Staining that was not cell associated were excluded from the analysis. Once ROIs were selected, the ROIs were overlaid to ARG1 and NOS2 channel images, the relative ARG1 and NOS2 staining in each region were determined using colour threshold function to generate intensity statistics (mean fluorescence intensity). The individual intensity statistics for each marker separately (NOS2 and ARG1) were applied to a frequency bin and allowed for a pie chart representing each maker frequency to be plotted. A full description of the image analysis work-flow can be found in **Section 4.3.6.1**.

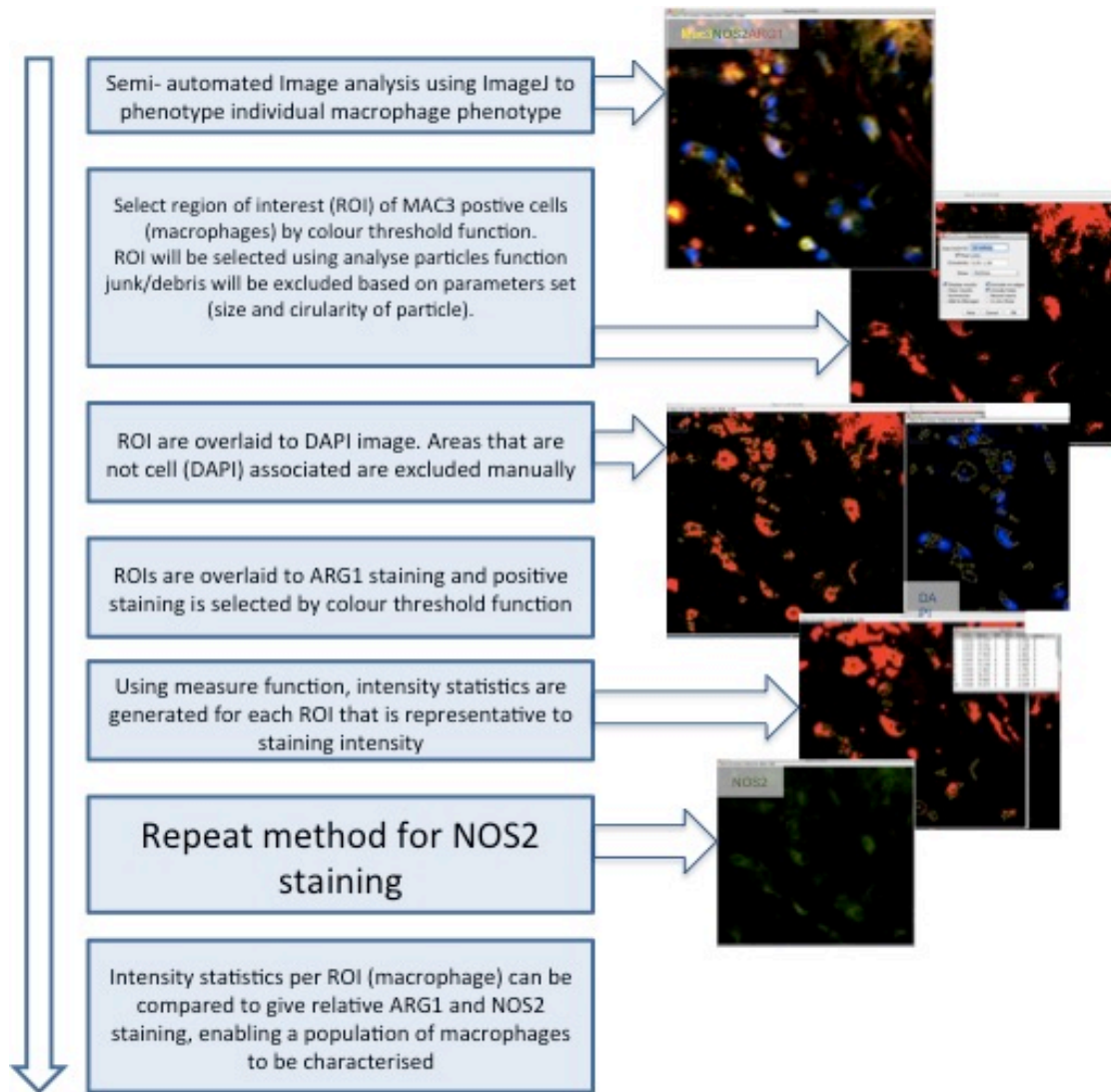


Figure 4.2: Flow chart summarising the analysis of plaque macrophage phenotype *in situ* by immunohistochemistry.

Flow chart illustrates the designed work-flow in ImageJ to characterise individual macrophages. Raw images were exported from Leica LAS AF Lite software to ImageJ for analysis. Functions in ImageJ (colour threshold and analyse particles; size pixel $^2=10$ -infinity, circularity= 0.05-10) allow Mac3 positive cells (macrophages) to be selected as multiple regions of interest (ROI). Once ROIs are selected, the relative ARG1 and NOS2 staining in each region were determined using colour threshold function to generate intensity statistics. Intensity statistics were used to generate data relating to individual macrophages in the plaque and therefore a population based on the NOS2/ARG1 marker staining intensity. The analysis allowed for the spectrum of phenotypes of macrophages *in vivo* to be considered.

4.3.6.3 Macrophage populations and ratios

To assess both NOS2 and ARG1 staining simultaneously in individual macrophages, mean fluorescence intensity values, generated by ImageJ were used to calculate NOS2: ARG1 ratio. To assess the populations further, we took the extreme mean intensity statistics to stratify the populations. A mean intensity statistic of ≤ 20 was

deemed negative, likewise a mean expression value of ≥ 70 was deemed positive. Using this analysis we have marked four populations; single positive for ARG1, double positive (NOS2-positive/ARG1-positive), double negative (NOS2-negative/ARG1-negative) and single positive for NOS2.

4.4 Results

4.4.1 Plaque macrophages can be simultaneously stained for MAC3, NOS2 and ARG1

Using the novel staining technique, it was possible to stain for three markers simultaneously in one tissue section (**Figure 4.4**). Note the different intensities of markers staining in each cell (arrow).

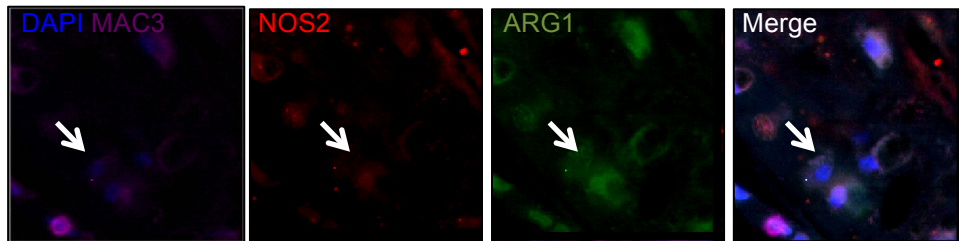


Figure 4.3: Plaque macrophages can be individually characterised by multi-colour immunohistochemistry and can be quantified by ImageJ.

To assess plaque macrophage phenotype, aortic root plaques from atherosclerotic mice were simultaneously stained for the pan macrophage marker MAC3 (CD107b, purple) and pro- vs. anti-inflammatory associated markers; inducible nitric oxide synthase (NOS2, red) and Arginase I (ARG1, green). Images were acquired by an Inverted wide field fluorescence microscope (Leica AF6000) using a 20x lens, NA 0.7.

4.4.2 ARG1 expressing plaque macrophages are less abundant in ApoE^{-/-}, compared to LDLR^{-/-} and PCSK9 animals.

Plaque macrophages (MAC3⁺) stained with NOS2 and ARG1 displayed marked heterogeneity for expression levels of both markers (**Figure 4.5**). Quantification of positive staining using standard techniques (number of positive cells / total number of cells) showed that LDLR^{-/-} plaque macrophages have a significantly increased expression of ARG1 compared to ApoE^{-/-} macrophages (**Figure 4.6A**). There was also a trend towards an increased expression of ARG1 in plaque macrophages in the PCSK9 induced model, however this was not significant ($p=0.1868$). In contrast, NOS2 staining showed no significant differences between each of the cohorts.

Using the developed method of quantification, it enabled mapping of fluorescence intensity statistics. **Figure 4.6B** illustrates the approach and emphasizes the spectral pattern of macrophage marker expression. Next, this approach was used to analyse NOS2 and ARG1 staining individually, across the three models of atherosclerosis. Whilst it was found that marker expression was heterogeneous, most cells displayed either high or low marker expression with a small proportion of macrophages that expressed moderate amounts in between, suggesting that the majority of plaque macrophages exist in a polarised state (**Figure 4.6C**). Further analysis revealed that the NOS2 profile of the plaque macrophages were not significantly different from one another (**Figure 4.6D**). In contrast, plaques from ApoE^{-/-} mice had 3-fold more low-ARG1 expressing macrophages than to LDLR^{-/-} mice (p=0.0275). It was also found that plaques from LDLR^{-/-} mice had significantly more high-ARG1 expressing macrophages than those from ApoE^{-/-} mice (p=0.0123). PCKS9 macrophages also had a trend towards increased levels of high-ARG1 expressing macrophages compared to ApoE^{-/-} but the difference was not statistically significant. Considered together, the data suggests that plaque macrophages from ApoE^{-/-} mice may have a more pro-inflammatory phenotype, compared to LDLR^{-/-} macrophages.

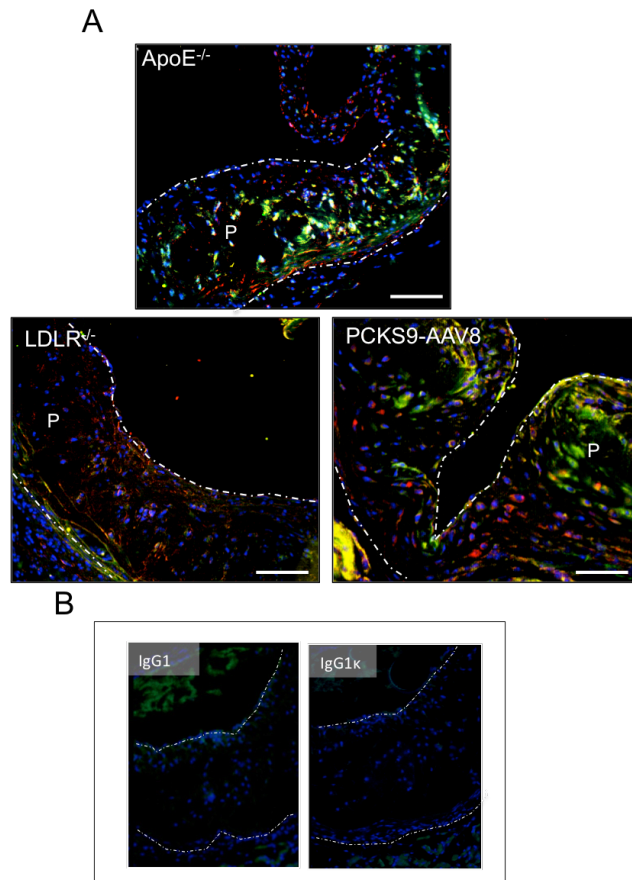


Figure 4.4: Representative images of simultaneous staining of murine plaque macrophages.

(A) Formalin fixed paraffin embedded (FFPE) aortic roots from ApoE^{-/-}, LDLR^{-/-} and PCSK9 mice were simultaneously stained for the pan macrophage marker, MAC3 (Yellow) (rat Biotin anti-mouse Mac 3 (CD107b) antibody) and ‘M1/M2’ macrophage markers inducible nitric oxide synthase (Green) (NOS2, mouse anti-mouse and ArginaseI (Red) (ARG1, rabbit anti-mouse Arginase I. Positive staining was detected by incubating with Streptavidin-NL637, Anti-mouse NL493 and Anti-rabbit NL557 (Northern Lights™, R&D Systems) and nuclei were counterstained with DAPI (blue). Images were captured using Leica inverted wide field fluorescence microscope AF6000 at x200 magnification, NA 0.7. Representative images of positive pseudo-coloured staining are shown. The plaque area (P) is outlined in white. (B) Isotype controls for NOS2 (IgG1) and MAC3 (IgG1 κ).

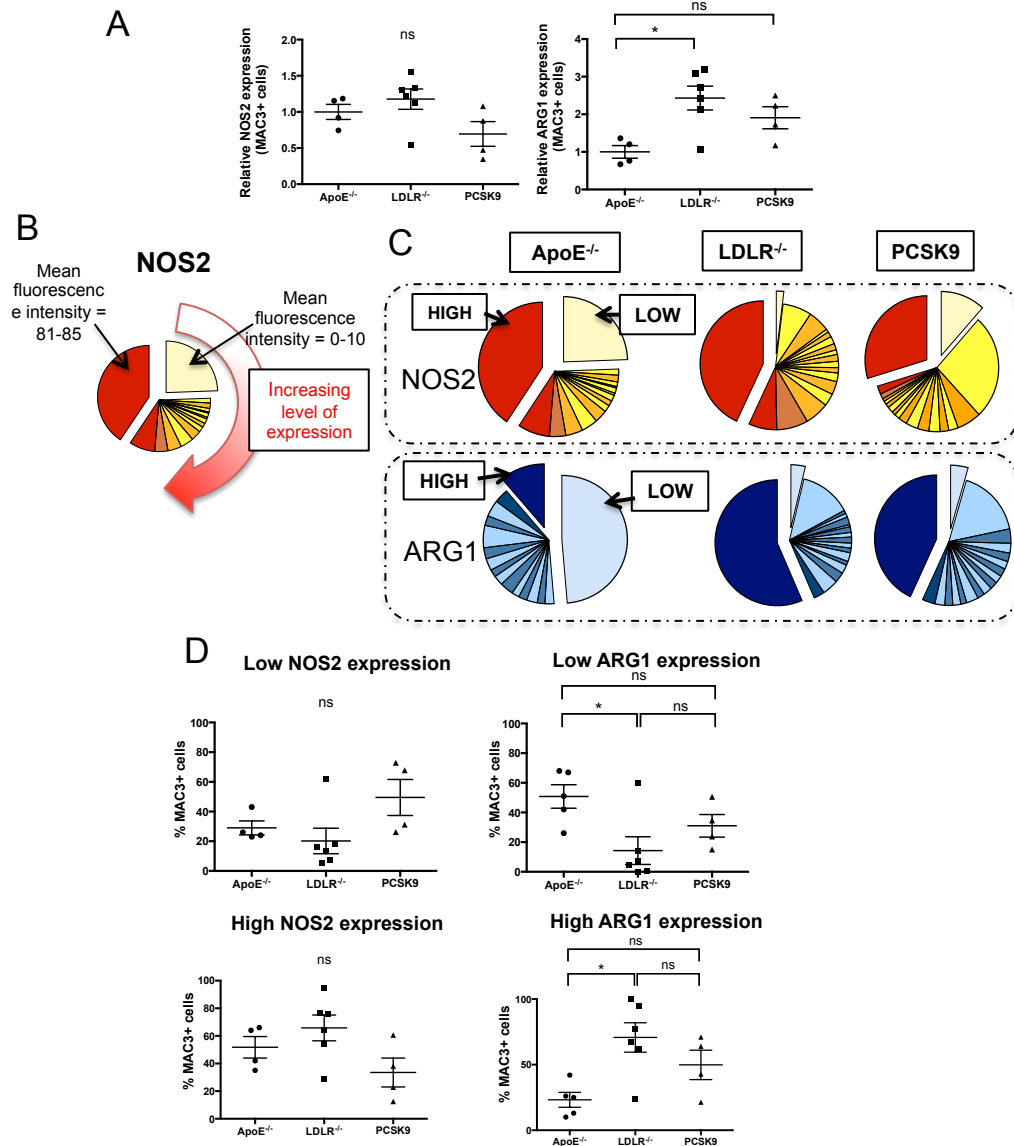


Figure 4.5: Single marker staining reveals ApoE^{-/-} plaque macrophages are more pro-inflammatory than LDLR^{-/-}.

Level of NOS2 and ARG1 staining intensity was quantified in each plaque, using standard methods and expressed relative to the mean intensity of ApoE^{-/-} plaques, showing that ApoE^{-/-} mice have reduced levels of ARG1. The graph illustrates the limited information produced using standard image quantification. **(B)** Using the image quantification technique described, it was possible to produce NOS2 and ARG1 intensity statistics (mean fluorescence intensity) for each MAC3 positive cell and apply a frequency bin. The pie chart represents low (0) to high expression (85) (clockwise) of each marker and indicates a spectrum of expression. **(C)** Plaque macrophages from each of the murine atherosclerotic models were quantified and shown as described. **(D)** The percentage of high and low NOS2 and ARG1 expressing MAC3 positive cells were also calculated and demonstrates ApoE^{-/-} mice have reduced population of high-ARG1 expressing macrophages but additionally have increase in low-ARG1 expressing cells compared to LDLR^{-/-} and PCSK9 induced murine plaques. Graphs present the mean \pm SEM, Ordinary one-way ANOVA with Kruskal-Wallis test. ns= non significant, *p<0.05, **p<0.01. Each data point represents one animal.

4.4.3 Enrichment of NOS2 positive/ARG1 negative macrophages is responsible for the pro-inflammatory phenotype of ApoE^{-/-} plaques

To investigate the plaque macrophage populations further, the expression of *both* markers *simultaneously* in one cell rather than individual expression profiles as described above (**Figure 4.7A**) was considered. Thus, the ratio of NOS2: ARG1 of macrophages in the plaque was calculated (**Figure 4.7B**). This analysis demonstrated that ApoE^{-/-} mice had a significantly greater proportion of cells with a ratio of >1 (NOS2^{HIGH} ARG1^{LOW}) compared to LDLR^{-/-} and PCSK9 models, indicating a pronounced pro-inflammatory phenotype. Conversely, both LDLR^{-/-} and PCSK9 plaque macrophages displayed a greater population of cells with a ratio of <1 (NOS2^{LOW} ARG1^{HIGH}) indicating a more anti-inflammatory phenotype, compared to ApoE^{-/-}. Interestingly, there was no difference between LDLR^{-/-} and PCSK9 plaque macrophages for either marker indicating the similarity in their plaque macrophage phenotype. To investigate in detail which cells were responsible for the pro-inflammatory phenotype of plaque macrophages that were enriched in ApoE^{-/-} plaques, the cell population was stratified based on simultaneous expression of polarisation markers. The most extreme NOS2 and ARG1 expression populations forward for analysis. As shown in a representative scatter plot for macrophages in ApoE^{-/-} plaques in **Figure 4.7C**, a mean expression value for either NOS2 or ARG1 of ≤ 20 was deemed negative while a mean expression value of ≥ 70 was deemed positive, the analysis enabled the enumeration of single positive (NOS2), single positive (ARG1), double positive and double negative cells (**Figures 4.7D-G**). This analysis revealed that the population responsible for the pro-inflammatory phenotype (**shown in Figure 4.7B**) was due to a significant increase in the single positive NOS2 population ($p < 0.05$) (**Figure 4.7G**). In contrast there were no significant differences in the other populations between the cohorts aside from a statistically significant increase in the proportion of double negative macrophages in the PCSK9 cohort ($p < 0.05$).

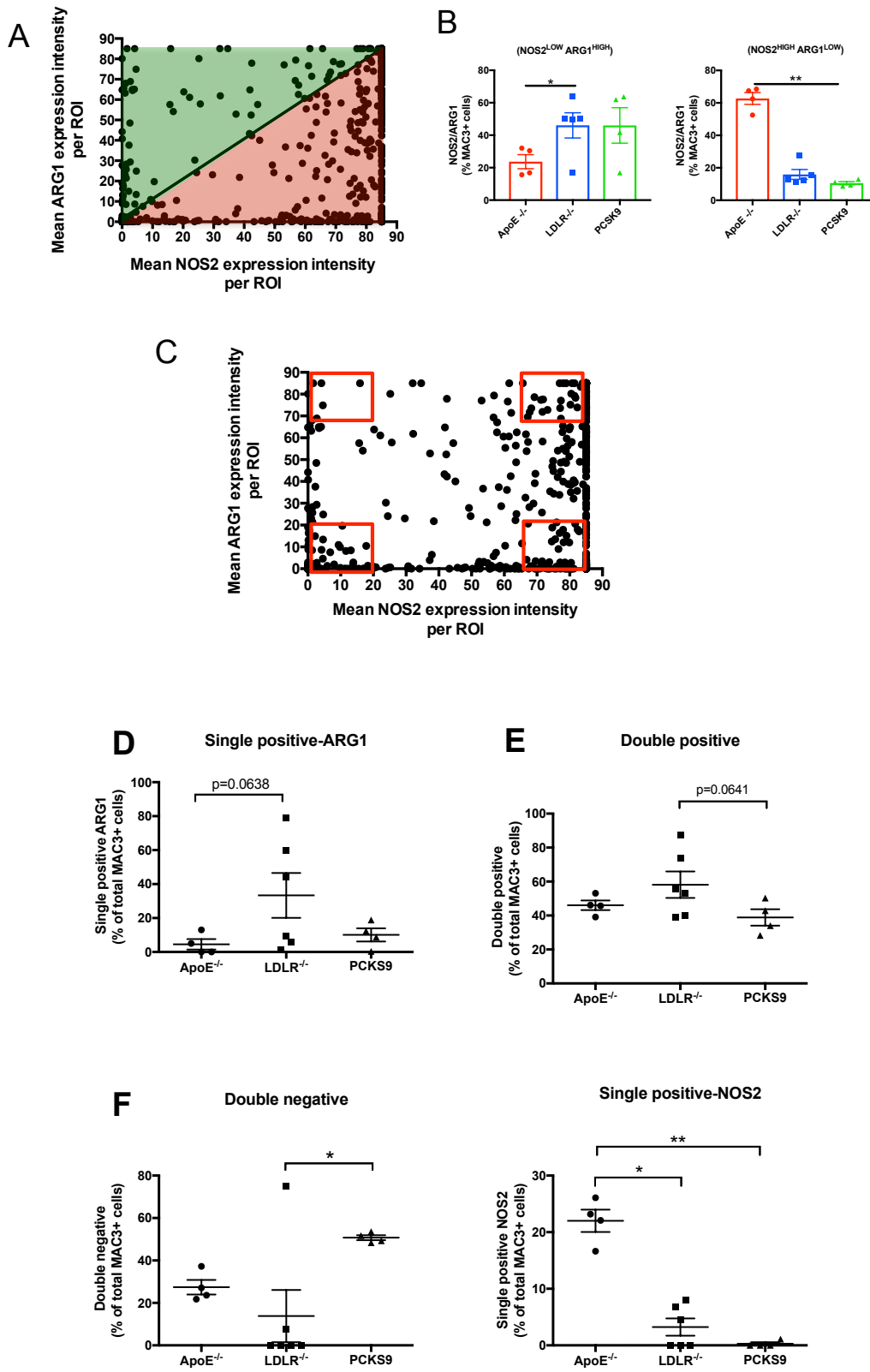
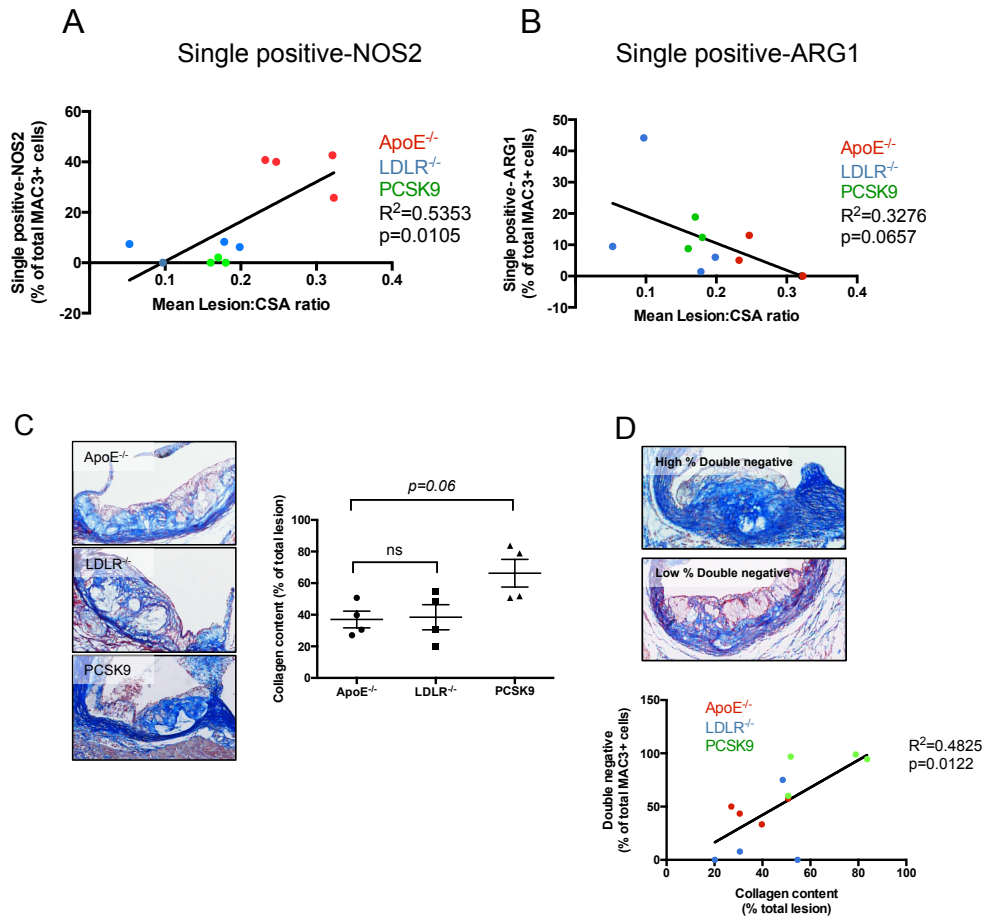


Figure 4.6: Dual marker analysis ApoE^{-/-} have an increased population of NOS2 positive/ARG1 negative plaque macrophages.

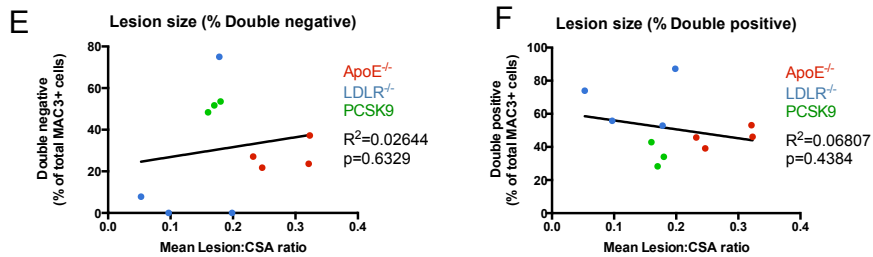
(A) Intensity statistics were used to calculate the NOS2:ARG1 ratio. The scatter graphs show mean NOS2 expression vs. mean ARG1 expression and each cell is represented by a single black dot. (B) The ratio of NOS2/ARG1 expression was calculated. A ratio of >1 indicates increased NOS2 expression (pro-inflammatory phenotype, red area), while a ratio of <1 indicates increased ARG1 expression (anti-inflammatory phenotype, green area). As before plaques from ApoE^{-/-} mice demonstrate an increased pro-inflammatory and reduced anti-inflammatory phenotype compared to both LDLR^{-/-} and PCSK9 plaques. (C) To understand the individual populations further, the extreme populations were taken forward for analysis. As an example, staining intensities of each macrophage detected in ApoE^{-/-} plaques are shown. A mean expression value of ≤ 20 was deemed negative, likewise a mean expression value of ≥ 70 was deemed positive. Using this analysis it was possible to generate data for four populations; single positive for ARG1 (D), double positive (E), double negative (F) and single positive for NOS2 (G) for each of the models analysed. Analysis revealed that the population responsible for the pro-inflammatory phenotype in ApoE^{-/-} plaques was single positive NOS2 cells (NOS2+/ARG1-). Graphs show mean \pm SEM, one-way ANOVA with Kruskal-Wallis test *p<0.05, **p<0.01.

4.4.4 Plaque macrophage phenotype correlates with plaque size and stability.

To examine whether the proportion of single positive NOS2 plaque macrophages have a role in plaque stability and structure, the mean cross sectional area (CSA): lesion area of the aortic root plaques was measured across the three experimental models and found a significant positive correlation ($p=0.0105$, $R^2= 0.5353$) between lesion size at the aortic sinus and the proportion of single positive NOS2 plaque macrophages, suggesting that NOS2 positive plaque macrophages are associated with and may promote lesion progression (**Figure 4.7A**). In line with this, a trend towards an inverse correlation between lesion size and the proportion of single positive ARG1 cells was seen (**Figure 4.7B**) ($p=0.0657$, $R^2=0.3276$). To examine plaque phenotype further, the stability of the lesions using collagen content as a surrogate by Martius, Scarlet and Blue (MSB) staining was measured. Whilst, no significant differences between the collagen content of the lesions in each of the cohorts were found, (**Figure 4.7C**), a positive and significant correlation ($p=0.0178$, $R^2=0.4451$) between collagen content in the lesion and the proportion of double negative macrophages was observed when all mouse models were combined (**Figure 4.7D**). There were no other significant correlations between collagen content and the other macrophage subpopulations (**Figure 4.7E-I**). Taken together, these results suggest that distinct macrophages subsets (as characterised by concurrent expression of NOS2 and ARG1) may play specific roles in lesion development and stability.



Lesion size & Plaque macrophage populations



Collagen content & Plaque macrophage populations

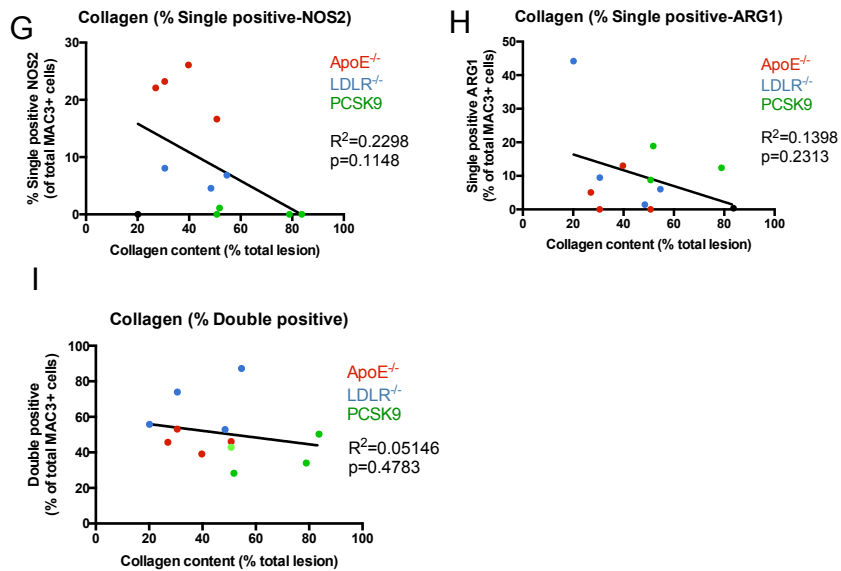


Figure 4.7: Plaque macrophage phenotype correlates with plaque size and stability.

(A) Levels of single positive NOS2 plaque macrophages show a positive correlation with plaque size, suggesting presence of pro-inflammatory macrophages drives lesion formation. **(B)** Levels of single positive ARG1 plaque macrophages show an inverse correlation with plaque size. **(C)** To investigate if any plaque macrophage population correlates with plaque stability, lesions were stained with Martius Scarlet Blue (MSB) to define collagen (blue). Quantification revealed that PSCK9 plaques have trend towards an increased collagen content, suggesting a more stable lesion. Graph shows mean \pm SEM, two way ANOVA with Sidak's multiple comparisons test. **(D)** The presence of double-negative macrophages in all three-mouse models shows a positive correlation with collagen content, suggesting they may have a role in controlling lesion stability. Further analysis of the plaque macrophage populations and lesion size revealed no significant correlation between lesion size and the presence of double negative **(E)** or double positive plaque macrophages **(F)**. Collagen content of the lesion also showed no correlation with the presence of single positive NOS2 **(G)**, single positive ARG1 **(H)** and double positive plaque macrophages **(I)**. Linear regression and Pearson correlation coefficient were performed to determine correlation. R^2 is reported along with level of significance, set at $p < 0.05$.

4.5 Summary

The work presented in this chapter has used a novel staining and imaging technique to assess plaque macrophage populations using two phenotypic markers *simultaneously*. In summary:

- Plaque macrophages can be *simultaneously* stained for MAC3, a pan macrophage marker; NOS2, a pro-inflammatory macrophage marker and ARG1, an anti-inflammatory macrophage marker.
- Intensity of marker staining can be quantified using ImageJ and be used to generate fluorescent intensity statistics that can be used to investigate different plaque macrophage populations.
- The novel tool was used to compare plaque macrophages in three models of murine atherosclerosis fed high-fat diet; ApoE^{-/-}, LDLR^{-/-} and PCSK9-overexpression mice.
- Analyses revealed plaque macrophages largely exist in a polarised state with high proportion of macrophages existing with either very high or low levels of marker expression.
- Single marker analysis revealed plaque macrophages from ApoE^{-/-} mice have significantly less ARG1 staining (less anti-inflammatory).
- Dual marker analysis enabled investigation into four macrophage populations; single positive NOS2, single-positive ARG1, double negative and double positive.
- This analysis revealed plaque macrophages from ApoE^{-/-} mice are enriched for single-positive NOS2 macrophages (more pro-inflammatory).
- Plaque macrophages from PCSK9-overexpressing mice had significantly higher proportion of double negative macrophages.
- The presence of single positive NOS2 macrophages significantly correlated with lesion size suggesting they may drive lesion formation. No other significant correlation was found for the other macrophage populations.
- The presence of double-negative macrophages significantly correlated with lesion collagen content suggesting they may have a role in plaque stability. No other significant correlation was found for the other macrophage populations.

4.6 Discussion

Plaque macrophages are intimately involved with the initiation, progression and rupture of atherosclerotic plaques (Chinetti-Gbaguidi et al., 2015). Understanding and defining plaque macrophage phenotypes in relation to plaque development is fundamental in order to exploit their potential as therapeutic targets. Plaque macrophage phenotypes atheroma sections from the three most commonly used murine atherosclerosis models were fully characterised.

Macrophage populations were defined using established and well-characterised macrophage polarisation markers: NOS2 and ARG1. NOS2 is traditionally associated with classical activation and is thought to be expressed in cells promoting inflammation. In contrast, ARG1 is associated with alternative activation and with promoting inflammation resolution and repair (Chinetti-Gbaguidi et al., 2015). To ensure macrophage specificity of the analysis, cells were simultaneously stained for MAC3 (CD107b); a well-established and widely used pan-macrophage marker. Whilst each of these markers has previously been used to characterize macrophages in atheromas as single markers, this is the first reported use in combination, enabling characterisation of plaque macrophages as the single cell level.

Murine models of atherosclerosis (discussed in more detail in **section 6.2**) enable researchers to study atherosclerosis relatively accurately to human disease. Work by Piedrahita et al. (1992) and Ishibashi et al. (1993) revolutionised modern atherosclerosis research by the development of apolipoprotein E (ApoE) and low-density lipoprotein receptor (LDLR) knockout mice strains, these particular strains have a rapid onset (a matter of weeks) of atherosclerosis that closely resemble lesions seen in human disease when fed a high-fat diet, both of these models are widely used in atherosclerosis research.

Recently, the discovery of PCSK9 has created a new wave of revolution in the atherosclerosis research field, allowing for the induction of atherosclerosis in murine models. Currently, research-using PCSK9 as a method to induce an atherosclerotic phenotype is in its infancy. However, it is envisaged that this method could be used as a background to induce atherosclerosis in single gene knockout animals thereby

eliminating the need to breed double knockout animals (ApoE^{-/-} or LDLR^{-/-}), thus reducing the time and costs associated with such experiments.

Overexpression of PCSK9 (Proprotein convertase subtilisin kexin type 9) via adeno-associated virus (AAV) injected directly into mice *in vivo* results in an LDLR^{-/-}-like phenotype (Somanathan et al., 2014, Maxwell and Breslow, 2004). Wild-type mice injected with PCSK9 present with 2- and 5-times increase in total and non-HDL cholesterol respectively. PCSK9 activity was additionally shown to be LDLR dependent as injected LDLR^{-/-} mice had no change in plasma lipid levels (Maxwell and Breslow, 2004). Adenovirus mediated gene expression has been previously demonstrated to be an effective way to achieve long-term gene expression. Kassim et al. (2010) demonstrated that AAV8 expressing human LDLR (AAV8.hLDLR) led to a decrease in plasma LDL to normal levels within seven days and levels were sustained for more than a year in a humanised mouse model of familial hypercholesterolaemia.

PCSK9 has a major role in LDLR mediated LDL clearance from plasma. PCSK9, a secreted protein acts as an inhibitor of LDLR by directly binding LDLR in the liver and mediates its lysosomal degradation (**Figure 4.8**). Interestingly, patients with familial hypercholesterolaemia (FH) have mutations associated with PCSK9. PCSK9 missense, gain of function mutations have been linked to autosomal dominant hypercholesterolaemia (ADH) a rare form of FH. Patients with these type of mutations appear to have enhanced PCSK9 activity that elevates both total and LDL cholesterol levels causing increased cholesterol deposition in the tissues and premature development of atherosclerosis (Lambert et al., 2009). Currently, research-using PCSK9 as a method to induce an atherosclerotic phenotype is in its infancy.

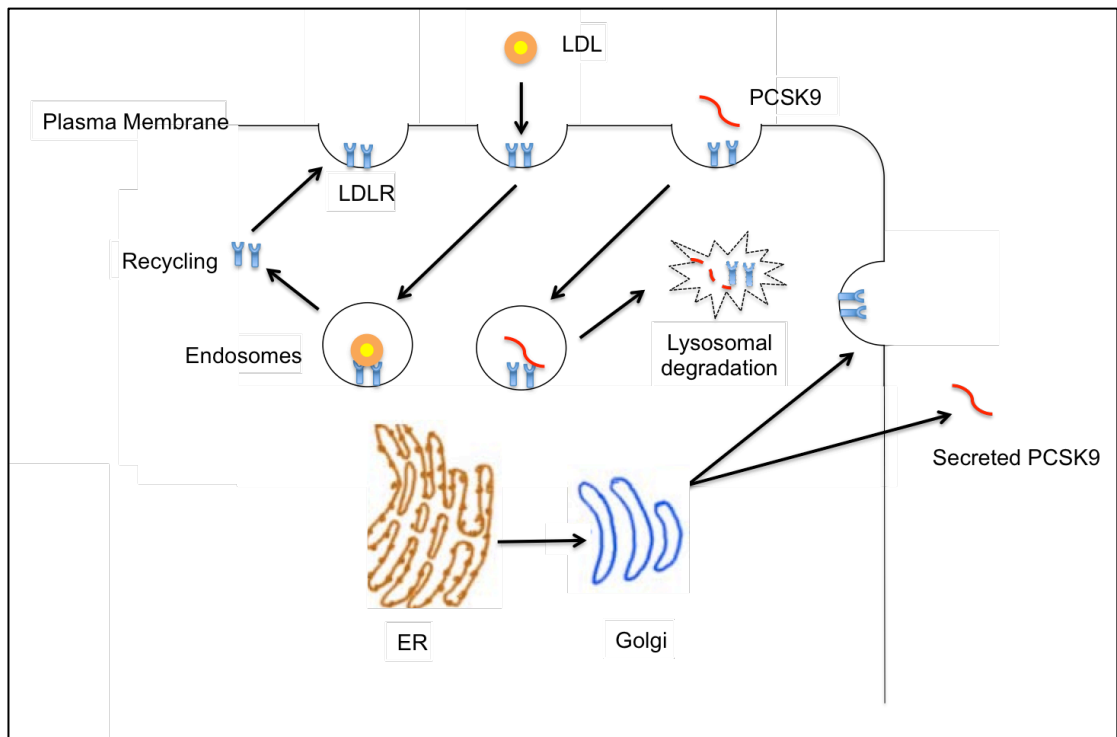


Figure 4.8: The mechanism of PCSK9 clearance of LDLR.

Circulating PCSK9 binds to the LDLR on the surface of hepatocytes causing internalisation of both LDLR and PCSK9. Once bound and in the endosome, PCSK9 targets LDLR for degradation in the lysosome, thus reducing surface expression of LDLR. As discussed above, circulating LDL binds LDLR causing its internalisation and progression into the cholesterol transport pathway and ultimate recycling and excretion. Increasing plasma levels of PCSK9 causes increased turnover and reduced surface expression of LDLR thereby raising circulating levels of LDL causing hypercholesterolaemia (Lambert et al., 2012).

In this study it was found that ApoE^{-/-} mice had larger lesions in the aortic root (data not shown). Comparison of murine models of atherosclerosis in the literature has demonstrated ApoE^{-/-} mice develop spontaneous lesions without the need for dietary supplement, unlike LDLR^{-/-} mice. When an atherogenic diet such as Western diet is introduced, ApoE^{-/-} mice typically develop more advanced lesions quicker than LDLR^{-/-} mice (Whitman, 2004). ApoE^{-/-} mice typically have higher plasma lipid levels, and this in part might be a reason why they typically develop lesions quicker (Ishibashi et al., 1993, Getz and Reardon, 2006) as elevated plasma lipid levels in man are one of the classical risk factors for developing atherosclerosis. Elevated levels of inflammatory mediators such as IL-6, TNF- α and C-reactive protein (CRP) secreted by pro-inflammatory macrophages have also been shown to have predictive value for future vascular events with increased vascular risk associated with

increased basal levels of these cytokines in human studies (Ridker et al., 2000, Danesh et al., 2000).

Additionally, the abundance of single positive NOS2 plaque macrophages positively correlate with lesion size in high fat diet fed mice, across the experimental models, suggesting that this macrophage population might be an important local driver of atheroma development. NOS2 expression in macrophages promotes the production of free radicals such as nitric oxide (NO), superoxide (O₂⁻) and peroxynitrite (ONOO⁻). These products are thought to cause protein nitration, DNA damage and PARP activation (Holvoet et al., 1995). However, whether elevated plasma lipid levels in the ApoE^{-/-} mice drive the polarisation towards single NOS2 positive macrophages or this is due to other factors, is currently unclear. Interestingly however, ApoE itself has been shown to be athero-protective independently of its effects on plasma lipid levels. In agreement with my observations ApoE can polarise pro-inflammatory macrophages to anti-inflammatory by simultaneously down-regulating NOS2 and up-regulating ARG1 expression (Baitsch et al., 2011). Similarly, ApoE was shown to have anti-oxidative properties and can induce significant regression of atherosclerotic lesions (Tangirala et al., 2001). Detmers et al. (2000) have previously investigated the role of NOS2 directly in *ApoE^{-/-}NOS2^{-/-}* double knockout mice fed on high fat diet for 16 and 22 weeks. Whilst NOS2 deficiency had no effect on plasma cholesterol and triglyceride, they reported a 30-50% and 45-70% reduction in atherosclerosis at 16 and 22 weeks respectively. Furthermore, the size of necrotic core and level of foam cells were unaffected by NOS2 deficiency. Similarly, NOS2 expression has been shown to correlate with lesion size in rabbits (Alfon et al., 1999). It has been suggested that NOS2 has direct effects at the site of the lesion by in part promoting inflammation and lipoperoxide formation such as malondialdehyde (MDA), which modifies low density lipoproteins (LDL) promoting foam cell generation (Kuhlencordt et al., 2001). Elevated levels of MDA-modified LDL may be a marker for unstable atherosclerotic lesions (Holvoet et al., 1995).

Interestingly, an abundant population of double positive macrophages was observed in the analysis; a macrophage subtype that has not previously been reported, to my best knowledge. Whilst the functional significance of these cells is currently unclear, it can be speculated that they may represent a population of cells that are

transitioning from one phenotype to another. In support of such hypothesis, cell-tracking experiments have previously demonstrated a switch between M1 and M2 macrophage phenotypes *in vivo* (Lee et al., 2011).

Furthermore, the presence of double negative macrophages significantly correlates with collagen content in the atherosclerotic lesion. Collagen is an important component of the extracellular matrix of the arterial wall and its presence is the result of a dynamic balance between its degradation and synthesis. Indeed, collagen is an important component of the fibrous cap and confers tensile strength to the developing atheroma. Dissolution of collagen weakens the fibrous cap causing it to become vulnerable to fracture when exposed to haemodynamic forces caused by the cardiac cycle (Newby, 2005, Libby, 2012). Typically, rupture prone plaques often exhibit a thin fibrous cap with lower collagen content (Davies, 2000). A possible rationale for the presence of double negative macrophages and their correlation with plaque collagen content is that they may secrete tissue inhibitors of matrix metalloproteinases (TIMPs). Matrix metalloproteinases (MMPs) are widely thought to be involved in the growth, de-stabilisation and eventual rupture of atherosclerotic lesions by degrading components of the extracellular matrix. TIMPs secreted by macrophages inhibit the activity of these proteases in the lesion and are thought to act as an important protective mechanism against plaque degradation (Newby, 2005).

Interestingly, MMP-14 expression is up regulated and TIMP3 expression is down regulated in foam cell macrophages compared to non-foamy macrophages isolated from high-fat diet vs. chow fed rabbits. These MMP14^{high}TIMP-3^{low} cells were found to be highly invasive and proliferated more rapidly than MMP14^{low}TIMP3^{high} cells suggesting that the MMP: TIMP balance is a fundamental characteristic of plaque stability (Johnson et al., 2008) *Timp3*^{-/-} mice show increased collagen degradation and *Timp3* overexpressing mice show reduced atherosclerosis with increased lesion collagen content and reduced necrotic core (Sahebjam et al., 2007, Casagrande et al., 2012). Therefore, the increased presence of double negative macrophages in this study may be an important source of TIMPs, thus inhibiting MMPs and promoting collagen synthesis. However, testing this hypothesis by simultaneous staining for MAC3/NOS2/ARG1 and additional proteins (MMPs and/or TIMPs) is a substantial technical challenge thus will be the subject of future

studies.

In addition, it is also feasible that some of the double negative macrophages are Mox macrophages that have been demonstrated to be present in the plaque and to react to oxidized phospholipids. These are distinct from M1 and M2 macrophages characterised by reduced expression of both NOS2 and ARG1 and have been reported to account for up-to 30% plaque macrophages in advanced lesions of mouse atheromas (Kadl et al., 2010).

As these double negative macrophages express no detectable (or low levels of) NOS2 and ARG1, these cells could also be so-called 'memory macrophages' that retain memory of past challenges. Although no long-term experiments have been performed and their existence has not been described in lesions before it is speculated that surviving macrophages after an inflammatory challenge may form a new population that have a low level of self-renewal and may behave as anti-inflammatory macrophages (Italiani and Boraschi, 2014).

The macrophage populations of a relatively new atherosclerosis model; PCSK9 were also investigated. Hepatic overexpression of a gain of function form of PCSK9 (incorporated into an adeno-associated virus (AAV) results in an LDLR^{-/-} like phenotype (Somanathan et al., 2014, Maxwell and Breslow, 2004). PCSK9 is a secreted protein and has a major role in LDLR mediated LDL clearance from plasma. PCSK9 binds directly to LDLR in the liver and mediates its lysosomal degradation resulting in reduced surface expression of LDLR, thereby raising circulating levels of LDL, thus inducing hypercholesterolaemia (Lambert et al., 2012, Lambert et al., 2009). In line with expectations, the analysis confirms that LDLR^{-/-} and PCSK9 plaques have a similar macrophage profile, thus further validating the utility of this relatively new model of experimental atherosclerosis. Induction of atherosclerosis by PCSK9 overexpression has promise to revolutionise atherosclerosis research as it could be used as a background to induce atherosclerosis in single gene knockout animals, thereby eliminating the need to breed double knockout animals, thus reducing time and costs associated with such experiments.

In summary, this study highlights that distinct macrophage populations are present in the plaques of atherosclerotic mouse models and these correlate with atheroma

phenotype. I have shown the enrichment of single positive NOS2 cells significantly correlates with lesion size and macrophages that are negative for both NOS2 and ARG1 significantly correlate with lesion stability. This approach of image analysis could be used to investigate and understand modulators of macrophage phenotype *in vivo*.

Chapter 5. Overexpression of *Trib1* in haematopoietic cells induces atherosclerosis and metabolic phenotype in ApoE^{-/-} mice

5.1 Introduction

Despite TRIB1's role in inflammation and plasma lipid homeostasis, both hallmarks of atherosclerosis there have been no direct studies that have elucidated its role in this disease. Work by Sung et al. (2007) and Liu et al. (2013) demonstrated *Trib1* to be involved in the chemotaxis and proliferation of smooth muscle cells and also the migration of macrophages, both important pathological features of developing atheromas (Sung et al., 2007, Liu et al., 2013). Interestingly, in plaque macrophages specifically, the percentage of TRIB1-expressing macrophages is decreased in the lesions of mice that lack the IL-1 receptor and therefore cannot signal via IL-1 (ApoE^{-/-}/IL1R1^{-/-} double knockout) compared to controls (ApoE^{-/-}) (Sung et al., 2012).

To investigate the role of myeloid *Trib1* in atherosclerosis directly, bone marrow transplants were performed. Due to the nature of atherosclerosis, many mice strains are highly resistant to the disease. However, in the first study of its kind it was discovered that C57BL/6 mice are mildly susceptible to atherosclerosis and develop small lesions when fed a highly atherogenic 'Paigen' diet (Paigen et al., 1987). Since then work by Piedrahita et al. (1992) and Ishibashi et al. (1993) has revolutionised modern atherosclerosis research by the development of apolipoprotein E (ApoE) and low-density lipoprotein receptor (LDLR) knockout mice strains, these particular strains have a rapid onset (a matter of weeks) of atherosclerosis that closely resemble lesions seen in human disease when fed a high-fat diet, both of these models are widely used in atherosclerosis research.

Since the *Trib1* x *LyzMCre* mouse strains used in **Chapter 3** were developed on a C57BL/6 genetic background, it was not possible to induce atherosclerosis to the extent that is physiologically relevant *in vivo*. Therefore bone marrow was transplanted from these mice into atherogenic ApoE^{-/-} mice. Transplantation of bone marrow into atherogenic mouse models are a useful tool to elucidate the role of circulating blood cells including monocytes in atherogenesis (Getz and Reardon,

2012). Whole body irradiation is used to destroy the recipient's bone marrow that contains the pre-cursors of the blood and immune cells. When bone marrow (either normal or genetically altered in this case) is reconstituted via transplantation, it can be used to discriminate between the contribution of the circulating blood cells from those from other cells in the developing plaque such as smooth muscle and endothelial cells.

5.2 Hypothesis

In this Chapter, the bone marrow from the same strains of mice used in **Chapter 3** were isolated and transplanted into irradiated ApoE^{-/-} mice. Based on the results presented in **Chapter 3** and the literature, I hypothesise myeloid *Trib1* derived from the bone marrow alters atheroma development and metabolic syndromes in ApoE^{-/-} mice fed on high fat diet.

5.3 Materials & Methods

5.3.1 Animals

Mixed gender *Trib1* x *LyzMCre* mice (*Trib1* *fl/fl* x *LyzMCre* & *ROSA26.Trib1* x *LyzMCre*) donor mice were bred and sourced from the University of Leeds, UK. To avoid potential gender-dependent differences in atherosclerosis development, all male *ApoE*^{-/-} were used and were also bred and sourced from the University of Leeds, UK. As bone marrow transplantation involves destruction of bone marrow, the recipient mice are essentially immunosuppressed; therefore the success of the transplant depends highly on keeping the environment sterile to avoid the likelihood of developing infections. To that end, all mice were housed in individually ventilated caging (IVC) with sterile bedding and fed standard laboratory chow diet (2018S, Tekland Global) and sterile water *ad libitum* until bone marrow transplant commenced at aged 12-13 weeks. Bone marrow transplants were carried out in two waves, separate for each *Trib1* model (myeloid *Trib1*-overexpressing vs. -knockout). Each experiment was carried out using litter-mate control mice (normal levels of *Trib1* expression) for each of the models.

5.3.2 Bone marrow transplantation

Recipient male *ApoE*^{-/-} mice were given sterile acidified water (1.1% (v/v) HCl) *ad libitum* one week prior to the procedure to reduce bacterial growth in the drinking water from regurgitated food, thereby reducing chances of infection.

5.3.2.1 Total body irradiation

Recipient male *ApoE*^{-/-} mice aged 13 weeks were treated with a lethal dose of whole body irradiation totalling 11 Grays (1000 rads), in two doses four hours apart. Following the final dose of irradiation, mice were placed in an incubator at 35°C for one hour prior to receiving bone marrow injection via the tail vein.

5.3.2.2 Bone marrow cell preparation and transplantation

Donor *Trib1* x *LyzMCre* mice were sacrificed humanely by cervical dislocation at 12-13 weeks. The femurs and tibias were removed under aseptic conditions and bone marrow was flushed from the bones with RPMI-1640 medium + 10% (v/v)

fetal calf serum (FCS) using a syringe and 26-gauge needle. The cell suspension was passed through a 40µm cell strainer and centrifuged at 500x g for 5 minutes. The supernatant was removed and discarded. The cell pellet was re-suspended in Hank's buffered salt solution (HBSS) + 10% (v/v) FCS to a single cell suspension. In order to count the cells accurately, 1% (v/v) acetic acid was added to a small volume of cell suspension to lyse the red blood cells. Cells were counted using a haemocytometer and placed on ice until tail vein injections commenced.

Recipient ApoE^{-/-} mice were injected with 200µl of mixed whole bone marrow via the tail vein. Each mouse received 2-4x10⁶ donor cells in total and was returned to the sterile ventilated caging. Mice were monitored daily for the first week after transplant and twice daily in the second week. If mice appeared unwell at any stage they were culled immediately. Mice were continually maintained on sterile acidified water (1.1% (v/v) HCl) until the end of the procedure.

5.3.2.3 High fat diet

Following seven weeks post transplant recovery in sterile conditions, mice were fed on a high-fat (21%) western diet (829100; Special Diet Services, Baintree, UK) for 12 weeks to enhance atherosclerosis. **Figure 5.1** Outlines the bone marrow transplant procedure and **Table 5.1** shows the number and nomenclature of the chimera mice produced from each experiment.

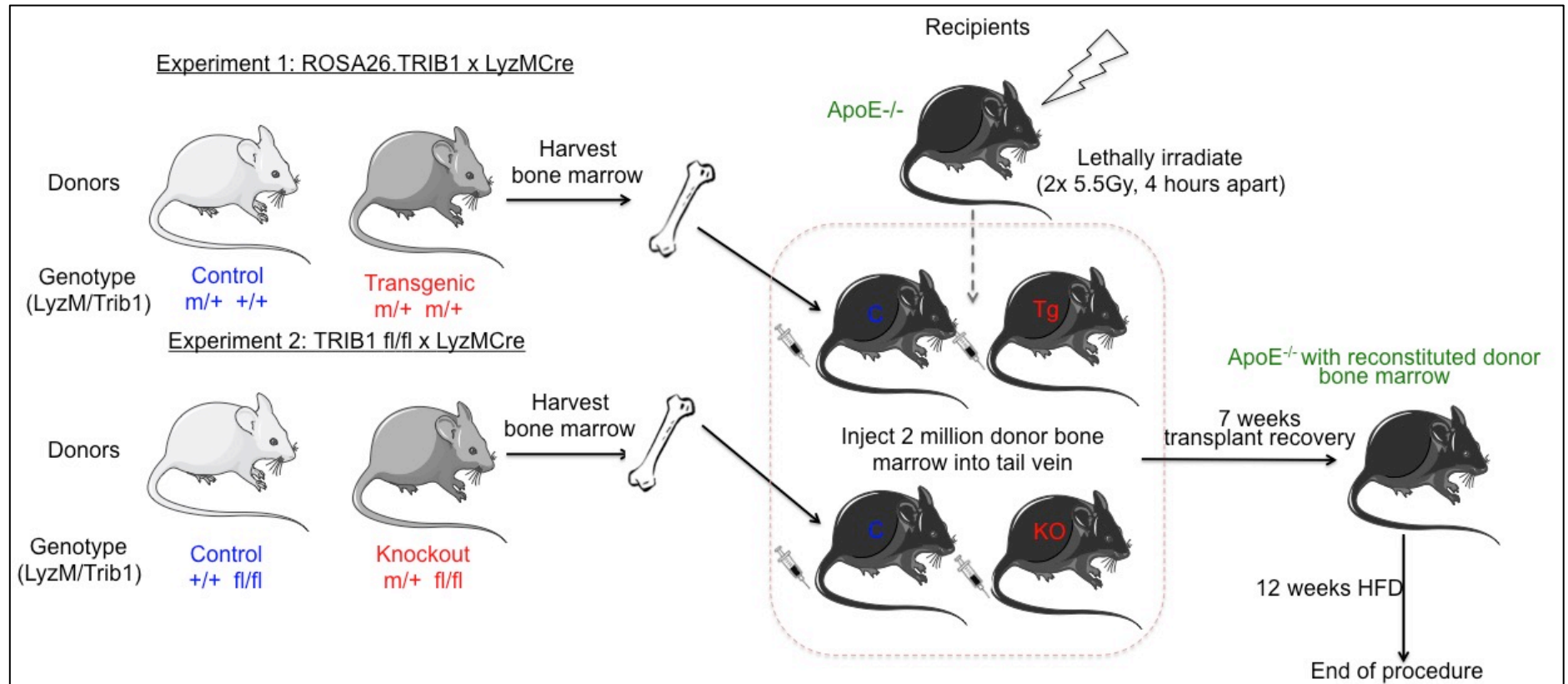


Figure 5.1: Schematic of bone marrow transplantation into ApoE^{-/-} mice and induction of experimental atherosclerosis.

Donor *Trib1* x *LyzMCre* mice were humanely killed via cervical dislocation. Bone marrow from femurs and tibias were isolated under sterile conditions. Recipient ApoE^{-/-} mice were given a lethal dose of irradiation (5.5Gy), 2 hours apart, following an hour at 35°C, the mice were given a tail vein injection of mixed donor bone marrow (2-4x10⁶ cells). Following seven weeks transplant recovery and reconstitution of bone marrow, the *Trib1*-ApoE^{-/-} chimera mice were fed on high fat 'Western' diet (HFD) for 12 weeks to induce atherosclerosis. Note the colour of the mice have no significance and are merely to illustrate the different genotypes of mice in these experiments for clarity.

Table 5.1: Outline of *Trib1* x *LyzMCre* → ApoE^{-/-} bone marrow transplantation.

Table shows donor and recipient genotype along with numbers of mice used in each experiment.

Donor	Recipient ApoE ^{-/-}	
	Control	Experimental
Experiment 1: <i>ROSA26.Trib1</i> x <i>LyzMCre</i> (<i>Trib1</i> transgenic)	10	12
Experiment 2: <i>Trib1 fl/fl</i> x <i>LyzMCre</i> (<i>Trib1</i> KO)	6	10

5.3.3 End of procedure and cardiac puncture

Mice weights were recorded and the animals were sacrificed humanely under a Home Office licensed procedure using a pharmacological overdose of sodium pentobarbital (200mg/ml). Following the loss of the pedal reflex, blood was collected by cardiac puncture directly into the heart through the chest wall into a heparinised syringe. For plasma, blood was centrifuged for 5 minutes at 200x g at room temperature.

5.3.4 Perfusion fixation

Once breathing had stopped, the abdominal cavity was exposed and the lower aorta was cut to provide a path for blood loss. The chest cavity was opened and the circulation was perfusion fixed by direct injection of 1ml PBS followed by 1ml 10% (v/v) Formalin/ FBS into the heart.

5.3.5 Tissue dissection

Organs of interest including the spleen, liver and adipose were removed from the mice via blunt dissection and placed into a bijou containing 2.5ml 10% (v/v) formalin. Tissues were then processed for histological analysis.

5.3.5.1 Dissection of the aortic tree

To expose the aortic tree, the ribs, thymus, lungs and oesophagus were removed by blunt dissection. The aorta was exposed *in situ* by careful removal of fat tissue and branching vessels from the aortic wall beginning at the descending aorta (above the

level of the diaphragm) to the aortic arch. The aortic arch and its main vessels including the brachiocephalic left common carotid and left subclavian arteries were removed from the surrounding tissue.

Fine cleaning and dissections were carried out in a petri dish using a dissecting microscope, ensuring the tissue was kept moist at all times. Any remaining adventitial fat was removed and the aorta was removed from its origin at the top of the heart.

The branching arteries: the brachiocephalic, left common carotid and left subclavian were removed from the aorta. The brachiocephalic artery, another common site of atherosclerosis was removed from its branch point at the aortic arch to the bifurcation into the right common carotid and right subclavian arteries and placed in 1ml of 10% (v/v) formalin.

The heart was cut along the midline below the atria at a slight angle to view the aortic sinus. Both pieces were placed in 2.5ml of 10% (v/v) formalin at 4°C for 24 hours, after 24 hours, tissues were placed in PBS and kept at 4°C until further processing

The aorta was dissected longitudinally under the arch to expose the inner surface and was also dissected down the outer curvature for its entire length. The aorta was placed in 4% (w/v) PFA at 4°C for 24 hours, after 24 hours aortae were placed in PBS and kept at 4°C until further processing (**Figure 5.2**).

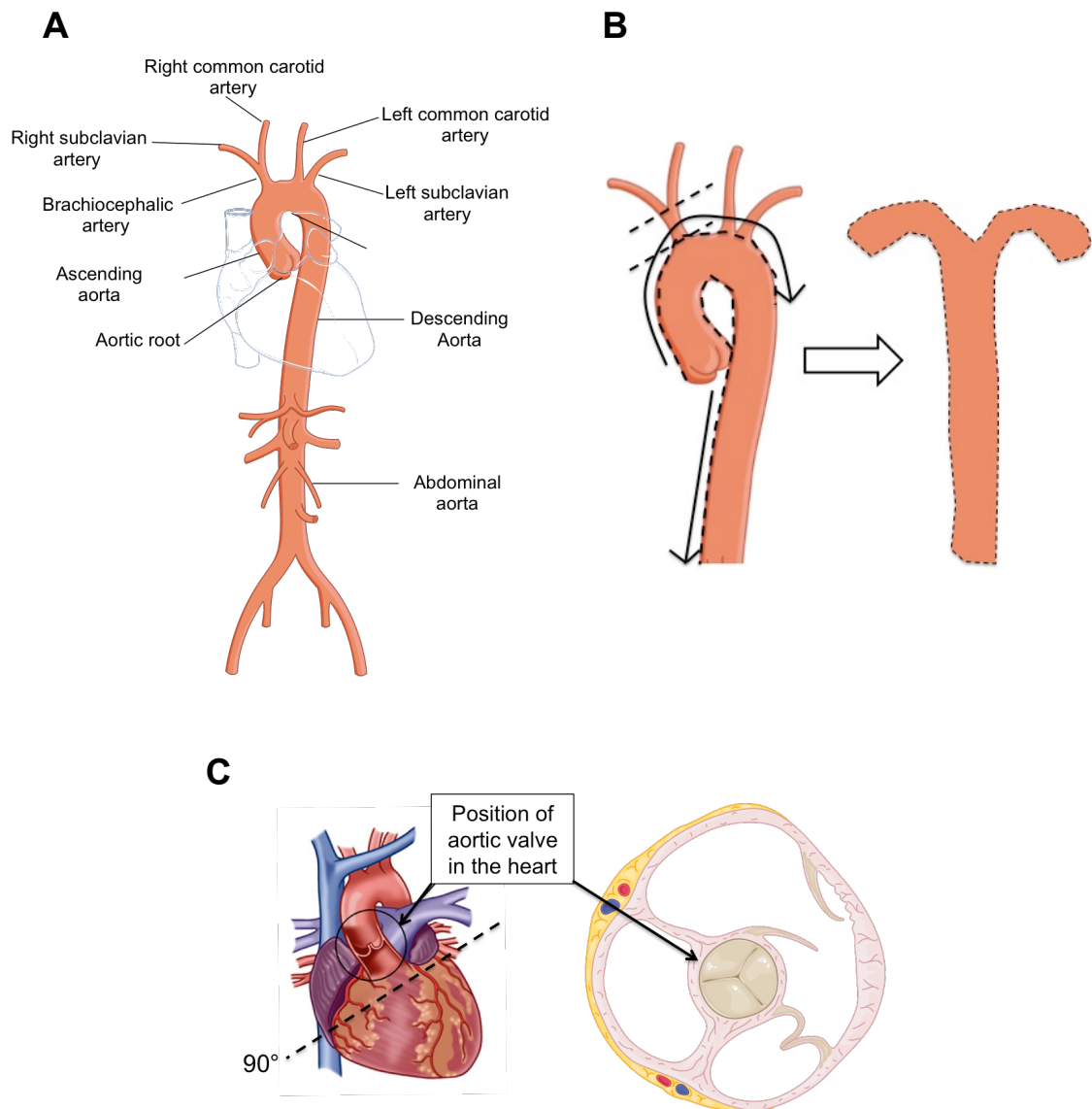


Figure 5.2: Schematic illustration of tissues excised for examination of atherosclerosis.

(A) Diagram to illustrate the blood vessel architecture. Note the location of the aortic root in relation to the whole aorta and heart. The aortic root is one of the dilations of the aorta present just above the aortic valve and a site of high atherosclerotic burden in mice. (B) The whole aorta was dissected from the mouse and cleaned of any remaining adventitial fat and cut open along the arch and down the inner surface of the descending aorta to expose the inner surface (along the dotted lines). The aortic arch branch vessels; the brachiocephalic, left common carotid and subclavian arteries were also removed. Note; the brachiocephalic artery is another site prone to atherosclerosis in mice and can be kept for histological analysis. (C) The heart was transected at a 90° angle to allow correct orientation for the visualisation of the aortic root (just above the valve) for histological analysis.

5.3.6 Blood biochemistry

Plasma was obtained from blood as described in **section 2.1.5** and stored at -80°C until analysis. Frozen plasma was sent to Royal Hallamshire Hospital (Sheffield Teaching Hospitals) Department of Clinical Chemistry. A full lipid profile including total cholesterol, low- (LDL) and high- density lipoproteins (HDL), triglycerides and glucose were obtained using Roche Cobas 8000 modular analyser series (study code CVTRIB- 70/7992). LDL- cholesterol was calculated using the following formula known as the Friedwald equation:

$$LDL = Cholesterol - HDL - \left(\frac{Triglyceride}{2.2} \right)$$

The Friedwald equation should not be used if plasma triglyceride concentration exceeds 4.52 mmol/L, but since all triglyceride concentrations were <3mmol/L the calculation was valid.

5.3.7 Histological processing and paraffin embedding of tissues

The aortic root and other tissues of interest were dehydrated and embedded in paraffin for histological analysis as follows; the tissue was sandwiched between two sheets of Whatman Grade 1 filter paper (aortic sinus facing up) and placed inside a processing cassette. The tissue was dehydrated sequentially in the following order: 50% (v/v) ethanol 1 hour, 70% (v/v) ethanol 1 hour/ overnight, 90% (v/v) ethanol 1 hour, 100% (v/v) ethanol 1 hour, 100% (v/v) ethanol 1 hour, 50:50 (v/v) ethanol/ xylene 1 hour, xylene 1 hour and xylene for 1 hour. Tissue cassettes were placed in molten paraffin at 60°C to infiltrate overnight. Tissues were then placed (aortic sinus facing up) into paraffin moulds and filled with molten paraffin. Embedding cassettes were then placed on top and left to set overnight. To section, wax blocks were placed on melting ice 1 hour prior to sectioning. Blocks were trimmed until the aortic sinus was reached and then subsequently cut at 5µm thickness using a microtome. The sections were placed in a pre-heated (~40°C) mounting bath and mounted on glass microscope slides. The slides were then dried at room temperature and transferred to a 37°C drying oven overnight.

5.3.8 Histological analysis

5.3.8.1 *En Face* staining of the Aorta

Whole aortas were dissected longitudinally and fixed in 4% (w/v) paraformaldehyde and stained with Oil Red O to visualise areas of atheromatous lesions. Oil Red O stain was prepared as follows; Oil Red O powder was added to 99% (v/v) isopropanol (Propan-2-ol) until the solution became saturated. The solution was then filtered using Whatman filter paper and diluted to a working solution of 60% (v/v) using H₂O. Aortas were rinsed in ddH₂O followed by 60% (v/v) isopropanol for 2 minutes and immersed in Oil Red O for 15 minutes. The aortas were then rinsed in 60% (v/v) isopropanol for 2 minutes followed by ddH₂O. Aortas were stored in ddH₂O at 4°C until pinning out and photographing.

5.3.8.2 Histology & Morphometry

Molten paraffin wax was poured into a petri dish to form a substrate for pinning. When the wax became firm (before fully setting), each aorta was pinned open using insect pins (Fine Science Tools) and immersed in PBS. Images of each aorta were captured using a Nikon camera at 10x and 15x magnification together with a ruler for scale. Image scale was calibrated and used to measure the total area of each aorta as well as detect and quantify areas of positive staining (user defined threshold). **Figure 5.3** gives an outline of the quantification procedure. The percentage lesion coverage was calculated by the following formula:

$$\% \text{ lesion coverage} = \frac{\text{number of objects} \times \text{mean lesion area} \times 100}{\text{Total aorta area}}$$

Image analysis was performed using the NIS-Elements software (Nikon Instruments, Kingston upon Thames, UK).

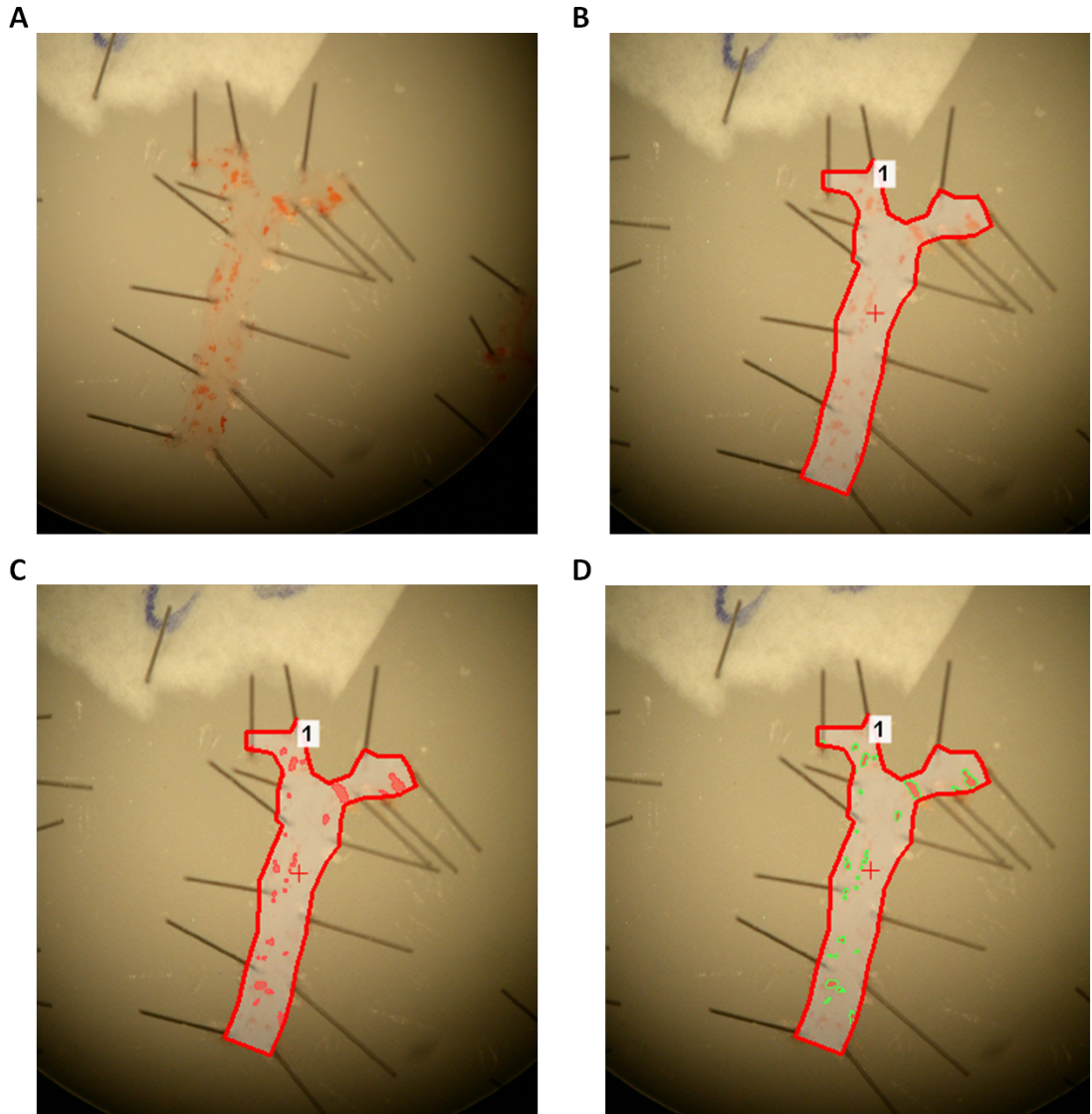


Figure 5.3: Quantification of *en face* Oil Red O staining in whole aorta.

(A) Image of whole murine aorta stained with Oil red O, showing positive staining in red, image captured at x10 magnification. (B) The area of positive staining was calculated using NIS Elements software by manually outlining the aorta (red). (C) The software was then used to highlight areas of positive staining by using a user-defined threshold based on hue, saturation and intensity filters. (D) The software highlights separate objects of positive staining (green) and the percentage lesion area can be calculated using the equation in **section 5.3.8.2**. The software was calibrated by capturing an image of a ruler at the same magnification.

5.3.8.3 Histological staining

The aortic sinus, liver and adipose tissue cross-sections were stained using histological dyes to identify tissue constituents and structure. Slides were de-waxed and rehydrated through graded alcohols to water. Sections were stained with various dyes including alcian blue/ elastic van Gieson (EVG), haematoxylin and eosin (H&E) or martius scarlet blue (MSB). Details of staining procedures can be found in

Appendix III. Following staining, slides were dehydrated and mounted using appropriate sized coverslips and DPX resin.

5.3.9 Assessment of lesion size and macrophage infiltrate in aortic roots

5.3.9.1 Lesion size

Aortic root plaques stained with elastic van Gieson were imaged and measured in an analogous way to Oil red O staining using NIS Elements Software. **Figure 5.4** Shows the anatomy of the aortic sinus, one of the most common sites of atherosclerosis in mice and outlines the image analysis tool used to measure lesion size.

5.3.9.2 Histological staining and plaque pathology

The aortic sinus, liver and adipose tissue cross-sections were stained using histological dyes to identify tissue constituents and structure. Slides were de-waxed and rehydrated through graded alcohols to water. Sections were stained with various dyes including alcian blue/ elastic van Gieson (EVG), haematoxylin and eosin (H&E) or martius scarlet blue (MSB). To assess if TRIB1 is present in human atheromas, human coronary plaques were stained dual with TRIB1 (1:100, Rabbit polyclonal anti-human TRIB1, Millipore, UK) and CD68 (1:100, Mouse monoclonal anti-human CD68, Dako). To assess macrophage infiltrate into the plaque, aortic root sections were stained with Mac3 (1:100, Rat monoclonal anti-mouse Mac3, BD Pharmingen, UK) using standard immunohistochemistry protocols. Details of staining procedures and specific protocols can be found in **Appendix V**. Following staining, slides were dehydrated and mounted using appropriate sized coverslips and DPX resin.

5.3.9.3 Quantification of Lesion size

Aortic sinus lesions were imaged at x40 magnification typically two sections per 150µm (approximately) along the length of the vessel generating typically 5 slides each with 3 valves present from each animal to give a mean value. Lesion size was measured by manually tracing around each lesion in NIS-Elements software (Nikon, UK). Lesion size was normalised to the vessel cross-sectional area (CSA) to account and normalise for the possible variability of vessel size between each animal. The CSA was measured by manually tracing around the circumference of the vessel wall (**Figure 5.4**).

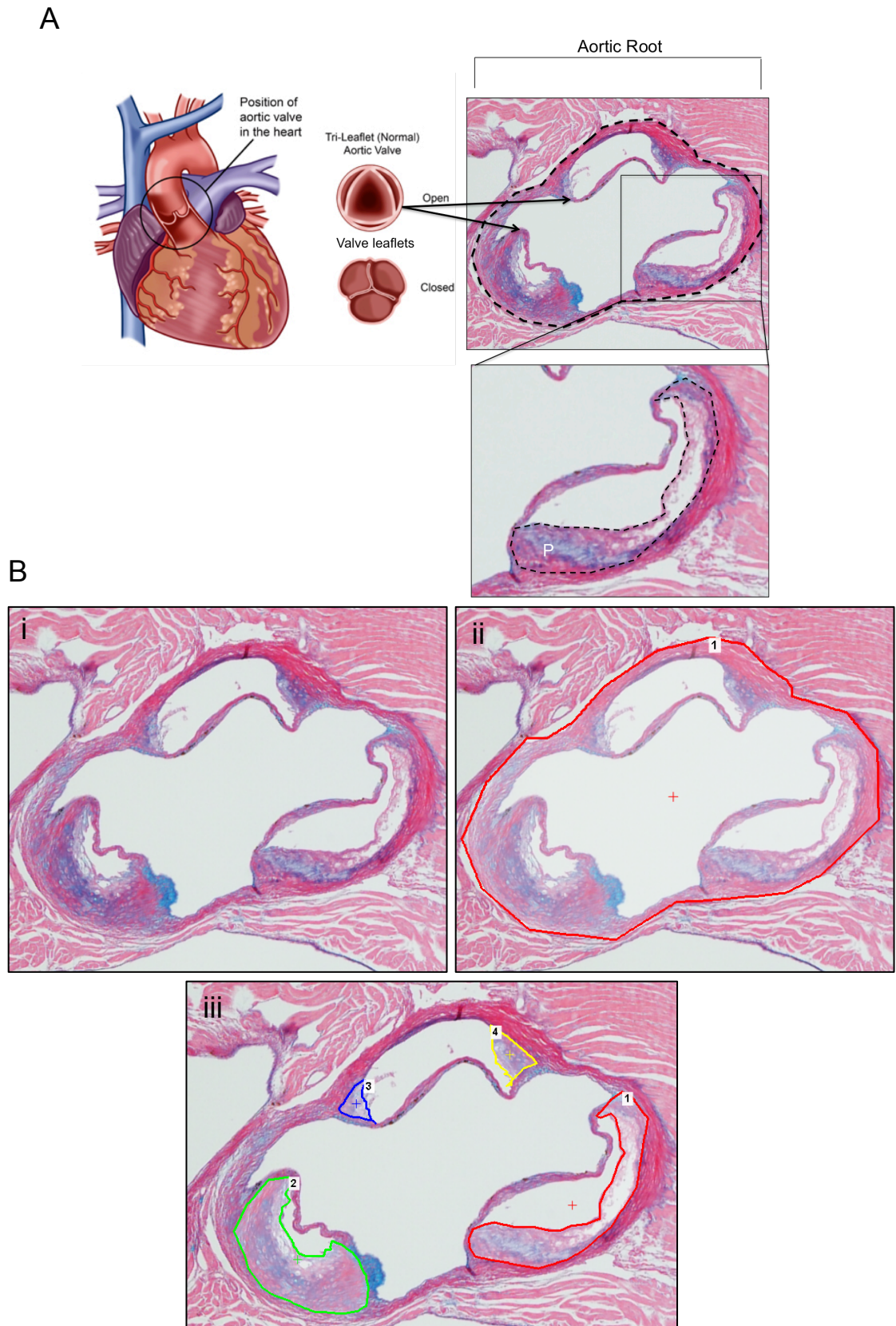


Figure 5.4: Anatomy of the mouse aortic sinus (root).

(A) A representative image of an aortic root histological section in the context of the heart. The aortic root (outlined) is one of the dilations of the aorta present just above the aortic valve and is a routine site for histological examination of atherosclerotic plaques in mice. The location and anatomy of the valve leaflets are shown. The presence of an atherosclerotic plaque is shown (inset, P). (B) Lesion size is calculated using NIS Elements software. (i) Original aortic root image. (ii) Using the ROI function, the total cross sectional area of the sinus was manually traced (outlined in red). (iii) Individual lesion areas were also manually traced (outlined in various colours and numbered 1-4), individual lesion areas were combined to give a total lesion area.

5.3.9.4 Quantification of Mac3 and Collagen staining

Mac3 content was determined by colourimetric immunohistochemistry using DAB and quantifying areas of brown staining. Collagen content was determined using MSB staining and quantifying areas of blue staining with the lesions. As with Oil Red O staining, Mac3 and collagen levels were quantified using the threshold function with HSI filters (NIS-Elements, Nikon, UK) to select areas of positive staining. The area of positive staining was expressed as a percentage of the total lesion area.

5.4 Results

5.4.1 Human plaque macrophages express TRIB1

TRIB1 expression has been positively stained for in the atherosclerotic lesions of mice (Sung et al., 2012), however to validate expression in humans, coronary plaques derived from human patients that underwent a coronary endarterectomy (removal of atherosclerotic plaque material) were stained for TRIB1. **Figure 5.5** shows a representative image of dual positive staining of TRIB1 in human plaque (CD68+) macrophages. Therefore confirmation of TRIB1 expression in human plaques provides support that findings in mice studies can be transferred to- and are relevant to human disease.

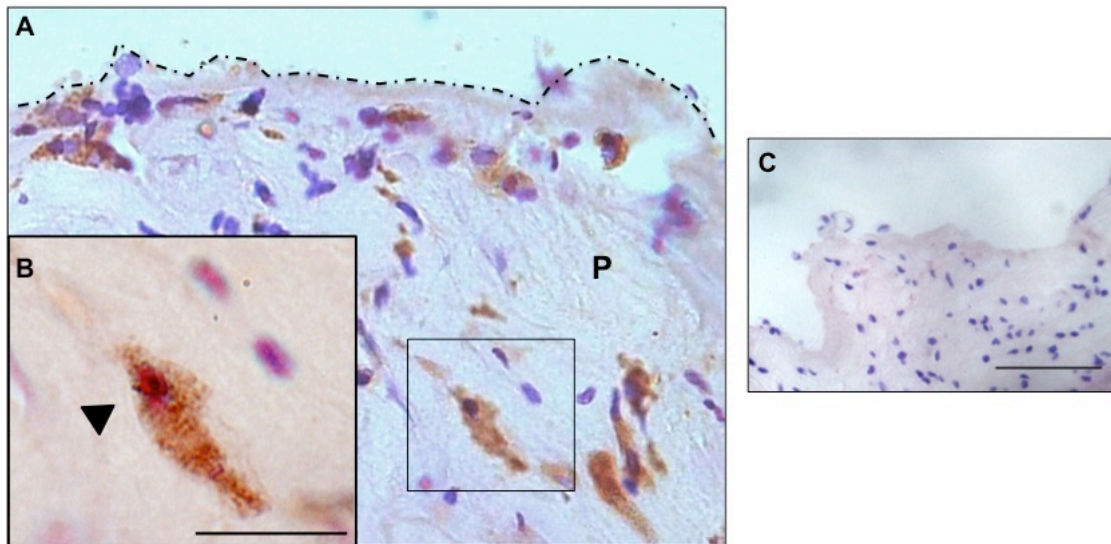


Figure 5.5: TRIB1 expression in human plaque macrophages.

(A) Dual staining of macrophage (CD68; brown) and TRIB1 (red) in human atherosclerotic plaque (P) counterstained with haematoxylin. (B) High power image of boxed area. Arrow indicates positive dual staining for CD68 and TRIB1 (C) Isotype control showing lack of staining. Scale= 50 μ m

5.4.2 Survival of *Trib1* x *LyzMCre* \rightarrow *ApoE*^{-/-} mice

Within the Department, irradiation and bone marrow reconstitution is known to cause up to 30% of sudden death in mice between days 7-14 post-procedure (unpublished data). In addition, altered chimera state in extreme cases may account for an additional 10-20% mortality. However, in both waves of my experiments, there was a 100% survival rate in *ApoE*^{-/-} mice reconstituted with *Trib1* bone marrow. Despite 100% survival, confirmation of bone marrow engraftment was not verified but will be the subject of future work.

5.4.3 *Trib1* x *LyzMCre* \rightarrow *ApoE*^{-/-} have altered atherosclerosis burden

5.3.2.1 Aorta

To date there has been no reported study that has investigated the role of myeloid *Trib1* in atherosclerosis, to determine the extent of atherosclerosis, whole aortae from the transplanted mice were stained with Oil Red O *en face* (**Figure 5.6A**). Oil Red O stains lipid and triglyceride deposits on tissue, and thus highlights lipid rich atherosclerotic lesions on the inner lumen of the aorta. The mean percentage area of oil red o staining was calculated for each mouse aorta. Staining revealed *Trib1*^{Tg} \rightarrow

ApoE^{-/-} mice have a 2-fold increase in disease burden compared to control mice (5.21 ± 0.89%; Trib1^{Tg}→ ApoE^{-/-} vs. 2.5 ± 0.85%; control, p<0.05). Equally, Trib1^{KO}→ ApoE^{-/-} mice displayed a significant attenuation of atherosclerosis in the aorta compared to Trib1^{Tg}→ ApoE^{-/-} mice (0.46 ± 0.8%; Trib1^{KO}→ ApoE^{-/-} vs. 5.21 ± 0.89%; Trib1^{Tg}→ ApoE^{-/-}, p<0.001). Although the myeloid *Trib1* KO mice showed a reduced trend of atheroma compared to control mice, these data were not statistically significant (**Figure 5.6B**).

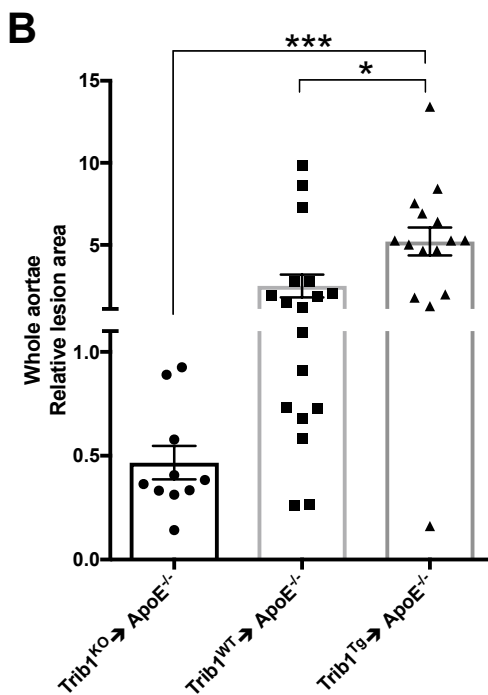
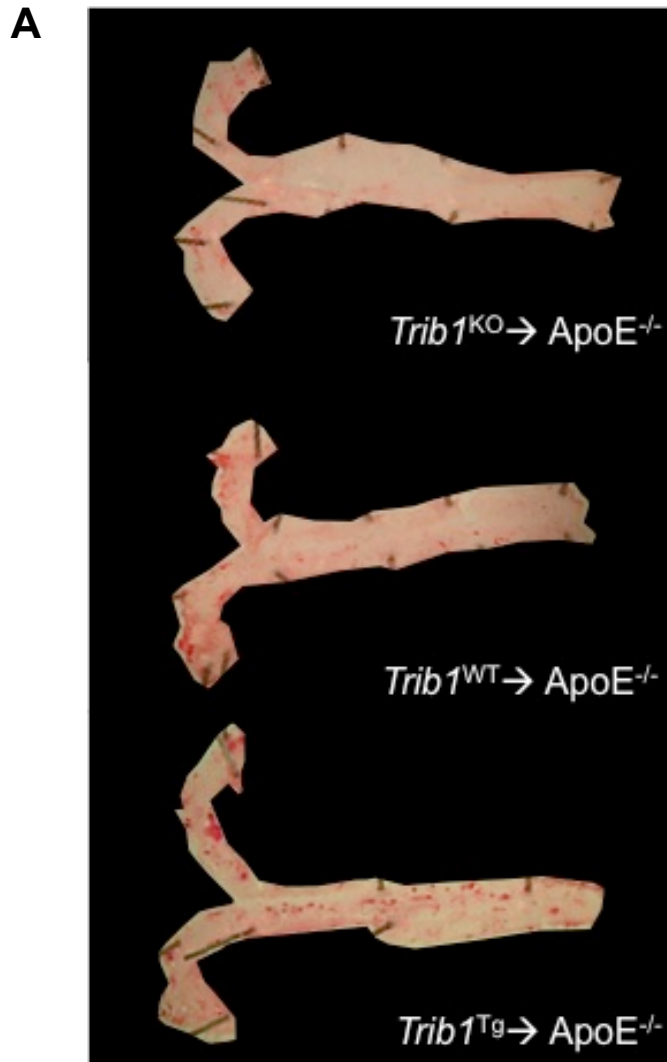


Figure 5.6: *en face* Oil Red O staining of *Trib1* x *LyzMCre* → *ApoE^{-/-}* mice.

Following bone marrow transplantation, mice were left to recover for 7 weeks and fed a high-fat diet for 12 weeks. (A) Aortae were stained with oil red O where fatty atherosclerotic lesions are stained red. (B) Lesion area was calculated as percentage of the total surface area of the whole aorta and was normalised to control mice (median). Data are presented as mean ± SEM, n=10-18. As data was not normally distributed, values were normalised to the median control. *p<0.05, ***p<0.001, ordinary one way ANOVA with Sidak's multiple comparisons post test.

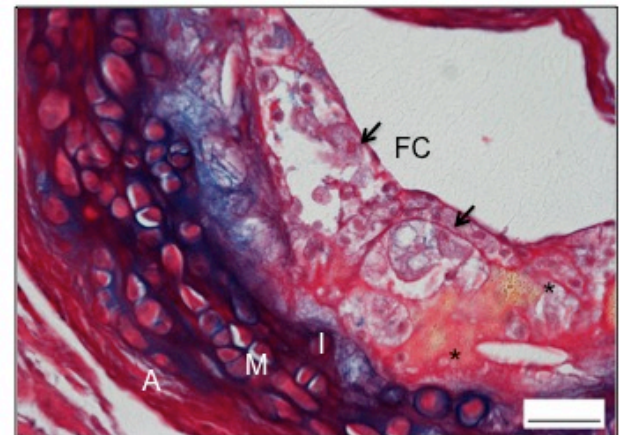
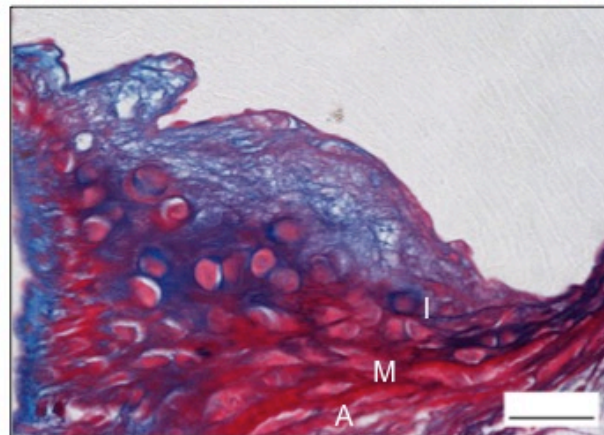
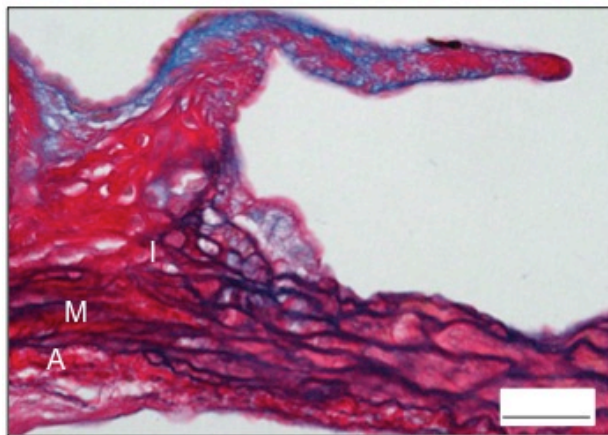
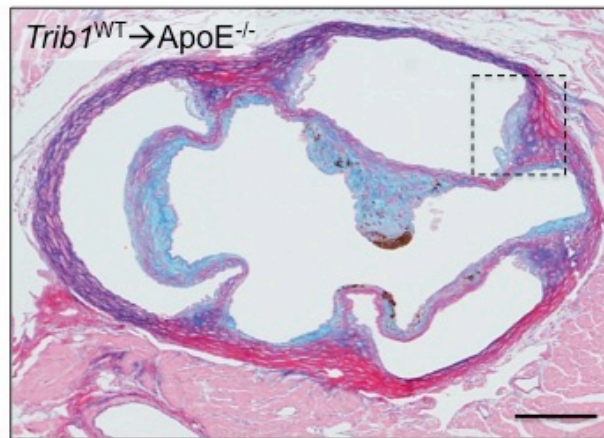
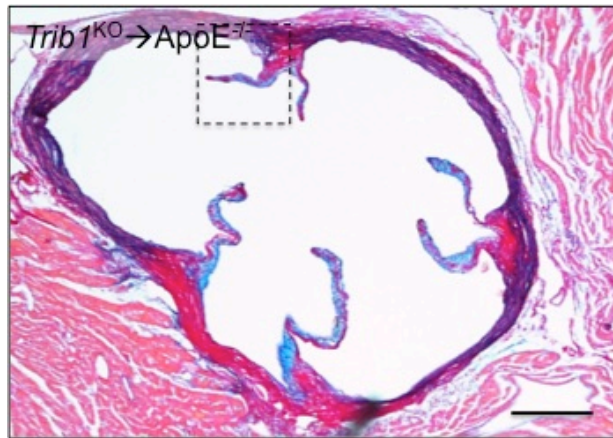
5.3.2.2 Lesion size and stability

To consider atherosclerosis further, the aortic sinus was also examined. Histological analysis of the aortic root is the gold standard method for analysis of atherosclerotic plaques in mice (**Figure 5.7A**).

Similar to the results in the aorta, Trib1^{Tg}→ApoE^{-/-} had on average 60% larger and more advanced atherosclerotic lesions compared to control mice (1.66 ± 0.24 vs. 0.99 ± 0.12 , $p < 0.05$) in the aortic sinus. Trib1^{Tg}→ApoE^{-/-} mice had large lesions with hallmarks of progressive advanced atherosclerotic plaques such as pathological media and intimal thickening with the presence of lipid rich foam cell macrophages (arrows), some evidence of red blood cells and/or cell lysis (yellow staining, asterisks), a sign of possible lesion neovascularisation, furthermore they also had evidence of thin fibrous cap formation. Trib1^{WT}→ApoE^{-/-} lesions on the other hand had some evidence of intimal-medial thickening but limited lipid accumulation and foam cell development. The lesions were primarily comprised of small intimal xanthomas (fatty streaks) with absence of fibrous cap formation indicating a much earlier stage of atherosclerosis. Trib1^{KO}→ApoE^{-/-} mice on the other hand had limited disease burden. The lesions that were present were limited to small fatty streaks, indicative of early atherosclerosis but were significantly much smaller than Trib1^{WT}→ApoE^{-/-} lesions (0.41 ± 0.04 , $p < 0.05$). Comparison of Trib1^{Tg} and Trib1^{KO} lesion size revealed a highly significant difference ($p < 0.0001$) (**Figure 5.7B**).

To assess the plaque phenotypes further, aortic root sections were stained with Martius, Scarlet, Blue (MSB), a stain to assess collagen deposition, a hallmark of atherosclerotic lesion stability. Quantification revealed no statistically significant difference between the groups (**Figure 5.7C**).

A



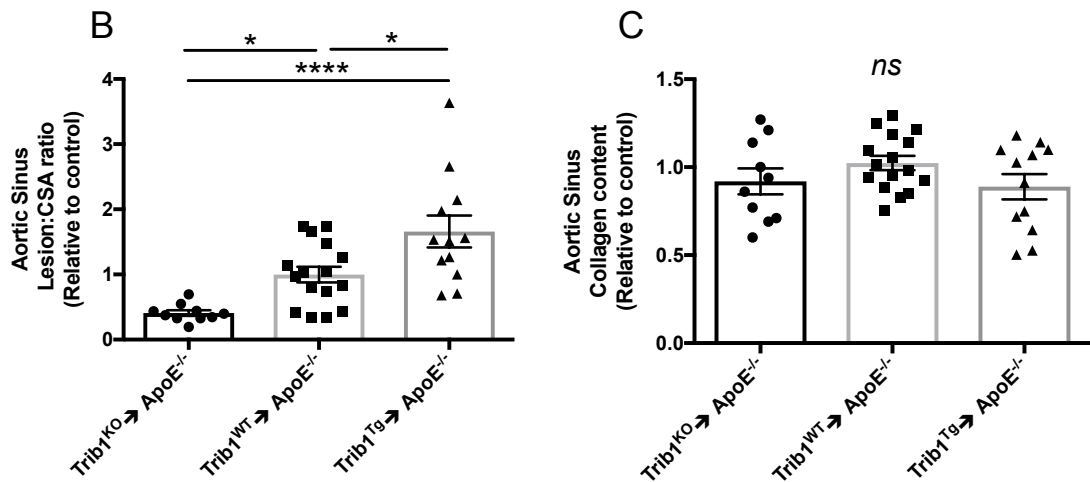


Figure 5.7: *Trib1* x *LyzMCre* → *ApoE*^{-/-} have altered atherosclerosis burden in the aortic sinus.

(A) The aortic root was sectioned and stained with Elastic van Gieson (EVG). Representative cross sections are shown along with plaque architecture; A, Adventitia; M, Media; I, Intima; FC, fibrous cap. Note presence of foamy cell macrophages in *Trib1* x *LyzMCre* → *ApoE*^{-/-} lesions (arrows). (B) The mean lesion: cross-sectional area (CSA) was calculated and normalised to control mice. (C) Lesion stability was assessed by staining with Martius Scarlet Blue (MSB) and quantified for collagen content. Data are presented as mean ± SEM, n=10-16. ns= not significant *p<0.05, ****p<0.0001, ordinary one way ANOVA with Sidak's multiple comparisons test.

5.4.3 *Trib1*^{Tg} → *ApoE*^{-/-} atheromas are rich in foamy cell macrophages

5.4.3.1 Mac-3 staining

At all stages of atheroma analysis, it was noted *Trib1*^{Tg} → *ApoE*^{-/-} were rich in pro-atherogenic lipid rich foam cell macrophages. To quantify the level of macrophage infiltrate in the atheromas, the aortic root sections were stained with Mac-3, a pan macrophage marker (**Figure 5.8**). Image analysis revealed that *Trib1*^{WT} → *ApoE*^{-/-} and *Trib1*^{Tg} → *ApoE*^{-/-} specimens had evident macrophage infiltrate but during image analysis *Trib1*^{Tg} → *ApoE*^{-/-} appeared to have larger macrophages at the luminal interface of the atherosclerotic plaque (data not shown), evidence of foam cell macrophage presence. Quantification revealed that *Trib1*^{Tg} → *ApoE*^{-/-} specimens had a trend towards increased Mac-3-positive staining compared control (1.2 ± 0.2; *Trib1*^{Tg} → *ApoE*^{-/-} vs. 0.88 ± 0.12; *Trib1*^{WT} → *ApoE*^{-/-}) however, the difference was not statistically significant. However, the difference was statistically significant

compared to $Trib1^{KO} \rightarrow ApoE^{-/-}$ specimens (0.18 ± 0.05 , $p < 0.001$). $Trib1^{KO} \rightarrow ApoE^{-/-}$ also showed a statistically significant reduction in Mac-3 positive staining compared to control sections ($p < 0.01$).

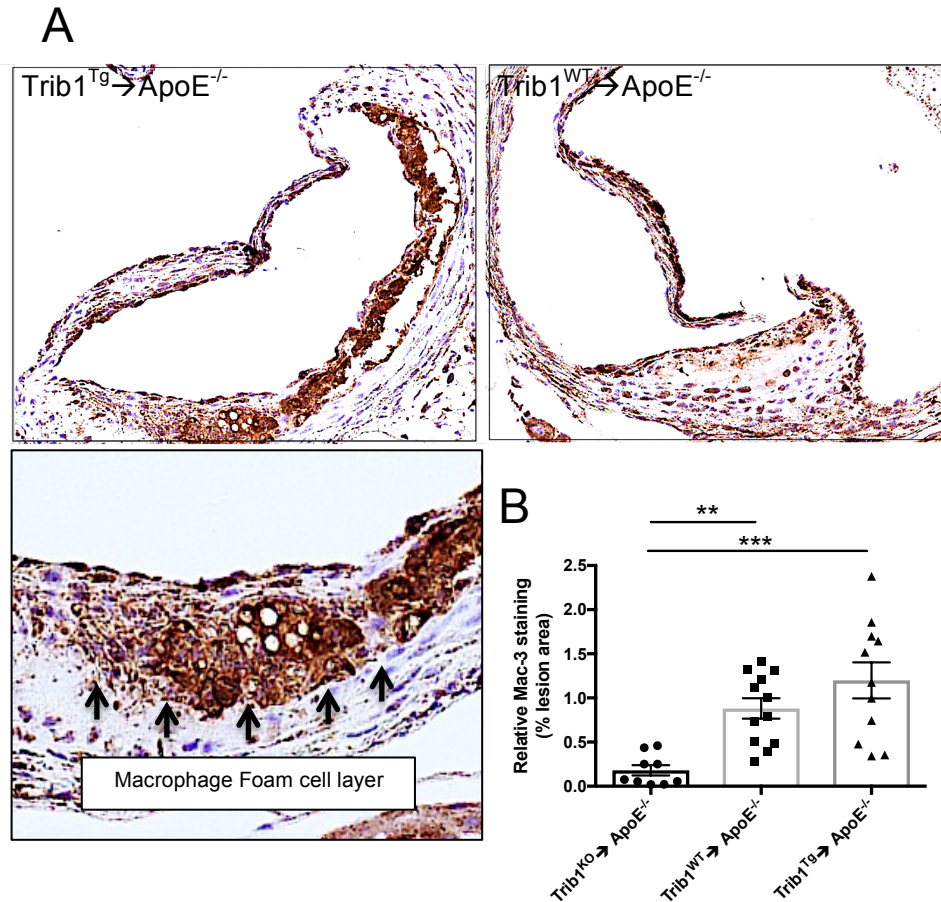


Figure 5.8: $Trib1^{Tg} \rightarrow ApoE^{-/-}$ mice have increased plaque macrophage infiltrate and presence of foamy cell macrophages.

(A) Representative images of aortic root cross-sections stained with Mac-3 (brown). Note high presence of foam cells in $Trib1^{Tg} \rightarrow ApoE^{-/-}$ mice (inset). (B) Quantification of Mac-3 staining relative to control mice. Data represents mean \pm SEM, $n=9-12$ $**p < 0.01$, $***p < 0.001$, ordinary one way ANOVA with Sidak's multiple comparison's test.

5.4.3.2 Scavenger receptors are up regulated in *TRIB1*-high human MDMs

To ascertain if the observations of high foam cell formation in $Trib1^{Tg} \rightarrow ApoE^{-/-}$ mice aortic sinus sections are relevant in humans, the expression of scavenger receptors was investigated in *TRIB1*-high human MDMs. Scavenger receptors are expressed by macrophages and they recognise amongst other things lipids (e.g. HDL and LDL) and modified LDL (e.g. oxLDL and acLDL), thus recognition and

internalisation of LDL is crucial for macrophage cholesterol metabolism and efflux and also in foam cell formation and the progression of the atheroma. **Table 5.2** outlines the various scavenger receptor gene expression in *TRIB1*-high human MDMs. Interestingly the analyses revealed significant change in expression of CD163 (1.1-fold change; haemoglobin/haptoglobin receptor) and CD68 (0.9-fold change cellular debris). However, much more intriguingly, there was a change in genes involved in lipid clearance and foam cell formation including up regulation of OLR1 (1.85-fold; oxLDL receptor) and down regulation of the reverse cholesterol transport gene SCARB1 (0.84-fold; HDL receptor) indicating that high-*TRIB1* expression in macrophages may lead to the increase in both lipid loading and the formation of foam cells due to oxLDL receptor expression and also a reduction in clearance by HDL receptor.

Table 5.2: Genes found to be differentially regulated in *TRIB1* high vs. *TRIB1* low human MDMs

Table shows NCBI gene accession number and name along with fold changes. Table shows p- (significance set at <0.05) and q-values (set at <0.05). Statistically significant genes are highlighted in grey

NCBI Gene	Gene ID	log.fold	fold.change	p.values	q.values
4973	OLR1	0.894	1.858	0.000	0.000
58191	CXCL16	0.188	1.139	0.000	0.000
9332	CD163	0.119	1.086	0.036	0.103
23166	STAB1	0.093	1.067	0.287	0.466
950	SCARB2	0.043	1.030	0.099	0.220
4481	MSR1	0.023	1.016	0.747	0.846
8578	SCARF1	0.006	1.004	0.773	0.866
948	CD36	-0.141	0.907	0.005	0.023
81035	COLEC12	-0.170	0.889	0.042	0.114
8685	MARCO	-0.234	0.850	0.012	0.043
949	SCARB1	-0.241	0.846	2.00E-08	5.10E-07
968	CD68	-0.267	0.831	1.46E-06	2.22E-05

5.4.3.3 Expression of scavenger receptors are up regulated in *Trib1* transgenic BMDMs

To confirm that the observed changes in the human microarray data were *TRIB1* dependent, the expression of the candidate scavenger receptor genes was verified in *Trib1* transgenic BMDMs via qPCR. **Figure 5.9** shows the relative expression of

each of the scavenger receptor genes. The majority of the genes examined mirrored the expression pattern seen in the human microarray data in terms of direction of expression (up-regulated vs. down-regulated). These genes included OLR1, CXCL16, SCARB1 and MARCO. However, CD68 expression was similar between WT and *Trib1* transgenic BMDMs and CD163 expression appeared to be marginally down regulated although the differences were not statistically significant. There were however two genes that were statistically significant between WT and *Trib1* transgenic BMDMs which included the oxLDL receptor OLR1 (0.59 ± 0.20 ; WT vs. 1.51 ± 0.17 ; *Trib1* transgenic, $p < 0.05$) and the HDL receptor SCARB1 (1.04 ± 0.03 ; WT vs 0.51 ± 0.05 ; *Trib1* transgenic, $p < 0.001$).

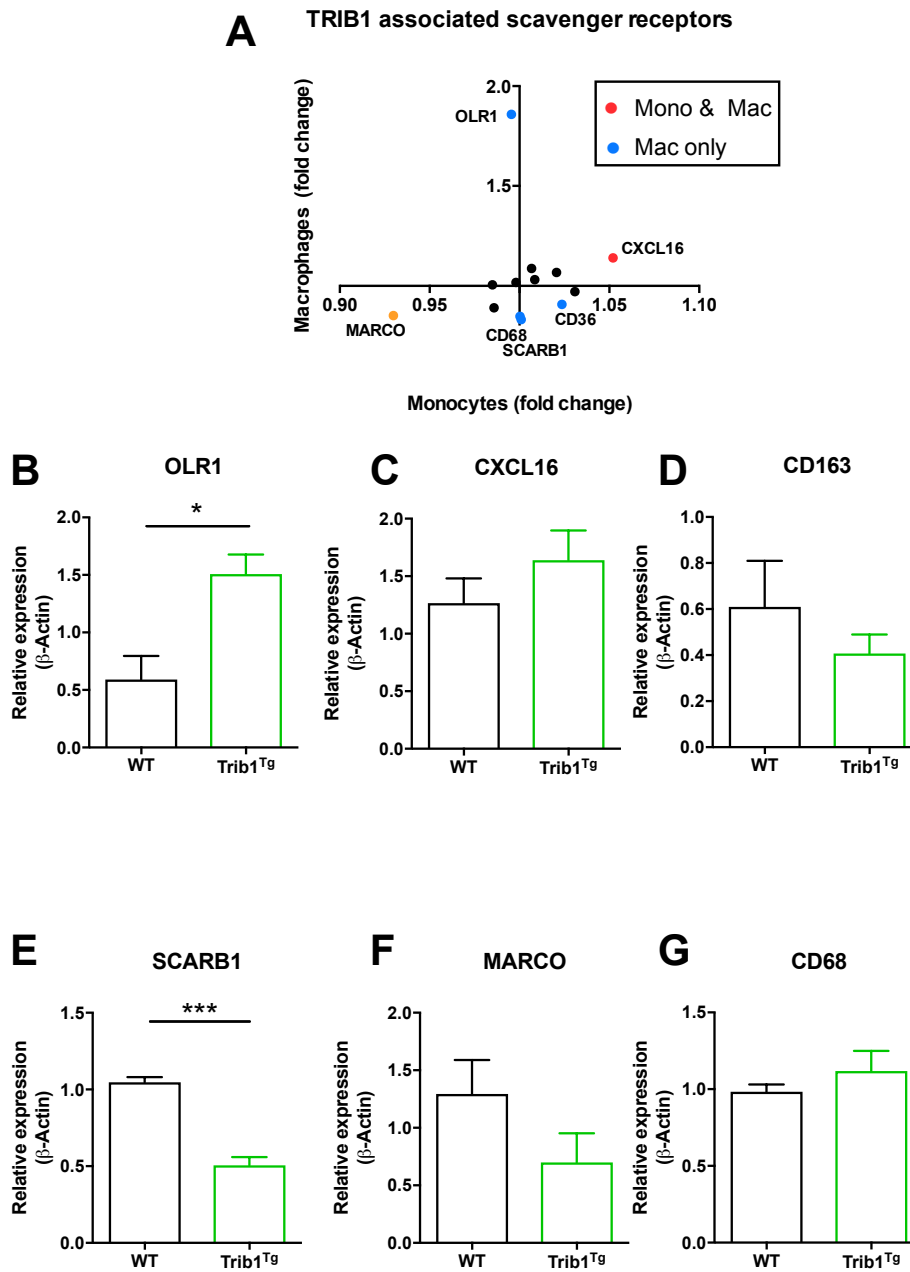


Figure 5.9: Scavenger receptor expression in *Trib1* transgenic BMDMs

(A) Log-fold changes of individual Scavenger receptor expression in *TRIB1*-high human MDMs in macrophages vs. monocytes. Identification of pathways was performed with QuSAGE. Relative mRNA expression (via qPCR) in *Trib1* M ϕ BMDMs of each of the candidate scavenger receptor genes identified in A, including OLR1 (B), CXCL16 (C), SCARB1 (D), CD68 (E), MARCO (F) and CD163 (G). Expression is normalised to β -actin. Graphs represent the mean \pm SEM, * $p < 0.05$, *** $p < 0.001$, student's t-test, $n = 3-6$.

5.4.4 ApoE^{-/-} mice with altered levels of *Trib1* in haematopoietic cells show differences in body weight and adipose tissue size

Upon dissection of the transplanted mice, it was noted the *Trib1* transgenic mice (Trib1^{Tg}→ ApoE^{-/-}) had higher level of abdominal and visceral adipose deposits, compared to the parallel, control cohort (**Figure 5.10A**). The Trib1^{KO}→ApoE^{-/-} mice also appeared leaner with visibly reduced adipose tissue volume compared to the recipients that received bone marrow from littermate control mice that express normal levels of *Trib1* (**Figure 5.10B**). Despite no differences in body weight, the ApoE^{-/-} transplanted mice had different body weights at the end of the diet (**Figure 5.1C-D**). As the experiments were carried out in two separate waves, it was found that there was also variation between the control mice (Trib1^{WT}→ApoE^{-/-}) between the two experiments. Therefore to consider the data together, the raw data was normalised to the median control to give a relative value. **Figure 5.10D** shows the *Trib1* transgenic transplanted (Trib1^{Tg}→ ApoE^{-/-}) mice were approximately 11% heavier (1.1 ± 0.02) compared to control mice (0.99 ± 0.03) ($p < 0.05$). Similarly, ApoE^{-/-} mice transplanted with *Trib1* KO bone marrow (Trib1^{KO} →ApoE^{-/-}) displayed the opposite phenotype and had significantly reduced body weight compared to transgenic *Trib1* transplanted mice (1.1 ± 0.02 ; *Trib1* transgenic vs. 0.92 ± 0.03 ; *Trib1* KO, $p < 0.01$). Trib1^{KO} →ApoE^{-/-} had approximately 7% lower body mass compared to control mice (0.92 ± 0.03 , *Trib1* KO vs. 0.99 ± 0.03 ; *Trib1* control), however the difference was not significant.

A. *ROSA26.Trib1* x *LyzMCre* → *ApoE*^{-/-}

***Trib1*^{WT} → *ApoE*^{-/-}**

***Trib1*^{Tg} → *ApoE*^{-/-}**

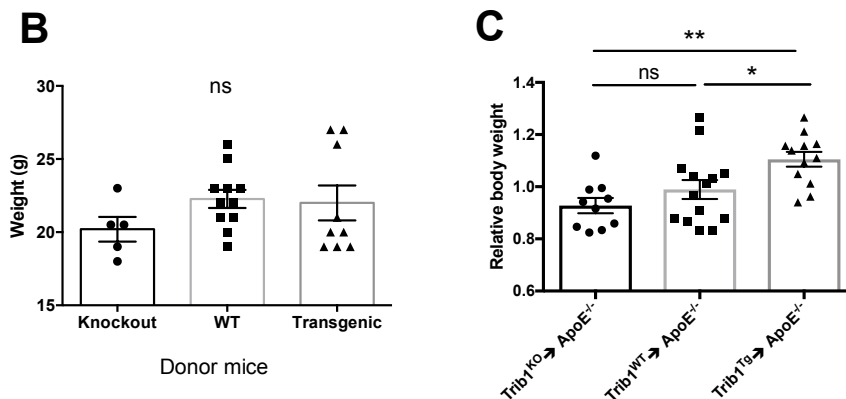
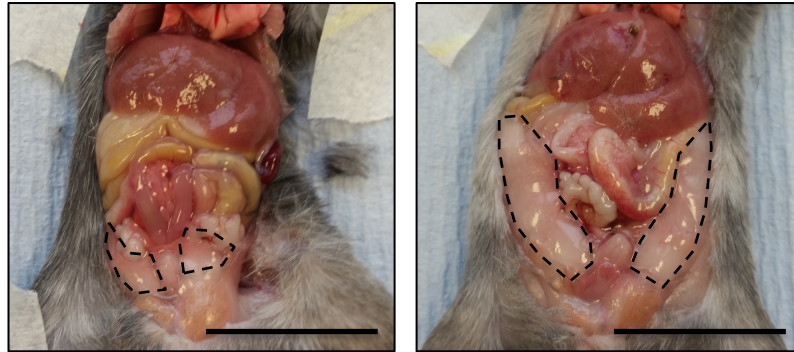


Figure 5.10: *Trib1*^{Tg} → *ApoE*^{-/-} mice have increased abdominal and visceral adipose tissue.

(A) Upon dissection it was noted *Trib1*^{Tg} → *ApoE*^{-/-} mice had increased abdominal and visceral adipose deposits compared to control mice (outlined), while *Trib1* KO mice were leaner (not shown). (B) Although the bone marrow donor mice had no differences in weight, *ApoE*^{-/-} mice transplanted with *Trib1*^{Tg} bone marrow were significantly heavier and *ApoE*^{-/-} mice transplanted with *Trib1*^{KO} bone marrow were leaner but the difference was not statistically significant (C). Scale= 2cm. Graph represents the mean ± SEM, each data point represents one mouse, n=10-16. One way ANOVA with Sidak's multiple comparisons post test, *p<0.05, **p<0.01.

5.4.4.1 Transgenic *Trib1* → *ApoE*^{-/-} mice have altered plasma lipids

Plasma from *Trib1* → *ApoE*^{-/-} transplanted mice was sent for biochemical analysis and lipid profiling including total cholesterol, triglycerides, HDL, LDL and glucose; graphs of each are presented in **Figure 5.11** (Raw data can be found in **Appendix V**). Analysis revealed that the transplanted mice have an altered plasma lipid profile compared to control mice. Unsurprisingly, *Trib1*^{Tg} → *ApoE*^{-/-} mice had significantly

elevated total cholesterol (approximately 50% more) compared to both control and Trib1^{KO}→ApoE^{-/-} animals (1.49 ± 0.12 vs. 1.043 ± 0.06 , $p < 0.01$). There were however, no significant differences between control and Trib1 KO transplanted animals (1.023 ± 0.08) (**Figure 5.11A**). Trib1 transgenic transplanted mice also showed a trend towards elevated levels of plasma triglyceride compared to control mice however the data was not significant (1.26 ± 0.16 vs. 0.973 ± 0.09). Nevertheless, they displayed a significant increase when compared to Trib1^{KO}→ApoE^{-/-} mice (1.26 ± 0.16 vs. 0.758 ± 0.07 , $p < 0.05$) (**Figure 5.11B**). Plasma HDL levels were also augmented in Trib1^{Tg}→ApoE^{-/-} mice as they displayed approximately 60% increase in HDL levels compared to both control and Trib1^{KO}→ApoE^{-/-} mice (1.606 ± 0.11 ; Trib1^{Tg} vs. 1.084 ± 0.08 ; Trib1^{WT} vs. 0.953 ± 0.03 ; Trib1^{KO}, $p < 0.001$) (**Figure 5.11C**). Interestingly, the level of LDL the lipoprotein with a pivotal role in the development of atherosclerosis did not change between the groups (**Figure 5.11D**). Trib1^{Tg}→ApoE^{-/-} also appeared hyperglycaemic with respect to both control and Trib1 KO transplanted mice with approximately 20% higher glucose concentration (1.197 ± 0.03 vs. 1.016 ± 0.03 ; Trib1^{WT} $p < 0.01$ vs. 0.909 ± 0.04 ; Trib1^{KO} $p < 0.0001$) (**Figure 5.11E**).

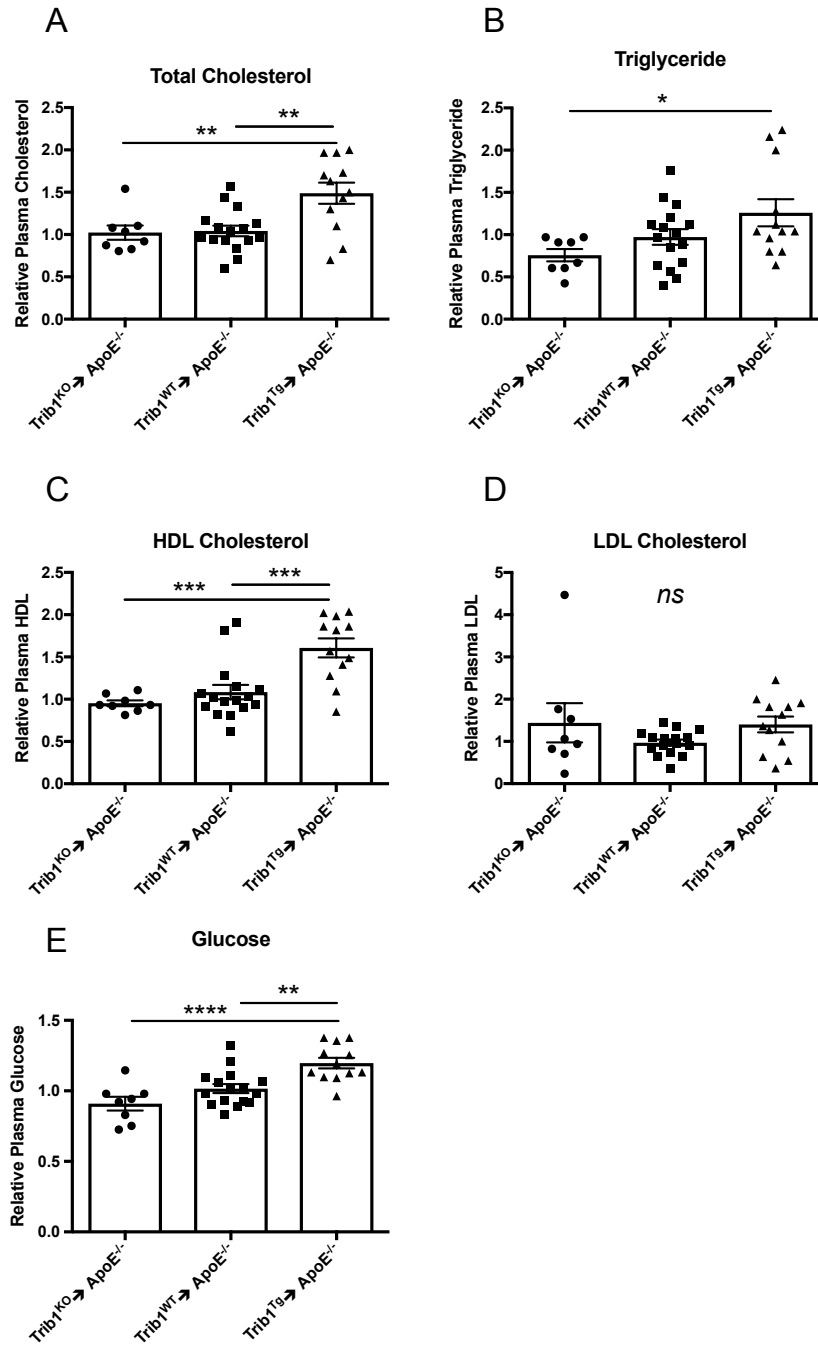


Figure 5.11: *Trib1*^{Tg} → ApoE^{-/-} mice have altered plasma lipids.

Full lipid and glucose profile was generated from the plasma of the transplanted mice, including total cholesterol (A), triglyceride (B), HDL (C), LDL (D) and glucose (E). Graphs represent the mean ± SEM, one data point represents an individual mouse, n=8-16. Ordinary one way ANOVA with Sidak's multiple comparisons post test, *p<0.05, **p<0.01, ***p<0.001, ****p<0.0001

5.4.5 Trib1 \rightarrow ApoE $^{-/-}$ mice have a metabolic phenotype

5.4.5.1 Trib1 Tg \rightarrow ApoE $^{-/-}$ mice have increased hepatic steatosis

To investigate the apparent metabolic phenotype further, livers from these mice were weighed and examined histologically by staining tissue sections with haematoxylin and eosin (H&E). There was no difference in liver weight between the groups (1.613g \pm 0.10, Trib1 WT \rightarrow ApoE $^{-/-}$ vs. 1.636g \pm 0.12, Trib1 Tg \rightarrow ApoE $^{-/-}$ vs. 1.563g \pm 0.09, Trib1 KO \rightarrow ApoE $^{-/-}$) (**Figure 5.12A**).

Despite no difference in liver weight, histological examination of liver cross sections stained with H&E showed Trib1 Tg \rightarrow ApoE $^{-/-}$ mice had increased levels of macrovesicular steatosis, large adipose deposits in cell vacuoles that distort the nucleus (**Figure 5.12Bii**) compared to control mice (**Figure 5.12Bi**). Upon further examination the *Trib1* transgenic transplanted mice had a high proportion of hepatocytes in microvesicular steatosis, small intra-cytoplasmic liposomes inside the cell (Figure 2Biii). Quantification revealed a significant increase ($p < 0.05$) in fatty areas in the Trib1 Tg \rightarrow ApoE $^{-/-}$ compared to controls (1.6 \pm 0.23 vs. 0.83 \pm 0.19). Similarly, it appeared livers from Trib1 KO \rightarrow ApoE $^{-/-}$ were less fatty than control mice. However, quantification showed that although there was a trend towards a decrease, the results were not significant (1.49 \pm 0.48 vs. 0.71 \pm 0.18, $p = 0.1602$).

To quantify the levels of lipid in the livers of these mice more accurately, hepatic cholesterol and triglyceride content was measured using a colorimetric assay. The results are presented in Figure 5.3E-F and in support of our image analysis data, Trib1 Tg \rightarrow ApoE $^{-/-}$ mice have increased hepatic triglyceride (141.8 \pm 23.6 mg/g vs. 72.89 \pm 14.2 mg/g, $p < 0.05$) and show a trend towards an increased cholesterol content also, however the data was not significant (11.58 \pm 1.790 mg/g vs. 8.821 \pm 1.268 mg/g).

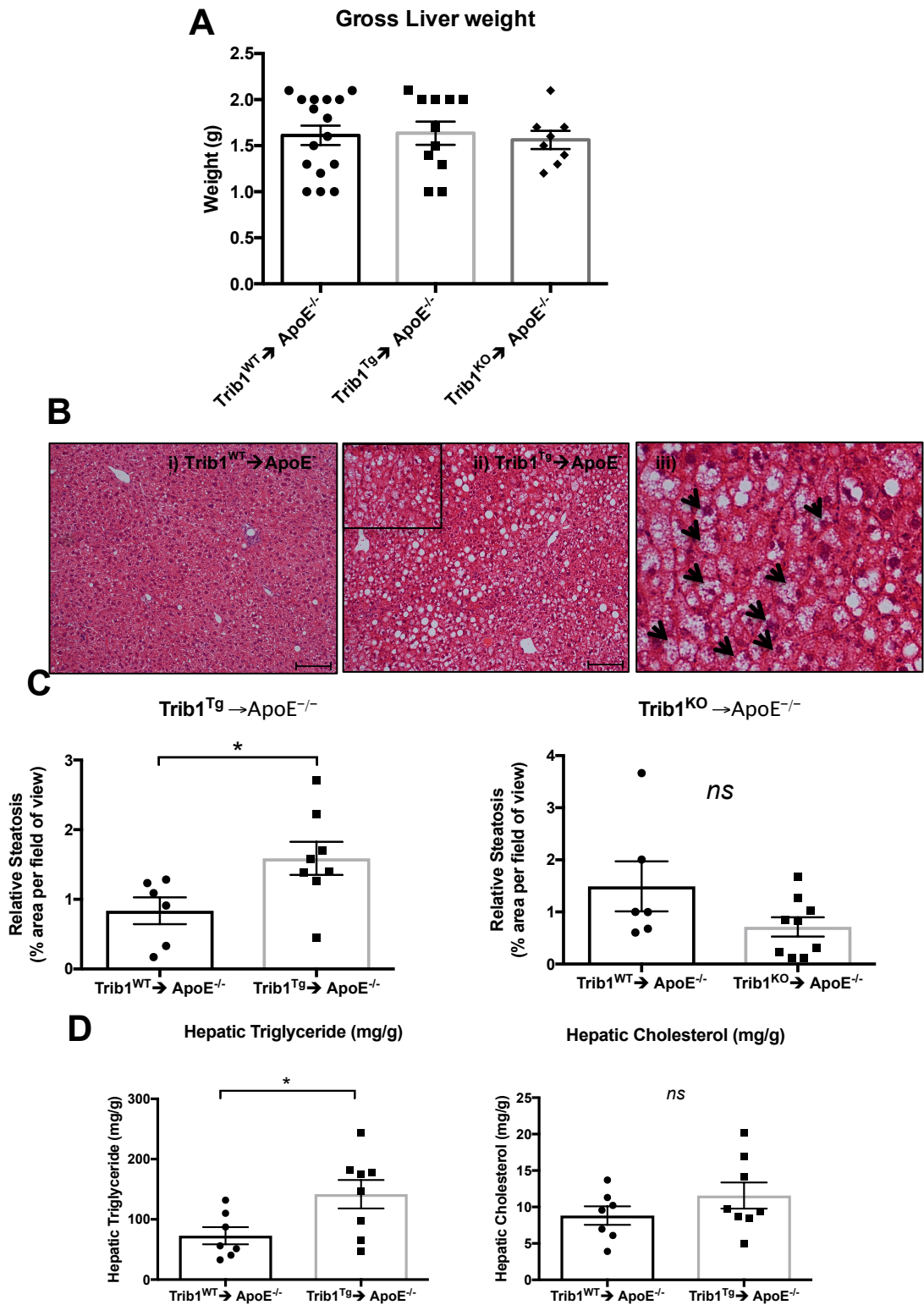


Figure 5.12: Transgenic *Trib1* ApoE^{-/-} mice have significantly more steatosis.

(A) Livers from *Trib1* x *LyzMCre* transplanted ApoE^{-/-} mice fed on high fat diet for 12 weeks show no difference in gross liver weight (n=8-16). (B) Liver cross sections were stained with H&E and show transgenic mice have an elevated degree of hepatic steatosis as illustrated by the clear spaces compared to control mice. Note elevated microvesicular steatosis (arrows, small intracytoplasmic liposomes inside the cell) (iii, zoomed area of ii). (C) Quantification revealed Trib1^{Tg}→ApoE^{-/-} mice have significantly more adipose deposits compared to Trib1^{WT}→ApoE^{-/-} mice (n=6-8). (D) Similarly, Trib1^{KO}→ApoE^{-/-} mice had less fatty liver deposits, however this was not significant (n=6-9). (E) Colorimetric assay using homogenised livers showed Trib1^{Tg}→ApoE^{-/-} have significantly elevated hepatic triglycerides and a trend towards elevated hepatic cholesterol but the difference was not significant (n=7-8) (F). Graphs represent the mean ± SEM, *p<0.05, unpaired student's t test. Scale = 100µm.

5.4.5.2 Adipocyte size is altered in Trib1^{Tg}→ApoE^{-/-} mice

In view of the fact that the adipose tissue deposits looked noticeably different in the mice at the time of harvest, subcutaneous adipose tissue was taken from the abdominal cavity of the mice and processed histologically. Tissue cross-sections were stained with H&E and examined (**Figure 5.13**). Adipocytes from Trib1^{Tg}→ApoE^{-/-} mice were two-fold larger than Trib1^{WT}→ApoE^{-/-} control mice (2.07 ± 0.16 ; *Trib1* transgenic vs. 1.03 ± 0.09 ; *Trib1* control, $p < 0.0001$). Likewise, Trib1^{KO}→ApoE^{-/-} adipocytes were significantly smaller compared to both control ($p < 0.05$) and Trib1^{Tg}→ApoE^{-/-} mice (0.48 ± 0.14 , $p < 0.0001$).

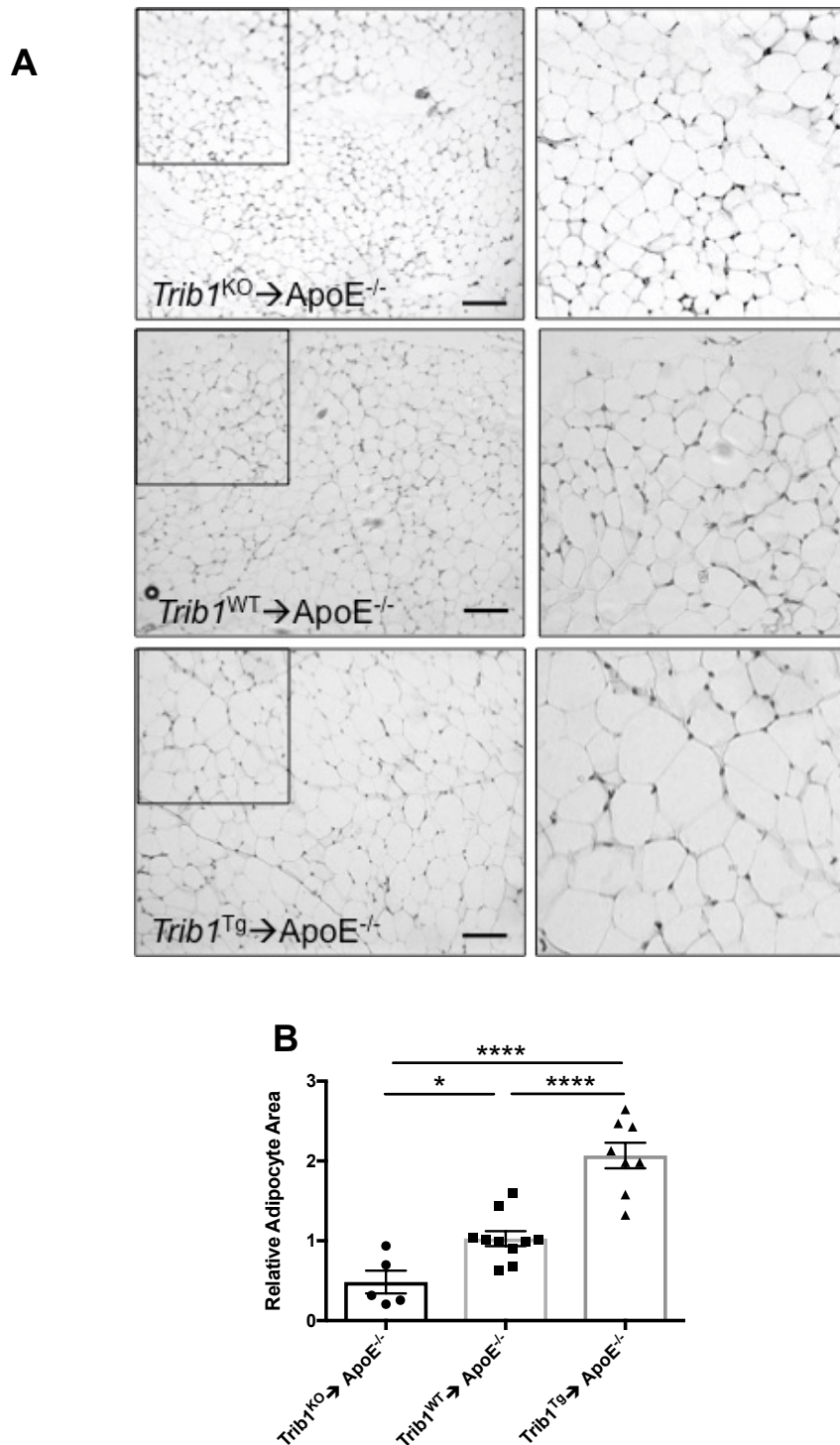


Figure 5.13: Adipocyte size is altered in *Trib1*→ *ApoE*^{-/-} mice.

(A) Adipose tissue from *Trib1* × *LyzMCre*→ *ApoE*^{-/-} transplanted mice were processed histologically. To visualise the size of the adipocytes, tissue cross sections were stained with H&E. The sizes of adipocytes were quantified using NIS-Elements software by measuring at least 10-15 cells per field of view (3 in total) per mouse. (B) Quantification revealed *Trib1*^{Tg}→*ApoE*^{-/-} mice have significantly larger adipocytes compared to control and *Trib1* KO transplanted mice. *Trib1*^{KO}→ mice have significantly smaller adipocytes compared to control mice, suggesting some lipodystrophy. Graphs represent the mean ± SEM, *****p*<0.0001, **p*<0.05, ordinary one way ANOVA with Sidak's multiple comparisons post-test.

5.4.6 Macrophage infiltrate in metabolic tissues

5.4.6.1 *Trib1*→ *ApoE*^{-/-} mice have comparable numbers of macrophages in the adipose tissue

Obesity and metabolic syndromes are associated with macrophage infiltration into the adipose tissue. Since adipogenesis appears to be altered in *Trib1* x *LyzMCre*→*ApoE*^{-/-} mice, adipose tissue cross-sections were stained with F4/80 to assess the extent of macrophage infiltration (**Figure 5.14A**). There were no significant differences between the level of F4/80+ cells between the groups (**Figure 5.14B**).

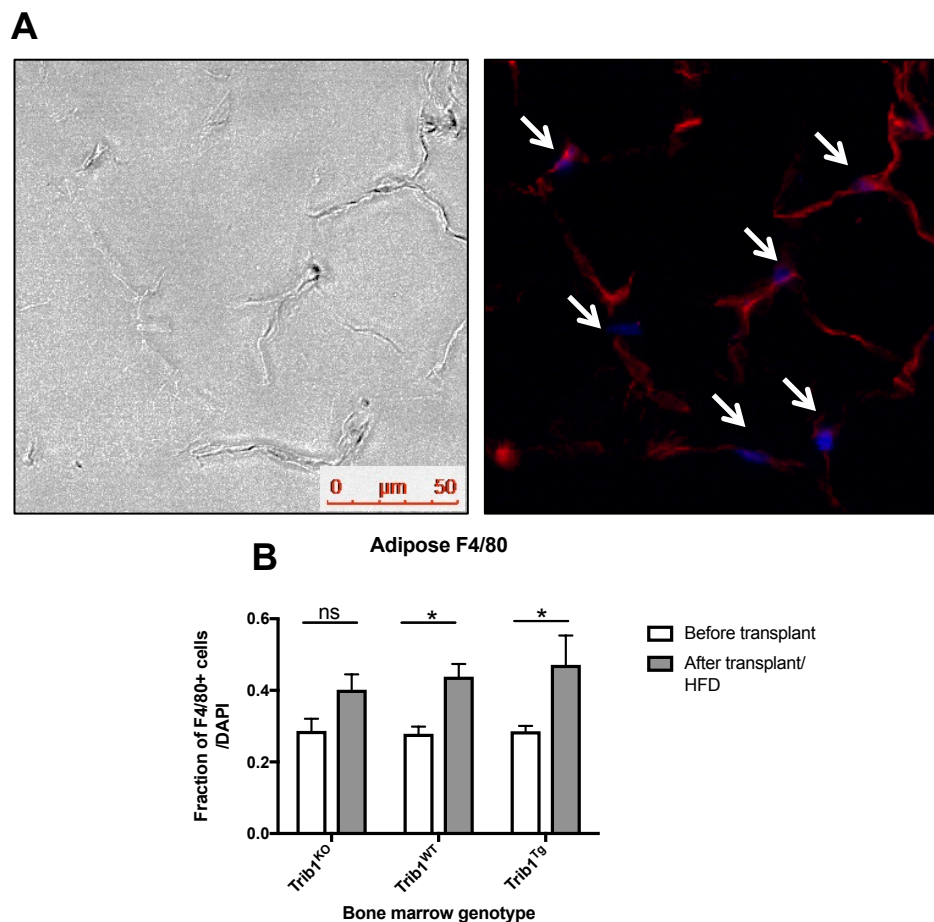


Figure 5.14: Levels of F4/80+ macrophages are unchanged in *Trib1*→*ApoE*^{-/-} mice.

(A) Adipose tissue was stained with F4/80 (red) to assess macrophage infiltrate, a change known to occur in obesity, (B) however no significant differences were found between the genotypes, however macrophage infiltrate in the adipose tissue increased after transplant and high fat diet, significantly in *Trib1*^{WT} and *Trib1*^{Tg} mice ($p<0.05$). Graph represents mean \pm SEM, ordinary one way ANOVA with Sidak's multiple comparisons post-test, $n=4-11$, ns= not significant, * $p<0.05$.

5.5 Summary

The work presented in this chapter has used bone marrow transplantation to examine the role of haematopoietic derived *Trib1* in altering the phenotype of ApoE^{-/-} mice fed on high-fat diet. In summary:

- TRIB1 is expressed in human atherosclerotic plaque macrophages
- *Trib1* transplanted mice showed differences in atherosclerotic burden in the aorta, Trib1^{Tg}→ ApoE^{-/-} had elevated levels of positive oil-red-o staining compared to control mice, while Trib1^{KO}→ ApoE^{-/-} had significant attenuation.
- The phenotype was mirrored at the aortic sinus and Trib1^{Tg}→ ApoE^{-/-} showed evidence of progressive atherosclerotic plaques with the presence of foamy cell macrophages. Trib1^{KO}→ ApoE^{-/-} mice however had limited disease burden with small fatty streaks, indicative of early atherosclerosis.
- There were no significant differences in plaque collagen content between the groups.
- Mac-3 staining of aortic sinus plaques indicated increased and decreased macrophage infiltrate in Trib1^{Tg}→ ApoE^{-/-} and Trib1^{KO}→ ApoE^{-/-} mice respectively. The staining confirmed the elevated levels of foamy cell macrophages in the lesions of Trib1^{Tg}→ ApoE^{-/-} mice, while Trib1^{KO}→ ApoE^{-/-} had significantly reduced levels.
- Microarray data from human MDMs revealed TRIB1- high MDMs express elevated levels of scavenger receptors including the oxLDL receptor (OLR1), a key step in the formation of foamy cell macrophages.
- qPCR analysis of Trib1 transgenic BMDMs validated the human microarray data and showed a significant increase in the expression of OLR1 and interestingly a significant decrease in the expression of the HDL receptor, SCARB1.
- Trib1^{Tg}→ ApoE^{-/-} mice had increased adipose deposits in the abdomen while Trib1^{KO}→ ApoE^{-/-} mice were leaner.
- Trib1^{Tg}→ ApoE^{-/-} mice were significantly heavier at the end of the procedure compared to Trib1^{WT}→ ApoE^{-/-} mice.
- Trib1 transplanted mice had altered plasma lipids, specifically Trib1^{Tg}→ ApoE^{-/-} had significantly elevated levels of plasma triglyceride,

HDL cholesterol and glucose. Trib1^{KO}→ ApoE^{-/-} however had significantly reduced HDL cholesterol and glucose. There were no significant differences between any of the groups for levels of LDL-cholesterol.

- Despite no change in gross liver weight, Trib1^{Tg}→ApoE^{-/-} mice had statistically significant elevated levels of steatosis in H&E stained liver sections and elevated levels of liver triglyceride.
- Adipocyte size was altered in *Trib1* transplanted mice; specifically Trib1^{Tg}→ ApoE^{-/-} mice had enlarged adipocytes (hypertrophy) while Trib1^{KO}→ ApoE^{-/-} had smaller adipocytes.
- There were comparable levels of F4/80+ macrophages in the adipose in all of the groups.

5.6 Discussion

To date, there has been no published study that has investigated the role of haematopoietic TRIB1 on atherosclerosis directly despite evidence implicating *TRIB1* as being a risk factor to the development of coronary artery disease in humans (Willer et al., 2008, Kathiresan et al., 2008). Most studies including the results presented in **Chapter 3** have indicated that *Trib1* expression in hepatocytes and macrophages control plasma lipid homeostasis. Elevated levels of plasma cholesterol and lipids particularly LDL and triglycerides are strong risk factors for the development of chronic inflammatory diseases including obesity and cardiovascular disease. Indeed, the National Institute for Health and Care Excellence (NICE) who provide national guidelines for treatment advice and regimes in the UK recommend treatment with lipid lowering agents e.g. statins to patients whose 10-year risk of CVD is $\geq 10\%$ (1 in 10 chance), which was reduced from $\geq 20\%$ (1 in 5 chance) (NICE, 2016).

The results presented in **Chapter 3** described the role of *Trib1* in tissue resident macrophages under normal physiological conditions (chow diet) using mouse strains that either over-express or do not express *Trib1* in myeloid cells. In this chapter, however the role of haematopoietic-derived *Trib1* was established by transplanting the bone marrow from these mice strains into atherogenic ApoE^{-/-} mice that were subsequently fed a high-fat diet. The results in this chapter demonstrate that myeloid *Trib1* induces changes in the adipose and liver tissue and induces atherosclerosis. Although the direction of change may seem counter-intuitive to data presented in **Chapter 3** and to the literature, which has established TRIB1 to have anti-inflammatory properties and reduces levels of circulating of what is considered to be athero-prone lipids including LDL and triglycerides, the data presented illustrates the consequences of myeloid *Trib1* expression in a tissue specific manner.

Since there are no reported studies to date, one of the main aims of the project was to investigate the role of myeloid-*Trib1* in the development of atherosclerosis. The results indicate that myeloid overexpression of *Trib1* is pro-atherogenic with significant increases in lipid deposition in the aorta and presence of large atherosclerotic lesions in the aortic sinus. Loss of myeloid-*Trib1* however is athero-protective; mice presented only small lesions indicative of early atherogenesis.

Atherosclerosis is a localised inflammatory disease of the vessel wall where monocytes and macrophages are central to its pathogenesis. Indeed, the formation of macrophage foam cells with subsequent fatty streak formation plays a key role in early atherogenesis and is one of the factors that amplify the inflammatory response perpetuating atherosclerosis (Kzhyshkowska et al., 2012).

Atherosclerotic lesions from $Trib1^{Tg} \rightarrow ApoE^{-/-}$ had significantly increased Mac-3+ macrophage infiltrate. Monocyte recruitment, infiltration into the plaque and subsequent differentiation into macrophages is a necessary step for the initiation of atherosclerosis, as mice deficient in macrophages (through deficiency of macrophage colony stimulating factor (M-CSF, a key cytokine that influences macrophage differentiation) are protected against atherosclerosis (Smith et al., 1995). TRIB1 has been shown to be involved in macrophage migration and silencing of *Trib1* in RAW264.7 cells reduces the migration response when cells are stimulated with CCL2/MCP1 (C-C motif chemokine ligand 2/ monocyte chemokine protein-1) (Liu et al., 2013). Interestingly, CCL2/MCP1 is a key chemokine that has been strongly linked to atherosclerosis and the deletion of either CCL2 or its receptor CCR-2 results in significant reduction in atherosclerosis (Coll et al., 2007, Combadiere et al., 2008). Indeed the experiments performed by Liu et al. (2013) indicate that TRIB1 regulates monocyte/macrophage migration through ERK1/2 and inhibition of C/EBP β , which modulates TNF- α production. C/EBP β and C/EBP δ have both been shown to stimulate the transcription of *Ccl2*, as does TNF- α through NF- κ B (Sato et al., 2007, Chen et al., 2004). Therefore collectively, these data suggest that TRIB1 may be involved in macrophage migration through regulation of C/EBP β and may provide rationale as to why, at least in part $Trib1^{KO} \rightarrow ApoE^{-/-}$ mice have reduced and $Trib1^{Tg} \rightarrow ApoE^{-/-}$ mice have increased plaque macrophage infiltrate respectively. However, as presented in **Chapter 3**, over-expression of TRIB1 in RAW 264.7 cells increased protein expression of C/EBP β , contrary to Liu et al. (2013) this may reflect the fact that the effects of Tribs are largely cell type and context specific.

Progression of atherosclerosis is also dependent on the formation of macrophage foam cells, which over time are progressively replaced by the lipid core in atherosclerotic lesions (Dalager et al., 2007). Histological analysis of the aortic root lesions from these mice showed a high degree of foamy cell Mac3+ cells in

Trib1^{Tg}→ mice. Foamy cell macrophages are characterised by high levels of intracellular lipid, which give it the ‘foamy’ appearance it is named after. The process of foam cell formation results from the imbalance of normal cholesterol homeostasis including cholesterol influx mediated by scavenger receptors. To elucidate why *Trib1*^{Tg}→ *ApoE*^{-/-} mice have more foam cell macrophages, the expression of scavenger receptors was investigated. It was found both in human *TRIB1*-high MDMs and *Trib1* transgenic BMDMs displayed increased expression of some scavenger receptors. In particular, *Trib1* transgenic BMDMs had elevated levels of OLR1 expression. The *OLR1* gene encodes for LOX-1 (lectin-like oxidized low density lipoprotein receptor 1) present on endothelial cells and macrophages and mediates the recognition, internalisation and degradation of oxLDL and has proven to be a central player in the development of atherosclerosis (reviewed in Mehta et al. (2006)). Indeed, LOX-1 expression is increased in the atherosclerotic aorta from hyperlipidaemic animals including rabbits, mice, rats and humans (Chen et al., 2000, Hamakawa et al., 2004, Kataoka et al., 1999).

Interestingly, the expression of LOX-1 appears to be most abundant on endothelial cells and is largely implicated in atherosclerosis through its role in promoting oxLDL uptake on endothelial cells and consequent endothelial dysfunction, indeed atherosclerosis is attenuated in LOX-1/LDLR double knockout mice compared to LDLR-KO or LOX-1-KO animals (Mehta et al., 2007). LOX-1 however is also expressed on the surface of monocytes and macrophages and its expression is increased in intimal macrophages of advanced human atherosclerotic plaques (Kataoka et al., 1999). Despite this, its direct role in macrophages to atherosclerosis is uncertain. The major scavenger receptor involved in oxLDL uptake in macrophages appears to be CD68, although *Trib1* transgenic BMDMs had increased expression of CD68, the results were not significant.

Trib1 transgenic BMDMs had significant decrease in SCARB-1 (SR-B1; scavenger receptor class B member 1) expression that is involved in reverse cholesterol transport. Indeed, its expression levels are correlated with the rate of cholesterol efflux from macrophages (Ji et al., 1997). However how much contribution the expression of SCARB-1 has on reverse cholesterol transport in macrophages is debated since macrophages also express the ABC transporters, ABCA1 and ABCG1. In one study, primary macrophages that lacked ABCA1 had significantly reduced

reverse cholesterol transport *in vivo*, however residual transport also remained which was attributed to the expression of ABCG1 as macrophages deficient in SCARB-1 did not contribute to cholesterol efflux *in vivo* (Wang et al., 2007). However, another study has characterised ABCA1/SCARB1 double knockout mice and concluded both are essential for maintaining reverse cholesterol transport in macrophages. Despite the notion that increased expression of SCARB-1 is thought to be anti-atherogenic, more work is needed to clarify its role in macrophages. Interestingly, SCARB-1 is also expressed on hepatocytes, therefore the increased lipid deposition in the liver of Trib1^{Tg}→ApoE^{-/-} in these experiments may be in part explained by reduced cholesterol efflux from hepatocytes, moreover, atherogenic diet has been shown to down-regulate SCARB-1 expression on hepatocytes further suggesting this may be the case (Terpstra et al., 2000, Niemeier et al., 2009).

Since, *Trib1* transgenic BMDMs showed increased expression of the postulated pro-atherogenic receptor OLR-1 and reduced expression of the anti-atherogenic receptor SCARB-1, it indicates that both may play a part in the observed increase in atherosclerosis development in these mice. However, future work is needed to elucidate the influence of TRIB1 on scavenger receptor and ABC transporter expression. Expression of OLR-1 is thought to be induced by a number of factors including oxidative stress, oxLDL levels, IL-1 β and TNF- α *in vitro* and hyperlipidemia, hypertension and diabetes amongst others *in vivo* (reviewed in Mehta et al. (2006)). OLR-1 expression may be regulated by a number of different signalling pathways, for example Hayashida et al. (2004) showed PPAR- α is one of the key regulators of OLR-1 up-regulation, while Chiba et al. (2001) proposed PPAR- γ activators inhibit TNF- α induced OLR-1 expression in aortic endothelial cells. Similarly, the PPAR- γ ligand pioglitazone can inhibit oxLDL induced oxidative stress and OLR-1 up regulation in coronary artery endothelial cells and fibroblasts (Mehta et al., 2003). Expression may be also up regulated through elevated glucose through activating protein-1 (AP-1), as Trib1^{Tg}→ ApoE^{-/-} had higher plasma glucose levels, this could be in part the mechanism of OLR-1 up regulation, however this needs to be clarified further. Regulation of OLR-1 expression seems rather complex as a number of signalling pathways including those regulated by TRIB1 are thought to have a role including p38 MAPK, p44/42 MAPK and protein kinase B (PKB) (Mehta et al., 2004, Li et al., 2003, Li et al., 2001),

certainly further work is required to elucidate the molecular mechanisms of TRIB1-regulated OLR-1 expression.

SCARB-1 expression is regulated by a number of pathways including the transcription factor SREBP-1a. The SCARB-1 promoter contains two sterol responsive elements (pSRE and dSRE), in which SREBP-1a binds to promote transcription (Lopez and McLean, 1999). Interestingly, SREBP-2 expression appears to down-regulate SCARB-1 as it is down-regulated in animal models of NAFLD through increased expression of SREBP-2 (van Rooyen et al., 2011). Furthermore, SCARB-1 expression is also regulated by LXR/RXR in hepatoma and preadipocytes (Malerod et al., 2002). In addition, both PPAR- α (human only) and PPAR γ , which are regulators of cholesterol efflux in macrophages enhance SCARB-1 expression (Chinetti et al., 2000, Li et al., 2004) (**Figure 5.15**).

Therefore it appears TRIB1 may regulate SCARB-1 and OLR-1 expression through the inhibition of some of these complex pathways (LXR and PPAR- γ) which may or may not overlap, interestingly, TRIB3 also inhibits PPAR- γ (Takahashi et al., 2008) and may have similar roles in this context, however further work is needed to clarify the exact molecular mechanisms.

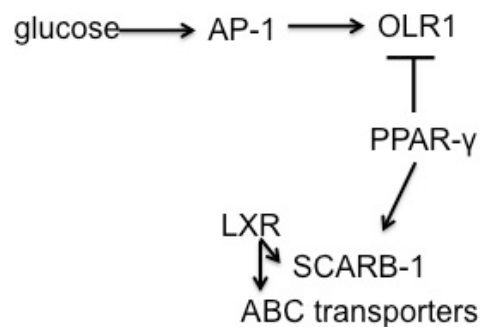


Figure 5.15: Regulation of OLR1 and SCARB-1 expression.

Intriguingly, increased expression of scavenger receptors has also been demonstrated in ‘M2’/ anti-inflammatory macrophages and they may have a role in their polarisation. The increased expression of these receptors is thought in part to aid clearance and suppress inflammation (reviewed in Canton et al. (2013)). Moreover, ‘M2’ anti-inflammatory macrophages are more likely to form foam cells under

inflammatory conditions *in vitro*, though the importance of this *in vivo* is unclear (Oh et al., 2012). These data suggest that although the atherosclerotic plaque is a complex microenvironment that influences macrophage polarisation, it is plausible that since over-expression of *Trib1* promotes an ‘M2’/ anti-inflammatory phenotype in monocytes and macrophages that they may have increased basal expression of these receptors with a higher propensity to form foam cells thereby promoting atherosclerosis. However this assumption is over-simplified and does not account for the complexity of atherosclerosis development, and the plasticity of plaque macrophage phenotype, but nevertheless does warrant future work to investigate the mechanism of myeloid-*Trib1* in atherosclerosis.

At the end of the procedure it was noted that $Trib1^{Tg} \rightarrow ApoE^{-/-}$ although were not obese, were significantly heavier than $Trib1^{WT} \rightarrow ApoE^{-/-}$ and $Trib1^{KO} \rightarrow ApoE^{-/-}$ mice with enlarged adipose deposits in the abdomen. Subsequent analysis of the adipose tissue showed a significant *Trib1* gene dose dependent increase in adipocyte size and adipocyte shrinkage in $Trib1^{KO} \rightarrow ApoE^{-/-}$ mice. Previous studies have shown that obesity is characterised by adipocyte hypertrophy and size of subcutaneous abdominal deposits are highly predictive for the development of diabetes, independent of insulin resistance (Skurk et al., 2007, Weyer et al., 2000). Therefore hypertrophy and hyperplasia of adipocytes in metabolic diseases indicate that the molecular mechanisms that regulate these processes have important roles in controlling energy balance and pathogenesis of disease.

Adipocytes are the main energy storage cells in white adipose tissue (WAT) where the lipid pool is in a constant state of flux resulting from a cycle of lipolysis followed by re-esterification. During times of low energy, the rate of lipolysis is increased causing the liberation of FFA and triglycerides. However, in obesity, where WAT is increased and adipocytes are enlarged due to excess triglyceride storage, lipolysis is frequently impaired (Duncan et al., 2007). A wealth of evidence has demonstrated obesity is also associated with increased macrophage infiltrate in the adipose and a phenotypic switch in adipose tissue macrophages from ‘M2’ anti-inflammatory to ‘M1’ pro-inflammatory (Li et al., 2010, Zeyda et al., 2010, Prieur et al., 2011). In these experiments however, the *Trib1* transplanted mice had no differences in the number of F4/80-positive macrophages in the adipose tissue. Although experiments were not performed to assess the phenotype of the ATMs,

data presented in **Chapter 3** demonstrated high expression of *Trib1* in BMDMs and *TRIB1* in human MDMs corresponds to increase in ‘M2’ anti-inflammatory markers, and a decrease in IL-15 expression. As most if not all data presented in this thesis from *Trib1* transgenic vs. *Trib1* KO mice have demonstrated opposite effects, it is with reasonable confidence that loss of *Trib1* promotes pro-inflammatory polarisation in tissue macrophages and may increase IL-15 expression. As discussed in **Chapter 3** IL-15 is expressed by activated KCs and is implicated in the pathogenesis of NAFLD. IL-15 also has a significant role in the adipose tissue, where numerous studies have indicated it to be involved in the reciprocal regulation of lipolysis between the skeletal muscle and adipose tissues in both humans and mice, where over-expression is associated with leaner WAT mass (reviewed in Argiles et al. (2005)), therefore could be the mechanism at least in part why $Trib1^{KO} \rightarrow ApoE^{-/-}$ mice have reduced adipose size.

There are few studies that have investigated the role of TRIB1 in adipose tissue, a study by Ostertag et al. (2010) demonstrated that *Trib1* expression is significantly elevated in the WAT of obese *db/db* mice compared to WT controls. Interestingly, following cell separation of the adipose, *Trib1* expression is increased in the adipocytes and stromal vascular cells and not in the CD11b+ (macrophage) cell fraction when stimulated with LPS. Haplo-insufficiency of *Trib1* (*Trib1*^{-/-}) also protected against high-fat diet induced obesity and reduced levels of pro-inflammatory cytokine expression such as IL-1 β and TNF- α . Knockdown of *Trib1* also decreased induction of pro-inflammatory cytokine expression (e.g. IL-6, IL1- β , TNF- α and IL-6) in primary adipocytes. They also show that TRIB1 serves as a nuclear transcriptional co-activator for the NF- κ B subunit RelA, suggesting TRIB1 up-regulates pro-inflammatory cytokine expression by this mechanism.

To provide explanation to how haematopoietic TRIB1 drives lipolysis in the adipose tissue, the question remains as to whether the ATMs in the transplanted mice are derived from the bone marrow recipient $ApoE^{-/-}$ mouse (i.e. *Trib1* WT) or from the bone marrow itself. This will then clarify if infiltrating macrophages can change the phenotype of resident ATMs or if the ATMs themselves are responsible for the phenotype. It has been shown that total body irradiation in mice not only destroys bone marrow but ATMs also as most (85%) of F4/80+ cells in adipose tissue are bone marrow derived (Weisberg et al., 2003). Therefore the differences in adipocyte

and tissue size in these experiments are likely attributable to the ATMs with altered *Trib1* expression. In agreement with my data, the prominent study published by Satoh et al. (2013) demonstrated transplantation of *Trib1*^{-/-} bone marrow into WT mice resulted in a lipodystrophic phenotype with reduced abdominal adipose tissue deposits. In contrast, *Trib1*^{-/-} transplanted with WT bone marrow showed no such phenotype suggesting that *Trib1* in bone marrow derived cells were responsible. They also observed a severe reduction of anti-inflammatory ‘M2’-like macrophages in the tissue and when *Trib1*^{-/-} mice were supplemented with ‘M2’-like macrophages, the epididymal adipose tissue were significantly larger than PBS treated controls suggesting altered macrophage phenotype driven by *Trib1* is responsible. Indeed, serum levels of non-esterified fatty acids (NEFAs) and glycerol were also significantly elevated indicating lipolysis. Interestingly, the lipolysis was attributed to decreased levels of *Il-10* and increased levels of *Tnf-α* and *Inos* mRNA expression. IL-10 has reported roles in repressing lipolysis in adipocytes and could be in part the mechanism by which lipodystrophy occurs in this setting (Lumeng et al., 2007). Interestingly, parameters often associated with metabolic abnormalities such as serum glucose, cholesterol, triglyceride and insulin were not detected between WT and *Trib1*^{-/-} bone marrow chimaeric mice fed on chow diet, elevated levels were only induced when the mice were fed high-fat diet and they subsequently developed glucose intolerance and insulin resistance. Although in agreement with my findings, the experiments performed used bone marrow from full-body *Trib1* knockout mice, display high perinatal mortality and are none viable. Therefore questions arise whether the phenotype Akira’s group saw was truly macrophage-*Trib1* driven. However the data presented in this chapter provides strong evidence that the lipodystrophy observed is macrophage specific driven by expression of *Trib1*. Evidently, further work is needed to clarify the mechanism by which macrophage expression of *Trib1* alters adipocyte lipolysis. **Figure 5.16** illustrates the proposed mechanism of haematopoietic-derived TRIB1 in atherosclerosis development and induction of a metabolic phenotype.

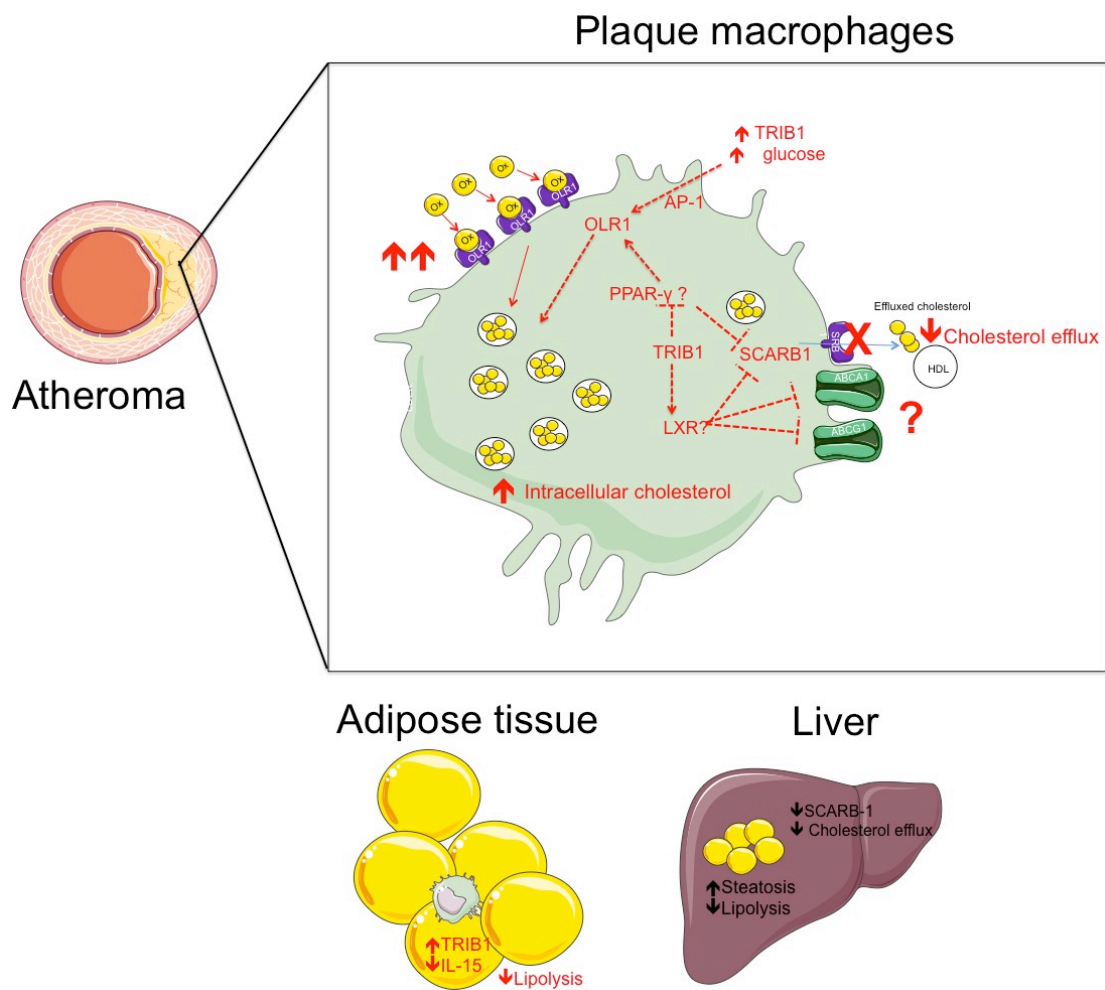


Figure 5.16: Proposed working model of local (atheroma) and systemic (adipose and liver) effects of *Trib1* expression in macrophages.

Over-expression of *Trib1* in plaque macrophages drives local foam cell formation by up-regulating expression of OLR-1 and down-regulating SCARB-1 expression, both contributing to increased intracellular cholesterol accumulation. TRIB1 may exert these effects by modulating expression of PPAR- γ and LXR. Over-expression of *Trib1* in ATMs may down-regulate IL-15 expression, leading to defective lipolysis. Similarly, reduced SCARB-1 expression may be also apparent in the liver causing reduced cholesterol efflux and increased hepatic steatosis from defective lipolysis.

Chapter 6. General Discussion

6.1 Major outcomes

Immuno-metabolic disorders including obesity, diabetes and cardiovascular disease cause significant morbidity and mortality, therefore increasing knowledge of the mechanisms that underpin these diseases will lead to more effective treatment strategies. The aim of this study was to contribute to a better understanding of the role of myeloid TRIB1 in the control of macrophage function and polarisation in the context of lipid metabolism and atherosclerosis. Moreover, a sub-aim was to develop multi-colour immunohistochemistry staining protocols to *simultaneously* stain atherosclerotic plaque macrophages *in situ* with phenotypic markers to clarify their role *in vivo*.

In this thesis, I have described the consequences of myeloid-*Trib1* using conditional knockout and over-expressor *Trib1* x *LyzMCre* mice, especially lipid metabolism and alteration of tissue macrophage phenotype. This appears to be mediated by C/EBP α and C/EBP β that may contribute towards hepatic inflammation and steatosis likely through an IL-15 dependent mechanism. Data from the mouse models were similar to in human MDM microarray data suggesting these may be relevant in humans. Additionally, the actions of TRIB1 in tissue macrophages are likely to be important not just in the liver but also in the context of adipose tissue, where macrophage activation and pro-inflammatory cytokine secretion contributes towards adipocyte lipolysis.

The role of bone marrow derived TRIB1 in the context of systemic inflammation also promoted atherogenesis (largely independent of modulating plasma lipid levels) through increased foam cell formation likely due to a combination of increased oxLDL uptake and defective cholesterol efflux. The transplant data further suggests that *Trib1* may be involved in lipolysis in the liver and adipose tissue (Argiles et al., 2005).

Collectively the data have uncovered previously unreported roles for TRIB1 using novel myeloid-specific *Trib1* *in vivo* models that together demonstrate TRIB1 to

control distinct aspect of macrophage biology that have local and systemic consequences.

Although, previous studies have shown TRIB1 to be a novel regulator of plasma lipid levels; these actions have been largely attributed to its expression in the liver using hepatic-specific knockout and over-expression models (Bauer et al., 2015, Burkhardt et al., 2010). However, it has not been shown until now (this thesis) that myeloid-derived *Trib1* can also significantly modify plasma lipid levels and hepatic lipid content in mice through its role in altering macrophage polarisation. The role of *Trib1* in macrophage polarisation has been reported before and discussed several times throughout this thesis, where full body *Trib1*-KO mice had severe reductions in tissue macrophages and ‘M2’-like macrophages in the bone marrow suggesting it is critical for the differentiation of these cells (Satoh et al., 2013). In some agreement with this finding, the phenotype of KCs in the livers of *Trib1 fl/fl* x *LyzMCre* mice had significantly reduced levels of Ym1+ expression; however, the levels of tissue macrophages (F4/80+) were not altered in the adipose or the liver questioning whether observations seen by Satoh et al. (2013) were truly myeloid- *Trib1* derived and not from other cells with potential influence (e.g. platelets, lymphocytes).

The functional consequences of *Trib1* loss in the context of lipogenesis and macrophage polarisation have been shown in several recent studies to involve C/EBP α , in agreement with this study (Bauer et al., 2015, Satoh et al., 2013, Ishizuka et al., 2014). However, the TRIB1-dependent molecular mechanisms involving C/EBP β in macrophage polarisation have not been fully described and data presented in this thesis show that TRIB1 may regulate distinct functions of macrophage biology through the degradation of C/EBP isoforms (C/EBP α and C/EBP β) with opposing function through COP1 and miR-155.

TRIB1 is involved in distinct aspects of macrophage biology depending on the tissue context and transplanting bone marrow from these mice into an atherogenic ApoE^{-/-} mouse model exposed this. These observations are also similar to work done by Satoh et al. (2013), where they noted *Trib1*^{-/-} \rightarrow WT bone marrow transplantation and subsequent high fat diet resulted in increased adipose tissue lipolysis and increased serum glucose and insulin resistance. Interestingly, high fat diet feeding also increased serum cholesterol and triglycerides. In the context of these experiments,

serum glucose was also increased as well as serum cholesterol, likely due to both increased triglyceride and HDL- cholesterol but independent of LDL cholesterol. Interestingly, in Satoh et al. (2013) experiments, changes were only seen upon high-fat diet feeding and no notable histological changes were seen in mice fed with chow diet, in context with my experiments where changes in the size of adipose tissue and adipocytes were more significant in a chronic inflammatory setting induced by high-fat diet feeding.

The effects of TRIB1 on adipocytes has been demonstrated in a study by Ostertag et al. (2010) using heterozygous *Trib1* (*Trib1*^{+/-}) mice. Ostertag et al. (2010) showed that haplo-insufficiency of *Trib1* protects against diet-induced obesity. Interestingly, the effects of *Trib1* were only revealed upon induction of high-fat diet and the metabolic phenotype was not present under basal conditions. This may explain why no obvious adipose phenotype were seen in the TRIB1 mouse strains prior to transplant and high fat diet in the Satoh et al. (2013) study and work presented in this thesis. As Ostertag et al. (2010) used a haplo-insufficiency model, it is difficult to ascertain the role of each cell type in the adipose tissue in relation to their observations *in vivo*, however both of these studies suggest that TRIB1 may behave differently upon induction of inflammation.

My data may suggest a mechanism for the observed phenotypes whereby IL-15 may play an important part in both lipogenesis in the liver and adipose. Indeed, three receptors for IL-15 have been shown to exist in fat tissue; IL-15R α , IL-2R β and IL-2R γ and interestingly, difference between expression of these receptors have been observed in lean vs. obese animals suggesting IL-15 has important roles in fat deposition (Alvarez et al., 2002). Several studies have implicated IL-15 to have direct roles on lipolysis and recombinant IL-15 stimulated lipolysis in primary porcine adipocytes, even more potently than known adipose pro-inflammatory cytokines including TNF- α , IL-6 and LPS (Ajuwon and Spurlock, 2004). Similar results have been obtained in rats, where treatment with IL-15 decreases WAT mass (Almendro et al., 2008). Likewise, transgenic mice over-expressing IL-15 have leaner bodies, do not gain weight and have smaller adipocytes due to adipocyte shrinkage, while IL-15^{-/-} mice have significant weight gain despite no alteration in appetite or food consumption (Barra et al., 2010). These findings are also relevant in humans where recombinant IL-15 treatment of human adipocytes reduces lipid

deposition (Barra et al., 2010). Interestingly, several SNPs in the human *IL-15* and *IL15RA* gene have been described that correlate with adiposity and markers of metabolic syndrome including levels of total cholesterol, LDL-cholesterol in female subjects and with BMI in males (Pistilli et al., 2008, Di Renzo et al., 2009). Equally, a study of human patients with a wide range of BMIs found negative associations between plasma concentrations of IL-15 and BMI, total fat mass, trunk fat mass and limb fat mass (Nielsen et al., 2008). Comparable results were also found by Barra et al. (2010), where obese subjects had lower circulating IL-15 levels than leaner subjects.

IL-15 expression has been shown to up regulated upon IFN- γ stimulation- a major inflammatory mediator and is thought to activate the JAK-STAT, NF- κ B and MAPK (PKA) pathways (Ajuwon and Spurlock, 2004, Bianchi et al., 2000, Bulfone-Paus et al., 1999, Adunyah et al., 1997). Indeed, it also regulates lipoprotein lipase (LPL) expression, the major regulator of adipocyte lipolysis which it itself is activated through PKA phosphorylation. Several studies have indicated IL-15 to activate several genes including PPAR α and PPAR δ and suppress several lipogenesis genes including ones regulated by TRIB1; *scd1* and *fas* (Almendro et al., 2008, Sun et al., 2016). IL-15 may also increase mitochondrial activity which may enhance fatty acid oxidation which may influence body weight and lipolysis (Barra et al., 2014). Interestingly, there have been reported negative correlations between the severity of obesity and the expression and activity of mitochondrial oxidative phosphorylation. To this end, IL-15-transgenic mice have elevated mitochondrial activity (Kaaman et al., 2007) . IL-15 treatment in mice is also reported to improve glucose homeostasis and insulin sensitivity (Barra et al., 2012). Intriguingly, glucose serum levels were increased in Trib1^{Tg}→ApoE^{-/-} mice and Trib1^{Tg} BMDMs express reduced levels of IL-15.

Most if not all of the studies have shown IL-15 is expressed by KCs, adipocytes or in adipose tissue but whether IL-15 is produced by ATMs specifically remains to be investigated. However, the results from these experiments indicating a loss of *Trib1* in myeloid cells causes adipocyte shrinkage may provide circumstantial evidence. Further work is evidently needed to elucidate how TRIB1 modulates IL-15 expression, especially in the context of adipose biology.

No study has been published that describes the role of *Trib1* in atherosclerosis despite its documented roles in lipid metabolism and therefore the data presented in this thesis is completely novel, particularly the suggestion that *Trib1* regulates the expression of scavenger receptor genes and that this may effect the propensity of plaque macrophages to form foam cells. Indeed, regulation of scavenger receptor gene expression and cholesterol metabolism in macrophages are attributed to LXR and PPAR and no study thus far has implicated *Trib1* to possibly regulate these transcription factors. Interestingly, TRIB3 is known to inhibit the transcriptional activity of PPAR γ by direct interaction (Takahashi et al., 2008) and therefore Trib1 may also have similar regulation which remains to be determined.

In vitro studies would suggest that PPARs have opposing roles in atherosclerosis and may have both atherogenic and anti-atherogenic effects (**Table 6.1**). PPAR α agonists for example can stimulate monocyte chemo-attractant protein (MCP-1), which promotes the infiltration of monocytes into the atherosclerotic plaque (Lee et al., 2000, Gosling et al., 1999). Likewise, PPAR γ agonists stimulate CD36 expression enabling oxLDL uptake and foam cell formation in macrophages (Tontonoz et al., 1998). Anti-atherogenic effects include the inhibition of pro-inflammatory gene expression including IL-1 β , TNF- α , IL-6 and IFN- γ . PPAR α and γ promote the expression of cholesterol efflux proteins through LXR. Studies *in vivo* however have given conflicting results. Mice lacking PPAR α and ApoE fed high fat diet developed less atherosclerosis compared to ApoE null control mice, suggesting PPAR α to be atherogenic (Tordjman et al., 2001). Contrary to this, PPAR α agonists in ApoE^{-/-} mice showed minimal atherogenic effects. It is likely myeloid TRIB1 may regulate atherosclerosis through PPAR γ as agonists have demonstrated anti-atherogenic effects in mice due to anti-inflammatory effects and increased cholesterol efflux in macrophages (Duez et al., 2002, Li et al., 2000). Additionally, transplants with PPAR γ - knockout bone marrow into LDLR^{-/-} mice showed a significant increase in atherosclerosis suggesting PPAR γ to be anti-atherogenic (Chawla et al., 2001). A study by Li et al. (2004) systematically assessed the role of PPAR α , β/δ and γ agonists on foam cell formation in experimental atherosclerosis in LDLR^{-/-} mice. They showed PPAR α and PPAR γ agonists both strongly inhibited atherosclerosis through reduced foam cell formation whereas PPAR β/δ failed to inhibit atheroma development. The anti-atherogenic effects of PPAR α was attributed to increased ABCA1 expression through LXR. However, PPAR γ agonists appear to

work through ABCA1-LXR independent pathways by increasing ABCG1 expression, reducing cholesterol re-esterification and stimulated HDL-dependent cholesterol efflux. Although there are no reported studies that have linked TRIB1 and PPAR γ specifically, TRIB3 has been shown to negatively regulate the transcriptional activity of PPAR γ in adipocytes (Takahashi et al., 2008). Whether these pathways overlap with TRIB1 in macrophages, remains to be elucidated.

Table 6.1: Summary of the effects of PPAR ligands on atherosclerosis.

Adapted from Li et al. (2004).

Effect on	PPAR α	PPAR β/δ	PPAR γ
Atherosclerosis	↓	-	↓
Body weight	↓	-	
Insulin levels	↓	-	↑
Cholesterol levels	-	-	-
CD36 expression	-	↑	↑↑
Inflammation	↓	↓	↓
Foam cell formation	↓	-	↓
ABCA1 expression	↑	-	-
ABCG1 expression	-	-	↑↑
Cholesterol esterification	-	-	↓

TRIB1 may also regulate LXRs either dependently or independently of PPAR γ . LXRs have important roles in atherosclerosis and the induction of anti-inflammatory gene expression in macrophages. Chronic treatment with LXR agonists or the use of *LXR α/β* double knockout mice has demonstrated that LXRs can modulate atherosclerosis through two independent ways; promotion of reverse cholesterol transport and direct suppression of pro-inflammatory signalling pathways. Moreover, these studies established that these effects are controlled by LXR expression in macrophages specifically. Furthermore, evidence has shown that protection from atherosclerosis occurs from LXR activity in bone marrow derived cells and are independent of LXR activity in other tissues of the body (Im and Osborne, 2011). Transplantation of *LXR α/β* double knockout mice into *LDLR^{-/-}* and *ApoE^{-/-}* demonstrated significant increase in lesion development (Tangirala et al., 2002). Similarly, macrophage specific over-expression of *LXR α* in *LDLR^{-/-}* mice resulted in a reduction of atherosclerosis (Teupser et al., 2008). Activation of LXRs increases reverse cholesterol transport from macrophages by increasing expression

of the cholesterol transporters (as mentioned) and by increasing expression of the HDL apolipoprotein-E (apoE).

LXRs also attenuate pro-inflammatory signalling in macrophages independent of its role in reverse cholesterol transport. Indeed, increased intracellular cholesterol can induce pro-inflammatory IL-1 β and NF- κ B signalling in macrophages, which exacerbates atherosclerosis. LXRs can inhibit pro-inflammatory cytokine expression after LPS, TNF- α or IL-1 β stimulation including iNOS, COX-2, IL-6, MCP-1 and MMP-9. LXR agonists inhibit pro-inflammatory cytokine production in peritoneal macrophages treated with bacterial LPS and *LXR α/β* double knockout mice produce an exacerbated response when challenged with LPS in the same way (Joseph et al., 2003, A-Gonzalez and Castrillo, 2011, Im and Osborne, 2011). Likewise, LXRs can positively regulate the expression of anti-inflammatory genes in macrophages such as arginase II (Arg II) (Marathe et al., 2006). ArgII together with ArgI are enzymes that catalyse the conversion of L-arginine to L-ornithine in the urea cycle. Arg activity in macrophages contributes to an anti-inflammatory phenotype by promoting wound healing and proliferation. Arg also competes with other arginine-dependent enzymes such as the pro-inflammatory iNOS, therefore reducing nitric oxide production and its associated injury. Therefore although LXRs are an attractive therapeutic target in the treatment of atherosclerosis, treatment of LXR agonists results in significant hepatic steatosis in mice (Gao et al., 2013). Consequently, understanding the influence of TRIB1 in these pathways would form the basis of future investigation.

Although it is likely from the discussed literature and my data that the loss of TRIB1 promotes a pro-inflammatory ‘M1’ phenotype in tissue macrophages, it is also possible that systemic inflammation through sustained high fat diet feeding overrides the potential influence TRIB1 has on macrophage polarisation, and therefore could be a phenotypic switch from ‘M2’ to ‘M1’, which is a well documented phenomenon that occurs during obesity, particularly in ATMs (Lumeng et al., 2007). It is also well known that pro-inflammatory lesional macrophages are intimately involved with atherosclerotic plaque development and vulnerability, while anti-inflammatory macrophages are more associated with resolution of inflammation (Chinetti-Gbaguidi et al., 2015). However, it is however important to note that macrophages are highly plastic cells and can switch from one phenotype to another

depending on environmental cues and atherosclerotic lesions are a prime example of complex microenvironments. Without assessing the phenotype of the tissue macrophages in the transplanted mice, it is difficult to determine the full consequences of TRIB1 on macrophage polarisation. **Figure 6.1** outlines the potential overall mechanism of myeloid TRIB1 in the context of normal physiological conditions and systemic inflammation.

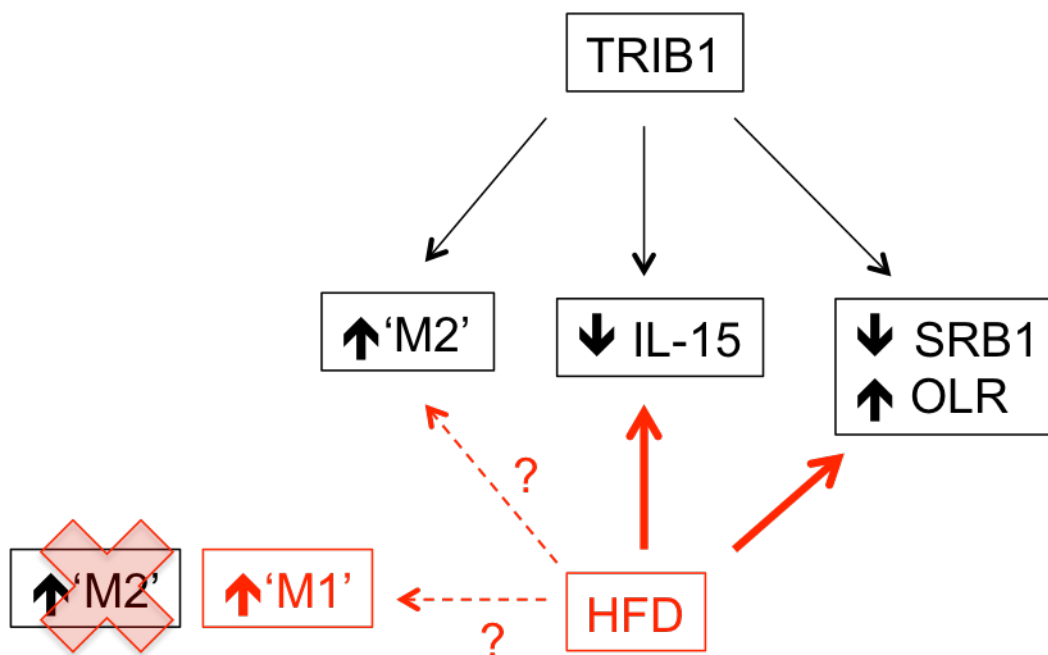


Figure 6.1: Myeloid TRIB1 has distinct roles in macrophage biology under normal physiological conditions and inflammation.

TRIB1 promotes ‘M2’ macrophage polarisation in tissue macrophages, decreases IL-15 expression and has roles in regulation of scavenger receptor expression. During high fat diet (HFD) the changes are more pronounced resulting in increased lipolysis in the liver and adipose and increased foam cell formation in plaque macrophages. The influence of TRIB1 on promoting ‘M2’ polarisation may be preserved during HFD or it may override its effects and switch to a pro-inflammatory ‘M1’ phenotype, which remains to be investigated.

6.2 Limitations

The use of animal models in biomedical research has offered critical insights into disease pathophysiology, characterisation of genes and the evaluation of novel therapeutic agents that cannot be gained from *in vitro* studies alone. However, there is debate about the accuracy and relevance of using animal models to mimic disease that may be largely human-specific. Additionally, differences in anatomy and

genetics highlight some of the fundamental limitations of animal models. This is best illustrated in models of atherosclerosis, which a number of useful and interesting recent reviews have been written that discuss the use of mice in atherosclerosis research (Allayee et al., 2003, Getz and Reardon, 2012, Daugherty, 2002, Fazio and Linton, 2001). Up until 1992 (when ApoE^{-/-} mouse models were developed), the vast majority of atherosclerosis research used rabbits but since then it has become accepted that these come with limitations, as they do not accurately reflect human disease (Getz and Reardon, 2012). Additionally, use of larger animal models such as pigs that are considered more relevant to human disease, have some disadvantages including the costs and difficulties associated with maintaining large animal colonies. These potential weaknesses prompted the need for small, genetically reproducible models that could overcome these potential difficulties. The use of murine models in atherosclerosis in particular therefore has become the most widely used model to replicate the disease.

To complicate matters further, many mice strains are naturally resistant to developing atherosclerosis and require genetic manipulation (e.g. ApoE^{-/-} and LDLR^{-/-}) or treatment (e.g. PCSK9) to develop disease. In spite of this, the models, particularly LDLR^{-/-} still require intervention with high fat diet feeding to induce atherosclerosis (ApoE^{-/-} mice can develop spontaneous lesions without the need for dietary intervention), which progresses in a matter of weeks that evidently do not reflect the true pathology of human atherosclerosis which develops chronically over decades. However, particularly in ApoE^{-/-} mice, lesions do reflect the morphology and phenotype seen in humans (Whitman, 2004, Nakashima et al., 1994), although the anatomical site of atherosclerosis is different as humans more frequently develop atheromas in the coronary arteries, carotids and peripheral vessels and mice develop lesions in the aortic root, aortic arch and innominate (brachiocephalic) artery, they still are a valuable model (Getz and Reardon, 2012).

Taken together therefore, when interpreting findings it must be considered that the research is carried out in a non-human species and thus conclusions drawn may not directly translate to be relevant in human disease. Despite the challenges animal models pose, the great advantages outweigh the potential weaknesses. Certainly, the use of genetically modified mouse lines (knockout or over-expressing) to elucidate

the role of a particular gene such as *Trib1* is invaluable and something that cannot be achieved easily in larger animal models.

Determining atherosclerosis burden in the mouse also has some limitations particularly when examining the aorta. *En face* oil red O staining of the aorta has become the standard technique to measure percentage lesion area. Oil red O stains for lipids and therefore is a rather crude method to assess atherosclerosis because the staining is only sensitive to lesion size/ lipid content rather than its composition. The accuracy of this method can also be questioned as residual fat present on the outside of the vessel wall may count towards positive staining, although extensive effort was made to remove all remaining adventitial fat there is a possibility this may have contributed to the measurements. Nonetheless, the contribution of this towards the results is expected to be very minimal.

Because of the described potential limitations of *en face* staining, serial sections of the aortic root lesions were cut and histologically measured at regular intervals along length of the vessel. As the aortic root contains well-recognised anatomical 'landmarks' it is possible to accurately and sensitively measure lesion burden in the same area across specimens derived from different mice and is considered the gold standard measurement of atherosclerosis burden in mice.

The work described in this thesis has used myeloid *Trib1* strains that were generated by crossing conditional *Trib1*-expressing transgenic mouse strain and a *Trib1*-floxed mouse strain with a line expressing cre recombinase under the control of the *Lyz2* promoter. Although this method has been used extensively to analyse genes involved in monocyte and macrophage function, the *Lyz2* promoter is expressed in cells of all myeloid origin, which include granulocytes (neutrophils, basophils and eosinophils), which may complicate the findings drawn from the observations *in vivo*. Nevertheless it is a valuable and useful tool to elucidate genes involved in macrophage function.

There are also potential confounding issues with the use of ApoE^{-/-} in bone marrow transplant experiments. Macrophages express both the ApoE and the LDL receptor but only ApoE is a secreted protein that participates in reverse cholesterol transport and is expressed in hepatic tissues and in macrophages and can therefore function

extracellularly (Getz and Reardon, 2016). ApoE has been shown to have numerous other functions independent of plasma lipid levels that may affect atherosclerosis including effects on the immune response, inflammation, smooth muscle cell proliferation and migration (reviewed in Getz and Reardon (2009)). Its anti-inflammatory and anti-atherogenic properties can rescue the phenotype of ApoE^{-/-} mice by reducing plasma lipoprotein levels and atherosclerosis. This was illustrated by Linton et al. (1995) with the transplantation of wild-type bone marrow expressing apoE into ApoE^{-/-} recipients. Indeed, VanEck et al. (1997) further demonstrated the effect of *ApoE* gene dosage on atherosclerosis development by transplantation of homozygous (apoE^{-/-}), heterozygous (apoE^{+/-}) and wild-type (apoE^{+/+}) bone marrow into apoE^{-/-} mice. They found both serum cholesterol levels (from reduction of VLDL) and atherosclerosis was significantly reduced in mice transplanted with wild-type bone marrow. Therefore to avoid these issues, transplantations can be done using LDLR^{-/-} recipient mice where the presence of LDLR-expressing bone marrow has little if any affect on atherosclerosis in LDLR^{-/-} mice (Getz and Reardon, 2016). As the experiments were performed using *Trib1* x *LyzMCre* donor mice that express wild-type levels of ApoE on their macrophages, it would be interesting to observe the results if LDLR^{-/-} recipients were used instead. Despite this, the gene dosage of ApoE in the donor mice are expected to be the same, therefore the results are still valid. Additionally, the increased atherosclerosis burden and presence of foam cell macrophages in the lesions of *Trib1*^{Tg}→ApoE^{-/-} regardless of these issues demonstrates that these findings may actually under-represent the true extent of atherosclerosis and disease burden may be even more advanced in LDLR^{-/-} transplanted mice.

Finally, some conclusions drawn were made on the basis of data generated from one and not both mouse strains that either over-express or do not express *Trib1* and in some cases was assumed the opposite trend would be seen in the other model (e.g. increased IL-15 expression in *Trib1*^{KO} BMDMs). However, these assumptions will need to be the focus of future work to thoroughly characterise these changes to accurately support the conclusions made.

6.3 Future work

The findings presented in this thesis raise new questions about the role of TRIB1 in regulating different aspect of macrophage biology. In order to obtain further insight, further investigation is required, which is discussed below.

6.3.1 The regulation of foam cell formation by TRIB1

The fundamental question remains as by what molecular mechanism TRIB1 is driving the observed phenotypes seen. Given the overlap of molecular regulation of cholesterol metabolism and inflammation by SREBP, LXR and PPARs, it is likely that TRIB1 may act by modulating these transcription factors or the associated downstream pathways. Therefore for future work it would be interesting to focus on dissecting these molecular pathways and how TRIB1 may affect in particular scavenger receptor expression and cholesterol metabolism in macrophages, specifically by fully assessing these genes and others such as the ABC transporter proteins that are also important in cholesterol efflux. Despite having gene expression data suggesting TRIB1 may regulate scavenger receptor expression, demonstrating increased oxLDL uptake *in vitro* using mouse BMDMs and human MDMs with differential *Trib1* expression (e.g siRNA vs. plasmid over-expression) will validate these ideas.

6.3.2 Assessment of macrophage phenotype in BMT mice

Although the literature and I have shown *Trib1* to modulate tissue macrophage phenotype, due to time constraints, the phenotype of macrophages in the transplanted mice were not investigated. Establishing macrophage phenotype particularly in the context of systemic inflammation will establish if the known effect of *Trib1* on promoting ‘M2’ polarisation is still evident or that inflammation may override its potential influence. In particular I would like to investigate the aortic plaque macrophages using the developed protocol described in **Chapter 4**, as this has major consequences on lesion development and stability (Chinetti-Gbaguidi et al., 2015). Furthermore, investigating the phenotype of ATMs and their cytokine expression profile, in particular IL-15 will no doubt help to understand the role of TRIB1 in adipocyte lipolysis and its systemic effects. Indeed, the phenotype of

ATMs can be investigated by fluorescence immunohistochemistry or by isolation of CD11b⁺ cells from stromal vascular cells in the adipose and subsequent flow cytometry and/or qPCR analyses (Cho et al., 2014).

6.3.3 High fat diet in *Trib1 x LyzMCre* mice

Giving the apparent opposing phenotypes presented in Chapter 3 and Chapter 5, it would be interesting to recapitulate the atherosclerotic phenotype in *Trib1 x LyzMCre* mice alone without using bone marrow transplantation in ApoE^{-/-} mice. These experiments were performed because *Trib1 x LyzMCre* mice fed high fat diet alone were unlikely to develop atherosclerosis, as C57BL/6 mice are inherently resistant to this disease. Hypercholesterolaemia and subsequent atherosclerosis could be achieved by injecting these mouse models with AAV-PCSK9 and would clarify the role of tissue resident macrophages vs. recruited monocytes in relation to the observed metabolic and atherosclerotic phenotype.

6.3.4 Measurement of lipolysis

As adipose lipolysis appears to be involved in the systemic effects of myeloid *Trib1* expression, work is needed to clarify if this is apparent, such as measurement of free fatty acid and adipokine concentration in the plasma of these mice. Additionally, although I have shown circumstantial evidence to implicate IL-15 expression as a potential mechanism, investigating IL-15 plasma levels are needed to establish if this is evident *in vivo*.

6.3.5 Measurement of plasma levels of cytokines

As several potential TRIB1 regulated cytokines were identified in the microarray study, it would be interesting to measure circulating levels of cytokines in the plasma of these mice, (by e.g. ELISA) particularly if they involved in the recruitment of monocytes into tissues including the adipose, liver and atherosclerotic plaques.

6.3.6 Measurement of apoB

To generate a more accurate analysis of the lipid profile data in the transplanted mice, it would be interesting to carry out a full lipid analysis of different lipoprotein particles, analogous to the results presented in Chapter 3. It would be also noteworthy to measure levels of apoB protein, the main protein constituent of both LDL and VLDL lipoprotein

particles. ApoB exists in two isoforms; apoB-48 (constituent of chylomicrons) and apoB-100 (constituent of VLDL), therefore having more in-depth understating of these relevant lipoproteins may yield interesting aspects of how myeloid *Trib1* may alter lipoprotein metabolism.

6.3.7 Measurement of fatty acid oxidation genes

Although the expression of lipogenesis (production of fatty acids and triglycerides) genes were not altered in the *Trib1x LyzMCre* mice in Chapter 3, the level of expression of fatty acid oxidation (breakdown of fatty acids) genes should also be assessed to see if potentially this pathway is affected, this may account for the increased levels of triglyceride in the livers *Trib1* KO mice (due to reduced fatty acid breakdown).

References

- Abram, C. L., Roberge, G. L., Hu, Y. & Lowell, C. A. 2014. Comparative Analysis Of The Efficiency And Specificity Of Myeloid-Cre Deleting Strains Using Rosa-Eyfp Reporter Mice. *Journal Of Immunological Methods*, 408, 89-100.
- A-Gonzalez, N. & Castrillo, A. 2011. Liver X Receptors As Regulators Of Macrophage Inflammatory And Metabolic Pathways. *Biochimica Et Biophysica Acta-Molecular Basis Of Disease*, 1812, 982-994.
- Adunyah, S. E., Wheeler, B. J. & Cooper, R. S. 1997. Evidence For The Involvement Of Lck And Map Kinase (Erk-1) In The Signal Transduction Mechanism Of Interleukin-15. *Biochemical And Biophysical Research Communications*, 232, 754-758.
- Ahmadian, M., Suh, J. M., Hah, N., Liddle, C., Atkins, A. R., Downes, M. & Evans, R. M. 2013. Ppar Gamma Signaling And Metabolism: The Good, The Bad And The Future. *Nature Medicine*, 19, 557-566.
- Ajuwon, K. M. & Spurlock, M. E. 2004. Direct Regulation Of Lipolysis By Interleukin-15 In Primary Pig Adipocytes. *American Journal Of Physiology-Regulatory Integrative And Comparative Physiology*, 287, R608-R611.
- Akira, S., Takeda, K. & Kaisho, T. 2001. Toll-Like Receptors: Critical Proteins Linking Innate And Acquired Immunity. *Nature Immunology*, 2, 675-680.
- Akira, S., Uematsu, S. & Takeuchi, O. 2006. Pathogen Recognition And Innate Immunity. *Cell*, 124, 783-801.
- Alfon, J., Guasch, J. F., Berrozpe, M. & Badimon, L. 1999. Nitric Oxide Synthase Ii (Nos Ii) Gene Expression Correlates With Atherosclerotic Intimal Thickening. Preventive Effects Of Hmg-Coa Reductase Inhibitors. *Atherosclerosis*, 145, 325-331.
- Allayee, H., Ghazalpour, A. & Lusis, A. J. 2003. Using Mice To Dissect Genetic Factors In Atherosclerosis. *Arteriosclerosis Thrombosis And Vascular Biology*, 23, 1501-1509.
- Almendro, V., Fuster, G., Busquets, S., Ametller, E., Figueras, M., Argiles, J. M. & Lopez-Soriano, F. J. 2008. Effects Of Il-15 On Rat Brown Adipose Tissue: Uncoupling Proteins And Ppars. *Obesity*, 16, 285-289.
- Alvarez, B., Carbo, N., Lopez-Soriano, J., Drivdahl, R. H., Busquets, S., Lopez-Soriano, F. J., Argiles, J. M. & Quinn, L. S. 2002. Effects Of Interleukin-15 (Il-15) On Adipose Tissue Mass In Rodent Obesity Models: Evidence For Direct Il-15 Action On Adipose Tissue. *Biochimica Et Biophysica Acta-General Subjects*, 1570, 33-37.
- Ameer, F., Scanduzzi, L., Hasnain, S., Kalbacher, H. & Zaidi, N. 2014. De Nova Lipogenesis In Health And Disease. *Metabolism-Clinical And Experimental*, 63, 895-902.
- Andreozzi, F., Formoso, G., Prudente, S., Hribal, M. L., Pandolfi, A., Bellacchio, E., Di Silvestre, S., Trischitta, V., Consoli, A. & Sesti, G. 2008. Trib3 R84 Variant Is Associated With Impaired Insulin-Mediated Nitric Oxide Production In Human Endothelial Cells. *Arteriosclerosis Thrombosis And Vascular Biology*, 28, 1355-1360.
- Argiles, J. M., Lopez-Soriano, J., Almendro, V., Busquets, S. & Lopez-Soriano, F. J. 2005. Cross-Talk Between Skeletal Muscle And Adipose Tissue: A Link With Obesity? *Medicinal Research Reviews*, 25, 49-65.
- Arranz, A., Doxaki, C., Vergadi, E., De La Torre, Y. M., Vaporidi, K., Lagoudaki, E. D., Ieronymaki, E., Androulidaki, A., Venihaki, M., Margioris, A. N., Stathopoulos, E. N., Tsihchlis, P. N. & Tsatsanis, C. 2012. Akt1 And Akt2 Protein Kinases Differentially Contribute To Macrophage Polarization. *Proceedings Of The National*

- Academy Of Sciences Of The United States Of America*, 109, 9517-9522.
- Avina-Zubieta, J. A., Choi, H. K., Sadatsafavi, M., Etminan, M., Esdaile, J. M. & Lacaille, D. 2008. Risk Of Cardiovascular Mortality In Patients With Rheumatoid Arthritis: A Meta-Analysis Of Observational Studies. *Arthritis & Rheumatism-Arthritis Care & Research*, 59, 1690-1697.
- Baffy, G. 2009. Kupffer Cells In Non-Alcoholic Fatty Liver Disease: The Emerging View. *Journal Of Hepatology*, 51, 212-223.
- Baitsch, D., Bock, H. H., Engel, T., Telgmann, R., Mueller-Tidow, C., Varga, G., Bot, M., Herz, J., Robenek, H., Von Eckardstein, A. & Nofer, J.-R. 2011. Apolipoprotein E Induces Antiinflammatory Phenotype In Macrophages. *Arteriosclerosis Thrombosis And Vascular Biology*, 31, 1160-U577.
- Bala, S., Csak, T., Saha, B., Zatsiorsky, J., Kodys, K., Catalano, D., Satishchandran, A. & Szabo, G. 2016. The Pro-Inflammatory Effects Of Mir-155 Promote Liver Fibrosis And Alcohol-Induced Steatohepatitis. *Journal Of Hepatology*, 64, 1378-1387.
- Bala, S., Marcos, M., Kodys, K., Csak, T., Catalano, D., Mandrekar, P. & Szabo, G. 2011. Up-Regulation Of Microrna-155 In Macrophages Contributes To Increased Tumor Necrosis Factor Alpha (Tnf Alpha) Production Via Increased Mrna Half-Life In Alcoholic Liver Disease. *Journal Of Biological Chemistry*, 286, 1436-1444.
- Barra, N. G., Chew, M. V., Holloway, A. C. & Ashkar, A. A. 2012. Interleukin-15 Treatment Improves Glucose Homeostasis And Insulin Sensitivity In Obese Mice. *Diabetes Obesity & Metabolism*, 14, 190-193.
- Barra, N. G., Palanivel, R., Denou, E., Chew, M. V., Gillgrass, A., Walker, T. D., Kong, J., Richards, C. D., Jordana, M., Collins, S. M., Trigatti, B. L., Holloway, A. C., Raha, S., Steinberg, G. R. & Ashkar, A. A. 2014. Interleukin-15 Modulates Adipose Tissue By Altering Mitochondrial Mass And Activity. *Plos One*, 9.
- Barra, N. G., Reid, S., Mackenzie, R., Werstuck, G., Trigatti, B. L., Richards, C., Holloway, A. C. & Ashkar, A. A. 2010. Interleukin-15 Contributes To The Regulation Of Murine Adipose Tissue And Human Adipocytes. *Obesity*, 18, 1601-1607.
- Bauer, R. C., Sasaki, M., Cohen, D. M., Cui, J., Smith, M. A., Yenilmez, B. D., Steger, D. J. & Rader, D. J. 2015. Tribbles-1 Regulates Hepatic Lipogenesis Through Posttranscriptional Regulation Of C/Ebp Alpha. *Journal Of Clinical Investigation*, 125, 3809-3818.
- Beier, J. I. & McClain, C. J. 2010. Mechanisms And Cell Signaling In Alcoholic Liver Disease. *Biological Chemistry*, 391, 1249-1264.
- Berliner, J. A., Territo, M. C., Sevanian, A., Ramin, S., Kim, J. A., Bamshad, B., Esterson, M. & Fogelman, A. M. 1990. Minimally Modified Low Density Lipoprotein Stimulates Monocyte Endothelial Interactions. *J Clin Invest*, 85, 1260-6.
- Berneis, K. K. & Krauss, R. M. 2002. Metabolic Origins And Clinical Significance Of Ldl Heterogeneity. *Journal Of Lipid Research*, 43, 1363-1379.
- Bianchi, M., Meng, C. & Ivashkiv, L. B. 2000. Inhibition Of Il-2-Induced Jak-Stat Signaling By Glucocorticoids. *Proceedings Of The National Academy Of Sciences Of The United States Of America*, 97, 9573-9578.
- Bjorklund, M. M., Hollensen, A. K., Hagensen, M. K., Dagnaes-Hansen, F., Christoffersen, C., Mikkelsen, J. G. & Bentzon, J. F. 2014. Induction Of Atherosclerosis In Mice And Hamsters Without Germline Genetic Engineering. *Circulation Research*, 114, 1684-+.
- Boden, G., She, P. X., Mozzoli, M., Cheung, P., Gumireddy, K., Reddy, P., Xiang, X. Q., Luo, Z. J. & Ruderman, N. 2005. Free Fatty Acids Produce Insulin Resistance And Activate The Proinflammatory Nuclear Factor-Kappa B Pathway In Rat Liver. *Diabetes*, 54, 3458-3465.
- Bou Ghosn, E. E., Cassado, A. A., Govoni, G. R., Fukuhara, T., Yang, Y., Monack, D. M., Bortoluci, K. R., Almeida, S. R., Herzenberg, L. A. & Herzenberg, L.

- A. 2010. Two Physically, Functionally, And Developmentally Distinct Peritoneal Macrophage Subsets. *Proceedings Of The National Academy Of Sciences Of The United States Of America*, 107, 2568-2573.
- Boyle, J. J., Weissberg, P. L. & Bennett, M. R. 2002. Human Macrophage-Induced Vascular Smooth Muscle Cell Apoptosis Requires No Enhancement Of Fas/Fas-L Interactions. *Arteriosclerosis Thrombosis And Vascular Biology*, 22, 1624-1630.
- Brestoff, J. R. & Artis, D. 2015. Immune Regulation Of Metabolic Homeostasis In Health And Disease. *Cell*, 161, 146-160.
- Brown, M. S., Goldstein, J. L., Krieger, M., Ho, Y. K. & Anderson, R. G. W. 1979. Reversible Accumulation Of Cholesteryl Esters In Macrophages Incubated With Acetylated Lipoproteins. *Journal Of Cell Biology*, 82, 597-613.
- Bulfone-Paus, S., Bulanova, E., Pohl, T., Budagian, V., Durkop, H., Ruckert, R., Kunzendorf, U., Paus, R. & Krause, H. 1999. Death Deflected: Il-15 Inhibits Tnf-Alpha-Mediated Apoptosis In Fibroblasts By Traf2 Recruitment To The Il-15r Alpha Chain (Retracted Article. See Vol 25, Pg 1118, 2011). *Faseb Journal*, 13, 1575-1585.
- Burkhardt, R., Toh, S.-A., Lagor, W. R., Birkeland, A., Levin, M., Li, X., Robblee, M., Fedorov, V. D., Yamamoto, M., Satoh, T., Akira, S., Kathiresan, S., Breslow, J. L. & Rader, D. J. 2010. Trib1 Is A Lipid- And Myocardial Infarction-Associated Gene That Regulates Hepatic Lipogenesis And Vldl Production In Mice. *Journal Of Clinical Investigation*, 120, 4410-4414.
- Burleigh, M. E., Babaev, V. R., Yancey, P. G., Major, A. S., Mccaleb, J. L., Oates, J. A., Marrow, J. D., Fazio, S. & Linton, M. F. 2005. Cyclooxygenase-2 Promotes Early Atherosclerotic Lesion Formation In Apoe-Deficient And C57bl/6 Mice. *Journal Of Molecular And Cellular Cardiology*, 39, 443-452.
- Burns, K. A. & Vanden Heuvel, J. P. 2007. Modulation Of Ppar Activity Via Phosphorylation. *Biochim Biophys Acta*, 1771, 952-60.
- Canton, J., Neculai, D. & Grinstein, S. 2013. Scavenger Receptors In Homeostasis And Immunity. *Nature Reviews Immunology*, 13, 621-634.
- Carmena, R., Duriez, P. & Fruchart, J. C. 2004. Atherogenic Lipoprotein Particles In Atherosclerosis. *Circulation*, 109, 2-7.
- Casagrande, V., Menghini, R., Menini, S., Marino, A., Marchetti, V., Cavalera, M., Fabrizi, M., Hribal, M. L., Pugliese, G., Gentileschi, P., Schillaci, O., Porzio, O., Lauro, D., Sbraccia, P., Lauro, R. & Federici, M. 2012. Overexpression Of Tissue Inhibitor Of Metalloproteinase 3 In Macrophages Reduces Atherosclerosis In Low-Density Lipoprotein Receptor Knockout Mice. *Arteriosclerosis Thrombosis And Vascular Biology*, 32, 74-U190.
- Caulfield, M. P., Li, S., Lee, G., Blanche, P. J., Salarneh, W. A., Benner, W. H., Reitz, R. E. & Krauss, R. M. 2008. Direct Determination Of Lipoprotein Particle Sizes And Concentrations By Ion Mobility Analysis. *Clinical Chemistry*, 54, 1307-1316.
- Cepero-Donates, Y., Lacraz, G., Ghobadi, F., Rakotoarivelo, V., Orkhis, S., Mayhue, M., Chen, Y. G., Rola-Pleszczynski, M., Menendez, A., Ilangumaran, S. & Ramanathan, S. 2016. Interleukin-15-Mediated Inflammation Promotes Non-Alcoholic Fatty Liver Disease. *Cytokine*, 82, 102-111.
- Cepero-Donates, Y., Rakotoarivelo, V., Mayhue, M., Ma, A., Chen, Y.-G. & Ramanathan, S. 2016. Homeostasis Of Il-15 Dependent Lymphocyte Subsets In The Liver. *Cytokine*, 82, 95-101.
- Chambers, J. C., Zhang, W., Sehmi, J., Li, X., Wass, M. N., Van Der Harst, P., Holm, H., Sanna, S., Kavousi, M., Baumeister, S. E., Coin, L. J., Deng, G., Gieger, C., Heard-Costa, N. L., Hottenga, J.-J., Kuehnel, B., Kumar, V., Lagou, V., Liang, L., Luan, J. A., Vidal, P. M., Leach, I. M., O'reilly, P. F., Peden, J. F., Rahmioglu, N., Soininen, P., Speliotes, E. K., Yuan, X., Thorleifsson, G., Alizadeh, B. Z., Atwood, L. D.,

- Borecki, I. B., Brown, M. J., Charoen, P., Cucca, F., Das, D., De Geus, E. J. C., Dixon, A. L., Doering, A., Ehret, G., Eyjolfsson, G. I., Farrall, M., Forouhi, N. G., Friedrich, N., Goessling, W., Gudbjartsson, D. F., Harris, T. B., Hartikainen, A.-L., Heath, S., Hirschfeld, G. M., Hofman, A., Homuth, G., Hypponen, E., Janssen, H. L. A., Johnson, T., Kangas, A. J., Kema, I. P., Kuehn, J. P., Lai, S., Lathrop, M., Lerch, M. M., Li, Y., Liang, T. J., Lin, J.-P., Loos, R. J. F., Martin, N. G., Moffatt, M. F., Montgomery, G. W., Munroe, P. B., Musunuru, K., Nakamura, Y., O'donnell, C. J., Olafsson, I., Penninx, B. W., Pouta, A., Prins, B. P., Prokopenko, I., Puls, R., Ruukonen, A., Savolainen, M. J., Schlessinger, D., Schouten, J. N. L., Seedorf, U., Sen-Chowdhry, S., Siminovitch, K. A., Smit, J. H., Spector, T. D., Tan, W., Teslovich, T. M., Tukiainen, T., Uitterlinden, A. G., Van Der Klauw, M. M., Vasani, R. S., Wallace, C., Wallaschofski, H., Wichmann, H. E., Willemsen, G., Wuertz, P., Xu, C., Yerges-Armstrong, L. M., Et Al. 2011. Genome-Wide Association Study Identifies Loci Influencing Concentrations Of Liver Enzymes In Plasma. *Nature Genetics*, 43, 1131-U129.
- Charriere, G., Cousin, B., Arnaud, E., Andre, M., Bacou, F., Penicaud, L. & Casteilla, L. 2003. Preadipocyte Conversion To Macrophage - Evidence Of Plasticity. *Journal Of Biological Chemistry*, 278, 9850-9855.
- Chawla, A., Boisvert, W. A., Lee, C. H., Laffitte, B. A., Barak, Y., Joseph, S. B., Liao, D., Nagy, L., Edwards, P. A., Curtiss, L. K., Evans, R. M. & Tontonoz, P. 2001. A Ppar Gamma-Lxr-Abca1 Pathway In Macrophages Is Involved In Cholesterol Efflux And Atherogenesis. *Molecular Cell*, 7, 161-171.
- Chen, M. Y., Kakutani, M., Minami, M., Kataoka, H., Kume, N., Narumiya, S., Kita, T., Masaki, T. & Sawamura, T. 2000. Increased Expression Of Lectinlike Oxidized Low Density Lipoprotein Receptor-1 In Initial Atherosclerotic Lesions Of Watanabe Heritable Hyperlipidemic Rabbits. *Arteriosclerosis Thrombosis And Vascular Biology*, 20, 1107-1115.
- Chen, X. L., Zhang, Q., Zhao, R. & Medford, R. M. 2004. Superoxide, H₂O₂, And Iron Are Required For Tnf-Alpha-Induced Mcp-1 Gene Expression In Endothelial Cells: Role Of Rac1 And NADPH Oxidase. *American Journal Of Physiology-Heart And Circulatory Physiology*, 286, H1001-H1007.
- Chiba, Y., Ogita, T., Ando, K. & Fujita, T. 2001. Ppar Gamma Ligands Inhibit Tnf-Alpha-Induced Lox-1 Expression In Cultured Endothelial Cells. *Biochemical And Biophysical Research Communications*, 286, 541-546.
- Chinetti, G., Gbaguidi, F. G., Griglio, S., Mallat, Z., Antonucci, M., Poulain, P., Chapman, J., Fruchart, J. C., Tedgui, A., Najib-Fruchart, J. & Staels, B. 2000. CLA-1/Sr-BI Is Expressed In Atherosclerotic Lesion Macrophages And Regulated By Activators Of Peroxisome Proliferator-Activated Receptors. *Circulation*, 101, 2411-2417.
- Chinetti-Gbaguidi, G., Baron, M., Bouhelle, M. A., Vanhoutte, J., Copin, C., Sebt, Y., Derudas, B., Mayi, T., Bories, G., Tailleux, A., Haulon, S., Zawadzki, C., Jude, B. & Staels, B. 2011. Human Atherosclerotic Plaque Alternative Macrophages Display Low Cholesterol Handling But High Phagocytosis Because Of Distinct Activities Of The Ppar Gamma And Lxr Alpha Pathways. *Circulation Research*, 108, 985-995.
- Chinetti-Gbaguidi, G., Colin, S. & Staels, B. 2015. Macrophage Subsets In Atherosclerosis. *Nature Reviews Cardiology*, 12, 10-17.
- Chistiakov, D. A., Bobryshev, Y. V. & Orekhov, A. N. 2016. Macrophage-Mediated Cholesterol Handling In Atherosclerosis. *Journal Of Cellular And Molecular Medicine*, 20, 17-28.
- Cho, K. W., Morris, D. L. & Lumeng, C. N. 2014. Flow Cytometry Analyses Of Adipose Tissue Macrophages. *Methods Of Adipose Tissue Biology, Pt A*, 537, 297-314.
- Clarke, M. C. H., Figg, N., Maguire, J. J., Davenport, A. P., Goddard, M., Littlewood, T. D. & Bennett, M. R. 2006. Apoptosis Of Vascular Smooth Muscle Cells Induces

- Features Of Plaque Vulnerability In Atherosclerosis. *Nature Medicine*, 12, 1075-1080.
- Combadiere, C., Potteaux, S., Rodero, M., Simon, T., Pezard, A., Esposito, B., Merval, R., Proudfoot, A., Tedgui, A. & Mallat, Z. 2008. Combined Inhibition Of Ccl2, Cx3cr1, And Ccr5 Abrogates Ly6c(Hi) And Ly6c(Lo) Monocytosis And Almost Abolishes Atherosclerosis In Hypercholesterolemic Mice. *Circulation*, 117, 1649-1657.
- Cousin, B., Munoz, O., Andre, M., Fontanilles, A. M., Dani, C., Cousin, J. L., Laharrague, P., Casteilla, L. & Penicaud, L. 1999. A Role For Preadipocytes As Macrophage-Like Cells. *Faseb Journal*, 13, 305-312.
- Cullen, P. 2000. Evidence That Triglycerides Are An Independent Coronary Heart Disease Risk Factor. *American Journal Of Cardiology*, 86, 943-949.
- Dalager, S., Paaske, W. P., Kristensen, I. B., Laurberg, J. M. & Falk, E. 2007. Artery-Related Differences In Atherosclerosis Expression - Implications For Atherogenesis And Dynamics In Intima-Media Thickness. *Stroke*, 38, 2698-2705.
- Danesh, J., Whincup, P., Walker, M., Lennon, L., Thomson, A., Appleby, P., Gallimore, J. R. & Pepys, M. B. 2000. Low Grade Inflammation And Coronary Heart Disease: Prospective Study And Updated Meta-Analyses. *British Medical Journal*, 321, 199-204.
- Daugherty, A. 2002. Mouse Models Of Atherosclerosis. *American Journal Of The Medical Sciences*, 323, 3-10.
- Davies, L. C., Jenkins, S. J., Allen, J. E. & Taylor, P. R. 2013. Tissue-Resident Macrophages. *Nature Immunology*, 14, 986-995.
- Davies, M. J. 2000. Coronary Disease - The Pathophysiology Of Acute Coronary Syndromes. *Heart*, 83, 361-366.
- Daynes, R. A. & Jones, D. C. 2002. Emerging Roles Of Ppars In Inflammation And Immunity. *Nature Reviews Immunology*, 2, 748-759.
- De Villiers, W. J. S. & Smart, E. J. 1999. Macrophage Scavenger Receptors And Foam Cell Formation. *Journal Of Leukocyte Biology*, 66, 740-746.
- Deloukas, P., Kanoni, S., Willenborg, C., Farrall, M., Assimes, T. L., Thompson, J. R., Ingelsson, E., Saleheen, D., Erdmann, J., Goldstein, B. A., Stirrups, K., Koenig, I. R., Cazier, J.-B., Johansson, A., Hall, A. S., Lee, J.-Y., Willer, C. J., Chambers, J. C., Esko, T., Folkersen, L., Goel, A., Grundberg, E., Havulinna, A. S., Ho, W. K., Hopewell, J. C., Eriksson, N., Kleber, M. E., Kristiansson, K., Lundmark, P., Lyytikainen, L.-P., Rafelt, S., Shungin, D., Strawbridge, R. J., Thorleifsson, G., Tikkanen, E., Van Zuydam, N., Voight, B. F., Waite, L. L., Zhang, W., Ziegler, A., Absher, D., Altshuler, D., Balmforth, A. J., Barroso, I., Braund, P. S., Burgdorf, C., Claudi-Boehm, S., Cox, D., Dimitriou, M., Do, R., Doney, A. S. F., El Mokhtari, N., Eriksson, P., Fischer, K., Fontanillas, P., Franco-Cereceda, A., Gigante, B., Groop, L., Gustafsson, S., Hager, J., Hallmans, G., Han, B.-G., Hunt, S. E., Kang, H. M., Illig, T., Kessler, T., Knowles, J. W., Kolovou, G., Kuusisto, J., Langenberg, C., Langford, C., Leander, K., Lokki, M.-L., Lundmark, A., Mccarthy, M. I., Meisinger, C., Melander, O., Mihailov, E., Maouche, S., Morris, A. D., Mueller-Nurasyid, M., Nikus, K., Peden, J. F., Rayner, N. W., Rasheed, A., Rosinger, S., Rubin, D., Rumpf, M. P., Schaefer, A., Sivananthan, M., Song, C., Stewart, A. F. R., Tan, S.-T., Thorgeirsson, G., Van Der Schoot, C. E., Wagner, P. J., Wells, G. A., Wild, P. S., Yang, T.-P., Amouyel, P., Et Al. 2013. Large-Scale Association Analysis Identifies New Risk Loci For Coronary Artery Disease. *Nature Genetics*, 45, 25-U52.
- Desai, N. R., Giugliano, R. P., Zhou, J., Kohli, P., Somaratne, R., Hoffman, E., Liu, T., Scott, R., Wasserman, S. M. & Sabatine, M. S. 2014. Amg 145, A Monoclonal Antibody Against Pcsk9, Facilitates Achievement Of National Cholesterol Education Program-Adult Treatment Panel Iii Low-Density Lipoprotein Cholesterol

- Goals Among High-Risk Patients. *Journal Of The American College Of Cardiology*, 63, 430-433.
- Detmers, P. A., Hernandez, M., Mudgett, J., Hassing, H., Burton, C., Mundt, S., Chun, S., Fletcher, D., Card, D. J., Lisnock, J., Weikel, R., Bergstrom, J. D., Shevell, D. E., Hermanowski-Vosatka, A., Sparrow, C. P., Chao, Y. S., Rader, D. J., Wright, S. D. & Pure, E. 2000. Deficiency In Inducible Nitric Oxide Synthase Results In Reduced Atherosclerosis In Apolipoprotein E-Deficient Mice. *Journal Of Immunology*, 165, 3430-3435.
- Dey, A., Allen, J. & Hankey-Giblin, P. A. 2015. Ontogeny And Polarization Of Macrophages In Inflammation: Blood Monocytes Versus Tissue Macrophages. *Frontiers In Immunology*, 5.
- Di Renzo, L., Gloria-Bottini, F., Saccucci, P., Bigioni, M., Abenavoli, L., Gasbarrini, G. & De Lorenzo, A. 2009. Role Of Interleukin-15 Receptor Alpha Polymorphisms In Normal Weight Obese Syndrome. *International Journal Of Immunopathology And Pharmacology*, 22, 105-113.
- Dobens, L. L. & Bouyain, S. 2012. Developmental Roles Of Tribbles Protein Family Members. *Developmental Dynamics*, 241, 1239-1248.
- Du, K. Y., Herzig, S., Kulkarni, R. N. & Montminy, M. 2003. Trb3: A Tribbles Homolog That Inhibits Akt/Pkb Activation By Insulin In Liver. *Science*, 300, 1574-1577.
- Duez, H., Chao, Y. S., Hernandez, M., Torpier, G., Poulain, P., Mundt, S., Mallat, Z., Teissier, E., Burton, C. A., Tedgui, A., Fruchart, J. C., Fievet, C., Wright, S. D. & Staels, B. 2002. Reduction Of Atherosclerosis By The Peroxisome Proliferator-Activated Receptor Alpha Agonist Fenofibrate In Mice. *Journal Of Biological Chemistry*, 277, 48051-48057.
- Duncan, R. E., Ahmadian, M., Jaworski, K., Sarkadi-Nagy, E. & Sul, H. S. 2007. Regulation Of Lipolysis In Adipocytes. *Annual Review Of Nutrition*, 27, 79-101.
- Eder, K., Guan, H., Sung, H. Y., Ward, J., Angyal, A., Janas, M., Sarmay, G., Duda, E., Turner, M., Dower, S. K., Francis, S. E., Crossman, D. C. & Kiss-Toth, E. 2008. Tribbles-2 Is A Novel Regulator Of Inflammatory Activation Of Monocytes. *International Immunology*, 20, 1543-1550.
- Edmondson, A. C., Braund, P. S., Stylianou, I. M., Khera, A. V., Nelson, C. P., Wolfe, M. L., Derohannessian, S. L., Keating, B. J., Qu, L., He, J., Tobin, M. D., Tomaszewski, M., Baumert, J., Klopp, N., Doering, A., Thorand, B., Li, M., Reilly, M. P., Koenig, W., Samani, N. J. & Rader, D. J. 2011. Dense Genotyping Of Candidate Gene Loci Identifies Variants Associated With High-Density Lipoprotein Cholesterol. *Circulation-Cardiovascular Genetics*, 4, 145-U182.
- Fabbrini, E., Sullivan, S. & Klein, S. 2010. Obesity And Nonalcoholic Fatty Liver Disease: Biochemical, Metabolic, And Clinical Implications. *Hepatology*, 51, 679-689.
- Faggioni, R., Moser, A., Feingold, K. R. & Grunfeld, C. 2000. Reduced Leptin Levels In Starvation Increase Susceptibility To Endotoxic Shock. *American Journal Of Pathology*, 156, 1781-1787.
- Fazio, S. & Linton, M. F. 2001. Mouse Models Of Hyperlipidemia And Atherosclerosis. *Frontiers In Bioscience*, 6, D515-D525.
- Ferre, P. & Foufelle, F. 2010. Hepatic Steatosis: A Role For De Novo Lipogenesis And The Transcription Factor Srebp-1c. *Diabetes Obesity & Metabolism*, 12, 83-92.
- Formoso, G., Di Tomo, P., Andreozzi, F., Succurro, E., Di Silvestre, S., Prudente, S., Perticone, F., Trischitta, V., Sesti, G., Pandolfi, A. & Consoli, A. 2011. The Trib3 R84 Variant Is Associated With Increased Carotid Intima-Media Thickness In Vivo And With Enhanced Mapk Signalling In Human Endothelial Cells. *Cardiovascular Research*, 89, 184-192.

- Friedrich, G. & Soriano, P. 1991. Promoter Traps In Embryonic Stem-Cells - A Genetic Screen To Identify And Mutate Developmental Genes In Mice. *Genes & Development*, 5, 1513-1523
- Gao, B. & Bataller, R. 2011. Alcoholic Liver Disease: Pathogenesis And New Therapeutic Targets. *Gastroenterology*, 141, 1572-1585.
- Gao, M. M., Bu, L., Ma, Y. J. & Liu, D. X. 2013. Concurrent Activation Of Liver X Receptor And Peroxisome Proliferator-Activated Receptor Alpha Exacerbates Hepatic Steatosis In High Fat Diet-Induced Obese Mice. *Plos One*, 8.
- Getz, G. S. & Reardon, C. A. 2006. Diet And Murine Atherosclerosis. *Arteriosclerosis Thrombosis And Vascular Biology*, 26, 242-249.
- Getz, G. S. & Reardon, C. A. 2009. Apoprotein E As A Lipid Transport And Signaling Protein In The Blood, Liver, And Artery Wall. *Journal Of Lipid Research*, 50, S156-S161.
- Getz, G. S. & Reardon, C. A. 2012. Animal Models Of Atherosclerosis. *Arteriosclerosis Thrombosis And Vascular Biology*, 32, 1104-+.
- Getz, G. S. & Reardon, C. A. 2016. Do The Apoe^{-/-} And Ldlr^{-/-} Mice Yield The Same Insight On Atherogenesis? *Arterioscler Thromb Vasc Biol*.
- Ghosh, S. 2011. Macrophage Cholesterol Homeostasis And Metabolic Diseases: Critical Role Of Cholesteryl Ester Mobilization. *Expert Rev Cardiovasc Ther*, 9, 329-40.
- Ginhoux, F., Greter, M., Leboeuf, M., Nandi, S., See, P., Gokhan, S., Mehler, M. F., Conway, S. J., Ng, L. G., Stanley, E. R., Samokhvalov, I. M. & Merad, M. 2010. Fate Mapping Analysis Reveals That Adult Microglia Derive From Primitive Macrophages. *Science*, 330, 841-845.
- Gong, H.-P., Wang, Z.-H., Jiang, H., Fang, N.-N., Li, J.-S., Shang, Y.-Y., Zhang, Y., Zhong, M. & Zhang, W. 2009. Trib3 Functional Q84r Polymorphism Is A Risk Factor For Metabolic Syndrome And Carotid Atherosclerosis. *Diabetes Care*, 32, 1311-1313.
- Gordon, S. 2003. Alternative Activation Of Macrophages. *Nature Reviews Immunology*, 3, 23-35.
- Gosling, J., Slaymaker, S., Gu, L., Tseng, S., Zlot, C. H., Young, S. G., Rollins, B. J. & Charo, I. F. 1999. Mcp-1 Deficiency Reduces Susceptibility To Atherosclerosis In Mice That Overexpress Human Apolipoprotein B. *Journal Of Clinical Investigation*, 103, 773-778.
- Grosshans, J. & Wieschaus, E. 2000. A Genetic Link Between Morphogenesis And Cell Division During Formation Of The Ventral Furrow In Drosophila. *Cell*, 101, 523-531.
- Hamakawa, Y., Omori, N., Ouchida, M., Nagase, M., Sato, K., Nagano, I., Shoji, M., Fujita, T. & Abe, K. 2004. Severity Dependent Up-Regulations Of Lox-1 And Mcp-1 In Early Sclerotic Changes Of Common Carotid Arteries In Spontaneously Hypertensive Rats. *Neurological Research*, 26, 767-773.
- Hansson, G. K. 2005. Mechanisms Of Disease - Inflammation, Atherosclerosis, And Coronary Artery Disease. *New England Journal Of Medicine*, 352, 1685-1695.
- Hayashida, K., Kume, N., Minami, M., Inui-Hayashida, A., Mukai, E., Toyohara, M. & Kita, T. 2004. Peroxisome Proliferator-Activated Receptor Alpha Ligands Activate Transcription Of Lectin-Like Oxidized Low Density Lipoprotein Receptor-1 Gene Through Gc Box Motif. *Biochemical And Biophysical Research Communications*, 323, 1116-1123.
- Hegedus, Z., Czibula, A. & Kiss-Toth, E. 2006. Tribbles: Novel Regulators Of Cell Function; Evolutionary Aspects. *Cellular And Molecular Life Sciences*, 63, 1632-1641.
- Hegedus, Z., Czibula, A. & Kiss-Toth, E. 2007. Tribbles: A Family Of Kinase-Like Proteins With Potent Signalling Regulatory Function. *Cellular Signalling*, 19, 238-250.

- Heinig, M., Petretto, E., Wallace, C., Bottolo, L., Rotival, M., Lu, H., Li, Y. Y., Sarwar, R., Langley, S. R., Bauerfeind, A., Hummel, O., Lee, Y. A., Paskas, S., Rintisch, C., Saar, K., Cooper, J., Buchan, R., Gray, E. E., Cyster, J. G., Erdmann, J., Hengstenberg, C., Maouche, S., Ouwehand, W. H., Rice, C. M., Samani, N. J., Schunkert, H., Goodall, A. H., Schulz, H., Roider, H. G., Vingron, M., Blankenberg, S., Munzel, T., Zeller, T., Szymczak, S., Ziegler, A., Tiret, L., Smyth, D. J., Pravenec, M., Aitman, T. J., Cambien, F., Clayton, D., Todd, J. A., Hubner, N., Cook, S. A. & Cardiogenics, C. 2010. A Trans-Acting Locus Regulates An Anti-Viral Expression Network And Type 1 Diabetes Risk. *Nature*, 467, 460-464.
- Hodis, H. N., Mack, W. J., Azen, S. P., Alaupovic, P., Pogoda, J. M., Labree, L., Hemphill, L. C., Krams, D. M. & Blankenhorn, D. H. 1994. Triglyceride-Rich And Cholesterol-Rich Lipoproteins Have A Differential Effect On Mild/Moderate And Severe Lesion Progression As Assessed By Quantitative Coronary Angiography In A Controlled Trial Of Lovastatin. *Circulation*, 90, 42-49.
- Hoeffel, G., Wang, Y. L., Greter, M., See, P., Teo, P., Malleret, B., Leboeuf, M., Low, D., Oller, G., Almeida, F., Choy, S. H. Y., Grisotto, M., Renia, L., Conway, S. J., Stanley, E. R., Chan, J. K. Y., Ng, L. G., Samokhvalov, I. M., Merad, M. & Ginhoux, F. 2012. Adult Langerhans Cells Derive Predominantly From Embryonic Fetal Liver Monocytes With A Minor Contribution Of Yolk Sac-Derived Macrophages. *Journal Of Experimental Medicine*, 209, 1167-1181.
- Holvoet, P., Perez, G., Zhao, Z., Brouwers, E., Bernar, H. & Collen, D. 1995. Malondialdehyde-Modified Low-Density Lipoproteins In Patients With Atherosclerotic Disease. *Journal Of Clinical Investigation*, 95, 2611-2619.
- Horton, J. D., Goldstein, J. L. & Brown, M. S. 2002. Srebps: Activators Of The Complete Program Of Cholesterol And Fatty Acid Synthesis In The Liver. *Journal Of Clinical Investigation*, 109, 1125-1131.
- Horton, J. D., Shah, N. A., Warrington, J. A., Anderson, N. N., Park, S. W., Brown, M. S. & Goldstein, J. L. 2003. Combined Analysis Of Oligonucleotide Microarray Data From Transgenic And Knockout Mice Identifies Direct Srebp Target Genes. *Proceedings Of The National Academy Of Sciences Of The United States Of America*, 100, 12027-12032.
- Hotamisligil, G. S., Arner, P., Caro, J. F., Atkinson, R. L. & Spiegelman, B. M. 1995. Increased Adipose-Tissue Expression Of Tumor-Necrosis-Factor-Alpha In Human Obesity And Insulin-Resistance. *Journal Of Clinical Investigation*, 95, 2409-2415.
- Hotamisligil, G. S., Shargill, N. S. & Spiegelman, B. M. 1993. Adipose Expression Of Tumor-Necrosis-Factor-Alpha - Direct Role In Obesity-Linked Insulin Resistance. *Science*, 259, 87-91.
- Huang, W., Metlakunta, A., Dedousis, N., Zhang, P., Sipula, I., Dube, J. J., Scott, D. K. & O'doherty, R. M. 2010. Depletion Of Liver Kupffer Cells Prevents The Development Of Diet-Induced Hepatic Steatosis And Insulin Resistance. *Diabetes*, 59, 347-357.
- Hulthe, J. & Fagerberg, B. 2002. Circulating Oxidized Ldl Is Associated With Subclinical Atherosclerosis Development And Inflammatory Cytokines (Air Study). *Arteriosclerosis Thrombosis And Vascular Biology*, 22, 1162-1167.
- Im, S. S. & Osborne, T. F. 2011. Liver X Receptors In Atherosclerosis And Inflammation. *Circulation Research*, 108, 996-1001.
- Ishibashi, S., Brown, M. S., Goldstein, J. L., Gerard, R. D., Hammer, R. E. & Herz, J. 1993. Hypercholesterolemia In Low-Density-Lipoprotein Receptor Knockout Mice And Its Reversal By Adenovirus-Mediated Gene Delivery. *Journal Of Clinical Investigation*, 92, 883-893.
- Ishii, I., Oka, M., Katto, N., Shirai, K., Saito, Y. & Hirose, S. 1992. Beta-Vldl-Induced Cholesterol Ester Deposition In Macrophages May Be Regulated By Neutral Cholesterol Esterase Activity. *Arterioscler Thromb*, 12, 1139-45.

- Ishizuka, Y., Nakayama, K., Ogawa, A., Makishima, S., Boonvisut, S., Hirao, A., Iwasaki, Y., Yada, T., Yanagisawa, Y., Miyashita, H., Takahashi, M., Iwamoto, S. & Jichi Med Univ Promotion Team, L. 2014. Trib1 Downregulates Hepatic Lipogenesis And Glycogenesis Via Multiple Molecular Interactions. *Journal Of Molecular Endocrinology*, 52, 145-158.
- Italiani, P. & Boraschi, D. 2014. From Monocytes To M1/M2 Macrophages: Phenotypical Vs. Functional Differentiation. *Frontiers In Immunology*, 5.
- Iynedjian, P. B. 2005. Lack Of Evidence For A Role Of Trb3/Nipk As An Inhibitor Of Pkb-Mediated Insulin Signalling In Primary Hepatocytes. *Biochemical Journal*, 386, 113-118.
- Jaeschke, H. & Ramachandran, A. 2011. Reactive Oxygen Species In The Normal And Acutely Injured Liver. *Journal Of Hepatology*, 55, 227-228.
- Jawien, J., Nastalek, P. & Korbut, R. 2004. Mouse Models Of Experimental Atherosclerosis. *Journal Of Physiology And Pharmacology*, 55, 503-517.
- Ji, Y., Jian, B., Wang, N., Sun, Y., Moya, M., Phillips, M. C., Rothblat, G. H., Swaney, J. B. & Tall, A. R. 1997. Scavenger Receptor Bi Promotes High Density Lipoprotein-Mediated Cellular Cholesterol Efflux. *Journal Of Biological Chemistry*, 272, 20982-20985.
- Jin, G., Yamazaki, Y., Takuwa, M., Takahara, T., Kaneko, K., Kuwata, T., Miyata, S. & Nakamura, T. 2007. Trib1 And Evl1 Cooperate With Hoxa And Meis1 In Myeloid Leukemogenesis. *Blood*, 109, 3998-4005.
- Jin, J. L., Iakova, P., Breaux, M., Sullivan, E., Jawanmardi, N., Chen, D. H., Jiang, Y. J., Medrano, E. M. & Timchenko, N. A. 2013. Increased Expression Of Enzymes Of Triglyceride Synthesis Is Essential For The Development Of Hepatic Steatosis. *Cell Reports*, 3, 831-843.
- Johnson, J. L., George, S. J., Newby, A. C. & Jackson, C. L. 2005. Divergent Effects Of Matrix Metalloproteinase-3, Metalloproteinase-7, Metalloproteinase-9, And Metalloproteinase-12 On Atherosclerotic Plaque Stability In Mouse Brachiocephalic Arteries. *Proceedings Of The National Academy Of Sciences Of The United States Of America*, 102, 15575-15580.
- Johnson, J. L. & Newby, A. C. 2009. Macrophage Heterogeneity In Atherosclerotic Plaques. *Current Opinion In Lipidology*, 20, 370-378.
- Johnson, J. L., Sala-Newby, G. B., Ismail, Y., Aguilera, C. N. M. & Newby, A. C. 2008. Low Tissue Inhibitor Of Metalloproteinases 3 And High Matrix Metalloproteinase 14 Levels Defines A Subpopulation Of Highly Invasive Foam-Cell Macrophages. *Arteriosclerosis Thrombosis And Vascular Biology*, 28, 1647-1653.
- Johnson, J. L., Sala-Newby, G. B., Ismail, Y., Aguilera, C. N. M. & Newby, A. C. 2008. Low Tissue Inhibitor Of Metalloproteinases 3 And High Matrix Metalloproteinase 14 Levels Defines A Subpopulation Of Highly Invasive Foam-Cell Macrophages. *Arteriosclerosis Thrombosis And Vascular Biology*, 28, 1647-1653.
- Johnston, J., Basatvat, S., Ilyas, Z., Francis, S. & Kiss-Toth, E. 2015. Tribbles In Inflammation. *Biochemical Society Transactions*, 43, 1069-1074.
- Joseph, S. B., Castrillo, A., Laffitte, B. A., Mangelsdorf, D. J. & Tontonoz, P. 2003. Reciprocal Regulation Of Inflammation And Lipid Metabolism By Liver X Receptors. *Nature Medicine*, 9, 213-219.
- Kaaman, M., Sparks, L. M., Van Harmelen, V., Smith, S. R., Sjolín, E., Dahlman, I. & Arner, P. 2007. Strong Association Between Mitochondrial Dna Copy Number And Lipogenesis In Human White Adipose Tissue. *Diabetologia*, 50, 2526-2533.
- Kadl, A., Meher, A. K., Sharma, P. R., Lee, M. Y., Doran, A. C., Johnstone, S. R., Elliott, M. R., Gruber, F., Han, J., Chen, W., Kensler, T., Ravichandran, K. S., Isakson, B. E., Wamhoff, B. R. & Leitinger, N. 2010. Identification Of A Novel Macrophage Phenotype That Develops In Response To Atherogenic Phospholipids Via Nrf2.

- Circulation Research*, 107, 737-U155.
- Karakucuk, I., Dilly, S. A. & Maxwell, J. D. 1989. Portal Tract Macrophages Are Increased In Alcoholic Liver-Disease. *Histopathology*, 14, 245-253.
- Kassim, S. H., Li, H., Vandenberghe, L. H., Hinderer, C., Bell, P., Marchadier, D., Wilson, A., Cromley, D., Redon, V., Yu, H., Wilson, J. M. & Rader, D. J. 2010. Gene Therapy In A Humanized Mouse Model Of Familial Hypercholesterolemia Leads To Marked Regression Of Atherosclerosis. *Plos One*, 5.
- Kataoka, H., Kume, N., Miyamoto, S., Minami, M., Moriwaki, H., Murase, T., Sawamura, T., Masaki, T., Hashimoto, N. & Kita, T. 1999. Expression Of Lectinlike Oxidized Low-Density Lipoprotein Receptor-1 In Human Atherosclerotic Lesions. *Circulation*, 99, 3110-3117.
- Kathiresan, S., Melander, O., Guiducci, C., Surti, A., Burtt, N. P., Rieder, M. J., Cooper, G. M., Roos, C., Voight, B. F., Havulinna, A. S., Wahlstrand, B., Hedner, T., Corella, D., Tai, E. S., Ordovas, J. M., Berglund, G., Vartiainen, E., Jousilahti, P., Hedblad, B., Taskinen, M.-R., Newton-Cheh, C., Salomaa, V., Peltonen, L., Groop, L., Altshuler, D. M. & Orho-Melander, M. 2008. Six New Loci Associated With Blood Low-Density Lipoprotein Cholesterol, High-Density Lipoprotein Cholesterol Or Triglycerides In Humans. *Nature Genetics*, 40, 189-197.
- Keeshan, K., Bailis, W., Dedhia, P. H., Vega, M. E., Shestova, O., Xu, L., Toscano, K., Uljon, S. N., Blacklow, S. C. & Pear, W. S. 2010. Transformation By Tribbles Homolog 2 (Trib2) Requires Both The Trib2 Kinase Domain And Cop1 Binding. *Blood*, 116, 4948-4957.
- Keeshan, K., He, Y., Wouters, B. J., Shestova, O., Xu, L., Sai, H., Rodriguez, C. G., Maillard, I., Tobias, J. W., Valk, P., Carroll, M., Aster, J. C., Delwel, R. & Pear, W. S. 2006. Tribbles Homolog 2 Inactivates C/Ebp Alpha And Causes Acute Myelogenous Leukemia. *Cancer Cell*, 10, 401-411.
- Kiss-Toth, E., Bagstaff, S. M., Sung, H. Y., Jozsa, V., Dempsey, C., Caunt, J. C., Oxley, K. M., Wyllie, D. H., Polgar, T., Harte, M., O'Neill, L. A. J., Qwarnstrom, E. E. & Dower, S. K. 2004. Human Tribbles, A Protein Family Controlling Mitogen-Activated Protein Kinase Cascades. *Journal Of Biological Chemistry*, 279, 42703-42708.
- Klein, I., Cornejo, J. C., Polakos, N. K., John, B., Wuensch, S. A., Topham, D. J., Pierce, R. H. & Crispe, I. N. 2007. Kupffer Cell Heterogeneity: Functional Properties Of Bone Marrow-Derived And Sessile Hepatic Macrophages. *Blood*, 110, 4077-4085.
- Klingenspor, M., Xu, P., Cohen, R. D., Welch, C. & Reue, K. 1999. Altered Gene Expression Pattern In The Fatty Liver Dystrophy Mouse Reveals Impaired Insulin-Mediated Cytoskeleton Dynamics. *Journal Of Biological Chemistry*, 274, 23078-23084.
- Kolios, G., Valatas, V. & Kouroumalis, E. 2006. Role Of Kupffer Cells In The Pathogenesis Of Liver Disease. *World Journal Of Gastroenterology*, 12, 7413-7420.
- Koo, S. H., Satoh, H., Herzig, S., Lee, C. H., Hedrick, S., Kulkarni, R., Evans, R. M., Olefsky, J. & Montminy, M. 2004. Pgc-1 Promotes Insulin Resistance In Liver Through Ppar-Alpha-Dependent Induction Of Trb-3. *Nature Medicine*, 10, 530-534.
- Kraja, A. T., Vaidya, D., Pankow, J. S., Goodarzi, M. O., Assimes, T. L., Kullo, I. J., Sovio, U., Mathias, R. A., Sun, Y. V., Franceschini, N., Absher, D., Li, G., Zhang, Q., Feitosa, M. F., Glazer, N. L., Haritunians, T., Hartikainen, A.-L., Knowles, J. W., North, K. E., Iribarren, C., Kral, B., Yanek, L., O'Reilly, P. F., McCarthy, M. I., Jaquish, C., Couper, D. J., Chakravarti, A., Psaty, B. M., Becker, L. C., Province, M. A., Boerwinkle, E., Quertermous, T., Palotie, L., Jarvelin, M.-R., Becker, D. M., Kardia, S. L. R., Rotter, J. I., Chen, Y.-D. I. & Borecki, I. B. 2011. A Bivariate Genome-Wide Approach To Metabolic Syndrome Stampede Consortium. *Diabetes*,

60, 1329-1339.

- Kuhlencordt, P. J., Chen, J. Q., Han, F., Astern, J. & Huang, P. L. 2001. Genetic Deficiency Of Inducible Nitric Oxide Synthase Reduces Atherosclerosis And Lowers Plasma Lipid Peroxides In Apolipoprotein E-Knockout Mice. *Circulation*, 103, 3099-3104.
- Kumar, V., Abbas, A., Aster, J. C. & Robbins, S. L. 2013. *Robbins Basic Pathology*, Philadelphia, Pa, Elsevier/Saunders.
- Kzhyshkowska, J., Neyen, C. & Gordon, S. 2012. Role Of Macrophage Scavenger Receptors In Atherosclerosis. *Immunobiology*, 217, 492-502.
- Lambert, G., Charlton, F., Rye, K.-A. & Piper, D. E. 2009. Molecular Basis Of Pcsk9 Function. *Atherosclerosis*, 203, 1-7.
- Lambert, G., Sjouke, B., Choque, B., Kastelein, J. J. P. & Hovingh, G. K. 2012. The Pcsk9 Decade. *Journal Of Lipid Research*, 53, 2515-2524.
- Lee, C. H. & Evans, R. M. 2002. Peroxisome Proliferator-Activated Receptor-Gamma In Macrophage Lipid Homeostasis. *Trends Endocrinol Metab*, 13, 331-5.
- Lee, H., Shi, W. B., Tontonoz, P., Wang, S., Subbanagounder, G., Hedrick, C. C., Hama, S., Borromeo, C., Evans, R. M., Berliner, J. A. & Nagy, L. 2000. Role For Peroxisome Proliferator-Activated Receptor Alpha In Oxidized Phospholipid-Induced Synthesis Of Monocyte Chemotactic Protein-1 And Interleukin-8 By Endothelial Cells. *Circulation Research*, 87, 516-521.
- Lee, S., Huen, S., Nishio, H., Nishio, S., Lee, H. K., Choi, B.-S., Ruhrberg, C. & Cantley, L. G. 2011. Distinct Macrophage Phenotypes Contribute To Kidney Injury And Repair. *Journal Of The American Society Of Nephrology*, 22, 317-326.
- Li, A. C., Binder, C. J., Gutierrez, A., Brown, K. K., Plotkin, C. R., Pattison, J. W., Valledor, A. F., Davis, R. A., Willson, T. M., Witztum, J. L., Palinski, W. & Glass, C. K. 2004. Differential Inhibition Of Macrophage Foam-Cell Formation And Atherosclerosis In Mice By Ppar Alpha, Beta/Delta, And Beta. *Journal Of Clinical Investigation*, 114, 1564-1576.
- Li, A. C., Brown, K. K., Silvestre, M. J., Willson, T. M., Palinski, W. & Glass, C. K. 2000. Peroxisome Proliferator-Activate Inhibit Development Of Atherosclerosis In Ldl Receptor-Deficient Mice. *Journal Of Clinical Investigation*, 106, 523-531.
- Li, D. Y., Chen, H. J. & Mehta, J. L. 2001. Statins Inhibit Oxidized-Ldl-Mediated Lox-1 Expression, Uptake Of Oxidized-Ldl And Reduction In Pkb Phosphorylation. *Cardiovascular Research*, 52, 130-135.
- Li, D. Y., Liu, L., Chen, H. J., Sawamura, R. & Mehta, J. L. 2003. Lox-1 Mediates Oxidized Low-Density Lipoprotein-Induced Expression Of Matrix Metalloproteinases In Human Coronary Artery Endothelial Cells. *Circulation*, 107, 612-617.
- Li, H., Xu, H. & Sun, B. 2012. Lipopolysaccharide Regulates Mmp-9 Expression Through Tlr4/Nf-Kappa B Signaling In Human Arterial Smooth Muscle Cells. *Molecular Medicine Reports*, 6, 774-778.
- Li, L., Sawamura, T. & Renier, G. 2004. Glucose Enhances Human Macrophage Lox-1 Expression Role For Lox-1 In Glucose-Induced Macrophage Foam Cell Formation. *Circulation Research*, 94, 892-901.
- Li, P. P., Lu, M., Nguyen, M. T. A., Bae, E. J., Chapman, J., Feng, D. R., Hawkins, M., Pessin, J. E., Sears, D. D., Nguyen, A. K., Amidi, A., Watkins, S. M., Nguyen, U. & Olefsky, J. M. 2010. Functional Heterogeneity Of Cd11c-Positive Adipose Tissue Macrophages In Diet-Induced Obese Mice. *Journal Of Biological Chemistry*, 285, 15333-15345.
- Li, Z. P., Lin, H. Z., Yang, S. Q. & Diehl, A. M. 2002. Murine Leptin Deficiency Alters Kupffer Cell Production Of Cytokines That Regulate The Innate Immune System. *Gastroenterology*, 123, 1304-1310.
- Libby, P. 2005. The Forgotten Majority - Unfinished Business In Cardiovascular Risk Reduction. *Journal Of The American College Of Cardiology*, 46, 1225-1228.

- Libby, P. 2012. Inflammation In Atherosclerosis. *Arteriosclerosis Thrombosis And Vascular Biology*, 32, 2045-2051.
- Libby, P., Ridker, P. M. & Hansson, G. K. 2011. Progress And Challenges In Translating The Biology Of Atherosclerosis. *Nature*, 473, 317-325.
- Libby, P., Ridker, P. M. & Hansson, G. K. 2011. Progress And Challenges In Translating The Biology Of Atherosclerosis. *Nature*, 473, 317-325.
- Linton, M. F., Atkinson, J. B. & Fazio, S. 1995. Prevention Of Atherosclerosis In Apolipoprotein E-Deficient Mice By Bone-Marrow Transplantation. *Science*, 267, 1034-1037.
- Liu, Y.-H., Tan, K. A. L., Morrison, I. W., Lamb, J. R. & Argyle, D. J. 2013. Macrophage Migration Is Controlled By Tribbles 1 Through The Interaction Between C/Ebp Beta And Tnf-Alpha. *Veterinary Immunology And Immunopathology*, 155, 67-75.
- Lopez, D. & Mclean, M. P. 1999. Sterol Regulatory Element-Binding Protein-1a Binds To Cis Elements In The Promoter Of The Rat High Density Lipoprotein Receptor Sr-Bi Gene. *Endocrinology*, 140, 5669-5681.
- Lumeng, C. N., Bodzin, J. L. & Saltiel, A. R. 2007. Obesity Induces A Phenotypic Switch In Adipose Tissue Macrophage Polarization. *Journal Of Clinical Investigation*, 117, 175-184.
- Lumeng, C. N. & Saltiel, A. R. 2011. Inflammatory Links Between Obesity And Metabolic Disease. *Journal Of Clinical Investigation*, 121, 2111-2117.
- Lutgens, E., Faber, B., Schapira, K., Evelo, C. T. A., Van Haaften, R., Heeneman, S., Cleutjens, K., Bijmens, A. P., Beckers, L., Porter, J. G., Mackay, C. R., Rennert, P., Bailly, V., Jarpe, M., Dolinski, B., Koteliensky, V., De Fougerolles, T. & Daemen, J. A. P. 2005. Gene Profiling In Atherosclerosis Reveals A Key Role For Small Inducible Cytokines - Validation Using A Novel Monocyte Chemoattractant Protein Monoclonal Antibody. *Circulation*, 111, 3443-3452.
- Luttun, A., Lutgens, E., Manderveld, A., Maris, K., Collen, D., Carmeliet, P. & Moons, L. 2004. Loss Of Matrix Metalloproteinase-9 Or Matrix Metalloproteinase-12 Protects Apolipoprotein E-Deficient Mice Against Atherosclerotic Media Destruction But Differentially Affects Plaque Growth. *Circulation*, 109, 1408-1414.
- Malerod, L., Juvet, L. K., Hanssen-Bauer, A., Eskild, W. & Berg, T. 2002. Oxysterol-Activated Lxr Alpha/Rxr Induces Hsr-Bi-Promoter Activity In Hepatoma Cells And Preadipocytes. *Biochemical And Biophysical Research Communications*, 299, 916-923.
- Manning, B. D. & Cantley, L. C. 2007. Akt/Pkb Signaling: Navigating Downstream. *Cell*, 129, 1261-1274.
- Manzi, S., Meilahn, E. N., Rairie, J. E., Conte, C. G., Medsger, T. A., Jansenmcwilliams, L., Dagostino, R. B. & Kuller, L. H. 1997. Age-Specific Incidence Rates Of Myocardial Infarction And Angina In Women With Systemic Lupus Erythematosus: Comparison With The Framingham Study. *American Journal Of Epidemiology*, 145, 408-415.
- Marathe, C., Bradley, M. N., Hong, C., Lopez, F., De Galarreta, C. M. R., Tontonoz, P. & Castrillo, A. 2006. The Arginase Ii Gene Is An Anti-Inflammatory Target Of Liver X Receptor In Macrophages. *Journal Of Biological Chemistry*, 281, 32197-32206.
- Martinez, F. O. & Gordon, S. 2014. The M1 And M2 Paradigm Of Macrophage Activation: Time For Reassessment. *F1000prime Reports*, 6, 13-13.
- Mata, J., Curado, S., Ephrussi, A. & Rorth, P. 2000. Tribbles Coordinates Mitosis And Morphogenesis In Drosophila By Regulating String/Cdc25 Proteolysis. *Cell*, 101, 511-522.
- Matlung, H. L., Neele, A. E., Groen, H. C., Van Gaalen, K., Tuna, B. G., Van Weert, A., De Vos, J., Wentzel, J. J., Hoogenboezem, M., Van Buul, J. D., Vanbavel, E. & Bakker, E. 2012. Transglutaminase Activity Regulates Atherosclerotic Plaque Composition

- At Locations Exposed To Oscillatory Shear Stress. *Atherosclerosis*, 224, 355-362.
- Matsusue, K., Gavrilova, O., Lambert, G., Brewer, H. B., Ward, J. M., Inoue, Y., Leroith, D. & Gonzalez, F. J. 2004. Hepatic Ccaat/Enhancer Binding Protein Alpha Mediates Induction Of Lipogenesis And Regulation Of Glucose Homeostasis In Leptin-Deficient Mice. *Molecular Endocrinology*, 18, 2751-2764.
- Maxwell, K. N. & Breslow, J. L. 2004. Adenoviral-Mediated Expression Of Pcsk9 In Mice Results In A Low-Density Lipoprotein Receptor Knockout Phenotype. *Proceedings Of The National Academy Of Sciences Of The United States Of America*, 101, 7100-7105.
- McInnes, I. B., Leung, B. P., Sturrock, R. D., Field, M. & Liew, F. Y. 1997. Interleukin-15 Mediates T Cell-Dependent Regulation Of Tumor Necrosis Factor-Alpha Production In Rheumatoid Arthritis. *Nature Medicine*, 3, 189-195.
- McLaren, J. E., Michael, D. R., Ashlin, T. G. & Ramji, D. P. 2011. Cytokines, Macrophage Lipid Metabolism And Foam Cells: Implications For Cardiovascular Disease Therapy. *Progress In Lipid Research*, 50, 331-347.
- Mcnelis, J. C. & Olefsky, J. M. 2014. Macrophages, Immunity, And Metabolic Disease. *Immunity*, 41, 36-48.
- Medzhitov, R. 2008. Origin And Physiological Roles Of Inflammation. *Nature*, 454, 428-435.
- Mehta, J. L., Chen, J., Yu, F. & Li, D. Y. 2004. Aspirin Inhibits Ox-Ldl-Mediated Lox-1 Expression And Metalloproteinase-1 In Human Coronary Endothelial Cells. *Cardiovascular Research*, 64, 243-249.
- Mehta, J. L., Chen, J. W., Hermonat, P. L., Romeo, F. & Novelli, G. 2006. Lectin-Like, Oxidized Low-Density Lipoprotein Receptor-1 (Lox-1): A Critical Player In The Development Of Atherosclerosis And Related Disorders. *Cardiovascular Research*, 69, 36-45.
- Mehta, J. L., Hu, B., Chen, J. W. & Li, D. Y. 2003. Pioglitazone Inhibits Lox-1 Expression In Human Coronary Artery Endothelial Cells By Reducing Intracellular Superoxide Radical Generation. *Arteriosclerosis Thrombosis And Vascular Biology*, 23, 2203-2208.
- Mehta, J. L., Sanada, N., Hu, C. P., Chen, J. W., Dandapat, A., Sugawara, F., Satoh, H., Inoue, K., Kawase, Y., Jishage, K., Suzuki, H., Takeya, M., Schnackenberg, L., Beger, R., Hermonat, P. L., Thomas, M. & Sawamura, T. 2007. Deletion Of Lox-1 Reduces Atherogenesis In Ldlr Knockout Mice Fed High Cholesterol Diet. *Circulation Research*, 100, 1634-1642.
- Molica, F., Morel, S., Kwak, B. R., Rohner-Jeanrenaud, F. & Steffens, S. 2015. Adipokines At The Crossroad Between Obesity And Cardiovascular Disease. *Thrombosis And Haemostasis*, 113, 553-566.
- Moore, K. J. & Freeman, M. W. 2006. Scavenger Receptors In Atherosclerosis: Beyond Lipid Uptake. *Arteriosclerosis Thrombosis And Vascular Biology*, 26, 1702-1711.
- Moore, K. J., Sheedy, F. J. & Fisher, E. A. 2013. Macrophages In Atherosclerosis: A Dynamic Balance. *Nature Reviews Immunology*, 13, 709-721.
- Nagiec, M. M., Skepner, A. P., Negri, J., Eichhorn, M., Kuperwasser, N., Comer, E., Muncipinto, G., Subramanian, A., Clish, C., Musunuru, K., Duvall, J. R., Foley, M., Perez, J. R. & Palmer, M. A. J. 2015. Modulators Of Hepatic Lipoprotein Metabolism Identified In A Search For Small-Molecule Inducers Of Tribbles Pseudokinase 1 Expression. *Plos One*, 10.
- Naiki, T., Saijou, E., Miyaoka, Y., Sekine, K. & Miyajima, A. 2007. Trb2, A Mouse Tribbles Ortholog, Suppresses Adipocyte Differentiation By Inhibiting Akt And C/Ebp Beta. *Journal Of Biological Chemistry*, 282, 24075-24082.
- Nakamura, T. 2005. Retroviral Insertional Mutagenesis Identifies Oncogene Cooperation. *Cancer Science*, 96, 7-12.

- Nakashima, Y., Plump, A. S., Raines, E. W., Breslow, J. L. & Ross, R. 1994. Apoe-Deficient Mice Develop Lesions Of All Phases Of Atherosclerosis Throughout The Arterial Tree. *Arteriosclerosis And Thrombosis*, 14, 133-140.
- Nerlov, C. 2008. C/Ebbs: Recipients Of Extracellular Signals Through Proteome Modulation. *Current Opinion In Cell Biology*, 20, 180-185.
- Newby, A. C. 2005. Dual Role Of Matrix Metalloproteinases (Matrixins) In Intimal Thickening And Atherosclerotic Plaque Rupture. *Physiological Reviews*, 85, 1-31.
- Nice 2016. Cardiovascular Disease: Risk Assessment And Reduction Including Lipid Modification. London: Nice.
- Niemeier, A., Kovacs, W. J., Strobl, W. & Stangl, H. 2009. Atherogenic Diet Leads To Posttranslational Down-Regulation Of Murine Hepatocyte Sr-Bi Expression. *Atherosclerosis*, 202, 169-175.
- Noto, D., Cefalu, A. B. & Averna, M. R. 2014. Beyond Statins: New Lipid Lowering Strategies To Reduce Cardiovascular Risk. *Current Atherosclerosis Reports*, 16.
- Odegaard, J. I., Ricardo-Gonzalez, R. R., Goforth, M. H., Morel, C. R., Subramanian, V., Mukundan, L., Eagle, A. R., Vats, D., Brombacher, F., Ferrante, A. W. & Chawla, A. 2007. Macrophage-Specific Ppar Gamma Controls Alternative Activation And Improves Insulin Resistance. *Nature*, 447, 1116-U12.
- Ohoka, N., Yoshii, S., Hattori, T., Onozaki, K. & Hayashi, H. 2005. Trb3, A Novel Er Stress-Inducible Gene, Is Induced Via Atf4-Chop Pathway And Is Involved In Cell Death. *Embo Journal*, 24, 1243-1255.
- Olefsky, J. M. & Glass, C. K. 2010. Macrophages, Inflammation, And Insulin Resistance. *Annual Review Of Physiology*, 72, 219-246.
- Ostertag, A., Jones, A., Rose, A. J., Liebert, M., Kleinsorg, S., Reimann, A., Vegiopoulos, A., Diaz, M. B., Strzoda, D., Yamamoto, M., Satoh, T., Akira, S. & Herzig, S. 2010. Control Of Adipose Tissue Inflammation Through Trb1. *Diabetes*, 59, 1991-2000.
- Otvos, J. D., Jeyarajah, E. J., Bennett, D. W. & Krauss, R. M. 1992. Development Of A Proton Nuclear-Magnetic-Resonance Spectroscopic Method For Determining Plasma-Lipoprotein Concentrations And Subspecies Distributions From A Single, Rapid Measurement. *Clinical Chemistry*, 38, 1632-1638.
- Paigen, B., Holmes, P. A., Mitchell, D. & Albee, D. 1987. Comparison Of Atherosclerotic Lesions And Hdl-Lipid Levels In Male, Female, And Testosterone-Treated Female Mice From Strains C57bl/6, Balb/C, And C3h. *Atherosclerosis*, 64, 215-221.
- Pepine, C. J. 1998. The Effects Of Angiotensin-Converting Enzyme Inhibition On Endothelial Dysfunction: Potential Role In Myocardial Ischemia. *American Journal Of Cardiology*, 82, 23s-27s.
- Perdiguero, E. G., Klapproth, K., Schulz, C., Busch, K., Azzoni, E., Crozet, L., Garner, H., Trouillet, C., De Bruijn, M. F., Geissmann, F. & Rodewald, H. R. 2015. Tissue-Resident Macrophages Originate From Yolk-Sac-Derived Erythro-Myeloid Progenitors. *Nature*, 518, 547-551.
- Phillips, N. R., Waters, D. & Havel, R. J. 1993. Plasma-Lipoproteins And Progression Of Coronary-Artery Disease Evaluated By Angiography And Clinical Events. *Circulation*, 88, 2762-2770.
- Piedrahita, J. A., Zhang, S. H., Hagaman, J. R., Oliver, P. M. & Maeda, N. 1992. Generation Of Mice Carrying A Mutant Apolipoprotein-E Gene Inactivated By Gene Targeting In Embryonic Stem-Cells. *Proceedings Of The National Academy Of Sciences Of The United States Of America*, 89, 4471-4475.
- Pistilli, E. E., Devaney, J. M., Gordish-Dressman, H., Bradbury, M. K., Seip, R. L., Thompson, P. D., Angelopoulos, T. J., Clarkson, P. M., Moyna, N. M., Pescatello, L. S., Visich, P. S., Zoeller, R. F., Gordon, P. M. & Hoffman, E. P. 2008. Interleukin-15 And Interleukin-15r Alpha Snps And Associations With Muscle, Bone, And Predictors Of The Metabolic Syndrome. *Cytokine*, 43, 45-53.

- Prieur, X., Mok, C. Y. L., Velagapudi, V. R., Nunez, V., Fuentes, L., Montaner, D., Ishikawa, K., Camacho, A., Barbarroja, N., O'rahilly, S., Sethi, J. K., Dopazo, J., Oresic, M., Ricote, M. & Vidal-Puig, A. 2011. Differential Lipid Partitioning Between Adipocytes And Tissue Macrophages Modulates Macrophage Lipotoxicity And M2/M1 Polarization In Obese Mice. *Diabetes*, 60, 797-809.
- Prudente, S., Hribal, M. L., Flex, E., Turchi, F., Morini, E., De Cosmo, S., Bacci, S., Tassi, V., Cardellini, M., Lauro, R., Sesti, G., Dallapiccola, B. & Trischitta, V. 2005. The Functional Q84r Polymorphism Of Mammalian Tribbles Homolog Trb3 Is Associated With Insulin Resistance And Related Cardiovascular Risk In Caucasians From Italy. *Diabetes*, 54, 2807-2811.
- Prudente, S., Sesti, G., Pandolfi, A., Andreozzi, F., Consoli, A. & Trischitta, V. 2012. The Mammalian Tribbles Homolog Trib3, Glucose Homeostasis, And Cardiovascular Diseases. *Endocrine Reviews*, 33, 526-546.
- Pruim, R. J., Welch, R. P., Sanna, S., Teslovich, T. M., Chines, P. S., Gliedt, T. P., Boehnke, M., Abecasis, G. R. & Willer, C. J. 2010. Locuszoom: Regional Visualization Of Genome-Wide Association Scan Results. *Bioinformatics*, 26, 2336-2337.
- Qi, L., Heredia, J. E., Altarejos, J. Y., Screaton, R., Goebel, N., Niessen, S., Macleod, I. X., Liew, C. W., Kulkarni, R. N., Bain, J., Newgard, C., Nelson, M., Evans, R. M., Yates, J. & Montminy, M. 2006. Trb3 Links The E3 Ubiquitin Ligase Cop1 To Lipid Metabolism. *Science*, 312, 1763-1766.
- Qiao, L. P., Maclean, P. S., You, H. N., Schaack, J. & Shao, J. H. 2006. Knocking Down Liver Ccaat/Enhancer-Binding Protein Alpha By Adenovirus-Transduced Silent Interfering Ribonucleic Acid Improves Hepatic Gluconeogenesis And Lipid Homeostasis In Db/Db Mice. *Endocrinology*, 147, 3060-3069.
- Qiao, L. P., Zou, C. H., Shao, P., Schaack, J., Johnson, P. F. & Shao, J. H. 2008. Transcriptional Regulation Of Fatty Acid Translocase/Cd36 Expression By Ccaat/Enhancer-Binding Protein Alpha. *Journal Of Biological Chemistry*, 283, 8788-8795.
- Raal, F., Scott, R., Somaratne, R., Bridges, I., Li, G., Wasserman, S. M. & Stein, E. A. 2012. Low-Density Lipoprotein Cholesterol-Lowering Effects Of Amg 145, A Monoclonal Antibody To Proprotein Convertase Subtilisin/Kexin Type 9 Serine Protease In Patients With Heterozygous Familial Hypercholesterolemia The Reduction Of Ldl-C With Pcsk9 Inhibition In Heterozygous Familial Hypercholesterolemia Disorder (Rutherford)
- Ridker, P. M., Rifai, N., Pfeffer, M., Sacks, F., Lepage, S., Braunwald, E. & Cholesterol Recurrent Events, C. 2000. Elevation Of Tumor Necrosis Factor-Alpha And Increased Risk Of Recurrent Coronary Events After Myocardial Infarction. *Circulation*, 101, 2149-2153.
- Ridker, P. M., Rifai, N., Stampfer, M. J. & Hennekens, C. H. 2000. Plasma Concentration Of Interleukin-6 And The Risk Of Future Myocardial Infarction Among Apparently Healthy Men. *Circulation*, 101, 1767-1772.
- Rigamonti, E., Chinetti-Gbaguidi, G. & Staels, B. 2008. Regulation Of Macrophage Functions By Ppar-Alpha, Ppar-Gamma, And Lxrs In Mice And Men. *Arteriosclerosis Thrombosis And Vascular Biology*, 28, 1050-1059.
- Robbe, P., Draijer, C., Borg, T. R., Luinge, M., Timens, W., Wouters, I. M., Melgert, B. N. & Hylkema, M. N. 2015. Distinct Macrophage Phenotypes In Allergic And Nonallergic Lung Inflammation. *American Journal Of Physiology-Lung Cellular And Molecular Physiology*, 308, L358-L367.
- Rock, K. L., Lai, J. J. & Kono, H. 2011. Innate And Adaptive Immune Responses To Cell Death. *Immunological Reviews*, 243, 191-205.
- Roethlisberger, B., Heizmann, M., Bargetzi, M. J. & Huber, A. R. 2007. Trib1 Overexpression In Acute Myeloid Leukemia. *Cancer Genetics And Cytogenetics*,

176, 58-60.

- Ross, R. 1999. Mechanisms Of Disease - Atherosclerosis - An Inflammatory Disease. *New England Journal Of Medicine*, 340, 115-126.
- Rotival, M., Zeller, T., Wild, P. S., Maouche, S., Szymczak, S., Schillert, A., Castagne, R., Deiseroth, A., Proust, C., Brocheton, J., Godefroy, T., Perret, C., Germain, M., Eleftheriadis, M., Sinning, C. R., Schnabel, R. B., Lubos, E., Lackner, K. J., Rossmann, H., Munzel, T., Rendon, A., Erdmann, J., Deloukas, P., Hengstenberg, C., Diemert, P., Montalescot, G., Ouwehand, W. H., Samani, N. J., Schunkert, H., Tregouet, D. A., Ziegler, A., Goodall, A. H., Cambien, F., Tiret, L., Blankenberg, S. & Cardiogenics, C. 2011. Integrating Genome-Wide Genetic Variations And Monocyte Expression Data Reveals Trans-Regulated Gene Modules In Humans. *Plos Genetics*, 7.
- Ruffell, D., Mourkioti, F., Gambardella, A., Kirstetter, P., Lopez, R. G., Rosenthal, N. & Nerlov, C. 2009. A Creb-C/Ebp Beta Cascade Induces M2 Macrophage-Specific Gene Expression And Promotes Muscle Injury Repair. *Proceedings Of The National Academy Of Sciences Of The United States Of America*, 106, 17475-17480.
- Sacks, F. M., Alaupovic, P., Moye, L. A., Cole, T. G., Sussex, B., Stampfer, M. J., Pfeffer, M. A. & Braunwald, E. 2000. Vldl, Apolipoproteins B, Ciii, And E, And Risk Of Recurrent Coronary Events In The Cholesterol And Recurrent Events (Care) Trial. *Circulation*, 102, 1886-1892.
- Sahebjam, S., Khokha, R. & Mort, J. S. 2007. Increased Collagen And Aggrecan Degradation With Age In The Joints Of Timp3(-/-) Mice. *Arthritis And Rheumatism*, 56, 905-909.
- Samarasekera, E. J., Neilson, J. M., Warren, R. B., Parnham, J. & Smith, C. H. 2013. Incidence Of Cardiovascular Disease In Individuals With Psoriasis: A Systematic Review And Meta-Analysis. *Journal Of Investigative Dermatology*, 133, 2340-2346.
- Sato, Y., Nishio, Y., Sekine, O., Kodama, K., Nagai, Y., Nakamura, T., Maegawa, H. & Kashiwagi, A. 2007. Increased Expression Of Ccaat/Enhancer Binding Protein-Beta And -Delta And Monocyte Chemoattractant Protein-1 Genes In Aortas From Hyperinsulinaemic Rats. *Diabetologia*, 50, 481-489.
- Satoh, T., Kidoya, H., Naito, H., Yamamoto, M., Takemura, N., Nakagawa, K., Yoshioka, Y., Morii, E., Takakura, N., Takeuchi, O. & Akira, S. 2013. Critical Role Of Trib1 In Differentiation Of Tissue-Resident M2-Like Macrophages. *Nature*, 495, 524-+.
- Schulz, C., Perdiguero, E. G., Chorro, L., Szabo-Rogers, H., Cagnard, N., Kierdorf, K., Prinz, M., Wu, B. S., Jacobsen, S. E. W., Pollard, J. W., Frampton, J., Liu, K. J. & Geissmann, F. 2012. A Lineage Of Myeloid Cells Independent Of Myb And Hematopoietic Stem Cells. *Science*, 336, 86-90.
- Schunkert, H., Konig, I. R., Kathiresan, S., Reilly, M. P., Assimes, T. L., Holm, H., Preuss, M., Stewart, A. F. R., Barbalic, M., Gieger, C., Absher, D., Aherrahrou, Z., Allayee, H., Altshuler, D., Anand, S. S., Andersen, K., Anderson, J. L., Ardissino, D., Ball, S. G., Balmforth, A. J., Barnes, T. A., Becker, D. M., Becker, L. C., Berger, K., Bis, J. C., Boekholdt, S. M., Boerwinkle, E., Braund, P. S., Brown, M. J., Burnett, M. S., Buysschaert, I., Carlquist, J. F., Chen, L., Cichon, S., Codd, V., Davies, R. W., Dedoussis, G., Dehghan, A., Demissie, S., Devaney, J. M., Diemert, P., Do, R., Doering, A., Eifert, S., El Mokhtari, N. E., Ellis, S. G., Elosua, R., Engert, J. C., Epstein, S. E., De Faire, U., Fischer, M., Folsom, A. R., Freyer, J., Gigante, B., Girelli, D., Gretarsdottir, S., Gudnason, V., Gulcher, J. R., Halperin, E., Hammond, N., Hazen, S. L., Hofman, A., Horne, B. D., Illig, T., Iribarren, C., Jones, G. T., Jukema, J. W., Kaiser, M. A., Kaplan, L. M., Kastelein, J. J. P., Khaw, K. T., Knowles, J. W., Kolovou, G., Kong, A., Laaksonen, R., Lambrechts, D., Leander, K., Lettre, G., Li, M. Y., Lieb, W., Loley, C., Lotery, A. J., Mannucci, P. M., Maouche, S., Martinelli, N., Mckeown, P. P., Meisinger, C., Meitinger, T.,

- Melander, O., Merlini, P. A., Mooser, V., Morgan, T., Muhleisen, T. W., Muhlestein, J. B., Munzel, T., Musunuru, K., Nahrstaedt, J., Nelson, C. P., Nothen, M. M., Olivieri, O., Et Al. 2011. Large-Scale Association Analysis Identifies 13 New Susceptibility Loci For Coronary Artery Disease. *Nature Genetics*, 43, 333-U153.
- Semenkovich, C. F. 2006. Insulin Resistance And Atherosclerosis. *Journal Of Clinical Investigation*, 116, 1813-1822.
- Shaw, P. X., Horkko, S., Chang, M. K., Curtiss, L. K., Palinski, W., Silverman, G. J. & Witztum, J. L. 2000. Natural Antibodies With The T15 Idiotype May Act In Atherosclerosis, Apoptotic Clearance, And Protective Immunity. *Journal Of Clinical Investigation*, 105, 1731-1740.
- Skurk, T., Alberti-Huber, C., Herder, C. & Hauner, H. 2007. Relationship Between Adipocyte Size And Adipokine Expression And Secretion. *Journal Of Clinical Endocrinology & Metabolism*, 92, 1023-1033.
- Smith, J. D., Trogan, E., Ginsberg, M., Grigaux, C., Tian, J. & Miyata, M. 1995. Decreased Atherosclerosis In Mice Deficient In Both Macrophage-Colony-Stimulating Factor (Op) And Apolipoprotein-E. *Proceedings Of The National Academy Of Sciences Of The United States Of America*, 92, 8264-8268.
- Stary, H. C., Chandler, A. B., Dinsmore, R. E., Fuster, V., Glagov, S., Insull, W., Rosenfeld, M. E., Schwartz, C. J., Wagner, W. D. & Wissler, R. W. 1995. A Definition Of Advanced Types Of Atherosclerotic Lesions And A Histological Classification Of Atherosclerosis - A Report From The Committee On Vascular-Lesions Of The Council On Arteriosclerosis, American-Heart-Association. *Circulation*, 92, 1355-1374.
- Steiner, T., Francescut, L., Byrne, S., Hughes, T., Jayanthi, A., Guschina, I., Harwood, J., Cianflone, K., Stover, C. & Francis, S. 2014. Protective Role For Properdin In Progression Of Experimental Murine Atherosclerosis. *Plos One*, 9.
- Stienstra, R., Saudale, F., Duval, C., Keshtkar, S., Groener, J. E. M., Van Rooijen, N., Staels, B., Kersten, S. & Muller, M. 2010. Kupffer Cells Promote Hepatic Steatosis Via Interleukin-1 Beta-Dependent Suppression Of Peroxisome Proliferator-Activated Receptor Alpha Activity. *Hepatology*, 51, 511-522.
- Stoger, J. L., Gijbels, M. J. J., Van Der Velden, S., Manca, M., Van Der Loos, C. M., Biessen, E. A. L., Daemen, M. J. A. P., Lutgens, E. & De Winther, M. P. J. 2012. Distribution Of Macrophage Polarization Markers In Human Atherosclerosis. *Atherosclerosis*, 225, 461-468.
- Storlazzi, C. T., Fioretos, T., Surace, C., Lonoce, A., Mastroilli, A., Strombeck, B., D'addabbo, P., Iacovelli, F., Minervini, C., Aventin, A., Dastugue, N., Fonatsch, C., Hagemeyer, A., Jotterand, M., Muhlematter, D., Lafage-Pochitaloff, M., Nguyen-Khac, F., Schoch, C., Slovak, M. L., Smith, A., Sole, F., Van Roy, N., Johansson, B. & Rocchi, M. 2006. Myc-Containing Double Minutes In Hematologic Malignancies: Evidence In Favor Of The Episome Model And Exclusion Of Myc As The Target Gene. *Human Molecular Genetics*, 15, 933-942.
- Su, G. L. 2002. Lipopolysaccharides In Liver Injury: Molecular Mechanisms Of Kupffer Cell Activation. *American Journal Of Physiology-Gastrointestinal And Liver Physiology*, 283, G256-G265.
- Sun, H., Ma, Y., Gao, M. & Liu, D. 2016. Il-15/Sil-15r Alpha Gene Transfer Induces Weight Loss And Improves Glucose Homeostasis In Obese Mice. *Gene Therapy*, 23, 349-356.
- Sung, H. Y., Francis, S. E., Arnold, N. D., Holland, K., Ernst, V., Angyal, A. & Kiss-Toth, E. 2012. Enhanced Macrophage Tribbles-1 Expression In Murine Experimental Atherosclerosis *Biology*, 43-57.
- Sung, H. Y., Francis, S. E., Crossman, D. C. & Kiss-Toth, E. 2006. Regulation Of

- Expression And Signalling Modulator Function Of Mammalian Tribbles Is Cell-Type Specific. *Immunology Letters*, 104, 171-177.
- Sung, H. Y., Guan, H., Czibula, A., King, A. R., Eder, K., Heath, E., Suvarna, S. K., Dower, S. K., Wilson, A. G., Francis, S. E., Crossman, D. C. & Kiss-Toth, E. 2007. Human Tribbles-1 Controls Proliferation And Chemotaxis Of Smooth Muscle Cells Via Mapk Signaling Pathways. *Journal Of Biological Chemistry*, 282, 18379-18387.
- Takahashi, Y., Ohoka, N., Hayashi, H. & Sato, R. 2008. Trb3 Suppresses Adipocyte Differentiation By Negatively Regulating Ppar Gamma Transcriptional Activity. *Journal Of Lipid Research*, 49, 880-892.
- Tangirala, R. K., Bischoff, E. D., Joseph, S. B., Wagner, B. L., Walczak, R., Laffitte, B. A., Daige, C. L., Thomas, D., Heyman, R. A., Mangelsdorf, D. J., Wang, X. P., Lusis, A. J., Tontonoz, P. & Schulman, I. G. 2002. Identification Of Macrophage Liver X Receptors As Inhibitors Of Atherosclerosis. *Proceedings Of The National Academy Of Sciences Of The United States Of America*, 99, 11896-11901.
- Tangirala, R. K., Pratico, D., Fitzgerald, G. A., Chun, S., Tsukamoto, K., Maugeais, C., Usher, D. C., Pure, E. & Rader, D. J. 2001. Reduction Of Isoprostanes And Regression Of Advanced Atherosclerosis By Apolipoprotein E. *Journal Of Biological Chemistry*, 276, 261-266.
- Tedgui, A. & Mallat, Z. 2006. Cytokines In Atherosclerosis: Pathogenic And Regulatory Pathways. *Physiological Reviews*, 86, 515-581.
- Terpstra, V., Van Amersfoort, E. S., Van Velzen, A. G., Kuiper, J. & Van Berkel, T. J. C. 2000. Hepatic And Extrahepatic Scavenger Receptors - Function In Relation To Disease. *Arteriosclerosis Thrombosis And Vascular Biology*, 20, 1860-1872.
- Teslovich, T. M., Musunuru, K., Smith, A. V., Edmondson, A. C., Stylianou, I. M., Koseki, M., Pirruccello, J. P., Ripatti, S., Chasman, D. I., Willer, C. J., Johansen, C. T., Fouchier, S. W., Isaacs, A., Peloso, G. M., Barbalic, M., Ricketts, S. L., Bis, J. C., Aulchenko, Y. S., Thorleifsson, G., Feitosa, M. F., Chambers, J., Orho-Melander, M., Melander, O., Johnson, T., Li, X., Guo, X., Li, M., Cho, Y. S., Go, M. J., Kim, Y. J., Lee, J.-Y., Park, T., Kim, K., Sim, X., Ong, R. T.-H., Croteau-Chonka, D. C., Lange, L. A., Smith, J. D., Song, K., Zhao, J. H., Yuan, X., Luan, J. A., Lamina, C., Ziegler, A., Zhang, W., Zee, R. Y. L., Wright, A. F., Wittteman, J. C. M., Wilson, J. F., Willemsen, G., Wichmann, H. E., Whitfield, J. B., Waterworth, D. M., Wareham, N. J., Waeber, G., Vollenweider, P., Voight, B. F., Vitart, V., Uitterlinden, A. G., Uda, M., Tuomilehto, J., Thompson, J. R., Tanaka, T., Surakka, I., Stringham, H. M., Spector, T. D., Soranzo, N., Smit, J. H., Sinisalo, J., Silander, K., Sijbrands, E. J. G., Scuteri, A., Scott, J., Schlessinger, D., Sanna, S., Salomaa, V., Saharinen, J., Sabatti, C., Ruukonen, A., Rudan, I., Rose, L. M., Roberts, R., Rieder, M., Psaty, B. M., Pramstaller, P. P., Pichler, I., Perola, M., Penninx, B. W. J. H., Pedersen, N. L., Pattaro, C., Parker, A. N., Pare, G., Oostra, B. A., O'donnell, C. J., Nieminen, M. S., Nickerson, D. A., Montgomery, G. W., Meitinger, T., Mcpherson, R., Mccarthy, M. I., Et Al. 2010. Biological, Clinical And Population Relevance Of 95 Loci For Blood Lipids. *Nature*, 466, 707-713.
- Teupser, D., Kretzschmar, D., Tennert, C., Burkhardt, R., Wilfert, W., Fengler, D., Naumann, R., Sippel, A. E. & Thiery, J. 2008. Effect Of Macrophage Overexpression Of Murine Liver X Receptor-Alpha (Lxr-Alpha) On Atherosclerosis In Ldl-Receptor Deficient Mice. *Arteriosclerosis Thrombosis And Vascular Biology*, 28, 2009-2015.
- Thurman, R. G. 1998. Mechanisms Of Hepatic Toxicity Ii. Alcoholic Liver Injury Involves Activation Of Kupffer Cells By Endotoxin. *American Journal Of Physiology-Gastrointestinal And Liver Physiology*, 275, G605-G611.
- Tontonoz, P., Nagy, L., Alvarez, J. G. A., Thomazy, V. A. & Evans, R. M. 1998. Ppar Gamma Promotes Monocyte/Macrophage Differentiation And Uptake Of Oxidized

- Ldl. *Cell*, 93, 241-252.
- Tordjman, K., Bernal-Mizrachi, C., Zeman, L., Weng, S., Feng, C., Zhang, F. J., Leone, T. C., Coleman, T., Kelly, D. P. & Semenkovich, C. F. 2001. Ppar Alpha Deficiency Reduces Insulin Resistance And Atherosclerosis In Apoe-Null Mice. *Journal Of Clinical Investigation*, 107, 1025-1034.
- Tosello-Trampont, A. C., Landes, S. G., Nguyen, V., Novobrantseva, T. I. & Hahn, Y. S. 2012. Kupffer Cells Trigger Nonalcoholic Steatohepatitis Development In Diet-Induced Mouse Model Through Tumor Necrosis Factor-Alpha Production. *Journal Of Biological Chemistry*, 287, 40161-40172.
- Traub, O. & Berk, B. C. 1998. Laminar Shear Stress - Mechanisms By Which Endothelial Cells Transduce An Atheroprotective Force. *Arteriosclerosis Thrombosis And Vascular Biology*, 18, 677-685.
- Tyagi, S., Gupta, P., Saini, A. S., Kaushal, C. & Sharma, S. 2011. The Peroxisome Proliferator-Activated Receptor: A Family Of Nuclear Receptors Role In Various Diseases. *J Adv Pharm Technol Res*, 2, 236-40.
- Van Rooyen, D. M. & Farrell, G. C. 2011. Srebp-2: A Link Between Insulin Resistance, Hepatic Cholesterol, And Inflammation In Nash. *Journal Of Gastroenterology And Hepatology*, 26, 789-792.
- Van Rooyen, D. M., Larter, C. Z., Haigh, W. G., Yeh, M. M., Ioannou, G., Kuver, R., Lee, S. P., Teoh, N. C. & Farrell, G. C. 2011. Hepatic Free Cholesterol Accumulates In Obese, Diabetic Mice And Causes Nonalcoholic Steatohepatitis. *Gastroenterology*, 141, 1393-U850.
- Vaneck, M., Herijgers, N., Yates, J., Pearce, N. J., Hoogerbrugge, P. M., Groot, P. H. E. & Vanberkel, T. J. C. 1997. Bone Marrow Transplantation In Apolipoprotein E Deficient Mice - Effect Of Apoe Gene Dosage On Serum Lipid Concentrations, (Beta)Vldl Catabolism, And Atherosclerosis. *Arteriosclerosis Thrombosis And Vascular Biology*, 17, 3117-3126.
- Vanfurth, R., Spector, W. G., Cohn, Z. A., Hirsch, J. G., Langevoog, H. & Humphrey, J. H. 1972. Mononuclear Phagocyte System - New Classification Of Macrophages, Monocytes, And Their Precursor Cells. *Bulletin Of The World Health Organization*, 46, 845-&.
- Varbo, A., Benn, M., Tybjaerg-Hansen, A., Grande, P. & Nordestgaard, B. G. 2011. Trib1 And Gckr Polymorphisms, Lipid Levels, And Risk Of Ischemic Heart Disease In The General Population. *Arteriosclerosis Thrombosis And Vascular Biology*, 31, 451-457.
- Verreck, F. A. W., De Boer, T., Langenberg, D. M. L., Hooft, M. A., Kramer, M., Vaisberg, E., Kastelein, R., Kolk, A., De Waal-Malefyt, R. & Ottenhoff, T. H. M. 2004. Human Il-23-Producing Type 1 Macrophages Promote But Il-10-Producing Type 2, Macrophages Subvert, Immunity To (Myco)Bacteria. *Proceedings Of The National Academy Of Sciences Of The United States Of America*, 101, 4560-4565.
- W.H.O, W. H. O. 2016. *Cardiovascular Diseases (Cvds) Fact Sheet, September 2016* [Online]. World Health Organisation. Available: <http://www.who.int/mediacentre/factsheets/fs317/en/> [Accessed 2016].
- Wang, J., Zhang, Y., Weng, W., Qiao, Y., Ma, L., Xiao, W., Yu, Y., Pan, Q. & Sun, F. 2013. Impaired Phosphorylation And Ubiquitination By P70 S6 Kinase (P70s6k) And Smad Ubiquitination Regulatory Factor 1 (Smurf1) Promote Tribbles Homolog 2 (Trib2) Stability And Carcinogenic Property In Liver Cancer. *Journal Of Biological Chemistry*, 288, 33667-33681.
- Wang, X., Collins, H. L., Ranalletta, M., Fuki, I. V., Billheimer, J. T., Rothblat, G. H., Tall, A. R. & Rader, D. J. 2007. Macrophage Abca1 And Abcg1, But Not Sr-Bi, Promote Macrophage Reverse Cholesterol Transport In Vivo. *Journal Of Clinical Investigation*, 117, 2216-2224.

- Wang, Z.-H., Shang, Y.-Y., Zhang, S., Zhong, M., Wang, X.-P., Deng, J.-T., Pan, J., Zhang, Y. & Zhang, W. 2012. Silence Of Trib3 Suppresses Atherosclerosis And Stabilizes Plaques In Diabetic Apoe(-/-)/Ldl Receptor(-/-) Mice. *Diabetes*, 61, 463-473.
- Watt, V., Chamberlain, J., Steiner, T., Francis, S. & Crossman, D. 2011. Trail Attenuates The Development Of Atherosclerosis In Apolipoprotein E Deficient Mice. *Atherosclerosis*, 215, 348-354.
- Weisberg, S. P., Mccann, D., Desai, M., Rosenbaum, M., Leibel, R. L. & Ferrante, A. W. 2003. Obesity Is Associated With Macrophage Accumulation In Adipose Tissue. *Journal Of Clinical Investigation*, 112, 1796-1808.
- Weismann, D., Erion, D. M., Ignatova-Todorava, I., Nagai, Y., Stark, R., Hsiao, J. J., Flannery, C., Birkenfeld, A. L., May, T., Kahn, M., Zhang, D., Yu, X. X., Murray, S. F., Bhanot, S., Monia, B. P., Cline, G. W., Shulman, G. I. & Samuel, V. T. 2011. Knockdown Of The Gene Encoding Drosophila Tribbles Homologue 3 (Trib3) Improves Insulin Sensitivity Through Peroxisome Proliferator-Activated Receptor-Gamma (Ppar-Gamma) Activation In A Rat Model Of Insulin Resistance. *Diabetologia*, 54, 935-944.
- Wellen, K. E. & Hotamisligil, G. S. 2005. Inflammation, Stress, And Diabetes. *Journal Of Clinical Investigation*, 115, 1111-1119.
- Weyer, C., Foley, J. E., Bogardus, C., Tataranni, P. A. & Pratley, R. E. 2000. Enlarged Subcutaneous Abdominal Adipocyte Size, But Not Obesity Itself, Predicts Type II Diabetes Independent Of Insulin Resistance. *Diabetologia*, 43, 1498-1506.
- Wheeler, M. D. 2003. Endotoxin And Kupffer Cell Activation In Alcoholic Liver Disease. *Alcohol Research & Health*, 27, 300-306.
- Whitman, S. C. 2004. A Practical Approach To Using Mice In Atherosclerosis Research. *The Clinical Biochemist. Reviews / Australian Association Of Clinical Biochemists*, 25, 81-93.
- Whitmarsh, A. J. 2006. The Jip Family Of Mapk Scaffold Proteins. *Biochemical Society Transactions*, 34, 828-832.
- Willer, C. J., Sanna, S., Jackson, A. U., Scuteri, A., Bonnycastle, L. L., Clarke, R., Heath, S. C., Timpson, N. J., Najjar, S. S., Stringham, H. M., Strait, J., Duren, W. L., Maschio, A., Busonero, F., Mulas, A., Albai, G., Swift, A. J., Morken, M. A., Narisu, N., Bennett, D., Parish, S., Shen, H., Galan, P., Meneton, P., Hercberg, S., Zelenika, D., Chen, W.-M., Li, Y., Scott, L. J., Scheet, P. A., Sundvall, J., Watanabe, R. M., Nagaraja, R., Ebrahim, S., Lawlor, D. A., Ben-Shlomo, Y., Davey-Smith, G., Shuldiner, A. R., Collins, R., Bergman, R. N., Uda, M., Tuomilehto, J., Cao, A., Collins, F. S., Lakatta, E., Lathrop, G. M., Boehnke, M., Schlessinger, D., Mohlke, K. L. & Abecasis, G. R. 2008. Newly Identified Loci That Influence Lipid Concentrations And Risk Of Coronary Artery Disease. *Nature Genetics*, 40, 161-169.
- Willer, C. J., Schmidt, E. M., Sengupta, S., Peloso, G. M., Gustafsson, S., Kanoni, S., Ganna, A., Chen, J., Buchkovich, M. L., Mora, S., Beckmann, J. S., Bragg-Gresham, J. L., Chang, H.-Y., Demirkan, A., Den Hertog, H. M., Do, R., Donnelly, L. A., Ehret, G. B., Esko, T., Feitosa, M. F., Ferreira, T., Fischer, K., Fontanillas, P., Fraser, R. M., Freitag, D. F., Gurdasani, D., Heikkila, K., Hypponen, E., Isaacs, A., Jackson, A. U., Johansson, A., Johnson, T., Kaakinen, M., Kettunen, J., Kleber, M. E., Li, X., Luan, J. A., Lyytikainen, L.-P., Magnusson, P. K. E., Mangino, M., Mihailov, E., Montasser, M. E., Mueller-Nurasyid, M., Nolte, I. M., O'connell, J. R., Palmer, C. D., Perola, M., Petersen, A.-K., Sanna, S., Saxena, R., Service, S. K., Shah, S., Shungin, D., Sidore, C., Song, C., Strawbridge, R. J., Surakka, I., Tanaka, T., Teslovich, T. M., Thorleifsson, G., Van Den Herik, E. G., Voight, B. F., Volcik, K. A., Waite, L. L., Wong, A., Wu, Y., Zhang, W., Absher, D., Asiki, G., Barroso, I., Been, L. F., Bolton, J. L., Bonnycastle, L. L., Brambilla, P., Burnett, M. S., Cesana, G., Dimitriou, M., Doney, A. S. F., Doering, A., Elliott, P., Epstein, S. E.,

- Eyjolfsson, G. I., Gigante, B., Goodarzi, M. O., Grallert, H., Gravito, M. L., Groves, C. J., Hallmans, G., Hartikainen, A.-L., Hayward, C., Hernandez, D., Hicks, A. A., Holm, H., Hung, Y.-J., Illig, T., Jones, M. R., Kaleebu, P., Kastelein, J. J. P., Khaw, K.-T., Kim, E., Et Al. 2013. Discovery And Refinement Of Loci Associated With Lipid Levels. *Nature Genetics*, 45, 1274-+.
- Wu, M., Xu, L. G., Zhai, Z. H. & Shu, H. B. 2003. Sink Is A P65-Interacting Negative Regulator Of Nf-Kappa B-Dependent Transcription. *Journal Of Biological Chemistry*, 278, 27072-27079.
- Wymann, M. P. & Schneider, R. 2008. Lipid Signalling In Disease. *Nature Reviews Molecular Cell Biology*, 9, 162-176.
- Wynn, T. A., Chawla, A. & Pollard, J. W. 2013. Macrophage Biology In Development, Homeostasis And Disease. *Nature*, 496, 445-455.
- Yaari, G., Bolen, C. R., Thakar, J. & Kleinstein, S. H. 2013. Quantitative Set Analysis For Gene Expression: A Method To Quantify Gene Set Differential Expression Including Gene-Gene Correlations. *Nucleic Acids Research*, 41.
- Yamamoto, M., Uematsu, S., Okamoto, T., Matsuura, Y., Sato, S., Kumar, H., Satoh, T., Saitoh, T., Takeda, K., Ishii, K. J., Takeuchi, O., Kawai, T. & Akira, S. 2007. Enhanced Tlr-Mediated Nf-Il6-Dependent Gene Expression By Trib1 Deficiency. *Journal Of Experimental Medicine*, 204, 2233-2239.
- Yokoyama, T., Kanno, Y., Yamazaki, Y., Takahara, T., Miyata, S. & Nakamura, T. 2010. Trib1 Links The Mek1/Erk Pathway In Myeloid Leukemogenesis. *Blood*, 116, 2768-2775.
- Yokoyama, T. & Nakamura, T. 2011. Tribbles In Disease: Signaling Pathways Important For Cellular Function And Neoplastic Transformation. *Cancer Science*, 102, 1115-1122.
- Yona, S., Kim, K. W., Wolf, Y., Mildner, A., Varol, D., Breker, M., Strauss-Ayali, D., Viukov, S., Guillemins, M., Misharin, A., Hume, D. A., Perlman, H., Malissen, B., Zelzer, E. & Jung, S. 2013. Fate Mapping Reveals Origins And Dynamics Of Monocytes And Tissue Macrophages Under Homeostasis. *Immunity*, 38, 79-91.
- Yoshida, A., Kato, J.-Y., Nakamae, I. & Yoneda-Kato, N. 2013. Cop1 Targets C/Ebp Alpha For Degradation And Induces Acute Myeloid Leukemia Via Trib1. *Blood*, 122, 1750-1760.
- Zanotti, I., Pedrelli, M., Poti, F., Stomeo, G., Gomasaschi, M., Calabresi, L. & Bernini, F. 2011. Macrophage, But Not Systemic, Apolipoprotein E Is Necessary For Macrophage Reverse Cholesterol Transport In Vivo. *Arterioscler Thromb Vasc Biol*, 31, 74-80.
- Zerneck, A., Shagdarsuren, E. & Weber, C. 2008. Chemokines In Atherosclerosis An Update. *Arteriosclerosis Thrombosis And Vascular Biology*, 28, 1897-1908.
- Zeyda, M., Gollinger, K., Kriehuber, E., Kiefer, F. W., Neuhofer, A. & Stulnig, T. M. 2010. Newly Identified Adipose Tissue Macrophage Populations In Obesity With Distinct Chemokine And Chemokine Receptor Expression. *International Journal Of Obesity*, 34, 1684-1694.
- Zhan, Y. T. & An, W. 2010. Roles Of Liver Innate Immune Cells In Nonalcoholic Fatty Liver Disease. *World Journal Of Gastroenterology*, 16, 4652-4660.
- Ziegler-Heitbrock, L., Ancuta, P., Crowe, S., Dalod, M., Grau, V., Hart, D. N., Leenen, P. J. M., Liu, Y.-J., Macpherson, G., Randolph, G. J., Scherberich, J., Schmitz, J., Shortman, K., Sozzani, S., Strobl, H., Zembala, M., Austyn, J. M. & Lutz, M. B. 2010. Nomenclature Of Monocytes And Dendritic Cells In Blood. *Blood*, 116, E74-E80.

Appendix I Genotyping protocols

8.1.1 DNA extraction from mouse earclips

DNA was extracted from mouse earclips which involved first incubating earclips in lysis buffer (50 μ M Tris-HCl (pH 8.5), 1 μ M EDTA (pH 8.0), 0.5% (v/v) Tween-20) and proteinase K (300 μ g/ml) overnight at 56°C to digest the tissue.

8.1.2 DNA isolation

- Add Proteinase K solution to lysis buffer to a final concentration of 300 μ g/ml (30 μ l stock per ml lysis buffer)
- Add 150 μ l lysis buffer +Proteinase K to each ear clip in 1.5 ml eppendorf tube
- Incubate ON at 55°C in waterbath
- Vortex briefly
- Heat inactivate Proteinase K by incubating samples at 100°C for 12 min
- Add 600 μ l sterile H₂O to each tube
- Vortex and store at 4°C
- Use 4 μ l DNA per reaction

8.1.3 Primers and PCR conditions

8.1.3.1 ROSA26.Trib1 transgene

Tribbles-1 primers:

FW: GTGATCTGCAACTCCAGTCTTTCTAG
WT REV: CGCGACACTGTAATTTTCATACTGTAG
TRANS REV: CCTTCTTGACGAGTTCTTCTGAGG

WT will generate a single band at 353 kD

Transgene will generate a single band at 263 kD

- **PCR & agarose gel analysis**

PCR mix (per sample):

Biomix Red (2x)	12.5 μ l
Primer Trb1 FW (20 μ M)	0.5 μ l
Primer Trb1 WT-R (20 μ M)	0.25 μ l
Primer Trb1 KO-R (20 μ M)	0.25 μ l
H ₂ O	7.5 μ l
DNA sample	4.0 μ l

	25.0 μ l

- **PCR conditions**

Step 1: 5 min at 94 °C	1 cycle
Step 2: 30 sec at 94 °C	40 cycles
30 sec at 58 °C	
30 sec at 72 °C	
Step 3: 5 min at 72 °C	1 cycle
Step 4: ∞ at 10 °C	

Run on 2% agarose gel, 80V (12 µl sample / slot)

8.1.3.2 Trib1 floxed

Tribbles-1 primers

dTRIB1cKO FL R: AAG TTC ACA TTT GAA CTG ATG GC

dTRIB1cKO WT R: AGC TGG TTT CAG GGG AAG AC

dTRIB1cKO F2: ACC TTG ATC TGC AGT CCT AGG

WT will generate a single band at 326 KD

Trib1 floxed will generate a single band at 420 KD

- **PCR & agarose gel analysis**

2x Master mix	5 µl
Primer mix 5µM	1 µl
DNA	1 µl
H ₂ O	3 µl

- **PCR conditions**

-

Step 1: 3 min at 94 °C	1 cycle
Step 2: 30 sec at 94 °C	35 cycles
1 min at 58 °C	
1 min at 72 °C	
Step 3: 5 min at 72 °C	1 cycle
Step 4: ∞ at 4 °C	

Run on 2% agarose gel, 80V

8.1.3.3 Lyz2Cre

Primers:

oIMR3066: CCC AGA AAT GCC AGA TTA CG **Mutant**

oIMR3067: CTT GGG CTG CCA GAA TTT CTC **Common**

oIMR3068: TTA CAG TCG GCC AGG CTG AC **Wild type**

Mutant will generate a single band ~700bp

Heterozygote will generate two bands ~700bp and 350bp

Wild type will generate single band at 350bp

Table A2.1 Reaction A: Mutant PCR

Reaction component	Volume (µl)	Final concentration	Total volume (µl)
ddH ₂ O	4.55		4.55
5x Kapa 2G HS buffer	2.40	1x	2.40
25 mM MgCl ₂	0.96	2 mM	0.96
10 mM dNTPS-kapa	0.24	0.2 mM	0.24
20 µM oIMR3066	0.30	0.5 mM	0.30
20 µM oIMR3067	0.30	0.5 mM	0.30
5 mM 10x Loading dye	1.20	0.5mM	1.2
2.5 U/µl Kapa 2G HS taq polymerase	0.05	0.01 U/µl	0.05
DNA	2.00		2.00

- Reaction A: PCR conditions**

Step 1: 2 min at 94 °C	1 cycle
Step 2: 20 sec at 94 °C	10 cycles (0.5°C per cycle decrease)
15 sec at 65 °C	
10 sec at 68 °C	
Step 3: 15 sec at 94 °C	
15 sec at 60°C	
10 sec at 72 °C	
Step 4: 2 min at 72 °C	
Step 5: Hold at 10 °C	

Table A2.2 Reaction B: Wildtype PCR

Reaction component	Volume (μl)	Final concentration	Total volume (μl)
ddH ₂ O	4.55		4.55
5x Kapa 2G HS buffer	2.40	1x	2.40
25 mM MgCl ₂	0.96	2 mM	0.96
10 mM dNTPS-kapa	0.24	0.2 mM	0.24
20 μ M oIMR3067	0.30	0.5 mM	0.30
20 μ M oIMR3068	0.30	0.5 mM	0.30
5 mM 10x Loading dye	1.20	0.5 mM	1.2
2.5 U/ μ l Kapa 2G HS taq polymerase	0.05	0.01 U/ μ l	0.05
DNA	2.00		2.00

- Reaction B: PCR Conditions**

Step 1: 2 min at 94 °C	1 cycle
Step 2: 20 sec at 94 °C 15 sec at 65 °C 10 sec at 68 °C	10 cycles (0.5°C per cycle decrease)
Step 3: 15 sec at 94 °C 15 sec at 60°C 10 sec at 72 °C	28 cycles
Step 4: 2 min at 72 °C	
Step 5: Hold at 10 °C	

Appendix II Mouse diets & drinking water

8.2.1 Chow diet

2018S-Tekland Global 18% protein rodent diet (Harlan, Indiana, USA), autoclaved and stored at room temperature.

Ingredients

Ground wheat, ground corn, wheat middlings, dehulled soybean meal, corn gluten meal, soybean oil, calcium carbonate, dicalcium phosphate, brewers dried yeast, iodized salt, Llysine, DL-methionine, choline chloride, kaolin, menadione sodium bisulfite complex (source of vitamin K activity), magnesium oxide, vitamin E acetate, calcium pantothenate, thiamin mononitrate, manganous oxide, niacin, ferrous sulfate, zinc oxide, riboflavin, vitamin A acetate, pyridoxine hydrochloride, copper sulfate, vitamin B12 supplement, folic acid, calcium iodate, biotin, vitamin D3 supplement, cobalt carbonate.

Macronutrients (% (w/w)): Crude Protein, 18.8; Crude Oil (Fat), 6.0; Crude Fibre, 3.8; Ash, 5.9; Carbohydrate, 50.0; Starch, 45.0; Sugar, 5.0. **Minerals (% (w/w)):** Calcium, 1.0; Phosphorus, 0.7; Sodium, 0.2; Potassium, 0.6; Chloride, 0.40; Magnesium, 0.20; Zinc 77.0 mg/kg; Manganese, 100.0 mg/kg; Copper, 15.0 mg/kg; Iodine, 6 mg/kg Iron, 200.0 mg/kg; Selenium 200 ug/kg. **Amino Acids (%):** Aspartic Acid, 1.4; Glutamic Acid, 3.4; Alanine, 1.1; Glycine, 0.8; Threonine, 0.7; Proline, 1.6; Serine, 1.1; Leucine, 1.8; Isoleucine, 0.8; Valine, 0.9; Phenylalanine, 1.0; Tyrosine, 0.6; Methionine, 0.6; Cystine, 0.3; Lysine, 1.1; Histidine, 0.4; Arginine, 1.0; Tryptophan, 0.2.

Vitamins (mg/kg): Vitamin A, 30.0 IU/g; Vitamin D3, 2.0 IU/g; Vitamin E, 135 IU/Kg; Vitamin K3, 100; Vitamin B1, 117; Vitamin B2, 27; Niacin, 115; Vitamin B6, 26; Pantothenic Acid, 140; Vitamin B12, 0.15; Biotin, 0.9; Folate, 9; Choline, 1200. **Fatty Acids (%):** C16:0 Palmitic, 0.7; C18:0 Steatic, 0.2; C18:1 ω 9 Oleic, 1.2; C18:2 ω 6 Linoleic, 3.1; C18:2 ω 3, 0.3; Total saturated, 0.9; total monounsaturated, 1.3; total polyunsaturated, 3.4; **Cholesterol, nil.**

8.2.2 Western diet

829100-Western Rodent Diet (Special Diet Services, UK), purified diet, stored at 4°C to prolong shelf life.

Ingredients (% (w/w))

Sucrose, 33.94; milk fat anhydrous, 20.00; casein, 19.50; maltodextrin, 10.00; corn starch, 5.00; cellulose, 5.00; corn oil, 1.00; calcium carbonate, 0.40; L-cystine, 0.30; choline bitartrate, 0.20; **Cholesterol, 0.15;** antioxidant, 0.01; AIN-76A-MX, 3.50; AIN-76A-VX, 1.00. **Specification: Crude Fat, 21.4; Crude Protein, 17.5; Crude Fibre, 3.5; Ash, 4.1; Carbohydrate, 50.0.**

8.2.3 Acidified drinking water

100x acidified water: 10ml concentrated (12M, 37%) HCl in 840ml sterile water (Baxter). HCl final concentration= 144mM.

1x acidified water: 10.1ml of 100x acidified water in 1L sterile water. HCl final concentration=1.44mM

Appendix III Histology

8.3.1 Fixatives

Neutral buffered formalin (10% v/v)

To make 1L:	4g	sodium phosphate (NaH ₂ PO ₄)
(Na ₂ HPO ₄)	7.1g	di-sodium hydrogen orthophosphate
	100ml	formaldehyde (37% w/v)
	~900ml	distilled water

Paraformaldehyde in PBS (PFA) (4% w/v)

To make 100ml	4g	paraformaldehyde
	100ml	1x PBS

Note: dissolve formaldehyde at ~60°C. Add several drops of NaOH to raise solution to pH 7.0, the solution will become clear.

8.3.2 Histological stains

8.3.2.1 Oil Red O

Solution:

- Add Oil Red O powder to 99% (v/v) isopropanol until it becomes saturated
- Filter the solution using Whatmann grade 1 filter paper
- The stock stain can be kept at room temperature
- Dilute to 60% (v/v) **fresh** using distilled water on day of staining

Staining:

- Aortas should be stained in individual 1.5ml eppendorf tubes
- Rinse aorta in distilled water followed by 60% (v/v) isopropanol for 2 minutes
- Immerse in 60% (v/v) Oil Red O for 10-15 minutes
- Rinse in 60% (v/v) isopropanol for 2 minutes followed by distilled water.
- Stained aorta can be stored at 4°C until pinning out.

8.3.2.2 Elastic van Gieson (EVG)

Staining:

- Dewax slides for 10 minutes in xylene and rehydrate through graded alcohols (100%, 90%, 70% and 50% (v/v) ethanol), finishing in water

- Oxidise with aqueous potassium permanganate (0.25% (w/v)) for 3 minutes, rinse in water
- Bleach with oxalic acid (1% w/v) for 3 minutes, rinse in water
- Stain nuclei with Carazzi's haematoxylin for 2 minutes
- Differentiate with acid alcohol (1% (v/v) HCl in 70% (v/v) ethanol) for 5 seconds
- "Blue" with hot running tap water for 5 minutes
- Stain with alcian blue (1% (w/v) in 3% aqueous acetic acid) for 5 minutes
- Rinse in water followed by 95% (v/v) ethanol
- Stain with Miller's elastin stain for 30 minutes
- Differentiate in 95% ethanol and rinse in water
- Stain with Curtis' modified van Gieson reagent (10 ml 1% (w/v) ponceau S in 90 ml saturated aqueous picric acid, 1 ml glacial acetic acid) for 6 minutes, rinse in water
- Dehydrate tissue through graded alcohols (reverse to step 1) ending in xylene
- Mount with coverslips using DPX mountant

Interpretation

- | | |
|----------------------------------|------------|
| • Elastin coarse and fine fibres | Blue/black |
| • Acid mucopolysaccharides | Black |
| • Collagen | Red |
| • Muscle | Yellow |

8.3.2.3 Haematoxylin and Eosin (H&E)

Staining:

- Dewax slides for 10 minutes in xylene and rehydrate through graded alcohols (100%, 90%, 70 and 50% (v/v) ethanol), finishing in water
- Stain with Carazzi's haematoxylin for 2 minutes, rinse in water
- Stain with eosin (1% (w/v)) for 30 seconds
- Rinse in water and quickly dehydrate through graded alcohols for 30 seconds in each, beginning at 90% (v/v) ethanol, ending in xylene
- Mount with coverslips using DPX mountant

Interpretation:

- | | |
|-----------------|-------------|
| • Nuclei | Purple/blue |
| • Cytoplasm | Pink |
| • Muscle fibres | Deep red |
| • RBCs | Orange/red |
| • Fibrin | Deep pink |

8.3.2.4 Maritus Scarlet Blue (MSB)

Staining:

- Dewax slides for 10 minutes in xylene and rehydrate through graded alcohols (100%, 90%, 70 and 50% (v/v) ethanol), finishing in water
- Stain with Celestine blue (1% (w/v)) for 5 minutes
- Stain with Harris' haematoxylin for 5 minutes, rinse in water
- Differentiate in acid alcohol (1% (v/v) HCl in 70% (v/v) ethanol) for a few seconds then "blue" in tap water for 5 minutes
- Rinse in 95% (v/v) ethanol
- Stain with martius yellow (0.5% (v/v) martius yellow, 2% (w/v) phosphotungstic acid in 95% (v/v) ethanol) for 2 minutes, rinse in water
- Stain with ponceau de xyline (1% (w/v) ponceau de xyline in 2% (v/v) glacial acetic acid) for 10 minutes
- Differentiate in 1% (w/v) phosphotungstic acid for 5 minutes and drain (do not wash in water)
- Stain with methyl blue (5% w/v methyl blue in 10% (v/v) glacial acetic acid) for 10 minutes
- Rinse in 1% (v/v) glacial acetic acid for 10 minutes
- Dehydrate in 100% (v/v) ethanol, then xylene
- Mount with coverslips using DPX mountant

Interpretation:

- | | |
|--|--------------|
| • Nuclei | Black/purple |
| • RBCs | Yellow |
| • Fibrin | Red |
| • Collagen/adventitia/ connective tissue | Blue |
| • Smooth muscle | Pink/red |

Appendix IV Immunohistochemistry

8.4.3.1 Dual CD68 and TRIB1

Human coronary atheromas were dual stained for CD68 and TRIB1. Following the de-waxing and H₂O₂ treatment in the standard protocol, antigen retrieval was performed using 0.01M Tris sodium citrate for 10 minutes in the microwave. Slides were rinsed with water and cooled. Sections were blocked using serum free protein block solution (Dako) for 20 minutes, RT. Slides were incubated with 1:100 (PBS) mouse anti-human CD68 antibody for 1 hour, RT and washed 3x with PBS. Slides were then incubated with 1:200 (PBS) biotinylated horse anti-mouse IgG 2° antibody using Elite Mouse ABC HRP kit (Vector Laboratories) according to the manufacturer's instructions for 30 minutes, RT. Sections were incubated with ABC complex for 30 minutes, RT and washed 3x in PBS. Following this, sections were incubated with enzyme substrate (SIGMAFAST 3, 3'-Diaminobenzidine; DAB) until colour development was observed under the microscope, the reaction was stopped by washing slides in dH₂O and subsequent rinse in PBS for 5 minutes. Sections were re-blocked as described and incubated with 1:100 (PBS) rabbit anti-human TRIB1 (Millipore, UK) for 1 hour, RT and washed 3x in PBS. Sections were then incubated with 1:200 (PBS) biotinylated goat anti-rabbit IgG 2° antibody using Rabbit ABC-Alkaline phosphatase kit as per manufacturer's instructions, for 30 minutes, RT (Vector Laboratories). Slides were washed 3x PBS and incubated with ABC-AP for 30 minutes, RT and washed 3x PBS, 5 mins. Positive TRIB1 staining was visualised using Vector Red Alkaline phosphatase substrate kit (Vector laboratories) as per manufacturer's instructions until colour development was observed under the microscope, the reaction was stopped by washing slides in dH₂O and subsequent rinse in PBS for 5 minutes. Slides were counterstained with Carazzi's haematoxylin for 1 minutes, dehydrated and mounted using coverslips and DPX mountant.

8.4.3.2 Mac-3

Mouse aortic sinus lesions were stained for Mac-3. Following the de-waxing and H₂O₂ treatment in the standard protocol, antigen retrieval was performed using

10mM sodium citrate buffer, pH 6 for 20 minutes at 95°C using a water bath, slides were then allowed to cool for a further 20 minutes at RT in the heated citrate buffer. Slides were rinsed with PBS and were blocked using 1% Marvel buffer for 30 minutes, RT. Slides were incubated with 1:100 (PBS) rat anti-mouse Mac-3 (BD Pharmingen) antibody overnight at 4°C, and washed 3x with PBS. Slides were then incubated with 1:200 (PBS) biotinylated rabbit anti-rat IgG 2° antibody (Vector Laboratories) for 30 minutes, RT. Sections were incubated with ABC complex for 30 minutes, RT and washed 3x in PBS. Following this, sections were incubated with enzyme substrate (SIGMAFAST 3, 3'-Diaminobenzidine; DAB) until colour development was observed under the microscope, the reaction was stopped by washing slides in dH₂O and subsequent rinse in PBS for 5 minutes. Slides were counterstained with Carazzi's haematoxylin for 1 minutes, dehydrated and mounted using coverslips and DPX mountant.

Table A4.1: Details of antibodies used for colourimetric immunohistochemistry

Antigen	Antibody	Source	Working Dilution and incubation time
<i>Primary</i>			
CD68	Mouse monoclonal anti-human CD68	Dako	1:100, 1 hour RT
TRIB1	Rabbit polyclonal anti-human TRIB1	Millipore	1:100, 1 hour RT
Mac-3	Rat monoclonal anti-mouse Mac-3	BD Pharmingen	1:100, O/N 4°C
<i>Secondary</i>			
CD68	Biotinylated horse anti-mouse	Vector Laboratories	1:200, 30 mins RT
TRIB1	Biotinylated goat anti-rabbit	Vector Laboratories	1:200, 30 mins RT
Mac-3	Biotinylated rabbit anti-rat	Vector Laboratories	1:200, 30 mins RT

Appendix V Raw data

Table A5.1: Plasma lipid analysis for *Trib1 x LyzMCre* → ApoE^{-/-} mice.

All results are presented as mmol/L.

Mouse ID	Genotype	Glucose	Cholesterol	TG	HDL	LDL
231	KO	18.2	4	1.6	2.6	0.7
232	KO	17.8	4.8	1	3.09	1.3
233	KO	22.1	4.5	1.6	2.98	0.8
234	KO	18.9	6.7	0.7	2.6	3.8
235	KO	18.9	4.7	1.1	2.74	1.5
240	KO	14.5	3.8	1	2.41	0.9
241	KO	14	3.6	1.5	2.27	0.6
244	KO	16	3.5	1.5	2.57	0.2

226	Control_KO	18.9	4.2	1.1	2.87	0.8
227	Control_KO	19.7	4.7	1.7	2.99	0.9
228	Control_KO	20.6	4.5	1.4	3.56	0.3
229	Control_KO	17.5	4.1	1.8	2.56	0.7
237	Control_KO	20.5	5.1	2.9	2.71	1.1
238	Control_KO	16	4.2	1.6	2.61	0.9

713	Tg	14.2	3.9	1.4	2.15	1.1
714	Tg	18.7	4.3	1	2.49	1.4
715	Tg	16.7	5.1	1.3	2.55	2
719	Tg	20	2.1	0.8	1.17	0.6
720	Tg	18.5	3.3	1.2	2.04	0.7
721	Tg	16.7	2.5	1.3	1.5	0.4
722	Tg	16.6	5.9	2.7	1.93	2.7
723	Tg	20.3	4.5	1.6	1.75	2
729	Tg	16.2	5.9	2.8	2.77	1.8
730	Tg	16.1	6	2.5	2.72	2.1
731	Tg	20.3	5.2	1	2.55	2.2
732	Tg	17.6	4.9	1.3	2.79	1.5

708	Control Tg	13.6	2.8	0.5	1.23	1.3
709	Control Tg	13.1	1.8	0.6	0.85	0.7
710	Control Tg	14.5	2.5	0.8	1.13	1
716	Control Tg	16.4	2.8	1.4	1.39	0.8
717	Control Tg	15	4	1.7	1.58	1.6
718	Control Tg	17.8	3.2	1.4	1.53	1
725	Control Tg	19.5	4.3	1.1	2.61	1.2
726	Control Tg	16.2	2.1	0.7	1.11	0.7
727	Control Tg	13.7	3.4	1.8	1.35	1.2
728	Control Tg	13.5	4.7	1.5	2.49	1.5